The Role of Leptin Action in States of Obesity

by

Warren W. Pan

A dissertation submitted in partial fulfillment
of the requirements for the degree of
Doctor of Philosophy
(Cellular and Molecular Biology)
In the University of Michigan
2017

Doctoral Committee:

Professor Martin G. Myers Jr., Chair
Professor Malcolm J. Low
Professor Carey N. Lumeng
Professor Audrey F. Seasholtz

Fortunate are those who are able to know the truth behind things

-Virgil

The truth is not always beautiful,

nor beautiful words the truth

-Laozi

Warren Wang Pan

warrenp@umich.edu

ORCID iD: 0000-0003-4931-8864

ACKNOWLEDGEMENTS

Ten years ago, I declared Economics as my College concentration. I could not then have imagined reaching this milestone today of fulfilling my dissertation requirements for a PhD in Cellular and Molecular Biology. The twists and turns of events, the serendipitous interactions, and the off-handed decisions that have proven life-defining all contributed to the winding path of my journey thus far. And, I eagerly look forward to where my path will lead.

There have been many who have supported me these last few years at Michigan, without whom I would not have made it to this point. There is, however, one person above the rest who has been instrumental in my development as a scientist. Martin has been tremendous as a mentor and I am deeply grateful to have trained under his tutelage. His uncanny ability to decrypt data and inspired approach to research, while at times intimidating, have sharpened my own scientific acumen and curiosity. Additionally, Martin's obvious love for science and boundless optimism are infectious and have empowered my own dream to pursue research. These last few years have been some of the most challenging and fulfilling of my life; I know the experiences will serve me well as I move forward.

I am also extremely thankful to the many Myers lab members, especially Christa

Polidori, Meg Allison, Jon Flak and Justin Jones. If Martin is the coxswain who steers the boat, they are the oarsmen/oarswomen who powered and set the pace for the boat. They taught me how to row. Without them, I would have had many ideas, but no way of testing them. Their instruction and friendship in the lab made my PhD a fun and relatively smooth experience. Additionally, work and guidance from the University of Michigan Phenotyping Core, DNA Sequencing Core, and Bioinformatics Core were pivotal in the completion of this dissertation.

Ultimately, research is a challenging road littered with failures and only occasionally punctuated by success. While Martin may have me believe that research is instead continued progress with the occasional set-back, I must acknowledge Dave Olson and Paula Goforth for their help in tempering my expectations after my many interactions with Martin. Research is a lot like banging your head against a wall and hoping the wall breaks before your head does; I very much appreciate the occasional reminder that the wall is made of brick and not of straw.

Numerous people and programs have all allowed me to complete this thesis. My dissertation committee of Martin, Malcolm, Carey and Audrey has helped guide and steer my scientific inquiry over the years and their feedback and questions have been invaluable in the progress of my projects. To Ron, Ellen, Hilkka, Laurie and Justine of the MSTP, thank you for taking a chance with me (despite my incongruous concentration/background) and supporting my training to become a physician-scientist. The members of the Cellular and Molecular Biology Program, along with Bob, Kathy, Margarita and Pat, have been extremely welcoming and helpful as I stumbled through my PhD years.

What I did not quite grasp as I began this journey is how long I would be in Ann Arbor; I continue to be here even as I watch my friends leave. Friends from College got married and had children. Close medical school friends with whom I explored a cadaver with left for residency. Even friends I made in graduate school pursued jobs and adventures in far-away lands after completing their master's programs. Despite this, my friends both new and old, and near and far have continued to remind me to appreciate life before it passes me by. Life really is too serious to take seriously. I, therefore, want to emphasize the love I hold for my friends. To the Bombsquad: we may be littered across the country now, but I continue cherish our (almost) annual reunions. To the Brickhouse: you are all irreplaceable as lifelong friends and I was able to get through each week by looking forward to the weekends with you all. To Munger Residences: a break from leptin and obesity was very much appreciated and I am extremely thankful to have had the opportunity and for the friends I made through it. And, most importantly, to my girlfriend Kelly: thank you for your patience, understanding and love during the volatility of the PhD; I look forward to our switching roles as you start your PhD and I restart medical school.

Finally, I would be nowhere without my family. You have encouraged me at my lowest moments and celebrated with me at my highest. Much of who I am can be attributed to your raising me and I cannot emphasize enough how much I draw upon that unconditional love. I love you all and can only continue down this path knowing that you will be there to support me every step of the way. Thank you!

TABLE OF CONTENTS

LIST OF FIGURES

Figure

LIST OF TABLES

Table

ABSTRACT

Over the last century, the United States has experienced a shift from underweight malnutrition maladies to obesity-associated complications. Today, over 70% of US adults are overweight and are at increased risk for various chronic diseases including diabetes, cardiovascular disease and cancer. The ubiquitous nature of obesity and its costs on the individual and societal level have elevated it to one of the most impactful diseases of the 21st century. The adipokine leptin is produced in proportion to the body's triglyceride content and binds to its receptor (LepRb) in the CNS to provide a snapshot of energy stores, resulting in the regulation of energy balance. Due to leptin's role in communicating fat stores and the hyperphagic obesity that results from its absence, leptin is clearly central to the homeostatic systems that regulate energy balance. And, while leptin replacement is an effective anti-obesity treatment in the few cases of obesity from leptin-deficiency, it fails to produce weight loss in diet-induced obese (DIO) individuals who express high levels of leptin (hyperleptinemia) commensurate with their elevated adipose content. Despite this, recent advances in genetic and sequencing technologies have allowed for a closer examination of DIO.

We first examined the hypothalamic transcriptome of LepRb neurons and characterized DIO as a state of leptin activity. Additional region-specific analyses confirm this understanding of DIO, and when coupled to immunohistochemical and phenotypic findings, broaden our understanding of the role DIO-hyperleptinemia plays in LepRb neurons and neighboring glial cells. These transcriptome findings additionally revealed STAT1 to be not only another LepRb-dependent signal, but to also significantly increase when STAT3 was ablated in neurons. This increase in *Stat1*, however, did not functionally compensate for the absence of STAT3. Moreover, we found STAT3 to be both necessary and sufficient in LepRb neurons for energy balance. However, while increased STAT3 activity does decrease weight in normoleptinemic mice (mimicking hyperleptinemia in lean animals) it does not produce weight loss in already hyperleptinemic DIO animals. Thus, the diminishing returns of additional STAT3/leptin action with increasing endogenous leptin levels were demonstrated transcriptionally, phenotypically and genetically. Our further investigation into the overlap between leptin and other metabolic hormones like calcitonin and amylin has broadened our understanding of leptin action and has identified potential molecular targets and locations for the already-proven synergistic amylin-leptin weight loss therapy. Together, these varied approaches underscore the complexity and importance of leptin action and paves a path for the discovery of novel anti-obesity therapies.

CHAPTER 1

INTRODUCTION

Chapter Summary

Obesity represents the single most important risk factor for early disability and death in developed societies, and the incidence of obesity remains at staggering levels. CNS systems that modulate energy intake and expenditure in response to changes in body energy stores serve to maintain constant body adiposity; the adipocyte-derived hormone, leptin, represents a crucial regulator of these systems. A variety of mechanisms (including feedback inhibition, inflammation, gliosis, and ER stress) have been proposed to impede the systems that control body energy homeostasis to promote or maintain obesity, although the relative importance and contribution of each of these remain unclear. Here, we review the state of the field regarding these processes and synthesize a framework for understanding potential mechanisms that may lead to or maintain elevated body weight.

I. OBESITY

Obesity, generally defined by a body mass index (BMI) ≥30kg/m^2, results from the accumulation of adiposity due to the storage of consumed calories that exceed metabolic needs. While obesity has always existed in humans, malnutrition and disease dictated that even developed countries struggled primarily with the problem of underweight (BMI < 18.5 kg/m^2) (rather than obesity) up through the late 19th and early 20th centuries.[1] The increasing production and availability of inexpensive high-calorie foods, coupled with the move from an agrarian society to a more sedentary working environment resulted in a steady rise in BMI over the 20th century, with an obesity prevalence of 15 percent in the United States by 1970.[1] Over the subsequent decades, obesity has exploded in incidence and impact: Today, 70% of the US adult population is overweight (BMI >25kg/m^2) and 37.7% is obese.[1]

This obesity epidemic has far-reaching consequences in health, medical care and economics. Obese individuals are more likely to develop chronic diseases like diabetes, cardiovascular disease and cancer; indeed, obese individuals have a shorter life expectancy and incur $2741 higher annual healthcare costs than normal-weight individuals.[2] On the societal level, obesity-related illnesses account for 20.6% of all US national health expenditures.[2]

Any change in adipose mass must reflect an imbalance between the intake (by feeding) and expenditure (on a combination of overall metabolic rate and voluntary locomotion) of energy.[3] Individuals (even if weight-stable and within the normal BMI range) differ in basal metabolic rate, exercise, and average daily food consumption;

furthermore, for each individual, each of these parameters also varies on a daily basis. Despite these differences, most people maintain relatively stable body weight and adiposity over the long term as a consequence of homeostatic systems that serve to counter fluctuations in energy consumption and expenditure. When energy stores (i.e., adipose mass) decrease, hunger increases and energy expenditure decreases due to the activation of an anabolic system that tends to increase energy stores to previous levels. This anabolic pathway works in opposition to a catabolic pathway that decreases hunger and augments energy utilization in response to increased energy stores. Together, these two pathways compose a homeostatic system that opposes energy surpluses or deficits, thus maintaining stable body energy (adipose) stores over the long term.[3]

While the control of energy expenditure is tightly coupled to adiposity in most instances, food intake more commonly becomes uncoupled from its appropriate control by energy stores. Thus, although individuals with very low adiposity due to anorexia nervosa demonstrate appropriately decreased energy expenditure compared to normal-weight people, they restrain food intake and resist gaining weight into the normal range.[4] More commonly, most obese individuals demonstrate increased basal metabolic rate compared to lean controls, but fail to suppress food intake to restore energy stores to within the normal range.[3] Indeed, even modest weight loss in obese individuals (to adiposity levels well above the norm) promotes the anabolic response (increasing hunger and decreasing energy expenditure) in a manner similar to that observed with weight loss in normal weight subjects.[5] Hence, this response opposes the maintenance of decreased body weight over the long term, and most obese individuals

who lose weight by dieting and exercise tend to regain the weight within a relatively short time, as recently highlighted for former contestants on *The Biggest Loser* television show.[6]

Thus, we require therapies that can countermand the anabolic response to weight loss to help patients lose weight and sustain weight loss. The development of such drugs will likely require an understanding of the systems that control energy balance and how they may be dysregulated in obesity.

II. MONOGENIC OBESITY SYNDROMES REVEAL CRUCIAL PLAYERS IN ENERGY BALANCE

Over the past 25 years, the elucidation of the molecular basis for some monogenic obesity syndromes in both human patients and rodent models has begun to define the systems that control energy homeostasis.[7] These findings have generally revealed the importance of specialized central nervous system (CNS) neurons for the control of food intake, energy expenditure, and overall body energy balance. Importantly, the finding that similar genetic systems mediate energy homeostasis in humans and rodents reveals the conservation of these systems across mammals and suggests the utility of rodent models for understanding the human systems that participate in the control of feeding.

A. The Melanocortin System.

The elucidation of the molecular basis for the *agouti* (A^y) autosomal dominant obesity phenotype revealed the importance of the hypothalamic melanocortin system in energy balance.[8] The *agouti* gene product, which is overexpressed throughout the

body in A^y mice, binds to and antagonizes melanocortin (MC) receptors, a class of guanine nucleotide binding protein (G protein)-coupled receptors that are activated by ligands derived from proopiomelanocortin (POMC).[8] Of the five MC receptors, MC3R and MC4R are primarily expressed in the hypothalamus, suggesting a role for these receptors in the control of body weight.[8] Indeed, mice null for MC4R demonstrate severe, early-onset, hyperphagic obesity.[9] MC3R-null mice develop late-onset obesity with a more modest 50% increase in fat mass [10]; mice null for both MC3R and MC4R are significantly heavier than mice with either mutation alone, suggesting that MC4R and MC3R each play independent roles in the regulation of energy balance.[10]

POMC-producing neurons of the hypothalamic arcuate (ARC) nucleus produce the ligand for these hypothalamic MCRs[11]; these project widely to CNS MC3R- and MC4R-containing neurons, but MC4R in the hypothalamic paraventricular nucleus (PVN) plays a particularly crucial role in the control of food intake.[11]

As in mice, humans with mutations in POMC or MC4R demonstrate severe early-onset obesity.[7] Indeed, coding mutations in *MC4R* represent the leading cause of monogenic obesity in humans: MC4R deficiency is estimated to be responsible for 5.8% of obesity in children, who display severe early-onset hyperphagic obesity, enhanced linear growth, and increased lean mass and bone mineral density.[12] The similarity of the melanocortin deficiency syndromes between humans and mice demonstrates the conserved role for this system in the control of feeding and overall energy balance.

B. Leptin plays essential roles in homeostatic systems that control energy balance.

The 1949 discovery of the autosomal recessive *obese* (*ob*) allele in mice (*ob/ob* mice are hyperphagic, obese, diabetic and sterile) revealed the existence of a gene crucial for the control of feeding, metabolism, and body weight.[13] Positional cloning of the *ob* allele in 1994 revealed the presence of a nonsense mutation in the coding region for a peptide hormone (termed, "leptin") that is secreted by adipocytes.[14] Adipocytes produce leptin in approximate proportion to their triglyceride stores; leptin thus represents a hormonal signal that circulates in proportion to body energy stores (Figure 1.1).[15]

Like *ob/ob* mice, rare humans lacking leptin due to genetic mutations display hyperphagic obesity, depressed energy expenditure and hyperinsulinemia.[16] Exogenous leptin decreases food intake, increases energy expenditure, and normalizes body weight in leptin-deficiency.[16]

The diabetic (*db/db*) mouse, which is phenotypically similar to the *ob/ob* mouse but arises from a different genetic locus is due to a splicing mutation that truncates the long isoform of the leptin receptor (LepRb).[17] LepRb is most highly expressed in hypothalamic nuclei known to be important for the control of feeding and energy expenditure (Figure 1.1).[18]

The hyperphagia and low energy expenditure exhibited by *ob/ob* and *db/db* mice, together with the ability of exogenous leptin to ameliorate these defects in *ob/ob* mice, suggest the importance of leptin as a regulator of energy balance.[18] Leptin and LepRb-deficient animal models and humans display other defects (high glucocorticoid levels, hypothalamic infertility, and decreased growth, thyroid, and immune function) that speak to the deeper physiologic function of leptin, however.[18,19] Indeed, deficiency in leptin

action mimics the response to starvation, suggesting that the withdrawal of leptin action plays a crucial role in the anabolic response to decreased fat stores.[19] Consistently, exogenous leptin not only ameliorates these defects in leptin deficiency, but also blunts these responses to nutritional deficiency in humans and rodent models.[19] Furthermore, exogenous leptin blunts many of the metabolic and neuroendocrine defects (hunger, high lipids, diabetes, and infertility) in humans and mice with lipodystrophy syndromes (which cause low body fat and thus very low leptin).[20] Thus, leptin plays a crucial role in modulating the pathways that maintain energy homeostasis, and low leptin represents a powerful signal to promote the anabolic response to negative energy balance .[19]

C. **Molecular and neural mediators of leptin action.**

LepRb is a type I cytokine receptor, which signals via an associated tyrosine kinase, Janus kinase 2 (JAK2).[18,21] Leptin binding to LepRb activates JAK2, which phosphorylates three conserved tyrosine residues (Tyr_{985}, Tyr_{1077}, and Tyr_{1138}) on the LepRb intracellular domain (Figure 1.2).[21] When phosphorylated, each of these tyrosine residues recruits distinct downstream signaling proteins: Tyr_{985} binds to SHP2 and SOCS3 to mediate ERK signaling and feedback inhibition of LepRb signaling, respectively.[21] Tyr_{1077} recruits the signal transducer and activator of transcription (STAT) 5, while Tyr_{1138} recruits STAT3; these STAT proteins represent latent transcription factors that become tyrosine phosphorylated upon their recruitment to the receptor, permitting their nuclear translocation and modulation of gene expression.[21]

Not only does the tyrosine phosphorylation of STAT3 (pSTAT3) during leptin action provide a convenient and sensitive histochemical marker for the activation of LepRb, but STAT3 plays a crucial role in leptin action: Mice mutated for Tyr_{1138} or

lacking STAT3 in LepRb neurons display a dramatic hyperphagic obese phenotype[22,23]; this phenotype is not identical to that of *ob/ob* or *db/db* mice, however, suggesting that additional physiologically-important leptin/LepRb signals must exist. Mutational analysis reveals that Tyr_{985} and Tyr_{1077} (and their binding partners) do not mediate such a signal, however, suggesting that there must exist another signal, independent of LepRb tyrosine phosphorylation, by which LepRb controls energy balance.[24] Leptin also controls phosphatidylinositol 3'-kinase (PI 3-kinase), and it is possible that the currently undefined LepRb moiety that recruits the putative SH2B-insulin receptor substrate-PI 3-kinase pathway could represent the missing LepRb signal.[25]

Most leptin-responsive (i.e., LepRb-expressing) neurons lie in hypothalamic nuclei that have known roles in the control of energy balance, and hypothalamic LepRb is required for the control of energy homeostasis by leptin[18]; the midbrain and hindbrain also contain some substantial populations of LepRb neurons, however (Figure 1.3). Of the populations of LepRb neurons, those of the ARC (which lies adjacent to the median eminence (ME), a circumventricular organ with fenestrated capillaries that permit the passage of circulating factors, like leptin) are best known. Many ARC LepRb neurons express the MC precursor, POMC.[11] Others express agouti-related protein (AgRP), the endogenous antagonist to CNS MCRs, along with the inhibitory neuropeptide Y (NPY) and the inhibitory neurotransmitter GABA.[26] POMC neurons decrease food intake and increase energy expenditure, while the so-called "NAG" (NPY, AgRP and GABA) neurons act oppositely.[18] Not surprisingly, leptin plays crucial roles in modulating the function of POMC and NAG neurons, increasing the activity of POMC neurons and the expression of *Pomc*, while inhibiting NAG cells and their expression of *Agrp* and other

orexigenic peptides (e.g., neuropeptide Y (NPY)).[18] Interestingly, however, deletion of LepRb from POMC and/or NAG neurons only modestly alters food intake and body weight,[27] and leptin mediates a substantial component of its control on POMC and NAG neurons indirectly, including via non-POMC/non-NAG LepRb neurons elsewhere in the hypothalamus.[28–30] Furthermore, recent single-cell sequencing analysis of ARC cells reveals the existence of additional, non-POMC, non-NAG ARC LepRb neurons of unknown functional relevance.[26]

III. Common obesity and the notion of leptin resistance

In contrast to the monogenetic rodent models of obesity, above, most obesity in humans does not result from a single genetic lesion, but rather appears to represent a common response to the availability of inexpensive, plentiful, tasty calories and the sedentary nature of modern society.[1] Furthermore, most obese humans, as well as "diet-induced obese" (DIO) rodents made obese by the provision of palatable, high-calorie diet (HCD), exhibit high circulating leptin concentrations, commensurate with their elevated adiposity.[15] This observation, coupled with the failure of treatment with exogenous leptin to decrease food intake and provoke weight loss in obese humans and DIO animals,[31] has led to the promulgation of the notion of "leptin resistance" (Figure 1.4). Classical hormone resistance syndromes result from impaired receptor signaling stemming from genetic lesions, circulating antagonists (e.g., anti-receptor antibodies), or uncoupling of the receptor from its intracellular signaling system (as in the case of most insulin resistance, which also accompanies obesity).[32] Since there is no evidence for genetic lesions or circulating antagonists in DIO animals or most obese

humans, any failure of leptin signaling presumably derives from the uncoupling of LepRb from its intracellular signaling mediators (as in insulin resistance).

Due to the relatively low expression of LepRb on relatively few neurons, the detection and quantification of most LepRb signals *in vivo* remains problematic. The detection of pSTAT3 represents a notable exception to this rule; most, if not all, hypothalamic pSTAT3 results from direct leptin action via LepRb.[21] Thus, given the importance of STAT3 signaling to leptin action and the relatively facile detection of leptin-stimulated pSTAT3 *in vivo*, most studies treat pSTAT3 detection as tantamount to the detection of LepRb intracellular signaling. Importantly, high-dose exogenous leptin not only fails to decrease food intake and body weight in obese humans and DIO animals,[31] but also poorly increases hypothalamic pSTAT3,[33] potentially consistent with an uncoupling of LepRb from its intracellular signaling cascade in common obesity.

Since pSTAT3 may be detected immunohistochemically, as well as by immunoblot, it is possible to examine the detailed anatomic distribution of leptin-stimulated pSTAT3 throughout the hypothalamus. Studies in lean mice reveal that exogenous leptin stimulates pSTAT3 in the ARC before it does in deeper CNS structures. The pSTAT3 response to exogenous leptin in DIO animals is most impaired in the ARC.[33] Hence, many consider the ARC to be the major site affected by leptin resistance.

A. Negative regulators of leptin/LepRb signaling

Many potential mechanisms have been proposed to explain the limited response to exogenous leptin during obesity, including cellular signaling pathways that inhibit

LepRb signaling (Figure 1.2). During leptin/LepRb signaling, pSTAT3 translocates into the nucleus to modulate the expression of target genes, including the suppressor of cytokine signaling 3 (*Socs3*).[34,35] SOCS3 binds to JAK2 and to phosphorylated Tyr_{985} on LepRb, thereby inhibiting JAK2 activity and LepRb signaling.[36] Consequently, mice mutated for LepRb Tyr_{985} or ablated for *Socs3* in the brain exhibit increased leptin-stimulated pSTAT3 and anorectic signaling by leptin, resulting in a mildly lean phenotype in chow-fed mice.[37,38] While mutation of LepRb Tyr_{985} or CNS ablation of *Socs3* tends to decrease body weight, these animals still gain substantial weight on high-fat diet. Furthermore, for reasons that are unclear, overexpression of *Socs3* in LepRb neurons results in a lean phenotype.[39] Thus, while *Socs3* limits the maximum amplitude of leptin action and interference with *Socs3* function decreases body weight, increased *Socs3* expression cannot explain leptin resistance.

The action of protein tyrosine phosphatases (PTPases) also limits leptin signaling by dephosphorylating LepRb, JAK2, and STAT3.[40] In particular, PTP1B dephosphorylates and deactivates JAK2 to suppress leptin/LepRb signaling *in vitro,* and mice null for *Ptpn1* (which encodes PTP1B) exhibit exaggerated responsiveness to leptin.[40] Furthermore, as for *Socs3*, HCD increases the expression of *Ptpn1* in the ARC, suggesting that PTP1B might play a role in the leptin resistance observed in DIO.[41] Indeed, mice lacking *Ptpn1* in the brain, like whole-body null animals, are lean and gain less weight than controls on high-fat diet (HFD).[42] These mice still gain a substantial amount of weight on HFD,[42] however, suggesting that increased PTP1B expression alone is unlikely to explain DIO and leptin resistance.

In addition to PTP1B, the tyrosine phosphatase, TCPTP, which directly dephosphorylates STAT3, contributes to the attenuation of LepRb signaling. Furthermore, obesity and elevated leptin increase the expression of *Ptpn2* (which encodes TCPTP), and the deletion of neuronal *Ptpn2* decreases body weight, increases leptin sensitivity, and blunts weight gain in DIO animals.[43] Moreover, the combined deletion of *Ptpn1* and *Ptpn2* in the brain augments leanness and further attenuates weight gain in DIO mice.[43] However, these mice still gain a substantial amount of weight on high-calorie diet.[43]

The finding that high-calorie diet increases body weight and adiposity in mice lacking *Socs3* or *Ptpn1* and *Ptpn2* in the brain suggest that none of these mediators of LepRb signal attenuation suffice to explain leptin resistance.[38,42,43] Furthermore, leptin itself promotes the expression of *Socs3* and *Ptpn2*,[21,43] suggesting that the increased expression of these genes in obese animals reflects an increase in LepRb signaling (presumably in response to the increased circulating leptin that accompanies increased adiposity), rather than any reduction in LepRb signaling. Thus, while the action of these LepRb signaling inhibitors may limit the maximal signaling response to high levels of leptin, they cannot diminish the LepRb signaling response to elevated endogenous leptin in DIO to below the level of signaling observed in response to endogenous leptin in lean mice. Hence, it is difficult to propose that these attenuators of LepRb signaling cause obesity by decreasing overall leptin action; they may limit the ability of elevated leptin to reduce adiposity in obese mice, however, by attenuating the increase in LepRb signaling that would otherwise be observed in response to elevated leptin levels in the absence of these signal attenuators.

IV. Other processes that may interfere with leptin action and/or energy balance

In addition to the systems that directly inhibit LepRb signaling, a variety of hypothalamic responses to high-fat feeding/DIO have been proposed to limit leptin/LepRb action. These include hypothalamic inflammation (including the activation of "proinflammatory" cellular signaling pathways and the production of cytokines), inflammatory-appearing alterations in glia surrounding ARC LepRb neurons, and alterations of endoplasmic reticulum (ER) and/or oxidative stress in LepRb neurons.

A. Hypothalamic inflammation

DIO is associated with a state of low grade inflammation (so-called "metabolic inflammation") in peripheral tissues (such as adipose tissue), including the production and secretion of pro-inflammatory cytokines, such as tumor necrosis factor alpha (TNFa) and interferons (IFNs), and by the recruitment and activation of immune cells including macrophages and various subtypes of T cells.[44] It makes teleologic sense that this metabolic inflammation might cause insulin resistance, since pathological inflammatory insults (such as infection) interfere with insulin action, and a variety of data support the notion that inflammatory cytokines and cellular signals associated with inflammation play roles in metabolic dysfunction in obesity.[44]

As in peripheral tissues, exposure to high-calorie diet and the onset of positive energy balance promotes the expression of inflammatory cytokines in the hypothalamus.[45] DIO has also been reported to activate intracellular signaling cascades associated with inflammation within the hypothalamus, including the NFkB pathway (which promotes cytokine expression), c-Jun Kinases (JNKs) and protein kinase C theta (PKCθ).[46,47]

Thus, DIO-associated hypothalamic inflammatory signaling might play a role in promoting positive energy balance and/or attenuating leptin action (much as it is proposed to promote peripheral insulin resistance). Indeed, intracerebroventricular (ICV) TNF-alpha promotes food intake, decreases energy expenditure and increases body weight.[48] Furthermore, anti-TNF-alpha antibody treatment reduces weight gain during HFD feeding and mice without TNFR1 are resistant to DIO.[49] Also, viral approaches that block NFkB signaling throughout the hypothalamus reduce food intake and body weight.[46] Similarly, deletion of JNK throughout the brain blunts DIO, while the constitutive activation of JNK in NAG neurons results in hyperphagic obesity.[50,51] And, ARC-specific knockdown of PKCθ attenuates DIO.[47]

In contrast, however, the genetic activation of NFkB in hypothalamic neurons in mice does not increase hypothalamic cytokine levels, and mice null for IKKb in the arcuate nucleus (the inhibitor of NFkB signaling) are not obese or hyperphagic.[52,53] Thus, while the complete ablation of the NFkB pathway in the hypothalamus produces weight loss, the activation of this pathway is not sufficient to promote obesity.

Further confusing the picture of how inflammatory hypothalamic signals impact energy balance is the role many cytokines (e.g., IL-4, IL-6) play in the brain to reduce food intake.[54,55] Moreover, genetic and pharmacological interventions that block various inflammatory cytokine signals and proinflammatory signals result in increased susceptibility to DIO.[56] Indeed, systemic inflammation (e.g., infection or cancer) promotes cachexia, a state of negative energy balance characterized by decreased feeding and increased energy expenditure.[57]

Thus, strong inflammatory stimuli in the hypothalamus can decrease food intake, increase energy expenditure, and decrease body weight. Conversely, manipulations of some cytokines and/or cellular signaling pathways involved in the response to inflammation suggest an anabolic role for such pathways. Multiple mechanisms could underlie this apparent contradiction—including that milder inflammatory stimuli (associated with chronic, low-grade cytokine production and inflammatory signaling pathway activation) could act oppositely to stronger signals. It is also possible that certain cytokines or signaling pathways promote anabolic responses, while others promote catabolic responses. However, many cytokines can be both proinflammatory and anti-inflammatory depending on the source, target and other aspects of the immune response.[58] It is then perhaps unsurprising that work studying different cytokines, concentrations, sources, targets, and backgrounds have resulted in inconsistent findings.

Also, cytokines in the CNS regularly participate in normal physiological processes that regulate energy balance.[59] Similarly, it is possible that some manipulations of the various signaling pathways that are activated by inflammatory stimuli (e.g., NFkB, JNKs, PKCθ) interfere with the roles that these signals play in normal cellular physiology at baseline, rather than in the response to inflammation. Additionally, many of the manipulations undertaken to examine the function of inflammatory signals within the hypothalamus do not target particular cell types, but rather affect multiple types of neurons, and in some cases non-neuronal cells (e.g., glia). Going forward, it will be important to learn more about cell-type specific roles for

each cytokine and signaling pathway that may participate in the hypothalamic control of energy balance.

B. Hypothalamic gliosis

In addition to the observed induction of cytokine expression in the hypothalamus with DIO, the onset of obesity also increases the number and histologic activation state of microglia (the resident macrophage-like cells of the brain) in the ARC.[45,60] While it is possible that these microglia represent the source of the increased cytokine expression observed in the hypothalamus of DIO animals: the proliferation and histological activation of ARC microglia with DIO requires the production of fractalkine (CXCL1) by neurons.[61] It is not clear whether neurons produce the other cytokines that have been observed in DIO hypothalami, as well.

Increased numbers of activated-appearing astrocytes (increased size and reactive morphology) in the ARC accompany the microgliosis observed in DIO (Figure 1.4); these glial changes are observed in humans, as well as rodents.[45,53] The microgliosis and astrocytosis observed in the ARC of DIO animals might play a role in hypothalamic inflammation or otherwise limit the function of hypothalamic neurons involved in energy balance (e.g., LepRb neurons). Alternative interpretations exist, however: Microglia play important physiologic roles in remodeling neurological circuits/synaptic pruning and otherwise modulating neurons.[62] Similarly, reactive astrocytes play key roles in maintaining synaptic plasticity and supplying neurons with nutrients.[63] Thus, the gliosis observed in DIO could mediate changes in synaptic function and plasticity during DIO (and/or with chronic leptin administration), and could reflect a homeostatic response, rather than a pathophysiologic process. Indeed, while

the macrophage and immune cell infiltration into adipose tissue in obese animals were initially hypothesized to represent a pathophysiologic process tied to insulin resistance, a variety of data now suggest the importance of these cells for adipocyte remodeling to maintain metabolic homeostasis during positive energy balance.[64]

C. Endoplasmic reticulum stress

Concomitant with the increased cytokine production, activation of inflammatory signals, and immune infiltration observed in adipose and other peripheral tissues in DIO mice, endoplasmic reticulum (ER) stress is also increased in these tissues. Similarly, a variety of observations suggest that hypothalamic neurons experience ER stress during DIO.[65] ER stress occurs when protein or lipid synthesis in the ER outstrips the ability of the organelle to complete the processing and export of fully functional molecules. This can occur due to environmental (e.g., heat, infection) or other alterations associated with increased misfolding of proteins, or due to elevated rates of synthesis that augment demand on the ER. The misfolding of proteins in the ER activates the unfolded protein response (UPR) by activating IRE1 and the IRE1-dependent transcription factor, X-box binding protein 1 (XBP1); these limit protein synthesis and increase the expression of proteins (such as heat shock proteins) that enhance the protein folding capacity of the ER.[66] The failure of cells to mitigate ER stress effectively can impair cellular function and even induce apoptosis.[66,67]

Consistent with a potential role for hypothalamic ER stress in obesity, pharmacologic induction of ER stress in the brain promotes obesity, and mice that lack XBP1 in nestin+ neurons experience increased neuronal ER stress, dramatic hyperleptinemia and weight gain.[65] Conversely, treatment with chemical chaperones

that decrease ER stress or constitutive expression of XBP1 in POMC neurons protects against DIO.[65,68] Furthermore, two compounds identified in a transcriptional screen to discover molecules that diminish ER stress decrease feeding and promote weight loss in DIO animals.[69,70] Thus, a variety of data are consistent with the notion that decreasing ER stress in the hypothalamus promotes the activity of the catabolic arm of the energy balance system, potentially by augmenting leptin action.

D. Potential roles for reactive oxygen species in energy balance

Given the immense energetic needs of neurons for maintaining membrane potential and supporting neurotransmitter synthesis and release (the brain accounts for 2% of body weight but uses 20% of the oxygen and calories consumed by the body), it is not surprising that neurons contain a large number of mitochondria and that their status plays a crucial role in neuronal function. The increased mitochondrial activity that accompanies increased neuronal activity not only produces ATP, but also increases the production of reactive oxygen species (ROS). In addition to hypothetical roles for ROS-induced oxidative stress in the activation of inflammatory pathways and/or gliosis, a variety of data suggest important regulatory roles for ROS in circuits that control energy balance.[71] ROS promotes the activity of POMC neurons, while decreasing the activity of NAG neurons.[71,72] Importantly, ARC ROS production may be diminished by the increased number of peroxisomes in POMC and NAG neurons during DIO, potentially limiting the activity of POMC cells and augmenting the activity of NAG neurons.[72]

V. What underlies the observed changes in hypothalamic function in obese animals?

Processes that are altered in the hypothalamus (especially the ARC) during DIO include the production of inhibitors (SOCS3, PTP1B, TCPTP) relatively selective for LepRb signaling, the activation of signaling pathways associated with inflammatory stimuli (e.g., NFkB) and the production of pro-inflammatory cytokines (such as TNFa). ARC gliosis (microglia and astrocytes) and ER stress are also observed, along with peroxisome proliferation and the decreased production of ROS. What process or processes might underlie these changes?

One mechanism that has received a great deal of attention is the influx of lipids, especially those that contain saturated fatty acids (SFAs) during HFD feeding. SFAs have been shown to increase inflammatory signaling pathways and increase cytokine production, as well as activate JNKs and PKCθ.[47,60,73–75] In contrast, however, unsaturated fatty acids lower inflammation.[60,76] Moreover, while free fatty acid levels do rise in obesity, they are more elevated after fasting, which sensitizes the hypothalamus to exogenous leptin.[15,19] Furthermore, brain-specific deletion of lipoprotein lipase decreases FA uptake into the brain and increases food intake and body weight, consistent with the notion that FAs in the brain mediate anorectic signaling.[77]

Some studies also suggest a potential role for the gut microbiome, which is altered by HFD and obesity, in the genesis and/or maintenance of obesity.[78] It is theoretically possible that the amount or type of circulating endotoxin might be elevated during HFD feeding and/or obesity, and that this could augment inflammatory signaling and cytokine production systemically and in the hypothalamus. To date, the observed changes in food intake and body weight with manipulations of the microbiome have been small, however.[79]

Hyperleptinemia and endogenous leptin signaling

With the exception of rare cases of leptin deficiency, obese patients and most animal models of obesity exhibit appropriately elevated circulating leptin for their adipose mass.[15] Their failure to mount a catabolic response to this elevated endogenous leptin represents one line of evidence in favor of leptin resistance.[15] Treatment of DIO mice with a leptin/LepRb antagonist increases food intake and body weight, demonstrating that leptin action continues to restrain food intake and body weight in obesity, however.[80] Furthermore, DIO animals and most models of obesity (except for animals mutant for leptin, LepRb, or STAT3) actually exhibit elevated pSTAT3 at baseline (especially in the ARC), [33] suggesting that LepRb→STAT3 signaling is augmented as expected in response to the increased endogenous leptin (Figure 1.4). Thus, endogenous leptin appropriately accesses hypothalamic LepRb and activates pSTAT3 in obesity, suggesting that obesity does not result from decreased leptin/LepRb signaling. (Note that this also argues against a causative role for defective leptin transport in obesity). Thus, obesity occurs not because of decreased leptin/LepRb signaling, but rather in spite of increased leptin/LepRb signaling.

It is therefore possible that increased leptin/LepRb signaling could underlie some of the hypothalamic changes associated with obesity. For instance, leptin is a cytokine of the IL-6 superfamily (and LepRb is a member of the IL-6R superfamily), and leptin increases inflammatory immune function (Figure 1.1).[21,81] Hence, increased leptin/LepRb signaling in the hypothalamus might promote local cytokine production, secondarily increasing inflammatory signaling pathways in local cells. Such a mechanism could also potentially underlie the ARC gliosis that is observed in obesity.

Since most data suggest that LepRb is not expressed by microglia and astrocytes,[82] this would imply that leptin-induced changes in LepRb neurons would elaborate signals to neighboring glia. Consistent with this notion, the proliferation and histological activation of ARC microglia with DIO requires the production of fractalkine (CXCL1) by non-microglial cells.[61]

Similarly, increased leptin/LepRb signaling could augment hypothalamic ER stress in obesity as the result of increased demand for the production of anorexigenic peptides (e.g., by POMC neurons and/or other LepRb-expressing cells).[83,84] Indeed, fasting (which increases the production of AgRP and NPY and augments the activity of NAG neurons) produces a cell-autonomous transcriptional signature consistent with ER stress in these cells.[85]

Thus, while this hypothesis requires extensive testing, many of the hypothalamic perturbations observed in DIO are consistent with the theoretical consequences of increased LepRb signaling due to elevated leptin levels. If this is the case, how, then do we explain the modest anorectic and pSTAT3 responses to exogenous leptin in DIO and other obese models, and how do we explain the persistence of obesity in the face of hyperleptinemia?

In addition to the changes (inflammatory cytokines/signals, gliosis, ER stress, etc.) noted above, leptin/LepRb signaling increases the expression of *Socs3* and *Ptpn2*, which increase feedback inhibition on LepRb; PTP1B is also reportedly increased with DIO. These inhibitors (potentially in concert with other processes), while unable to decrease the amplitude of LepRb signaling to levels lower than those observed in lean

animals with normal leptin levels, could nonetheless limit the maximal amplitude of leptin signaling so that further increases in pSTAT3 and leptin-mediated anorexia are effectively blunted.

This model thus proposes that elevated leptin limits the magnitude of the signaling and catabolic responses to further increases in leptin concentrations. Indeed, Knight et al. demonstrated that DIO mice whose leptin levels were clamped to those observed in lean animals responded normally to exogenous leptin- exhibiting both an appropriately robust acute induction of pSTAT3 and decreased food intake and body weight, consistent with the notion that chronically elevated leptin concentrations and consequent LepRb signaling, rather than obesity *per se*, limit further increases in the amplitude of LepRb signaling and action.[84] This finding also highlights an important limitation of many publications that propose "leptin resistance" as a mechanism by which a manipulated pathway promotes obesity- the analysis of leptin responsiveness is often carried out in obese (hyperleptinemic) animals. Rather, this analysis must be carried out in pre-obese animals with demonstrably normal leptin levels to understand whether the pathway in question directly alters LepRb signaling, rather than promoting obesity and secondary leptin insensitivity.

Putting aside for a moment the limited response to pharmacologic levels of leptin in obesity,[31] the problem remains as to why obesity occurs in the face not only of increased endogenous leptin, but also in the face of increased baseline LepRb signaling.[33,80] Explanations include the potential inability to sufficiently increase LepRb signaling to promote long-term catabolic signaling.[33] If this were true, we would predict that it should be possible to reverse obesity with sufficient elevations in LepRb

signaling. A thoughtful and thought-provoking recent perspective argued persuasively in favor of this notion, and suggested that we have not sufficiently tested this possibility (especially in humans).[86] Testing this will be difficult, however, since it presumably requires promoting LepRb signaling without increasing the activity of feedback inhibitors (or other potential leptin-stimulated processes that limit leptin action).

It is also possible that maximal LepRb signaling cannot mediate a sufficiently strong signal to the correct neurons to counteract the augmentation of feeding by palatable, high-calorie foods. Indeed, leptin/LepRb signaling promotes changes in neuronal gene expression more powerfully than it activates (or inactivates) neurons. Thus, this theory would predict that stronger activators of specific LepRb-regulated pathways might reverse obesity. Furthermore, many of the currently-available CNS-acting molecules that produce weight loss (e.g., agonists of the GLP1 receptor, the amylin receptor, and the serotonin 2c receptor) tend to directly activate neurons or circuits that overlap with those controlled by LepRb.[87–89]

Note that it is also possible (even likely) that mechanisms that limit maximal leptin action and the relatively modest modulation of neuronal function by leptin both contribute. The existence of mechanisms to limit the catabolic function makes evolutionary sense. While there was selective pressure during evolutionary times to permit adipose accrual when food was plentiful (to permit survival during periods of caloric insufficiency), there was likely little to no selective pressure for leptin (or other signals) to strongly limit food intake and body weight, since there was not enough palatable, high-calorie, readily available food in the environment to promote obesity. Hence, because death by famine was a much more likely event than an obesity-related

demise, limiting the amplitude of LepRb signaling and the potential anorectic potency of leptin likely provided a long-term survival benefit.

VI. Summary and conclusions

The ongoing worldwide epidemic of obesity represents a serious threat to human health and economic productivity; current obesity therapies are inadequate and new medicines are required to combat this disease. Identifying such therapies will require a detailed understanding of the mechanisms that maintain adipose stores relatively constant over the long term, and how these may be dysregulated to permit the establishment and maintenance of elevated adiposity. Leptin, which is produced by adipose tissue in approximate proportion to triglyceride stores, controls the major hypothalamic systems that modulate food intake and energy expenditure and plays an important role in maintaining constant energy stores; low leptin augments food intake and suppresses energy expenditure, both of which tend to restore depleted energy stores. Conversely, adequate leptin suppresses feeding and normalizes energy expenditure.

Because obesity is defined by elevated adipose mass, leptin concentrations are increased in obesity. The failure of this high endogenous leptin (and even exogenous leptin) to normalize body weight in obese individuals has suggested the possibility of leptin resistance in obesity, spurring a great deal of research aimed at understanding this failure. A number of potential mechanisms that limit leptin/LepRb signaling in obesity (e.g., obesity-induced inhibitors of the LepRb signaling pathway, the activation of inflammatory signaling pathways and cytokines or ER stress in the hypothalamus, hypothalamic gliosis) have been suggested to impair LepRb signaling in obesity, and

thus permit positive energy balance. Proposed stimuli for these processes include the inundation of the hypothalamus with SFAs and/or low levels of endotoxin during obesity, but more compelling evidence exists for the notion that elevated leptin concentrations in obesity play a crucial role in limiting leptin action. Indeed, hypothalamic LepRb signaling is elevated in obesity, as would be expected given increased endogenous leptin, and increased LepRb signaling augments the expression of a variety of inhibitors of LepRb signaling; it is possible that increased LepRb signaling mediates some or all of the other changes in hypothalamic processes suggested to attenuate LepRb signaling, as well. This would imply that increased leptin/LepRb signaling limits the potential maximal amplitude of LepRb signaling, such that the strength of the leptin signal in hyperleptinemic obesity is less than it would be otherwise, and that the response to exogenous leptin would also be blunted (as is observed). Thus, important questions for future research include not only the mechanisms and relative roles for each potential process proposed to limit leptin action, but also the roles for leptin/LepRb signaling in the genesis of each process. Furthermore, it will be crucial to understand whether augmenting the leptin/LepRb signal and/or whether other means of more strongly activating leptin-regulated neural pathways can reverse obesity.

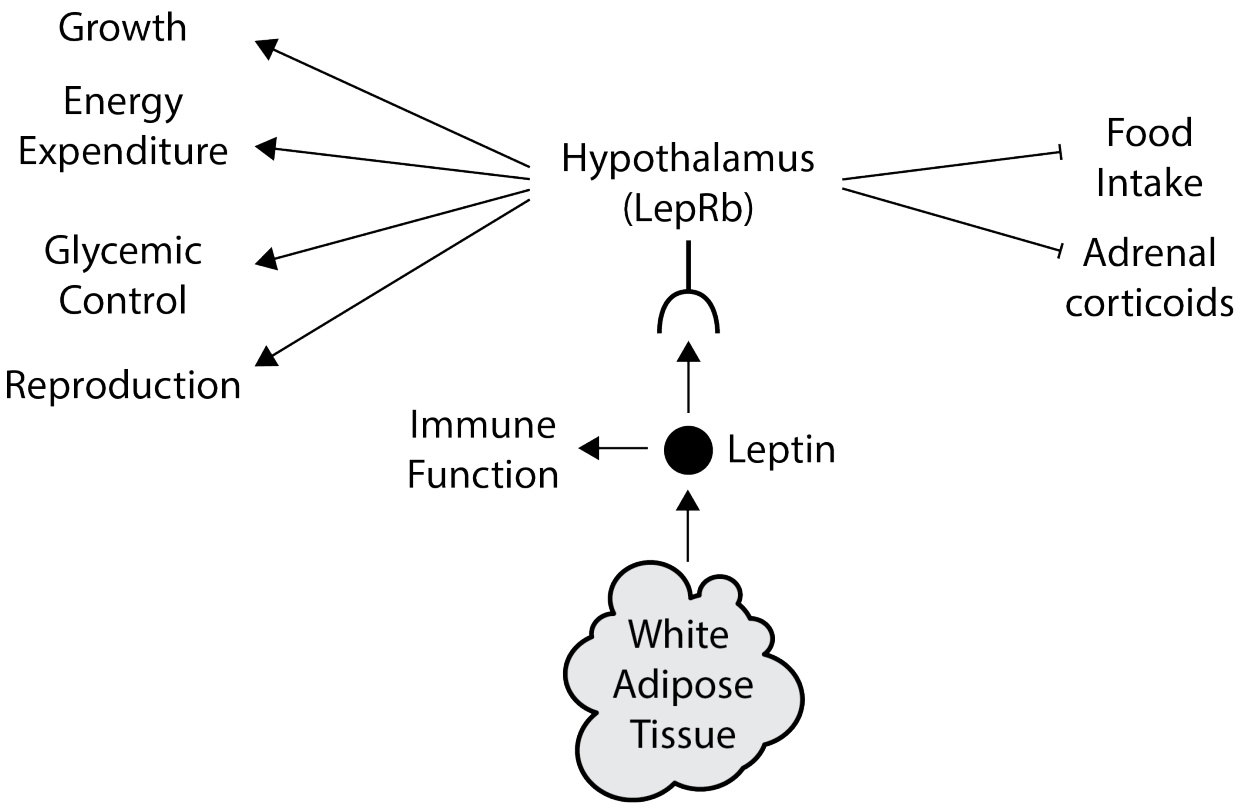

Figure 1.1: Leptin action. White adipose cells secrete leptin in approximate proportion to their triglyceride content. Leptin binds to the long form of the leptin receptor (LepRb) in the hypothalamus and brainstem to promote growth, energy expenditure, glycemic control, and reproduction. Leptin also suppresses food intake and the production of adrenal corticosteroids. Additionally, leptin permits the production and function of immune cells.

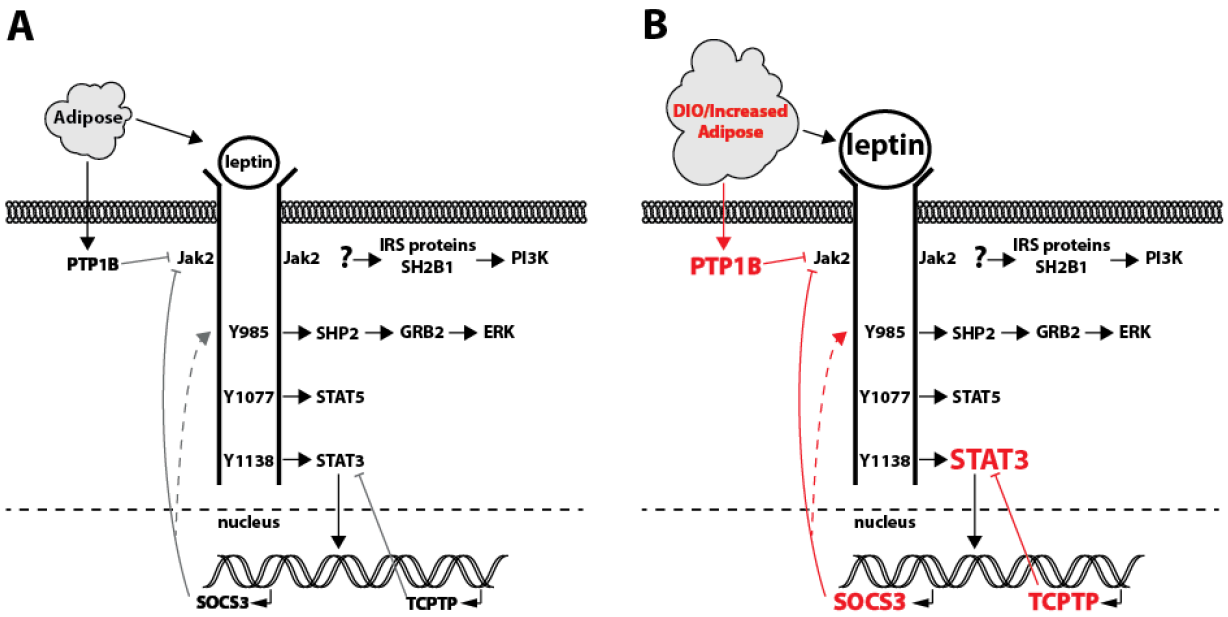

Figure 1.2: Leptin signaling and mechanisms that mediate its inhibition. **(A)** In individuals with normal body weight, circulating leptin binds to its receptor, which activates Jak2 tyrosine kinase activity, resulting in the phosphorylation of LepRb tyrosine residues Y_{985}, Y_{1077}, and Y_{1138}. Phosphorylated Y_{985} recruits and permits the phosphorylation of SHP-2, which recruits GRB2 and activates the ERK pathway in cultured cells. Phosphorylated Y_{1077} recruits STAT5, which could contribute to aspects of leptin-regulated gene expression. Phosphorylated Y_{1138} engages STAT3, resulting in its phosphorylation and translocation into the nucleus to mediate important aspects of gene expression. In addition to mediating changes in gene expression that contribute to the control of energy balance by leptin, STAT3 mediates the expression of SOCS3, which binds to phosphorylated Y_{985} and blunts leptin signaling. The tyrosine phosphatases PTP1B and TCPTP dephosphorylate Jak2 and STAT3, respectively. While LepRb→STAT3 represents a major means by which leptin regulates energy balance, leptin also recruits IRS proteins and SH2B1 by a poorly-defined mechanism. LepRb also mediates important, but not mechanistically understood, signals that operate independently of LepRb tyrosine phosphorylation. **(B)** In obesity, increased adipose mass increases leptin production and thus circulating leptin concentrations. The consequent increase in LepRb signaling promotes increased expression of SOCS3 and TCPTP; obesity also increases PTP1B expression. These mechanisms blunt the amplitude of the response to the increase in leptin.

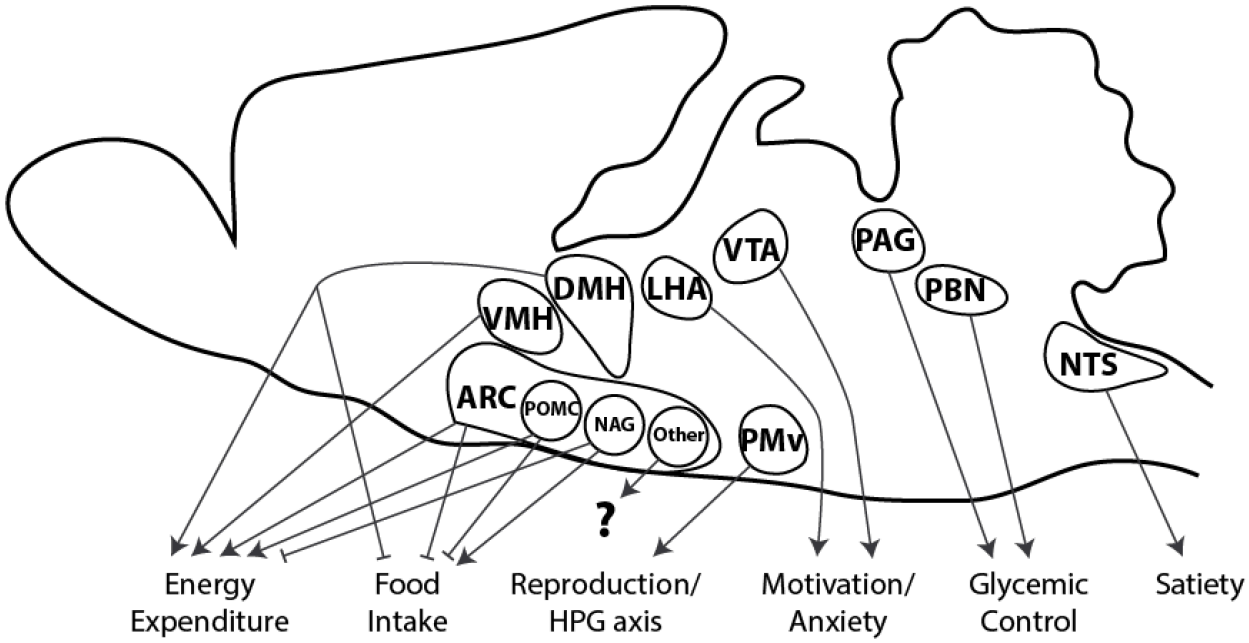

Figure 1.3: CNS leptin action. Leptin acts on its receptor in various discrete nuclei to regulate a variety of actions. Leptin promotes the function of arcuate nucleus (ARC) POMC-expressing cells to increase energy expenditure and decrease feeding, as well as attenuates the activity of oppositely-acting ARC NPY, AgRP and GABA (NAG)-containing neurons. Other (as yet molecularly undefined) ARC LepRb neurons presumably also modulate energy expenditure and food intake in response to leptin. Outside of the ARC, roles for LepRb neurons have been examined in a variety of regions. In the ventromedial hypothalamic nucleus (VMH), LepRb deletion decreases basal metabolic rate and other determinants of energy expenditure, resulting in mild obesity independently of leptin action in the ARC.[90] LepRb neurons in the large and dispersed dorsomedial hypothalamic nucleus (DMH) play roles in the control of thermogenesis and feeding,[91] and poorly-characterized subpopulations of DMH LepRb neurons play important roles in the control of POMC and NAG neurons.[29] The ventral premammilary nucleus (PMv) has been shown to be involved in the hypothalamic control of reproduction. Lateral hypothalamic area (LHA) LepRb neurons directly innervate the ventral tegmental area (VTA) to modulate the mesolimbic dopamine system and motivation; these cells play a modest role in energy balance [92]; other LepRb neurons in the VTA may play distinct roles in modulating the mesolimbic dopamine system and/or anxiety.[93] In the brainstem, leptin acts on LepRb neurons in the nucleus of the solitary tract (NTS) to modulate gastrointestinal satiety signals,[94] while LepRb neurons in the parabrachial nucleus (PBN) and nearby periaqueductal gray (PAG) modulate the sympathetic response to metabolic emergencies appropriately for the status of energy stores.[95,96]

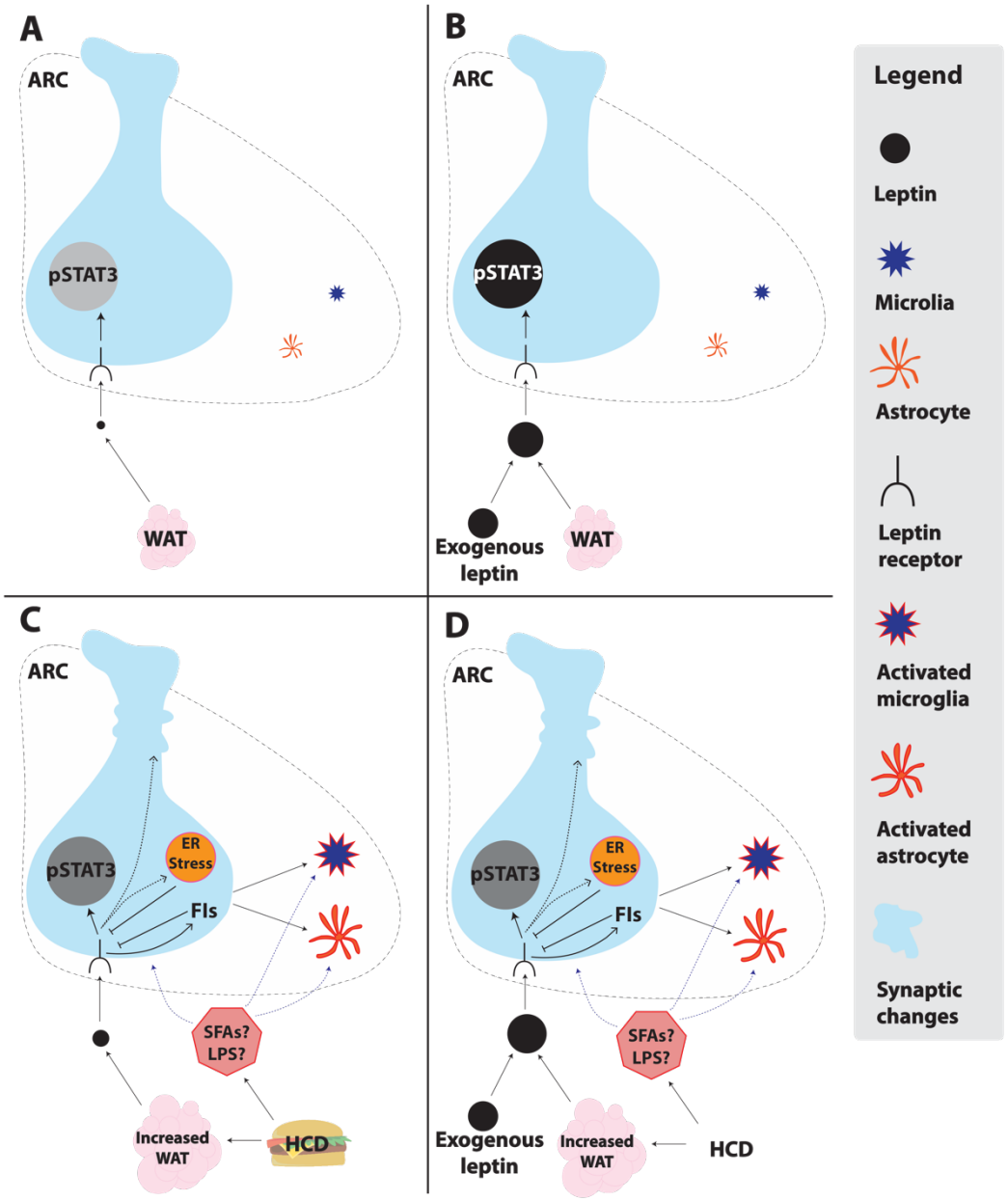

Figure 1.4: Hypothalamic leptin action and changes during DIO. In lean individuals **(A, B)**, white adipose tissue (WAT) produces leptin in proportion to triglyceride content and binds to LepRb in the arcuate nucleus (ARC) resulting in a baseline level of pSTAT3 activation and quiescent microglia and astrocytes. **(B)** Acute exogenous leptin injection adds to the endogenous leptin from WAT, augmenting LepRb→STAT3 signaling. **(C, D)** In DIO, high-calorie feeding increases WAT and leptin production; saturated fatty acids (SFAs) and circulating LPS are also hypothesized to be increased. **(C)** The increased endogenous leptin production increases baseline LepRb activation, leading to increased pSTAT3 and other changes in neuronal and function activity. This increased LepRb signaling also increases the expression of feedback inhibitors (FIs) including SOCS3 and TCPTP. DIO also increases PTP1B expression. Increased leptin action may also alter ER stress, synaptic inputs and potentially other functional

parameters in specific subsets of LepRb neurons; this could result in the activation of neighboring microglia and astrocytes. Additionally (or alternatively), SFAs, LPS, or other responses to high-calories diet may also contribute to the alterations in neuron and glia in the ARC. **(D)** The presence of feedback inhibitors or other modifiers of LepRb signaling limits the further amplification of LepRb signaling following the administration of exogenous leptin in DIO.

References:

1. Cutler DM, Glaeser EL, Shapiro JM. American Economic Association Why Have Americans Become More Obese? *Source J Econ Perspect*. 2003;17(3):93-118. doi:10.1257/089533003769204371.
2. Cawley J, Meyerhoefer C. The medical care costs of obesity: An instrumental variables approach. *J Health Econ*. 2012;31(1):219-230. doi:10.1016/j.jhealeco.2011.10.003.
3. Schwartz MW, Woods SC, Porte D, Seeley RJ, Baskin DG. Central nervous system control of food intake. *Nature*. 2000;404(6778):661-671. doi:10.1038/35007534.
4. Hebebrand J, Muller TD, Holtkamp K, Herpertz-Dahlmann B. The role of leptin in anorexia nervosa: clinical implications. *Mol Psychiatry*. 2007;12(1):23-35. doi:10.1038/sj.mp.4001909.
5. Rosenbaum M, Goldsmith R, Bloomfield D, et al. Low-dose leptin reverses skeletal muscle, autonomic, and neuroendocrine adaptations to maintenance of reduced weight. *J Clin Invest*. 2005;115(12):3579-3586. doi:10.1172/JCI25977.
6. Kolata G. Afer “The Biggest Loser,” Their Bodies Fought to Regain Weight. *New York Times*. 2016.
7. Ramachandrappa S, Farooqi IS. Genetic approaches to understanding human obesity. *J Clin Invest*. 2011;121(6):2080-2086. doi:10.1172/JCI46044.2080.
8. Fan W, Boston BA, Kesterson RA, Hruby VJ, Cone RD. Role of melanocortinergic neurons in feeding and the agouti obesity syndrome. *Nature*. 1997;385(6612):165-168. doi:10.1038/385165a0.
9. Huszar D, Lynch CA, Fairchild-Huntress V, et al. Targeted Disruption of the Melanocortin-4 Receptor Results in Obesity in Mice. *Cell*. 1997;88(1):131-141. doi:10.1016/S0092-8674(00)81865-6.
10. Chen AS, Marsh DJ, Trumbauer ME, et al. Inactivation of the mouse melanocortin-3 receptor results in increased fat mass and reduced lean body mass. *Nat Genet*. 2000;26(1):97-102. doi:10.1038/79254.
11. Mountjoy KG, Mortrud MT, Low MJ, Simerly RB, Cone RD. Localization of the melanocortin-4 receptor (MC4-R) in neuroendocrine and autonomic control circuits in the brain. *Mol Endocrinol*. 1994;8(December):1298-1308. doi:10.1210/mend.8.10.7854347.
12. Skene A, D P, Steg PG, Storey RF, Harrington RA. Clinical Spectrum of obesity and mutations in the melanocortin 4 receptor gene. *N Engl J Med*. 2003;348:1085-1095. doi:10.1056/NEJMoa1310480.
13. Harbor B. Zirkle : Introgression in Oaks OBESE , A NEW MUTATION IN THE HOUSE MOUSE *. 1949.
14. Zhang Y, Proenca R, Maffei M, Barone M, Leopold L, Friedman JM. Positional cloning of the mouse obese gene and its human homologue. *Nature*. 1994;372(6505):425-432. doi:10.1038/372425a0.
15. Frederich RC, Hamann A, Anderson S, Lollmann B, Lowell BB, Flier JS. Leptin Levels Reflect Body Lipid-Content in Mice - Evidence for Diet-Induced Resistance To Leptin Action. *Nat Med*. 1995;1(12):1311-1314. doi:10.1038/nm1295-1311.
16. Farooqi S, Jebb S, Langmack G, Lawrence E, Cheetham C, Prentice A, Hughes I, McCamish M OS. Effects of recombinant leptin therapy in a child with congenital

leptin deficiency. *N Engl J Med*. 1999:879-884.
17. Chua SC, Chung WK, Wu-peng XS, et al. Phenotypes of Mouse Diabetes and Rat Fatty Due to Mutations in the OB (Leptin) Receptor Shun-Mei Liu , Louis Tartaglia and Rudolph L . Leibel Published by : American Association for the Advancement of Science Stable URL : http://www.jstor.org/stable/289. 2016;271(5251):994-996.
18. Flak JN, Myers MG. Minireview : CNS Mechanisms of Leptin Action. 2016;30(January):3-12. doi:10.1210/me.2015-1232.
19. Ahima RS, Prabakaran D, Mantzoros C, et al. Role of leptin in the neuroendocrine response to fasting. *Nature*. 1996;382(6588):250-252. doi:10.1038/382250a0.
20. Oral EA, Simha V, Ruiz E, et al. Leptin-Replacement Therapy for Lipodystrophy. *N Engl J Med*. 2002;346(8):570-578. doi:10.1056/NEJMoa012437.
21. Allison MB, Myers MG. Connecting leptin signaling to biological function. *J Endocrinol*. 2014;223(1):T25-T35. doi:10.1530/JOE-14-0404.
22. Piper ML, Unger EK, Myers MG, Xu AW. Specific physiological roles for signal transducer and activator of transcription 3 in leptin receptor-expressing neurons. *Mol Endocrinol*. 2008;22(3):751-759. doi:10.1210/me.2007-0389.
23. Bates SH, Stearns WH, Dundon T a, et al. STAT3 signalling is required for leptin regulation of energy balance but not reproduction. *Nature*. 2003;421(6925):856-859. doi:10.1038/nature01388.
24. Jiang L, You J, Yu X, et al. Tyrosine-dependent and -independent actions of leptin receptor in control of energy balance and glucose homeostasis. *Proc Natl Acad Sci U S A*. 2008;105(47):18619-18624. doi:10.1073/pnas.0804589105.
25. Niswender KD, Morton GJ, Stearns WH, Rhodes CJ, Myers MG, Schwartz MW. Intracellular signalling. Key enzyme in leptin-induced anorexia. *Nature*. 2001;413(6858):794-795. doi:10.1038/35101657.
26. Campbell JN, Macosko EZ, Fenselau H, et al. A molecular census of arcuate hypothalamus and median eminence cell types. *Nat Neurosci*. 2017;(February). doi:10.1038/nn.4495.
27. Van De Wall E, Leshan R, Xu AW, et al. Collective and individual functions of leptin receptor modulated neurons controlling metabolism and ingestion. *Endocrinology*. 2008;149(4):1773-1785. doi:10.1210/en.2007-1132.
28. Vong L, Ye C, Yang Z, Choi B, Chua S, Lowell BB. Leptin Action on GABAergic Neurons Prevents Obesity and Reduces Inhibitory Tone to POMC Neurons. *Neuron*. 2011;71(1):142-154. doi:10.1016/j.neuron.2011.05.028.
29. Garfield AS, Shah BP, Burgess CR, et al. Dynamic GABAergic afferent modulation of AgRP neurons. *Nat Neurosci*. 2016;19(12):1628-1635. doi:10.1038/nn.4392.
30. Leshan RL, Greenwald-Yarnell M, Patterson CM, Gonzalez IE, Myers MG. Leptin action through hypothalamic nitric oxide synthase-1-expressing neurons controls energy balance. *Nat Med*. 2012;18(5):820-823. doi:10.1038/nm.2724.
31. El-Haschimi K, Pierroz DD, Hileman SM, Bjørbæk C, Flier JS. Two defects contribute to hypothalamic leptin resistance in mice with diet-induced obesity. *J Clin Invest*. 2000;105(12):1827-1832. doi:10.1172/JCI9842.
32. Jameson J. *Hormone Resistance Syndromes*. Springer Science & Business Media; 1999.

33. Münzberg H, Flier JS, Bjørbæk C. Region-specific leptin resistance within the hypothalamus of diet-induced obese mice. *Endocrinology*. 2004;145(11):4880-4889. doi:10.1210/en.2004-0726.
34. Bjørbaek C, Elmquist JK, Frantz JD, Shoelson SE, Flier JS. Identification of SOCS-3 as a potential mediator of central leptin resistance. *Mol Cell*. 1998;1(4):619-625. doi:10.1016/S1097-2765(00)80062-3.
35. Bjørbæk C, Buchholz RM, Davis SM, et al. Divergent Roles of SHP-2 in ERK Activation by Leptin Receptors. *J Biol Chem*. 2001;276(7):4747-4755. doi:10.1074/jbc.M007439200.
36. Bjørbæk C, El-Haschimi K, Frantz JD, Flier JS. The role of SOCS-3 in leptin signaling and leptin resistance. *J Biol Chem*. 1999;274(42):30059-30065. doi:10.1074/jbc.274.42.30059.
37. Bjornholm M, Munzberg H, Leshan R, et al. Mice lacking inhibitory leptin receptor signals are lean with normal endocrine function. *J Clin Invest*. 2007;117(5). doi:10.1172/JCI30688DS1.
38. Mori H, Hanada R, Hanada T, et al. Socs3 deficiency in the brain elevates leptin sensitivity and confers resistance to diet-induced obesity. *Nat Med*. 2004;10(7):739-743. doi:10.1038/nm1071.
39. Reed AS, Unger EK, Olofsson LE, Piper ML, Jr MGM, Xu AW. Functional Role of Suppressor of Cytokine Signaling 3 Long-Term Energy Homeostasis. *Diabetes*. 2010;59(April):894-906. doi:10.2337/db09-1024.A.S.R.
40. Zabolotny JM, Bence-Hanulec KK, Stricker-Krongrad A, et al. PTP1B regulates leptin signal transduction in vivo. *Dev Cell*. 2002;2(4):489-495. doi:10.1016/S1534-5807(02)00148-X.
41. White CL, Whittington A, Barnes MJ, Wang Z, Bray GA, Morrison CD. HF diets increase hypothalamic PTP1B and induce leptin resistance through both leptin-dependent and -independent mechanisms. *AJP Endocrinol Metab*. 2008;296(2):E291-E299. doi:10.1152/ajpendo.90513.2008.
42. Bence KK, Delibegovic M, Xue B, et al. Neuronal PTP1B regulates body weight, adiposity and leptin action. *Nat Med*. 2006;12(8):917-924. doi:10.1038/nm1435.
43. Loh K, Fukushima A, Zhang X, et al. Elevated hypothalamic TCPTP in obesity contributes to cellular leptin resistance. *Cell Metab*. 2011;14(5):684-699. doi:10.1016/j.cmet.2011.09.011.
44. Lumeng CN, Saltiel AR. Inflammatory links between obesity and metabolic disease. *J Clin Invest*. 2011;121(6):2111-2117. doi:10.1172/JCI57132.
45. Thaler J, Yi C, Schur E, et al. Obesity is associated with hipothalamic injury in rodents and humans. *J Clin Investig*. 2011;122(1):153. doi:10.1172/JCI59660.adjacent.
46. Zhang X, Zhang G, Zhang H, Karin M, Bai H, Cai D. Hypothalamic IKKb/NF-kB ER Stress Link Overnutrition to Energy Imbalance and Obesity. *Cell*. 2008;135(1):61-73. doi:10.1016/j.cell.2008.07.043.
47. Benoit SC, Kemp CJ, Elias CF, et al. Palmitic acid mediates hypothalamic insulin resistance by altering PKC-θ subcellular localization in rodents. *J Clin Invest*. 2009;119(9):2577-2589. doi:10.1172/JCI36714.
48. Romanatto T, Cesquini M, Amaral ME, et al. TNF-a acts in the hypothalamus inhibiting food intake and increasing the respiratory quotient-Effects on leptin and

insulin signaling pathways. *Peptides*. 2007;28(5):1050-1058. doi:10.1016/j.peptides.2007.03.006.
49. Arruda AP, Milanski M, Coope A, et al. Low-grade hypothalamic inflammation leads to defective thermogenesis, insulin resistance, and impaired insulin secretion. *Endocrinology*. 2011;152(4):1314-1326. doi:10.1210/en.2010-0659.
50. Sabio G, Cavanagh-Kyros J, Barrett T, et al. Role of the hypothalamic-pituitary-thyroid axis in metabolic regulation by JNK1. *Genes Dev*. 2010;24(3):256-264. doi:10.1101/gad.1878510.
51. Tsaousidou E, Paeger L, Belgardt BF, et al. Distinct Roles for JNK and IKK Activation in Agouti-Related Peptide Neurons in the Development of Obesity and Insulin Resistance. *Cell Rep*. 2014;9(4):1495-1506. doi:10.1016/j.celrep.2014.10.045.
52. Benzler J, Ganjam GK, Pretz D, et al. Central Inhibition of IKKb/NF-kB Signaling Attenuates High-Fat Diet–Induced Obesity and Glucose Intolerance. *Diabetes*. 2015;64(6):2015-2027. doi:10.2337/db14-0093.
53. Milanski M, Degasperi G, Coope A, et al. Saturated Fatty Acids Produce an Inflammatory Response Predominantly through the Activation of TLR4 Signaling in Hypothalamus: Implications for the Pathogenesis of Obesity. *J Neurosci*. 2009;29(2):359-370. doi:10.1523/JNEUROSCI.2760-08.2009.
54. Butti E, Bergami a, Recchia a, et al. Absence of an intrathecal immune reaction to a helper-dependent adenoviral vector delivered into the cerebrospinal fluid of non-human primates. *Gene Ther*. 2008;15(3):233-238. doi:10.1038/sj.gt.3303050.
55. Ropelle ER, Flores MB, Cintra DE, et al. IL-6 and IL-10 anti-inflammatory activity links exercise to hypothalamic insulin and leptin sensitivity through IKKβ and ER stress inhibition. *PLoS Biol*. 2010;8(8):31-32. doi:10.1371/journal.pbio.1000465.
56. Dong ZM, Gutierrez-Ramos JC, Coxon a, Mayadas TN, Wagner DD. A new class of obesity genes encodes leukocyte adhesion receptors. *Proc Natl Acad Sci U S A*. 1997;94(14):7526-7530. doi:10.1073/pnas.94.14.7526.
57. Langhans W. Signals generating anorexia during acute illness. *Proc Nutr Soc*. 2007;66(3):321-330. doi:10.1017/S0029665107005587.
58. Gadient RA, Otten UH. Interleukin-6 (IL-6) - A molecule with both beneficial and destructive potentials. *Prog Neurobiol*. 1997;52(5):379-390. doi:10.1016/S0301-0082(97)00021-X.
59. Leon LR. Cytokine regulation of fever: studies using gene knockout mice. *J Appl Physiol*. 2002;92(6):2648-2655. doi:10.1152/japplphysiol.01005.2001.
60. Valdearcos M, Robblee MM, Benjamin DI, Nomura DK, Xu AW, Koliwad SK. Microglia Dictate the Impact of Saturated Fat Consumption on Hypothalamic Inflammation and Neuronal Function. *Cell Rep*. 2014;9(6):2124-2139. doi:10.1016/j.celrep.2014.11.018.
61. Dorfman MD, Krull JE, Douglass JD, et al. Sex differences in microglial CX3CR1 signalling determine obesity susceptibility in mice. *Nat Commun*. 2017;8(May 2016):14556. doi:10.1038/ncomms14556.
62. Schafer DP, Lehrman EK, Kautzman AG, et al. Microglia Sculpt Postnatal Neural Circuits in an Activity and Complement-Dependent Manner. *Neuron*. 2012;74(4):691-705. doi:10.1016/j.neuron.2012.03.026.
63. Allen NJ. Astrocyte Regulation of Synaptic Behavior. *Annu Rev Cell Dev Biol*.

2014;30(1):439-463. doi:10.1146/annurev-cellbio-100913-013053.
64. Ye J, McGuinness OP. Inflammation during obesity is not all bad: evidence from animal and human studies. *AJP Endocrinol Metab*. 2013;304(5):E466-E477. doi:10.1152/ajpendo.00266.2012.
65. Ozcan L, Ergin AS, Lu A, et al. Endoplasmic Reticulum Stress Plays a Central Role in Development of Leptin Resistance. *Cell Metab*. 2009;9(1):35-51. doi:10.1016/j.cmet.2008.12.004.
66. Back SH, Kaufman RJ. Endoplasmic reticulum stress and type 2 diabetes. *Annu Rev Biochem*. 2012;81:767-793. doi:10.1146/annurev-biochem-072909-095555.
67. Marciniak SJ, Ron D. Endoplasmic Reticulum Stress Signaling in Disease. *Physiol Rev*. 2006;86(4):1133-1149. doi:10.1152/physrev.00015.2006.
68. Williams KW, Liu T, Kong X, et al. Xbp1s in pomc neurons connects ER stress with energy balance and glucose homeostasis. *Cell Metab*. 2014;20(3):471-482. doi:10.1016/j.cmet.2014.06.002.
69. Liu J, Lee J, Hernandez MAS, Mazitschek R, Ozcan U. Treatment of obesity with celastrol. *Cell*. 2015;161(5):999-1011. doi:10.1016/j.cell.2015.05.011.
70. Lee J, Liu J, Feng X, et al. Withaferin A is a leptin sensitizer with strong antidiabetic properties in mice. 2016;(August). doi:10.1038/nm.4145.
71. Andrews ZB, Liu Z-W, Walllingford N, et al. UCP2 mediates ghrelin's action on NPY/AgRP neurons by lowering free radicals. *Nature*. 2009;459(7247):736-736. doi:10.1038/nature08132.
72. Diano S, Liu Z-W, Jeong JK, et al. Peroxisome proliferation–associated control of reactive oxygen species sets melanocortin tone and feeding in diet-induced obesity. *Nat Med*. 2011;17(10):1320-1320. doi:10.1038/nm1011-1320a.
73. Solinas G, Vilcu C, Neels JG, et al. JNK1 in Hematopoietically Derived Cells Contributes to Diet-Induced Inflammation and Insulin Resistance without Affecting Obesity. *Cell Metab*. 2007;6(5):386-397. doi:10.1016/j.cmet.2007.09.011.
74. Nguyen MTA, Favelyukis S, Nguyen AK, et al. A subpopulation of macrophages infiltrates hypertrophic adipose tissue and is activated by free fatty acids via toll-like receptors 2 and 4 and JNK-dependent pathways. *J Biol Chem*. 2007;282(48):35279-35292. doi:10.1074/jbc.M706762200.
75. Saberi M, Woods NB, de Luca C, et al. Hematopoietic Cell-Specific Deletion of Toll-like Receptor 4 Ameliorates Hepatic and Adipose Tissue Insulin Resistance in High-Fat-Fed Mice. *Cell Metab*. 2009;10(5):419-429. doi:10.1016/j.cmet.2009.09.006.
76. Cintra DE, Ropelle ER, Moraes JC, et al. Unsaturated fatty acids revert diet-induced hypothalamic inflammation in obesity. *PLoS One*. 2012;7(1). doi:10.1371/journal.pone.0030571.
77. Wang H, Astarita G, Taussig MD, et al. Deficiency of lipoprotein lipase in neurons modifies the regulation of energy balance and leads to obesity. *Cell Metab*. 2011;13(1):105-113. doi:10.1016/j.cmet.2010.12.006.
78. Ridaura VK, Faith JJ, Rey FE, et al. Gut Microbiota from Twins Discordant for Obesity Modulate Metabolism in Mice. *Science (80-)*. 2013;341(6150):1241214-1241214. doi:10.1126/science.1241214.
79. Reijnders D, Goossens GH, Hermes GDA, et al. Effects of Gut Microbiota Manipulation by Antibiotics on Host Metabolism in Obese Humans: A

Randomized Double-Blind Placebo-Controlled Trial. *Cell Metab*. 2016;24(1):63-74. doi:10.1016/j.cmet.2016.06.016.
80. Ottaway N, Mahbod P, Alessio DAD, et al. Diet-Induced Obese Mice Retain Endogenous Leptin Short Article Diet-Induced Obese Mice Retain Endogenous Leptin Action. *Cell Metab*. 2015;21(6):1-6. doi:10.1016/j.cmet.2015.04.015.
81. Lord GM, Matarese G, Howard JK, Baker RJ, Bloom SR, Lechler RI. Leptin modulates the T-cell immune response and reverses starvation-induced immunosuppression. *Nature*. 1998;394(6696):897-901. doi:10.1038/29795.
82. Allison MB, Patterson CM, Krashes MJ, Lowell BB, Myers MG, Olson DP. TRAP-seq defines markers for novel populations of hypothalamic and brainstem LepRb neurons. *Mol Metab*. 2015;4(4):299-309. doi:10.1016/j.molmet.2015.01.012.
83. Ron D, Walter P. Signal integration in the endoplasmic reticulum unfolded protein response. *Nat Rev Mol Cell Biol*. 2007;8(7):519-529. doi:10.1038/nrm2199.
84. Knight ZA, Hannan KS, Greenberg ML, Friedman JM. Hyperleptinemia is required for the development of leptin resistance. *PLoS One*. 2010;5(6):1-8. doi:10.1371/journal.pone.0011376.
85. Henry FE, Sugino K, Tozer A, Branco T, Sternson SM. Cell type-specific transcriptomics of hypothalamic energy-sensing neuron responses to weight-loss. *Elife*. 2015;4(September 2015):1-30. doi:10.7554/eLife.09800.
86. Flier JS, Maratos-Flier E. Leptin's Physiologic Role: Does the Emperor of Energy Balance Have No Clothes? *Cell Metab*. 2017:1-3. doi:10.1016/j.cmet.2017.05.013.
87. Müller TD, Sullivan LM, Habegger K, et al. Restoration of leptin responsiveness in diet-induced obese mice using an optimized leptin analog in combination with exendin-4 or FGF21. *J Pept Sci*. 2012;18(6):383-393. doi:10.1002/psc.2408.
88. Roth JD, Roland BL, Cole RL, et al. Leptin responsiveness restored by amylin agonism in diet-induced obesity: Evidence from nonclinical and clinical studies. *Proc Natl Acad Sci*. 2008;105(20):7257-7262. doi:10.1073/pnas.0706473105.
89. Burke LK, Heisler LK. 5-Hydroxytryptamine Medications for the Treatment of Obesity. *J Neuroendocrinol*. 2015;27(6):389-398. doi:10.1111/jne.12287.
90. Dhillon H, Zigman JM, Ye C, et al. Leptin directly activates SF1 neurons in the VMH, and this action by leptin is required for normal body-weight homeostasis. *Neuron*. 2006;49(2):191-203. doi:10.1016/j.neuron.2005.12.021.
91. Rezai-Zadeh K, Yu S, Jiang Y, et al. Leptin receptor neurons in the dorsomedial hypothalamus are key regulators of energy expenditure and body weight, but not food intake. *Mol Metab*. 2014;3(7):681-693. doi:10.1016/j.molmet.2014.07.008.
92. Leinninger GM, Opland DM, Jo YH, et al. Leptin action via neurotensin neurons controls orexin, the mesolimbic dopamine system and energy balance. *Cell Metab*. 2011;14(3):313-323. doi:10.1016/j.cmet.2011.06.016.
93. Liu J, Perez SM, Zhang W, Lodge DJ, Lu X-Y. Selective deletion of the leptin receptor in dopamine neurons produces anxiogenic-like behavior and increases dopaminergic activity in amygdala. *Mol Psychiatry*. 2011;16(10):1024-1038. doi:10.1038/mp.2011.36.
94. Hayes MR, Skibicka KP, Leichner TM, et al. Endogenous Leptin Signaling in the Caudal Nucleus Tractus Solitarius and Area Postrema Is Required for Energy Balance Regulation. *Cell Metab*. 2010;11(1):77-83.

doi:10.1016/j.cmet.2009.10.009.
95. Flak JN, Patterson CM, Garfield AS, et al. Leptin-inhibited PBN neurons enhance responses to hypoglycemia in negative energy balance. *Nat Neurosci*. 2014;17(12):1744-1750. doi:10.1038/nn.3861.
96. Flak JN, Arble D, Pan W, Patterson C, Lanigan T, Goforth PB, Sacksner J, Joosten M, Morgan DA, Allison MB, Hayes J, Feldman E, Seeley RJ, Olson DP, Rahmouni K MJM. A leptin-regulated circuit controls glucose mobilization during noxious stimuli. *J Clin Invest*. 2017;In Press.

CHAPTER 2

THE PRESERVATION OF LEPTIN ACTION IN DIET-INDUCED OBESITY

Chapter Summary

Leptin controls the body's homeostatic systems that regulate energy balance by acting through its receptors (LepRb) primarily in the hypothalamus. The arcuate nucleus of the hypothalamus (ARC) is the most populous LepRb neuronal region and is unique for the presence of leptin-responsive transcripts not made in any other LepRb population. Additionally, diet-induced obesity (DIO) coincides with the development of gliosis and leptin resistance, both of which are attributed primarily to the ARC. Here, we examine the transcriptional regulation, glial activation, and phenotypic consequence of the many aspects of DIO. RNA isolated by Translating Ribosome Affinity Purification (TRAP) in hypothalamic and ARC cells into the LepRb-expressing cell fraction and the non-LepRb fraction identified DIO as a leptin-active state. Furthermore, the increased leptin signaling that defines DIO drives the gliosis typically observed in obese animals. Thus, we characterized the state of DIO in LepRb neurons and neighboring cells transcriptionally, phenotypically, and immunohistochemically.

Introduction

Diet-induced obesity (DIO) is the defining ailment of the 21st century. And as technological advances continue to transform the World, calorically dense foods will only become increasingly affordable and omnipresent.[1] Obesity results when an individual's homeostatic systems are unable to maintain energy balance and instead, in the face of the obesogenic environment, continued positive energy surpluses result in the accumulation of more and more adipose tissue.[2] At the center of these homeostatic systems evolved to maintain energy balance is the adipocyte hormone leptin, which is produced in proportion to the body's fat content and circulates in the blood to bind to its receptor (LepRb), located primarily in the hypothalamus of the brain, to provide a snapshot of energy stores and a commensurate response.[3–5] The most important leptin signaling pathway is LepRb→STAT3, such that when STAT3 is phosphorylated (pSTAT3) and translocates into the nucleus, pSTAT3 is responsible for the majority of leptin's negative energy balance effects to decrease food intake and increase energy expenditure.[6,7]

LepRb-expressing neurons in the arcuate nucleus of the hypothalamus (ARC) account for one-quarter of all hypothalamic LepRb neurons and uniquely express a number of leptin-regulated transcripts known to modulate energy balance (e.g. *Pomc*, *AgRP*, *Npy*).[8–11] The ARC lies adjacent to the median eminence, a circumventricular organ, and is exposed to a number of circulating factors, like leptin. In DIO, individuals exhibit high levels of circulating leptin (hyperleptinemia) consistent with their elevated adiposity.[12,13] Additionally, exogenous leptin treatment not only fails to provoke weight loss in DIO patients and rodents, but it also immunohistochemically fails to elicit an

increase in ARC pSTAT3 (in contrast to other LepRb hypothalamic populations that are responsive).[14–16] Thus, the ARC is considered to be the major site of “leptin resistance”, or the state of leptin unresponsiveness/deficiency in DIO. Another histochemical finding localized to the ARC that may limit LepRb neuronal function and explain leptin resistance is the gliosis observed in male DIO humans and rodents.[17–19] This gliosis, which can result from elevated cytokine and endotoxin levels in DIO individuals, may then contribute to the genesis of obesity and be a target of future anti-obesity therapies.[20,21] However, complicating this is the finding that female rodents on high-fat diets (HFD) do not experience gliosis, even when obese/DIO.[22]

There are a number of metabolically significant phenomena that impact only the ARC that hold clues to treating DIO. And, given the heterogeneous nature of LepRb neurons, particularly within the ARC LepRb neuronal population, and the differences observed between male and female mice, a careful examination of metabolism, transcriptional regulation and histochemical manifestations is necessary to clarify our understanding of DIO. Our hypotheses are that DIO is a leptin active, rather than impaired, state and that the hyperleptinemia (and not obesity *per se*) as a consequence of DIO drives the reactive gliosis observed.

Results

Regulation of the hypothalamic LepRb transcriptome reveal similarities among conditions

Using LepR^{eGFP} mice previously described,[23] we were able to perform anti-eGFP TRAP-seq on dissected hypothalami from mice under a variety of conditions: 1.

LepR^{eGFP} mice treated with PBS 10-hours prior to sacrifice, 2. LepR^{eGFP} mice treated with leptin 10-hours prior to sacrifice, 3. LepR^{eGFP} mice treated with PASylated superactive mouse leptin antagonist (SMLA) 20-hours prior to sacrifice, 4. LepR^{eGFP} mice weaned onto a high-fat diet, and 5. LepR^{eGFP} mice bred onto the *ob/ob* background to generate LepR^{eGFP};*ob/ob* mice. From the analyses performed, we identified over 300 genes that were enriched in LepRb neurons (FPKM in TRAP/FPKM in TRAP-depleted >1.5) and whose fold changes differentially changed from the 10-hour PBS treated condition to at least one of the four other conditions (10-hour leptin treated, SMLA treated, high-fat diet-induced *ob*ese (DIO) or *ob/ob*). These genes underwent Clustered Image Map (CIM) generation to determine the similarities between these four conditions (when compared to the same baseline of PBS-treated LepR^{eGFP} mice) (Figure 2.1A). Two groups clearly form: 10h leptin and DIO, and SMLA and *ob/ob*. SMLA is a transient form of leptin deficiency; therefore, it is not unexpected that it would mimic *ob/ob* genetic leptin deficiency. However, it is unexpected that DIO is most similar to 10-hour leptin treated mice, given the notion of leptin resistance. To better characterize the relationships, we plotted the fold changes for all genes of the various conditions and, through linear regression, found the coupling between DIO and 10-hour leptin treatment to be the tightest (Figure 2.1B-G).

A curated list of these 341 genes whose fold changes under the four conditions move in opposing directions based on their coupling (i.e. fold changes that moves in one direction for the 10h-leptin and DIO coupling and not in the same direction for the SMLA and *ob/ob* coupling, and vice versa) defined in Figure 2.1 is detailed in Table 2.1. Using fold change cutoffs of 1.5 and 0.667, there are clearly a number of genes that are

significantly changed in all four conditions (Group I), in three conditions (Group II) and in two conditions (Group III) (Table 2.1). Next, to determine whether these groups are transcriptionally regulated together, we performed Enrichr analyses to identify transcription factor protein-protein interactions (TF-PPI) and found that the most significant transcription factor for Group I to be STAT3, the key leptin signal (Table 2.2). The resemblance of DIO to 10h leptin treated mice and the identification of STAT3 as the transcription factor responsible for the most significant gene fold changes demonstrate that DIO is a leptin active state like treatment with leptin.

Regulation of the arcuate-specific LepRb transcriptome

To further explore the relationship of DIO and states of leptin action, arcuate-specific anti-eGFP TRAP-seq was performed in male mice under a number of conditions: 1. 10-hour PBS treated chow-fed $LepRb^{eGFP}$ mice, 2. 10-hour leptin treated chow-fed $LepRb^{eGFP}$ mice, 3. 10-hour PBS treated high-fat diet fed $LepRb^{eGFP}$ mice, 4. 10-hour PBS treated high-fat diet fed $LepRb^{eGFP}$ mice, 5. PBS-filled osmotic minipump implanted $LepRb^{eGFP}$ mice, and 6. leptin-filled osmotic minipump implanted $LepRb^{eGFP}$ mice. Genes enriched (FPKM in TRAP/FPKM in TRAP-depleted) at baseline (10-hour PBS treated $LepRb^{eGFP}$ mice or PBS minipump implanted $LepRb^{eGFP}$ mice) or that became enriched under any of the other conditions were included. We further sifted the gene list to only include those enriched genes that had differentially expressed fold changes under the five comparisons from baseline (1. Leptin-treated DIO vs PBS-treated DIO, 2. Leptin minipump vs PBS minipump, 3. 10-hour leptin treated vs 10-hour PBS treated, 4. PBS-treated DIO vs PBS treated, and 5. Leptin treated DIO vs PBS treated) and arrived at 148 genes. These genes underwent CIM analyses and

similarities between the conditions were identified (Figure 2.2A). Next, we, like in the hypothalamus-specific TRAP-seq analyses, plotted the 10-hour leptin treatment condition against the DIO condition and a similar, if not stronger, relationship exists in the ARC (Figure 2.2B). Clearly, the leptin action relationship first identified in the hypothalamus between DIO and 10h-leptin treated mice is maintained in the ARC.

Effect of exogenous leptin on the setting of hyperleptinemic diet-induced obesity

We examined relationship between the two most similar conditions in Figure 2.2A (PBS-treated DIO and leptin-treated DIO, both versus the baseline of 10-hour PBS-treated chow-fed mice) by plotting their fold change gene values (Figure 2.3A). The close coupling suggests that DIO mice treated with exogenous leptin are physiologically, immunohistochemically,[15,16] and transcriptionally similar to DIO mice given vehicle. We further parsed this exogenous leptin treatment in the setting of DIO condition by using the 10-hour PBS treated DIO condition as the baseline for the 10-hour leptin treated DIO condition (DIO leptin vs DIO PBS) and plotted the gene fold changes values against the PBS DIO condition (which is versus PBS treated chow mice) (Figure 2.3 B). Clearly, the regulation of genes with the extra leptin do not resemble the regulation of genes under DIO (Figure 2.3 B). This exogenous leptin condition (DIO leptin vs DIO PBS) was also plotted against 10-hour leptin treatment in chow-fed mice and was found to have a weak positive relationship (Figure 2.3 C). Last, we compared 10-hour leptin treated chow-fed animals and 10-hour leptin treated DIO animals and found the relationship to be a strong positive one (Figure 2.3D). In fact, this relationship was stronger than that between DIO and 10-hour leptin treated mice, suggesting that while exogenous leptin does marginally less in the context of

endogenous hyperleptinemia in DIO, it is still effective in regulating genes transcriptionally like that of 10-hour leptin treatment in normoleptinemic (leptin levels expected of lean animals) chow-fed mice.

ARC-specific regulation of LepRb transcriptome in leptin minipump implanted mice

Chow-fed male $LepR^{eGFP}$ mice were implanted with minipumps containing PBS or leptin for two weeks. Leptin minipump infused animals weighed significantly less than PBS minipump implanted littermates (Figure 2.5A). Indeed, over the two-week span, leptin minipump implanted mice lost over 10% of their body weight, most of which was adipose tissue (Figure 2.5B, 2.5C). One set of these mice underwent anti-LepRb TRAP-seq and gene fold change values are plotted against the other conditions (Figure 2.4). The strongest relationship is between leptin minipump implanted mice and the 10-hour leptin injected animals (Figure 2.4A). And, while there exist trending relationships between leptin minipump implanted animals and DIO (+/- leptin) animals, they are quite weak (Figure 2.4B, 2.4D). Because the leptin levels of these leptin minipump infused mice are comparable to high-fat diet fed animals, the adipose loss versus gain in leptin minipump animals versus in DIO animals, respectively, may be counterbalancing the leptin-driven relationships between the conditions (Figure 2.5D).

Gliosis in leptin active and deficient states

An area of intense interest is the manner by which gliosis in the ARC contributes to obesity. Here, we explored gliosis with many of the same groups we performed ARC-specific TRAP-seq analyses: 1. Chow fed mice, 2. High-fat diet fed mice, 3. PBS

osmotic minipump implanted mice, and 4. Leptin minipump implanted mice. As expected, high-fat DIO mice are significantly heavier, have more adipose tissue and are hyperleptinemic compared to chow-fed littermate controls (Figure 2.5A, 2.5B, 2.5D). Over the two-week period of minipump implantation, leptin minipump animals lost a significant amount of weight (while PBS minipump animals had unchanged weights) from fat due presumably to the increased leptin levels (Figure 2.5A-D). We therefore are able to study mice of comparable hyperleptinemic levels that are either obese (HFD) or extra-lean (leptin minipump) (Figure 2.5A-D).

Then, using immunohistochemical methods to detect Iba1 (microglia marker) and GFAP (astrocyte marker), we found the number of microglia/astrocyte and average area per microglia/astrocyte to indeed be increased in the high-fat diet fed male mice (compared to chow controls) as described by other researchers (Figure 2.5E-G).[17,22] Additionally, we detected a comparable increase in both microglia/astrocyte number and area in leptin minipump implanted mice (compared to PBS minipump implanted mice) (Figure 2.5E, 2.5H, 2.5I).

Because we found gliosis to occur in extra-lean leptin minipump animals, the gliosis may be driven by the hyperleptinemia experienced in DIO (and not the obesity). To investigate this, we employed three obese mouse models with varying degrees of leptin deficiency. It is worth differentiating between these three models of obesity: 1. The *ob/ob* leptin deficient animal is hypoleptinemic (no baseline leptin) and has largely absent LepRb signaling; 2. the *db/db* LepRb truncated mutant is hyperleptinemic and has completely absent LepRb signaling; and 3. the mouse with STAT3 conditionally deleted in LepRb neurons ($STAT3^{LepR}KO$) is hyperleptinemic and possesses intact

leptin action outside of leptin→STAT3 activity. Immunohistochemical analyses of Iba1 and GFAP reveal not only the absence of gliosis, but also a decrease in the number and average size of glia in *ob/ob* mice, *db/db* mice, and STAT3^{LepR}KO mice (Figure 2.6). Therefore, gliosis is not directly linked to obesity; instead, gliosis is a consequence of hyperleptinemia and increased leptin action in neighboring LepRb neurons.

Endotoxemia and diet-induced obesity

DIO mice are hyperleptinemic and obese; they also experience elevated endotoxin levels in their blood.[20] We implanted male mice with osmotic minipumps filled with low-dose lipopolysaccharide (using the same LPS concentration as the previous publication), high-dose LPS, or vehicle control. Body weights across the three groups were comparable (Figure 2.7A, 2.7B). Immunohistochemical analysis of Iba1 and GFAP revealed significant gliosis in both LPS minipump conditions when compared to PBS minipump control (Figure 2.7C-2.7H).

Whole hypothalamus TRAP-seq was then performed in male mice treated with LPS 10-hours before sacrifice and compared to DIO animals (both using 10-hour PBS injected chow-fed animals as a baseline). We plotted genes that were enriched (FPKM in TRAP/FPKM in TRAP-depleted > 1.5) in any of the three conditions and differentially expressed in the LPS treated or DIO conditions (Figure 2.7I). Here, genes that are positively regulated with both DIO and LPS are identified; the majority of the genes, however, crowd the two axes, suggesting that LPS and DIO are different conditions. Next, we plotted those genes that were differentially expressed in the non-LepRb cell (TRAP-depleted) fraction and similarly see genes crowding the axes (Figure 2.7J). All

together, while DIO animals may experience endotoxemia that can cause gliosis, the state of DIO is not comparable to one of endotoxin-driven inflammation.

Sex differences in gliosis

Female mice were placed into the same groups as their male counterparts: 1. Chow-fed, 2. High fat-diet fed, 3. PBS minipump, 4. Leptin minipump, 5. Low-dose LPS minipump, and 6. High-dose LPS minipump. Similar to male mice, females on high-fat diet weighed more from increased adipose tissue and were hyperleptinemic (Figure 2.8A, 2.8C, 2.8D). Female mice implanted with leptin minipumps lost a significant amount of weight over the two-week period due to decreased adipose tissue and were hyperleptinemic (Figure 2.8A-D). LPS minipump implanted females had comparable weights (the high-dose LPS minipump mice even unexpectedly gained weight) compared to PBS minipump control mice (Figure 2.8A, 2.8B). These similarities to their male littermates underscore the diet- and treatment-driven phenotypic similarities regardless of sex.

As others have demonstrated,[22] the gliosis associated with diet-induced obesity is absent in female mice (Figure 2.8E-I). Likewise, the gliosis we observed in leptin minipump implanted male mice disappeared in females (we found microglia/astrocytes to instead decrease in number) (Figure 2.8E-I). In contrast, female mice implanted with LPS minipumps (both concentrations) did experience gliosis like their male littermates (Figure 2.8E-I).

Because leptin action may be mediating DIO-induced gliosis, we employed anti-LepRb TRAP-seq in ARC-specific dissections of male and female mice in four

conditions: 10-hour PBS injected chow-fed mice, 10-hour PBS injected high-fat diet fed mice, PBS minipump implanted mice, and leptin minipump implanted mice. There are 77 genes that were enriched (FPKM in TRAP/FPKM in TRAP-depleted) and differentially expressed in at least one of the four conditions when compared to baseline controls (1. Male mice implanted with leptin minipumps vs male mice implanted with PBS minipumps, 2. Female mice implanted with leptin minipumps vs female mice implanted with PBS minipumps, 3. Male DIO mice vs male chow-fed mice, and 4. Female DIO mice vs female chow-fed mice) (Table 2.3). The CIM generated from these gene fold change values reveals a relationship not based on presence/absence of gliosis (i.e. both male DIO and male leptin minipump conditions have gliosis, but female DIO and female leptin minipump conditions do not); rather, there is clear coupling based on treatment type regardless of sex (Figure 2.8J). Upon plotting the fold change values of each treatment comparing gene regulation in male mice versus female mice, the genes are generally coordinately regulated by both male and female conditions (Figure 2.8K, 2.8L).

Regulation of non-LepRb cells transcriptome in the hypothalamus and ARC

Using our $LepR^{eGFP}$ mice, the LepRb pull-down fraction of TRAP does not include microglia or astrocytes; therefore, transcriptional changes in glia should exist in the LepRb-depleted cell fraction. Here, we examined our TRAP-depleted fold change values for the aforementioned hypothalamic- and arcuate-specific TRAP-seq conditions. Interestingly, we find that the non-LepRb hypothalamic cell transcriptome of DIO mice most resembles that of 10-hour leptin treated mice; therefore, the transcriptional changes in DIO (whether in LepRb neurons or not) is markedly similar to that of 10-hour

leptin treated mice (Figure 2.9A, 2.9B). In contrast, analyses of our ARC-specific TRAP-seq data demonstrates that DIO is very different from the other conditions of leptin action (Figure 2.9C). Plotting the fold changes of genes in the non-LepRb cells in DIO condition versus those in the 10-hour leptin treated condition (both with the baseline of PBS-treated chow-fed mice) reveals no relationship (Figure 2.9D). In addition, despite the difference noted in the regulation of the LepRb transcriptome of 10-hour leptin treated condition compared to the leptin minipump condition, the regulation of the non-LepRb transcriptome of these two conditions are consistent (Figure 2.9C, 2.9E).

Discussion

The rise of diet-induced obesity (DIO) is a particularly concerning development, given its profound impact on other diseases, overall health, and the well-fare of nations.[1,24–26] Hence, there is a clear need to develop effective anti-obesity therapies, which may hinge on the understanding of homeostatic systems that control energy balance and their dysregulation in DIO. Indeed, DIO-induced leptin resistance and gliosis in the ARC are particularly interesting phenomena worth exploring as part of homeostatic dysregulation.

We found the ARC-specific gliosis described in male DIO mice to exist in lean hyperleptinemic mice, but absent in obese leptin deficient mice. In contrast to the interpretation that gliosis may drive the development of obesity,[17] we instead find it to be a consequence of LepRb action. Additionally, we explored the gliosis that results from chronically elevated endotoxemia (another characterization of DIO) with translational profiling of LepRb and non-LepRb cells to find that DIO is not at all transcriptionally

similar to a state of endotoxin exposure. Therefore, while DIO can be characterized as a state of hyperleptinemia, obesity and endotoxemia, the gliosis observed appears to be driven by the hyperleptinemia. Furthermore, the bidirectional nature we observe in number and area of glia and the correlated level of leptin action suggest that gliosis is a sensitive marker for neighboring LepRb neuronal activity. Indeed, our analyses of transcriptional regulation of non-LepRb neurons suggests concordant changes based on leptin levels and actions. So, while glia may not respond directly to leptin, leptin-driven neuronal activity may affect nearby glial activity.

This relationship, however, does not appear to extend to female mice. DIO female mice do not experience gliosis like their male counterparts. Further supporting hyperleptinemia driven gliosis, lean hyperleptinemic female mice similarly do not display gliosis, while mice with varying degrees of endotoxemia do still experience gliosis. Our sex- and ARC-specific TRAP analyses also reveal that the presence or absence of gliosis does not define LepRb neurons transcriptionally, for genes are largely coordinately regulated between sexes. Truly, DIO is not an exclusively male condition, in fact the prevalence of obesity is higher for females in the United States;[27] therefore, it would follow that DIO and leptin resistance are similar condition for males and females and the absence of female DIO gliosis may instead suggest that gliosis does not cause leptin resistance or obesity.

If male gliosis is a measure of leptin action in neighboring LepRb neurons, our gliosis data would suggest that DIO is a state of increased leptin action, rather than one of leptin resistance or deficiency. Hypothalamus- and ARC-specific TRAP-seq analyses reveal that indeed DIO is a state of leptin action; this finding fits well with a recent

publication detailing continued leptin action from endogenous DIO-hyperleptinemia.[28] Upon further examination, we found the LepRb transcriptome of DIO mice and exogenous leptin-treated DIO mice to be remarkably similar. Additionally, while exogenous leptin treatment in DIO mice does not affect the transcription of LepRb neurons to the extent that exogenous leptin treatment in lean mice does, we did find a noticeable effect. In sum, our TRAP-seq analyses demonstrate the diminishing returns from the same marginal unit of exogenous leptin with increasing endogenous leptin levels. Therefore, future studies amplifying leptin action and augmenting marginal returns may hold the key to combating DIO by manually rebalancing the body's homeostatic systems.

Materials and Methods

Mice.

Mice were bred in our colony in the Unit for Laboratory Animal Medicine at the University of Michigan. All procedures were approved by the University of Michigan University Committee on the Use and Care of Animals in accordance with AAALAC and NIH guidelines. Animals were bred at the University of Michigan and maintained in a 12-hour light/12-hour dark cycle with *ad libitum* access to food and water. We purchased male and female C57BL/6 mice (Jackson stock #000664), *ob/ob* mice (Jackson stock #000632), *ob/+* mice (Jackson stock #000632), *db/db* mice (Jackson stock #000664), *db/+* mice (Jackson stock stock #000664) for experiments and breeding studies from Jackson Labs. $STAT3^{flox}$ (Jackson stock #016923) mice were also from Jackson.

We generated LepR^{eGFP} mice by crossing LepR^{cre} mice[29] onto the eGFP-L10a background to generate LepR$^{cre/+}$;Rosa26$^{eGFP-10a/+}$ mice,[30] which we then intercrossed to generate double homozygous LepR$^{cre/cre}$;Rosa$^{eGFP-10a/eGFP-L10a}$ (LepR^{eGFP}) study animals. LepR^{eGFP} mice were backcrossed to *ob/ob* mice until LepR$^{cre/cre}$;Rosa$^{eGFP-L10a/eGFP-L10a}$;*ob/*+ mice were obtained. These mice were subsequently intercrossed to generate LepR$^{cre/cre}$;Rosae$^{GFP-L10a/eGFP-L10a}$;*ob/ob* (LepR^{eGFP}*ob/ob*) and LepR^{crecre};Rosa$^{eGFP-L10a/eGFP-L10a}$;+/+ (LepR^{eGFP}) control mice for study. STAT3^{flox} mice were backcrossed to LepR^{eGFP} mice to generate LepR$^{eGFP-L10a}$;STAT3$^{flox/+}$ mice. These mice were then intercrossed to generate LepR$^{cre/cre}$;Rosa$^{eGFP-L10a/eGFP-L10a}$;STAT3$^{flox/flox}$ (STAT3^{LepR}KO) and LepR$^{cre/cre}$;Rosa$^{eGFP-L10a/eGFP-L10a}$;STAT3+/+ (LepR^{eGFP}) control mice for study.

High-fat diet, leptin treatment, LPS treatment and SMLA treatment

For fold induction TRAP-seq experiments, mice were weaned onto either a standard chow diet (Purina Lab Diet 5001) or a 60% high-fat diet (Research Diets D12492, 60% kcal from fat) for at least 8 weeks and were dissected at 12-14 weeks of age. Mice were treated 10 hours prior to sacrifice with metreleptin (5mg/kg, i.p.) (a generous gift from AstraZenica, Inc.), 10 hours prior to sacrifice with lipopolysaccharide (Sigma escherichia coli 055:B5, St. Louis; 100ug/kg; i.p.), 10 hours prior to sacrifice with vehicle (0.9% saline; Hospira; i.p.), or 20 hours prior to sacrifice with PASylated superactive mouse leptin antagonist (SMLA; Protein Laboratories Rehovot; 100pmol/g; i.p.). A separate group of LepR^{eGFP} mice were implanted subcutaneously with osmotic minipumps (Alzet Model 1002; Alza, Palo Alto, CA) filled with either metreleptin (2.2mg/kgday), low-dose lipopolysaccharide (300ug/kgday), high-dose lipopolysaccharide (9.6mg/kgday), or vehicle (0.9% sodium chloride; Hospira; i.p.). All

conditions were compared to the control LepR^{eGFP} vehicle injected or minipump implanted animals raised on standard chow, except for the 10-hour leptin treated DIO condition, which was compared to the PBS-treated DIO condition.

Hypothalamic and arcuate dissections for TRAP-seq

At the midpoint of the light cycle, adult homozygous mice were anesthetized with isoflurane, had their brains removed and placed onto a mouse coronal brain matrix (1mm sections). For whole hypothalamic dissections, a 3x3x3mm block was dissected from the ventral diencephalon immediately caudal to the optic chiasm and then homogenized for TRAP-seq analysis. For arcuate specific dissections, 3 consecutive 1mm sections were removed immediately caudal to the optic chiasm, and arcuate nuclei were dissected bilaterally by hand from the hypothalamus of each section, and pooled for TRAP-seq analysis.

Translating ribosome affinity purification (TRAP).

Messenger RNA was isolated from eGFP-tagged ribosomes, as well as from the eGFP-depleted fraction. RNA was assessed for quality using TapeStation (Agilent, Santa Clara, CA). Samples with RINs (RNA Integrity Numbers) of 8 or greater were prepped using the Illumina TruSeq mRNA Sample Prep v2 kit (Catalog #s RS-122-2001, RS-122-2002) (Illumina, San Diego, CA), where 0.1-3ug of total RNA was converted to mRNA using a polyA purification. The mRNA was fragmented via chemical fragmentation and copied into first strand cDNA using reverse transcriptase and random primers. The 3' ends of the cDNA were adenylated, and 6-nucleotide-barcoded adapters ligated. The products were purified and enriched by PCR to create the final

cDNA library. Final libraries were checked for quality and quantity by TapeStation (Agilent) and qPCR using Kapa's library quantification kit for Illumina Sequencing platforms (catalog # KK4835) (Kapa Biosystems, Wilmington MA). They were clustered on the cBot (Illumina) and sequenced 4 samples per lane on a 50 cycle single end run on a HiSeq 2000 (Illumina) using version 2 reagents according to manufacturer's protocols.

RNA sequencing.

50 base pair single end reads underwent QC analysis prior to alignment to mouse genome build mm10 using TopHat and Bowtie alignment software.[31] Differential expression was determined using Cufflinks Cuffdiff analysis, with thresholds for differential expression set to fold change >1.5 or <0.66 and a false discovery rate of <0.05.[32] Lists of differentially expressed genes were then queried against the Uniprot Database for gene ontology and protein class analysis.[33] Lists of differentially expressed genes were run through One Matrix CIMminer (with log transformation) and Enrichr databases.[34,35]

Immunohistochemistry.

Prior to perfusion, mice were anesthetized with a lethal dose of pentobarbital and transcardially perfused with phosphate buffered saline (PBS) followed by 10% buffered formalin. Brains were removed, placed in 10% buffered formalin overnight, and dehydrated in 30% sucrose for one week. Using a freezing microtome (Leica), brains were cut into 30 um sections. Sections were treated sequentially with 1% hydrogen peroxide/0.5% sodium hydroxide, 0.3% glycine, 0.03% sodium dodecyl sulfate, and

blocking solution (PBS with 0.1% triton, 3% Normal Donkey Serum). Immunostaining was performed using primary antibodies for pSTAT3 (Cell Signaling #9145, 1:1000), Iba1 (Wako, 1:1000), and GFAP (Millipore, 1:500). All antibodies were processed with the avidin-biotin/diamin*ob*enzidine (DAB) method (ABC kit, Vector Labs, 1:500; DAB reagents, Sigma). Images were collected on an Olympus BX53F microscope. Quantification was performed on anatomically matched brain regions with pre-set regions of interest using the Olympus BX53F software. Both sides of the arcuate nucleus were counted and groups means were determined (n=7-14 animals per group).

Phenotyping studies.

LepR^{eGFP} mice fed chow and high-fat diet had their body weights and body composition measured using an NMR-based analyzer (Minispec LF90II, Bruker Optics) (mice were 12-14 weeks old). Mice with implanted minipumps had their body weights measured the day of surgery and two weeks later at time of sacrifice. Body composition was also assessed at time of sacrifice (mice were 12-15 weeks old). Leptin was assayed by commercial ELISA (Crystal Chem) using serum of implanted mice one week after implantation and the day of sacrifice.

Statistics.

Physiological data are reported as mean +/- SEM. Statistical analysis of data was performed using Prism (version 7.0) software. Correlation analyses were also performed using Prism (version 7.0). Unpaired t-tests were used to assess significance; $p < 0.05$ was considered statistically significant.

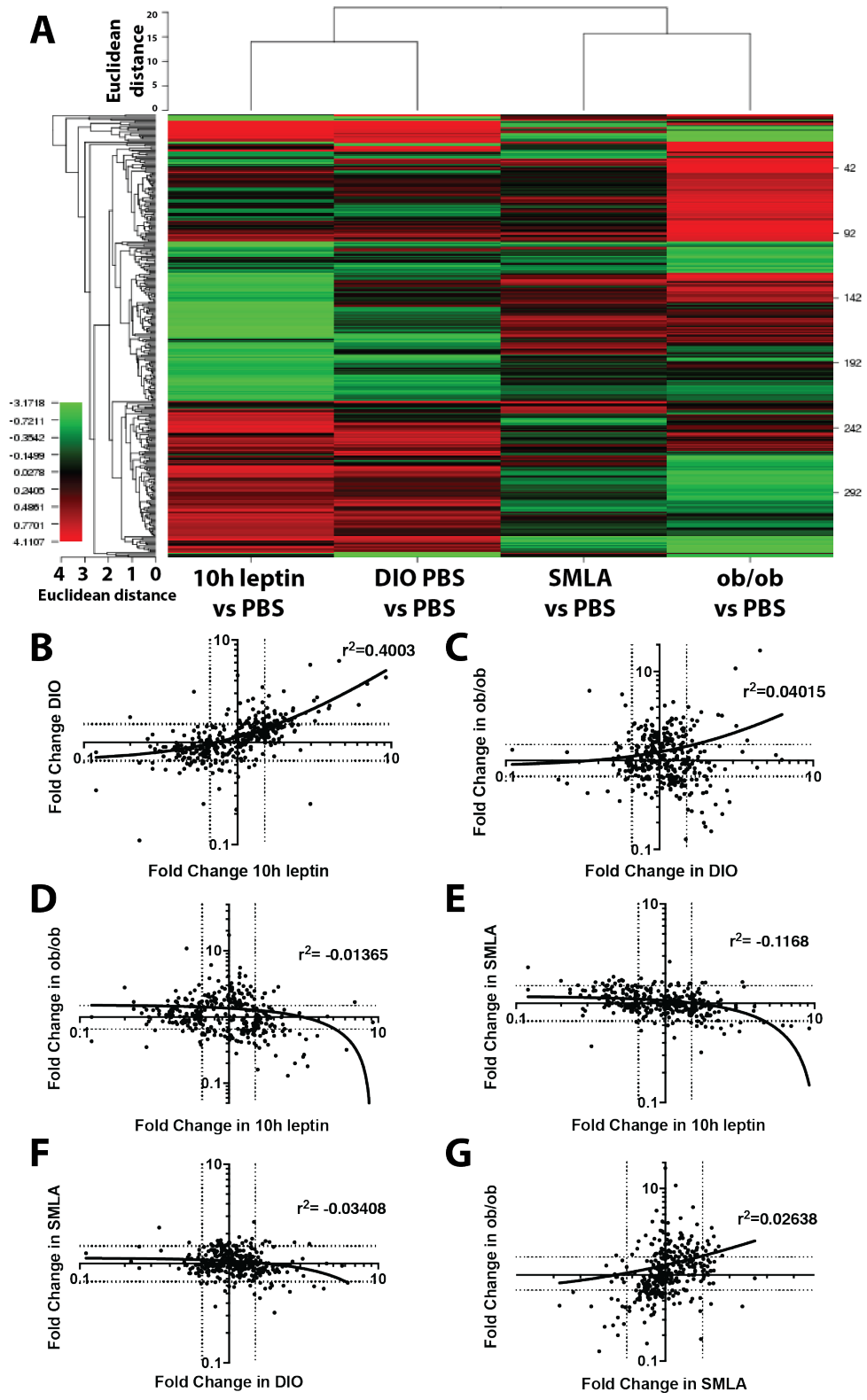

Figure 2.1: Fold change similarities in hypothalamic LepRb-enriched genes. Translating ribosome affinity purification (TRAP) was performed in LepR^{eGFP} and

LepR^{eGFP}*ob/ob* mice fed either normal chow or high-fat diet and treated with either PBS , SMLA, or leptin. Fold change values for each group were calculated and compared to littermate control PBS-treated LepR^{eGFP} mice. **(A)** Heat map detailing the relationship via dendrogram between genes (left axis) and conditions (top axis). **(B)** Fold change in 10-hour leptin treated mice versus fold change in DIO mice. **(C)** Fold change in DIO vs fold change in *ob/ob* mice. **(D)** Fold change in 10-hour leptin treated mice versus fold change in *ob/ob* mice. **(E)** Fold change in 10-hour leptin treated mice versus fold change in 20-hour SMLA treated mice. **(F)** Fold change in DIO mice versus fold change in 20-hour SMLA treated mice. **(G)** Fold change in 20-hour SMLA treated mice versus fold change in *ob/ob* mice. Genes enriched (FPKM in TRAP/FPKM in TRAP-depleted > 1.5) at baseline or in any of the conditions were included in this analysis. Dashed lines are at FC=1.5 and FC=0.667 for axis in **(B-G)**. Each sample comprised of pooled hypothalami for 4-6 adult mice. N=3-4 samples per group.

Gene	10h leptin	DIO	SMLA	*ob/ob*	Group
C1qtnf7	1.74	2.02	0.32	0.44	
Serpina3h	6.15	2.32	0.60	0.32	
Serpina3n	2.06	1.89	0.57	0.26	
Serpina3f	3.19	1.62	0.64	0.27	
Serpina3c	2.77	1.94	0.60	0.20	I
Socs3	3.14	2.56	0.52	0.25	
Bcl3	1.75	1.92	0.63	0.43	
Traf3ip3	2.36	1.75	0.56	0.53	
Serpina3i	2.48	1.48	0.49	0.13	
Sprr1a	9.22	4.31	0.56	0.83	
Atf3	4.58	6.26	0.64	1.02	
Serpina3m	3.92	2.14	0.84	0.52	
H2-Q6	1.60	2.85	0.86	0.34	
Serpina3k	3.37	1.99	1.47	0.18	
Pomc	1.56	2.17	0.82	0.16	
Cd44	1.98	1.74	0.87	0.61	
Prokr2	2.29	2.04	0.82	0.61	II
Asb4	1.74	1.62	0.76	0.61	
Vwf	0.23	0.63	1.38	1.69	
Pglyrp1	0.34	0.54	1.63	1.11	
Ccnb1ip1	1.15	1.61	0.45	0.43	
Pecam1	0.56	1.12	1.51	1.53	
Ly6a	0.45	1.17	1.85	1.67	
R*obo*4	0.51	0.88	1.72	1.91	
Apol10b	3.97	2.28	0.93	0.87	
Cd38	2.97	5.72	0.95	1.15	
Gpr151	2.30	2.15	0.97	0.77	
Gna14	2.03	1.69	0.91	0.72	
Crem	1.53	1.78	0.94	1.10	
Lamc2	1.78	1.53	0.72	1.07	
Gal	1.60	1.77	1.01	1.01	III
Sdc1	1.59	1.51	1.07	0.98	
Rrad	1.59	1.84	1.01	1.24	
Tac2	2.25	1.65	1.29	0.99	
Nr5a2	2.26	1.51	1.03	1.00	
Gpc2	1.64	1.53	1.30	1.24	
Prr19	1.81	1.63	1.07	0.92	

Slc39a4	**0.28**	**0.63**	**0.75**	**0.77**
Lix1	**0.67**	**0.60**	**0.80**	**0.76**
En2	**0.45**	**0.55**	**0.80**	**0.78**
Sult5a1	**0.42**	**0.50**	**1.03**	**1.06**
Bnc2	**0.59**	**0.62**	**0.89**	**0.93**
Elovl3	**0.52**	**0.66**	**1.06**	**1.04**
Th	**0.59**	**0.66**	**0.82**	**0.78**
BC002163	**0.23**	**0.11**	**1.27**	**1.32**
Rnase6	**0.60**	**0.25**	**1.48**	**1.24**
H2-Aa	**0.60**	**0.65**	**0.85**	**0.95**
Chrna3	**0.47**	**0.62**	**1.15**	**1.02**
Hsd17b2	**0.60**	**0.63**	**0.98**	**1.03**
Ntn1	**0.50**	**0.63**	**0.98**	**0.87**
Ces1d	**0.53**	**0.65**	**0.85**	**0.74**
Foxc2	**0.55**	**0.54**	**1.23**	**1.44**
D830030K20Rik	**0.62**	**0.56**	**1.12**	**1.40**
Col5a3	**1.09**	**0.97**	**1.55**	**1.90**
Apoa1	**1.22**	**1.40**	**1.60**	**2.25**
Mgp	**0.69**	**1.43**	**1.78**	**2.14**
Krtap17-1	**1.07**	**0.94**	**1.50**	**2.07**
Gbp9	**1.04**	**1.39**	**0.60**	**0.51**

Table 2.1: Fold change in hypothalamic LepRb-enriched genes. Translating ribosome affinity purification (TRAP) was performed in LepR^{eGFP} and LepR^{eGFP}*ob/ob* mice fed either normal chow or high-fat diet and treated with either PBS or leptin. Genes enriched (FPKM in TRAP/FPKM in TRAP-depleted >1.5) at baseline, or that became enriched in a condition in which they were also significantly changed, were included in this analysis. Per Figure 2.1, genes whose fold change moved in opposing directions based on coupling were included and grouped into 3 groups (Column 6). **(I)** Genes that were differentially regulated under all four conditions. **(II)** Genes whose fold change were significantly changed under three of the conditions. **(III)** Genes that were differentially regulated in two of the conditions. Each sample comprised of pooled hypothalami for 4-6 adult mice. N=3-4 samples per group.

Term	P-value	Group
STAT3	**5.12E-03**	
NFKB1	**5.45E-03**	
TBL1XR1	**1.61E-02**	
RCOR1	**1.92E-02**	
NCOA1	**3.94E-02**	
NOD2	**2.01E-02**	
GTF2B	**3.80E-02**	
RXRA	6.09E-02	
TBP	6.98E-02	**I**
FOS	8.61E-02	
STAT1	8.48E-02	
JUN	1.06E-01	
FOXP3	1.47E-01	
SMAD3	1.57E-01	
CTNNB1	1.66E-01	
EP300	1.94E-01	
ESR1	3.30E-01	
ATF2	**1.33E-02**	
JUND	**3.25E-02**	
JUNB	**3.54E-02**	
PPARG	8.36E-02	
HSF1	7.87E-02	
CEBPB	1.01E-01	
RXRA	9.94E-02	
STAT1	1.37E-01	
SMARCA4	1.52E-01	**II**
JUN	1.71E-01	
STAT3	1.69E-01	
NFKB1	1.75E-01	
SMAD3	2.47E-01	
HDAC2	2.54E-01	
SMAD2	2.52E-01	
CTNNB1	2.60E-01	
EP300	3.02E-01	
TP53	3.80E-01	
FOXA2	**2.52E-02**	
ATF1	5.30E-02	**III**
TAF7	8.17E-02	

ELF1	7.38E-02	
SPI1	1.06E-01	
KDM5B	1.02E-01	
PPARGC1A	1.03E-01	
CREB1	2.04E-01	
TBP	2.39E-01	
ILF3	3.99E-01	
MYC	8.11E-01	

Table 2.2: Transcription factors responsible for TRAP-seq gene fold changes. The genes clustered into groups I-III in Table 2.1 were linked to the corresponding list of transcription factors, as determined by the Transcription Factors Protein-Protein Interactions database through Enrichr. Genes highlighted in red were significant for each of the groups.

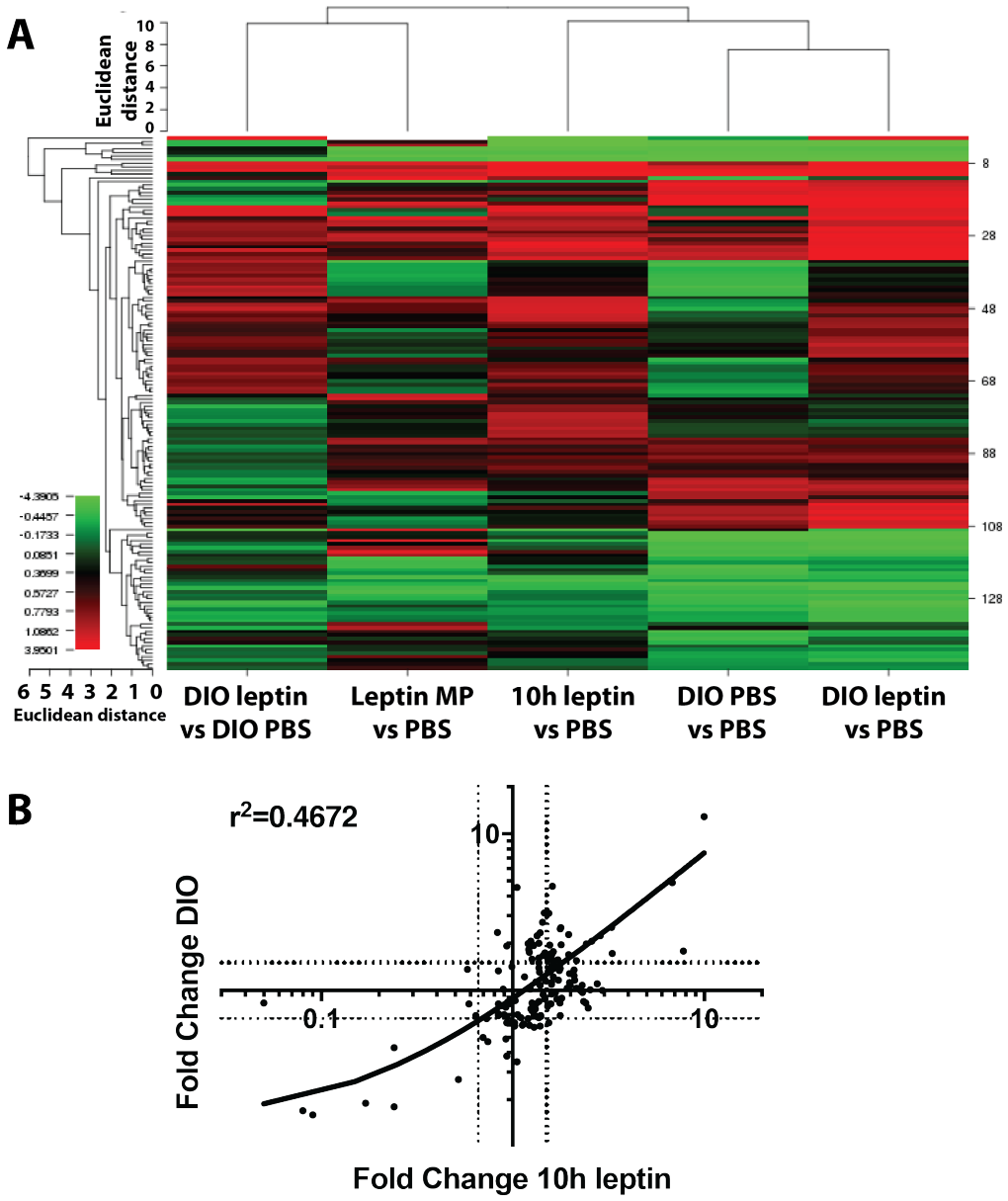

Figure 2.2: Fold changes in LepRb-enriched genes in the arcuate nucleus. Translating ribosome affinity purification (TRAP) was performed in male LepR^{eGFP} mice fed either normal chow or high-fat diet and treated with either PBS or leptin (via 10h injection or 2-week minipump implantation) (leptin: 5mg/kg i.p. injection or 2.2mg/kgday minipump). Fold change values for each group were calculated and compared to littermate control PBS-treated LepR^{eGFP} mice. **(A)** Heat map detailing the relationship via dendrogram between genes (left axis) and conditions (top axis). **(B)** Fold change in 10-hour leptin treated mice versus fold change in DIO mice. Genes enriched (FPKM in TRAP/FPKM in TRAP-depleted > 1.5) at baseline or in any of the conditions were included in this analysis. Dashed lines are at FC=1.5 and FC=0.667 for axis in **(B)**. Each sample comprised of pooled arcuate nuclei for 10-22 adult mice. N=3-5 samples per group.

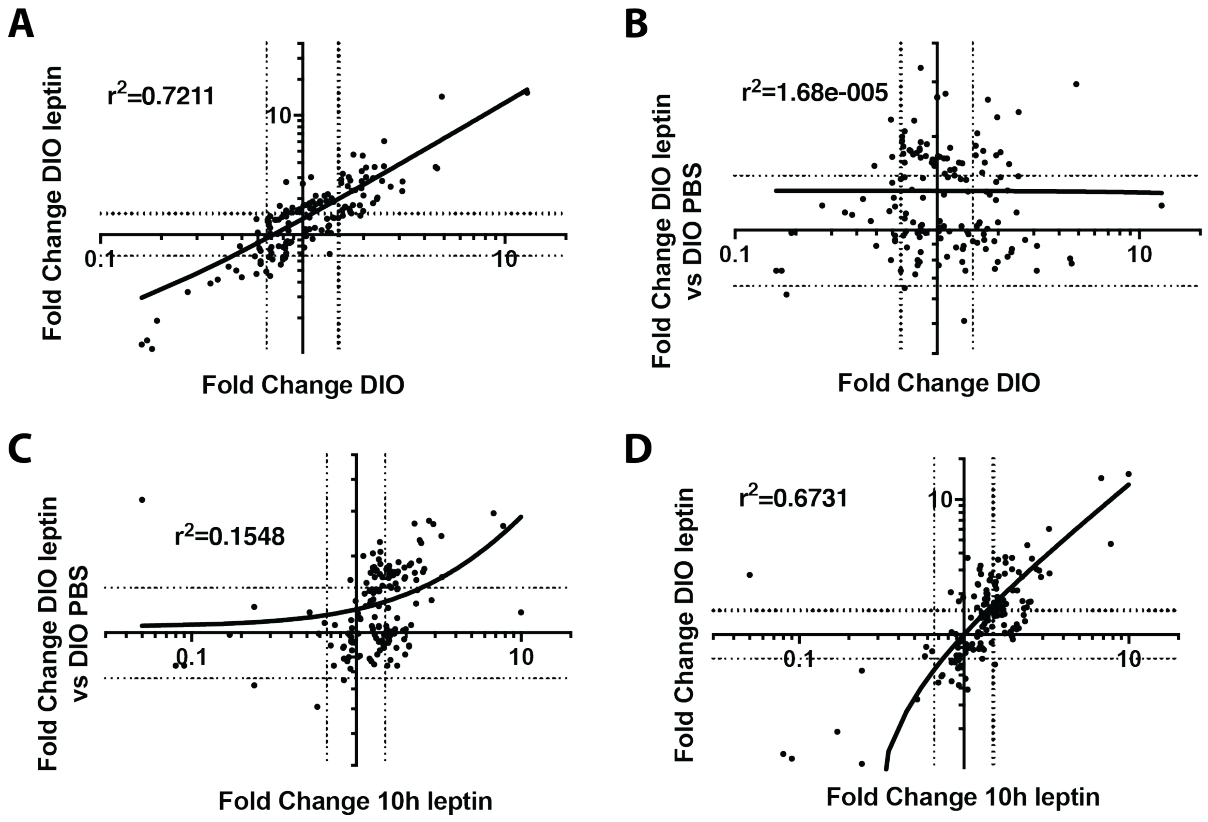

Figure 2.3: Fold changes in LepRb-enriched genes in the arcuate nucleus of DIO mice. Translating ribosome affinity purification (TRAP) was performed in male LepR^{eGFP} mice fed either normal chow or high-fat diet and treated with either PBS or leptin (via 10h injection). Fold change values for each group were calculated and compared to littermate control PBS-treated LepR^{eGFP} mice. **(A)** Fold change in PBS-treated DIO mice versus fold change in 10h leptin-treated DIO mice. **(B)** Fold change in PBS-treated DIO mice versus fold change between 10h leptin-treated DIO mice and PBS-treated DIO mice. **(C)** Fold change in 10-hour leptin treated mice versus fold change between 10h leptin-treated DIO mice and PBS-treated DIO mice. **(D)** Fold change in 10h leptin-treated mice versus fold change in 10h leptin-treated DIO mice. Genes enriched (FPKM in TRAP/FPKM in TRAP-depleted > 1.5) at baseline or in any of the conditions were included in this analysis. Dashed lines are at FC=1.5 and FC=0.667 for axis. Each sample comprised of pooled arcuate nuclei for 10-22 adult mice. N=3-6 samples per group.

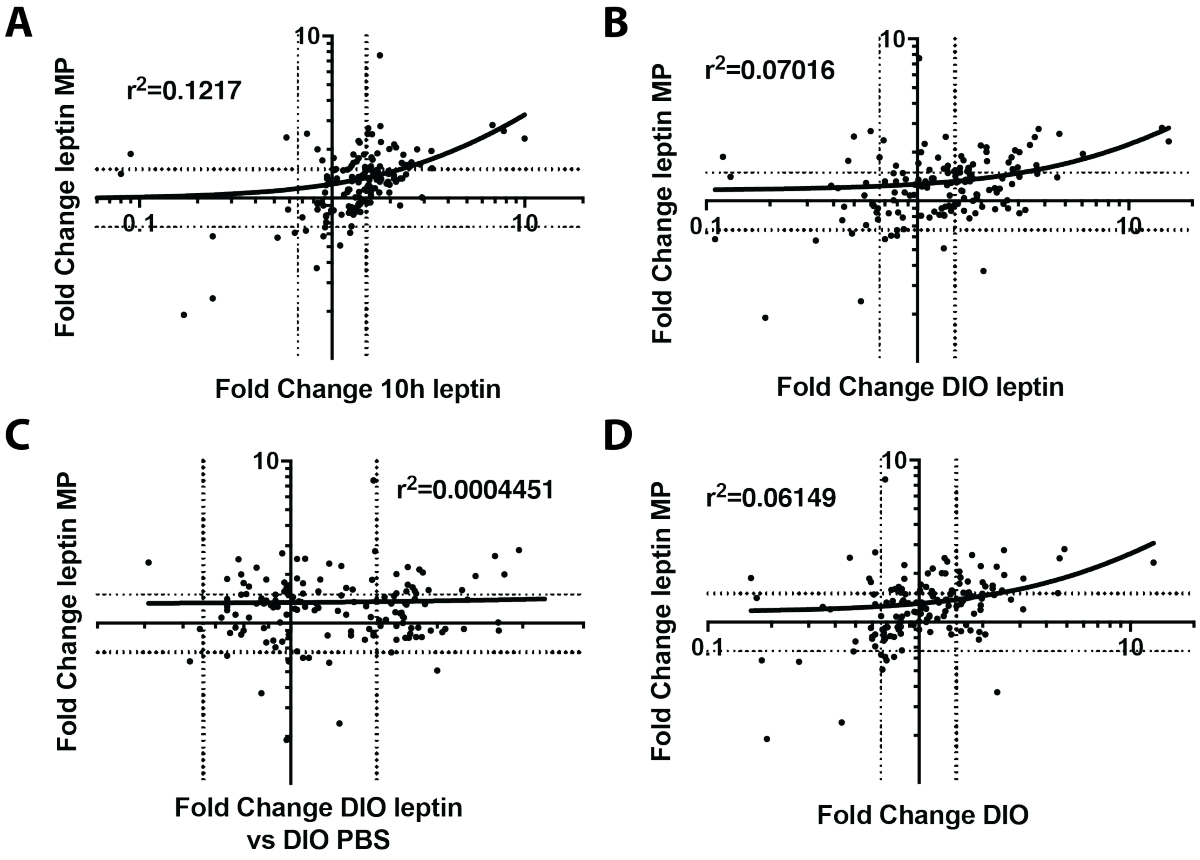

Figure 2.4: Fold changes in arcuate LepRb-enriched genes of leptin minipump mice. Translating ribosome affinity purification (TRAP) was performed in male $LepR^{eGFP}$ mice fed either normal chow or high-fat diet and treated with either PBS or leptin (via 10h injection or 2-week minipump implantation) (leptin: 5mg/kg i.p. injection or 2.2mg/kgday minipump). Fold change values for each group were calculated and compared to littermate control PBS-treated $LepR^{eGFP}$ mice or PBS-treated DIO $LepR^{eGFP}$ mice. **(A)** Fold change in 10h leptin-treated mice versus fold change in leptin minipump implanted mice. **(B)** Fold change in 10h leptin-treated DIO mice versus fold change in leptin minipump implanted mice. **(C)** Fold change between 10h leptin-treated DIO mice and PBS-treated DIO mice verses leptin minipump implanted mice. **(D)** Fold change in PBS-treated DIO mice and leptin minipump implanted mice. Genes enriched (FPKM in TRAP/FPKM in TRAP-depleted > 1.5) at baseline or in any of the conditions were included in this analysis. Dashed lines are at FC=1.5 and FC=0.667 for axis. Each sample comprised of pooled arcuate nuclei for 10-22 adult mice. N=3-6 samples per group.

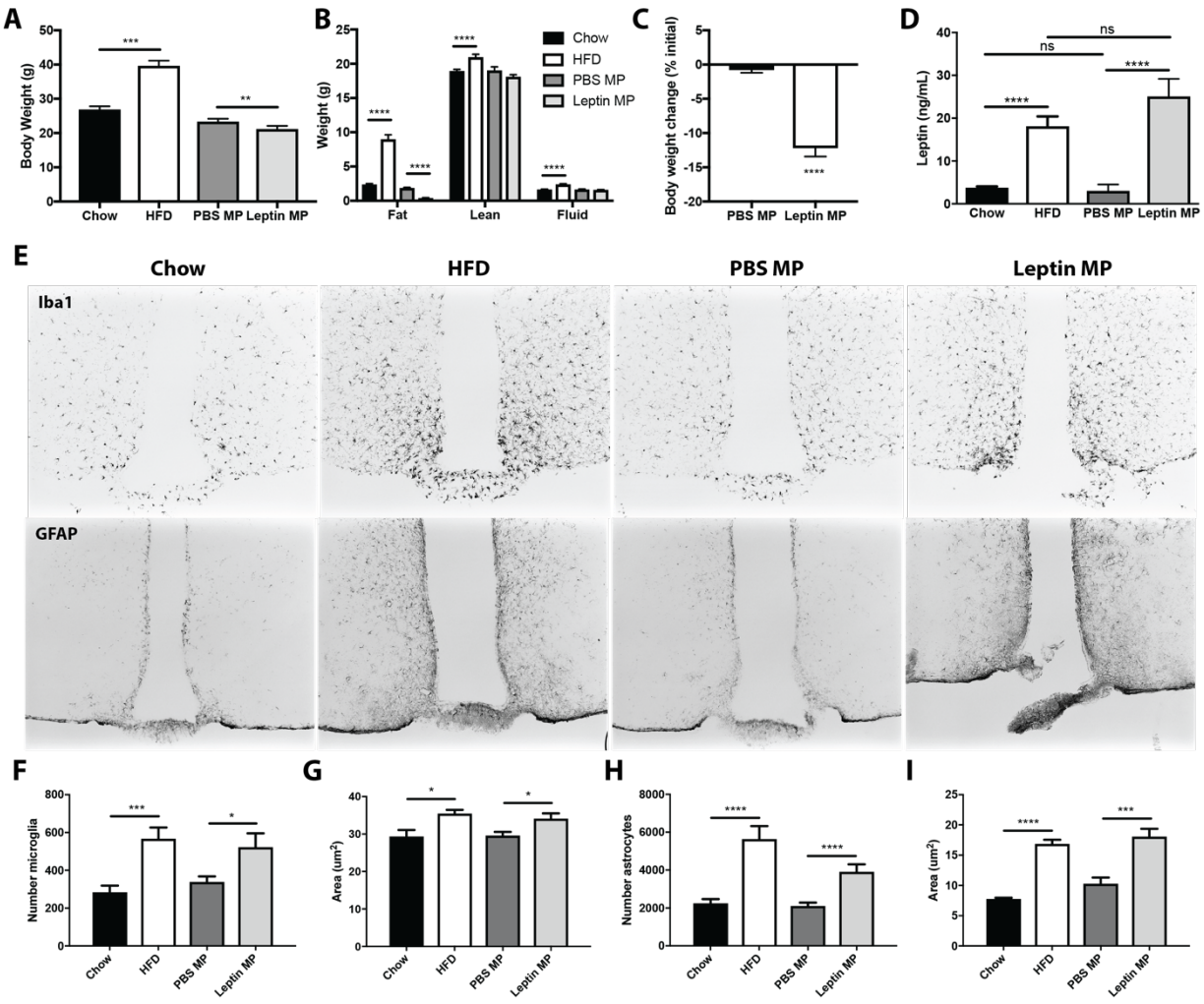

Figure 2.5: Histochemical analysis of gliosis in the arcuate nucleus of male mice fed normal chow or high-fat diet (HFD), fasted, and implanted with PBS or leptin minipumps. Body weights **(A)** and body composition **(B)** of mice on day of sacrifice. **(C)** Percent change in body weight over the two-week span with PBS or leptin minipumps (leptin: 2.2mg/kgday) implanted. **(D)** Leptin levels of the various conditions from serum collected at time of sacrifice. **(E)** Immunohistochemical detection of microglia (via Iba1 protein) and astrocytes (via GFAP protein) in mice fed chow, HFD, implanted with PBS minipumps for 2 weeks, and implanted with leptin minipumps for 2 weeks. Quantification of total ARC microglia **(F)** or ARC astrocyte **(H)** cell number and average area per microglia **(G)** or astrocyte **(I)**. Immunohistochemical analyses **(A-E)** were performed in 8-15 male mice per condition. Mean+/- SEM is shown for **(B-I)**. *p<0.05, **p<0.01, ***p<0.001, ****p<0.0001 by t-test.

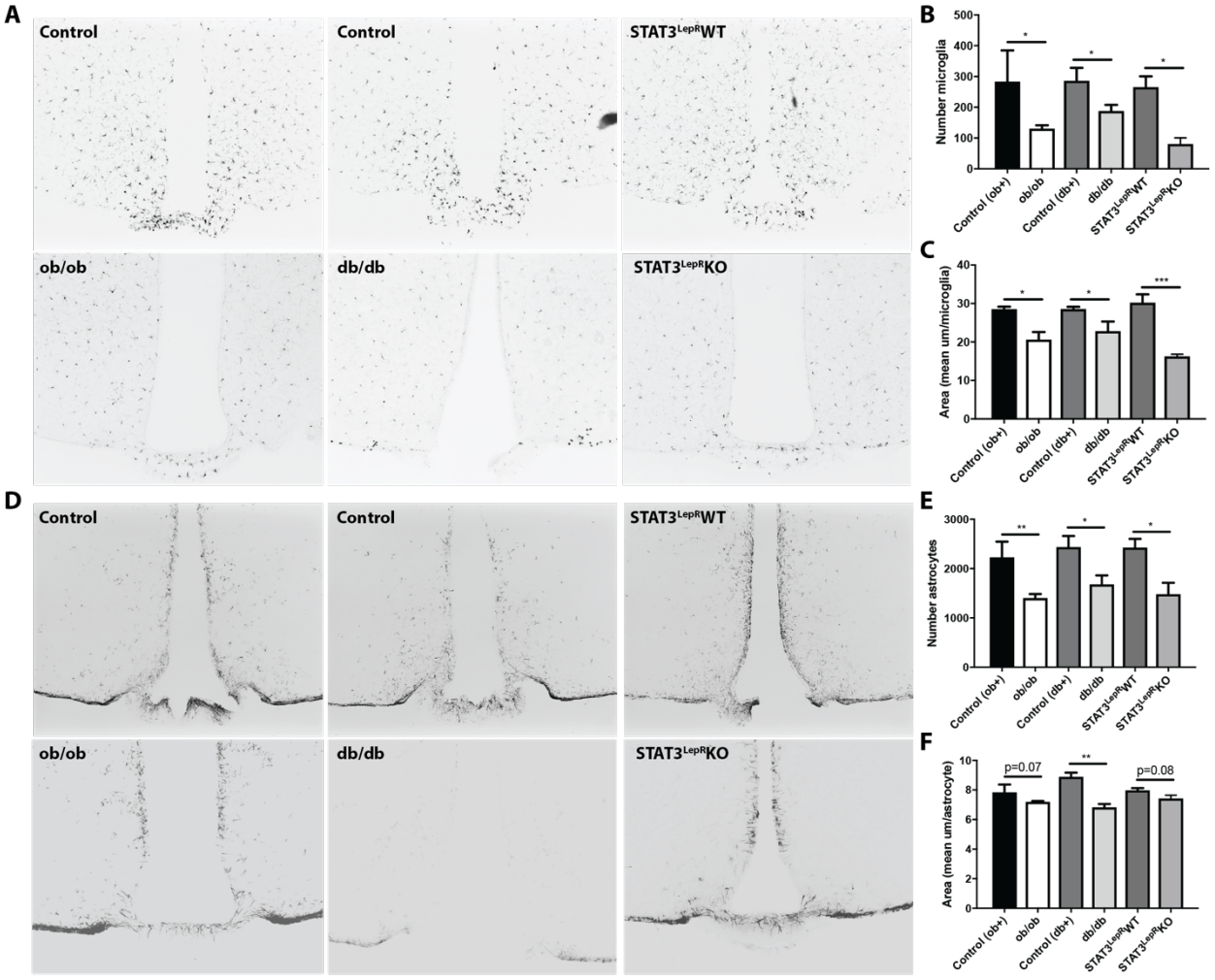

Figure 2.6: Histochemical analysis of gliosis in the arcuate nucleus of male mouse models of leptin deficiency. (A) Immunohistochemical detection of Iba1 protein (microglial marker) in leptin deficient *ob/ob* mice (with *ob*/+ littermate controls), LepRb deficient *db*/*db* mice (with *db*/+ littermate controls) and STAT3 null mice in LepRb neurons (STAT3^{LepR}KO) with STAT3^{LepR}WT littermate controls. Quantification of total ARC microglia **(B)** and average area per microglia **(C)**. **(D)** Representative images of histochemical detection of GFAP protein (astrocyte marker) in *ob/ob* (with *ob*+ controls), *db*/*db* (with *db/*+ controls), and STAT3^{LepR}KO (with STAT3^{LepR}WT controls) mice. Quantification of total ARC astrocyte **(E)** and average area per astrocyte **(F)**. Immunohistochemical analyses **(A-E)** were performed in 7-10 male mice per condition. Mean+/- SEM is shown for **(B,C,E,F)**. *p<0.05, **p<0.01, ***p<0.001 by t-test.

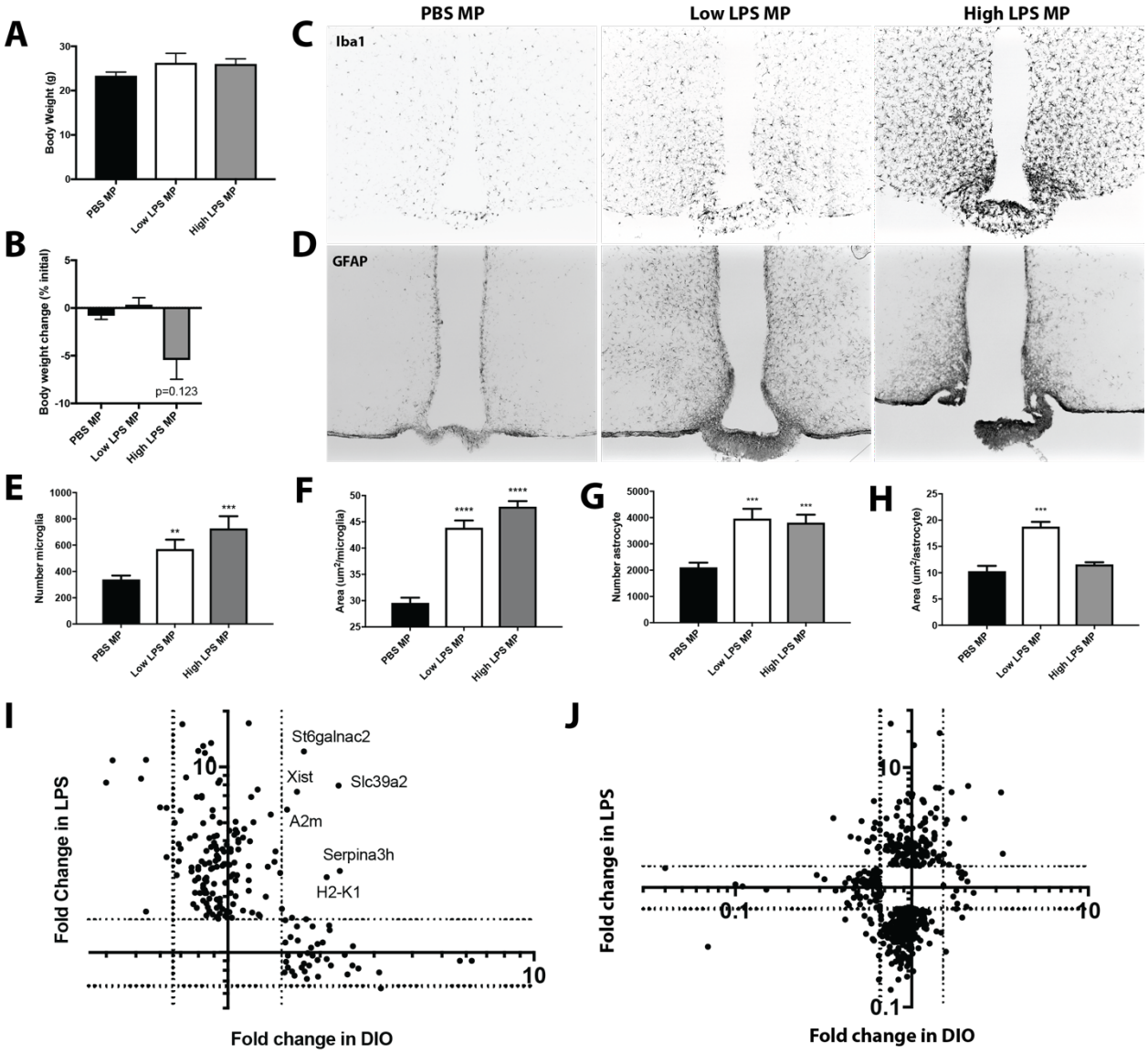

Figure 2.7: ARC glial histochemical and TRAP-seq analyses of male mice treated with lipopolysaccharide. (A) Body weights of mice on day of sacrifice. **(B)** Percent change in body weight over the two-week span with PBS, low-dose LPS (300ug/kgday), or high-dose LPS (9.6mg/kgday) minipumps implanted. Immunohistochemical detection of **(C)** microglia (via Iba1 protein) and **(D)** astrocytes (via GFAP protein) in chow-fed mice implanted with PBS, low-dose LPS (300ug/kgday), or high-dose LPS (9.6mg/kgday) minipumps for 2 weeks. Quantification of total ARC microglia **(E)** or ARC astrocyte **(G)** cell number and average area per microglia **(F)** or astrocyte **(H)**. **(I)** Translating ribosome affinity purification (TRAP) was performed in male $LepR^{eGFP}$ mice fed either chow or high-fat diet and treated with LPS (100ug/kg) or PBS 10 hours prior to sacrifice, respectively. Fold change values for each group were calculated and compared to littermate control PBS-treated $LepR^{eGFP}$ mice to generate the fold change in PBS-treated DIO mice versus fold change in 10h LPS-treated chow-fed mice. Genes enriched (FPKM in TRAP/FPKM in TRAP-depleted > 1.5) at baseline or in either

condition were included in this analysis. **(J)** Fold change values for the non-LepRb TRAP-depleted fraction are plotted here for PBS-treated DIO mice against 10h LPS-treated chow-fed mice; genes that were differentially changed in either condition were included. **(A-H)** were performed in 7-12 male mice per condition. Mean+/- SEM is shown for **(A,B,E-H)**. **p<0.01, ***p<0.001, ****p<0.0001 by t-test **(A-B, E-H)**. Dashed lines are at FC=1.5 and FC=0.667 for axis in **(I-J)**. Each sample comprised of pooled hypothalami for 4-6 adult mice **(I-J)**. N=3-4 samples per group **(I-J)**.

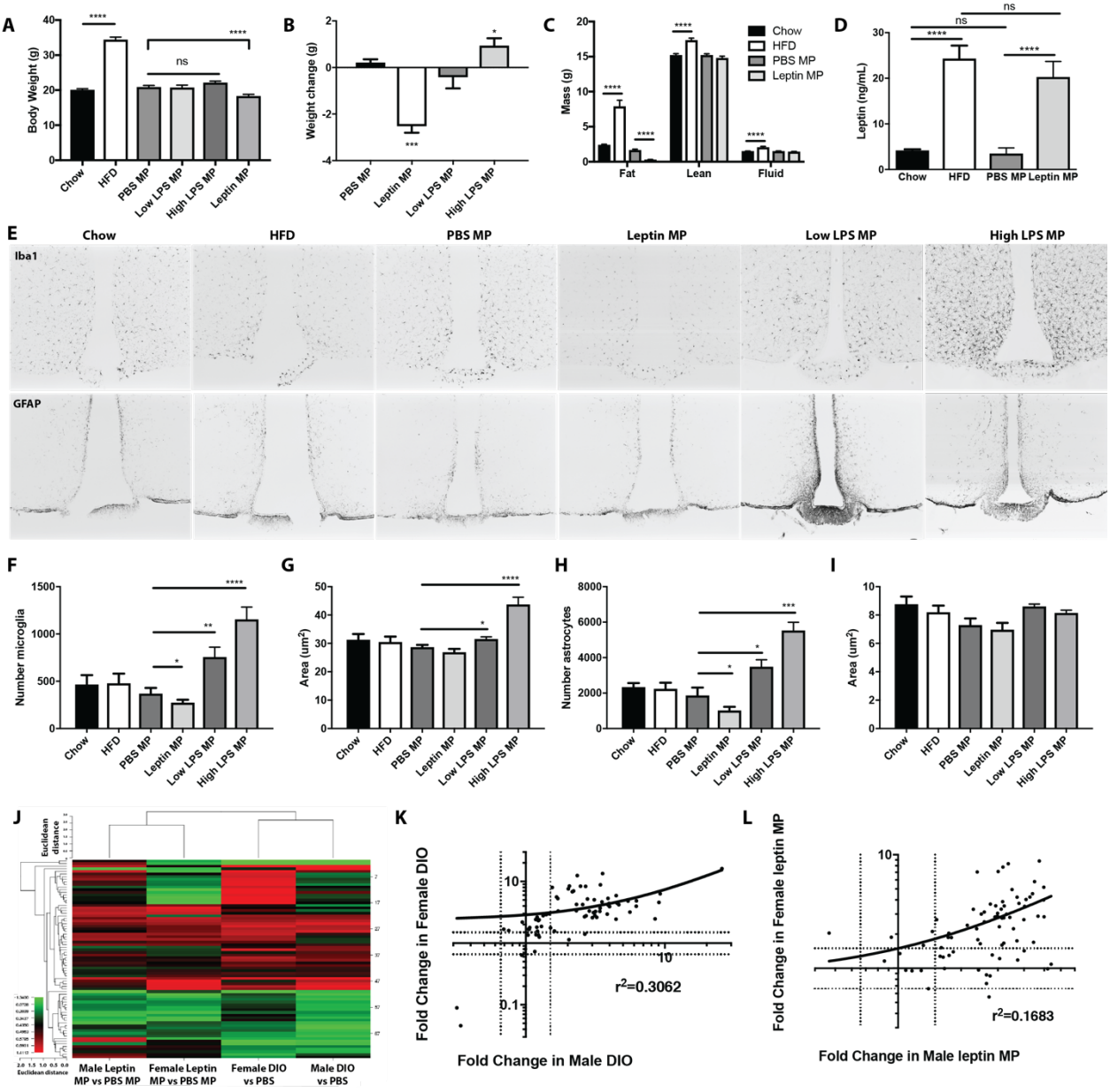

Figure 2.8: ARC glial histochemical and TRAP-seq analyses of female mice. (A) Body weights of mice on day of sacrifice. **(B)** Percent change in body weight over the two-week span with PBS, leptin (2.2mg/kgday), low-dose LPS (300ug/kgday), or high-dose LPS (9.6mg/kgday) implanted minipumps. **(C)** Body composition of animals on day of sacrifice. **(D)** Leptin levels assayed from serum collected on day of sacrifice. **(E)** Immunohistochemical detection of microglia (via Iba1 protein) and astrocytes (via GFAP protein) in mice fed either chow or high-fat diet (HFD), and mice implanted with PBS, leptin (2.2mg/kgday), low-dose LPS (300ug/kgday), or high-dose LPS (9.6mg/kgday) minipumps for 2 weeks. Quantification of total ARC microglia **(F)** or ARC astrocyte **(H)** cell number and average area per microglia **(G)** or astrocyte **(I)**. **(J)** Translating ribosome affinity purification (TRAP) was performed in male and female LepR^{eGFP} mice fed either chow or HFD, and male and female mice implanted with PBS or leptin

(2.2mg/kgday) minipumps. Fold change values for each group were calculated and compared to littermate control PBS-treated $LepR^{eGFP}$ mice (either PBS injected for HFD fed mice or PBS minipump for leptin minipump mice) of the same sex. **(K)** Fold change in PBS-treated male DIO mice versus fold change in PBS-treated female DIO mice. **(L)** Fold change in leptin minipump implanted male mice versus leptin minipump implanted female mice. **(A-I)** were performed in 7-15 female mice per condition. Mean+/- SEM is shown for **(A-D, F-I)**. p<0.05, **p<0.01, ***p<0.001, ****p<0.0001 by t-test **(A-D, F-I)**. Genes enriched (FPKM in TRAP/FPKM in TRAP-depleted > 1.5) at baseline or in any of the conditions were included in this analysis **(J-L)**. Dashed lines are at FC=1.5 and FC=0.667 for axis in **(K, L)**. Each sample comprised of pooled arcuate nuclei for 10-20 adult mice **(J-L)**. N=3-4 samples per group **(J-L)**.

Gene	Male DIO	Female DIO	Male Leptin MP	Female Leptin MP	DIO M/F	Leptin MP M/F
Olfr1033	0.34	0.05	2.82	1.31	7.42	2.15
A130040M12Rik	0.32	0.09	3.73	1.18	3.56	3.16
Tac2	8.51	2.47	0.86	1.16	3.45	0.74
Cd38	9.07	4.57	3.01	7.12	1.98	0.42
Socs2	2.66	1.40	4.00	2.68	1.90	1.49
Gbp9	4.45	2.44	3.37	8.32	1.82	0.40
Arid5b	2.04	1.14	3.43	2.81	1.79	1.22
Ifi47	5.61	3.19	3.18	7.79	1.76	0.41
Sprr1a	25.78	16.18	4.67	2.87	1.59	1.62
BC002163	1.16	0.73	0.47	2.04	1.59	0.23
Gbp6	6.23	3.97	2.39	7.05	1.57	0.34
Atf3	9.25	6.34	4.97	4.00	1.46	1.24
Foxq1	0.93	0.64	4.99	2.84	1.46	1.76
Psmb8	3.85	2.96	1.75	2.03	1.30	0.86
Erg	6.24	4.86	3.71	4.23	1.29	0.88
Cd24a	3.24	2.62	3.05	2.32	1.24	1.31
Yeats2	0.99	0.80	1.53	2.68	1.24	0.57
Prkar2b	3.01	2.59	2.50	3.00	1.16	0.83
Fam163a	5.44	4.82	2.76	3.68	1.13	0.75
Vwa5a	3.14	2.80	3.79	3.73	1.12	1.02
Socs3	4.67	4.19	4.40	4.54	1.11	0.97
2010011I20Rik	3.40	3.28	3.56	2.23	1.04	1.60
Cxcl12	4.54	4.45	2.93	3.55	1.02	0.83
Filip1	1.60	1.57	3.30	3.00	1.02	1.10
St18	4.00	3.93	3.51	4.93	1.02	0.71
Fgfr4	1.25	1.25	5.40	1.09	1.00	4.96
Nhlh2	3.12	3.16	2.14	2.39	0.99	0.90
Serpina3i	2.64	2.68	4.97	5.18	0.98	0.96
Stat1	3.07	3.13	2.29	3.31	0.98	0.69
Serpina3h	2.71	2.78	4.74	8.81	0.97	0.54
Irf9	3.17	3.27	2.59	3.13	0.97	0.83
Fgl2	3.91	4.15	4.44	1.70	0.94	2.62
Rgs4	3.42	3.71	3.00	2.86	0.92	1.05
Otp	1.23	1.34	2.58	2.56	0.92	1.01
Bcl3	3.97	4.39	2.99	3.05	0.90	0.98
Ddn	1.18	1.37	1.46	2.11	0.86	0.69
Gch1	2.86	3.31	3.14	2.77	0.86	1.13

2410004N09Rik	1.50	1.77	1.09	0.96	0.85	1.13
Bahcc1	1.21	1.56	2.97	2.86	0.78	1.04
Heatr8	1.04	1.35	1.80	1.87	0.77	0.96
Asb4	3.53	4.65	2.91	2.84	0.76	1.02
Gna14	4.46	5.90	3.22	3.54	0.76	0.91
B2m	3.90	5.31	2.38	2.23	0.73	1.07
Hrh3	1.29	1.87	1.32	1.59	0.69	0.83
Irs4	2.31	3.35	3.11	3.31	0.69	0.94
Prr7	1.20	1.81	1.67	0.99	0.66	1.68
Pcsk1n	1.06	1.68	1.75	1.30	0.63	1.35
C1ql2	1.04	1.68	0.93	1.88	0.62	0.49
Serpina3n	3.10	5.05	4.09	4.03	0.61	1.01
Glp1r	2.56	4.22	4.03	3.51	0.61	1.15
Kcnk12	1.07	1.79	1.74	1.87	0.60	0.93
Lepr	2.31	4.26	4.28	4.24	0.54	1.01
Cartpt	2.78	5.21	1.84	1.40	0.53	1.32
BC018242	1.23	2.32	1.61	1.52	0.53	1.06
Npdc1	1.25	2.39	1.64	1.26	0.52	1.31
Ghsr	1.71	3.32	4.49	5.80	0.51	0.78
Acvr1c	1.47	2.99	3.17	3.86	0.49	0.82
Ccdc107	1.18	2.42	1.29	0.96	0.49	1.35
Ghrh	1.40	2.90	1.17	0.95	0.48	1.23
Pomc	1.33	2.78	1.02	1.35	0.48	0.76
Agrp	0.75	1.60	2.40	1.79	0.47	1.35
Spint2	1.21	2.63	1.59	1.27	0.46	1.25
Rec8	0.94	2.19	1.40	0.66	0.43	2.12
Npy	0.69	1.69	2.47	1.65	0.41	1.50
Car12	3.44	8.81	3.06	1.22	0.39	2.51
C130021I20Rik	2.69	8.32	2.75	0.86	0.32	3.21
Slc6a3	1.70	5.29	3.70	1.75	0.32	2.12
Irx5	2.16	6.81	2.43	0.97	0.32	2.51
Ngfr	2.21	7.00	4.01	1.43	0.31	2.81
Adamts2	1.66	5.60	3.20	2.79	0.30	1.15
Foxa1	2.47	8.38	2.65	0.88	0.30	3.02
Egflam	2.02	7.58	3.14	1.60	0.27	1.96
Gucy2c	3.57	13.43	5.19	0.99	0.27	5.25
Tac1	2.06	8.45	2.65	0.74	0.24	3.60
Ret	1.55	7.98	3.21	1.66	0.19	1.93
Pitx2	2.34	12.43	2.72	0.56	0.19	4.87
Cxcl1	*0.93*	*3.81*	*0.74*	*NA*	*0.24*	*NA*

Table 2.3: Fold change in ARC LepRb-enriched genes in male and female diet-induced obese and chow-fed leptin minipump implanted mice. TRAP-seq was performed in male and female $LepR^{eGFP}$ mice fed either normal chow or high-fat diet and treated with PBS 10 hours prior to sacrifice. A separate cohort of male and female $LepR^{eGFP}$ mice mice had minipumps implanted for two weeks filled with leptin or vehicle. Genes enriched (FPKM in TRAP/FPKM in TRAP-depleted > 1.5) at baseline (or that became enriched in any of the conditions) and whose fold changes were differentially regulated compared to baseline (sex-specific PBS-treated chow fed mice or vehicle implanted mice) were included in this analysis. **Column 6** calculates the fold change in the DIO conditions for male and female mice. **Column 7** calculates the fold change in leptin minipump implanted male and female mice. Each sample comprised of pooled arcuate nuclei of 10-20 adult mice. N=3-4 per group. The last gene (Cxcl1) is italicized because it was not significantly enriched in any of the conditions but is included due to a recent publication implicating it in the sex-differences seen in gliosis response to diet-induced obesity.

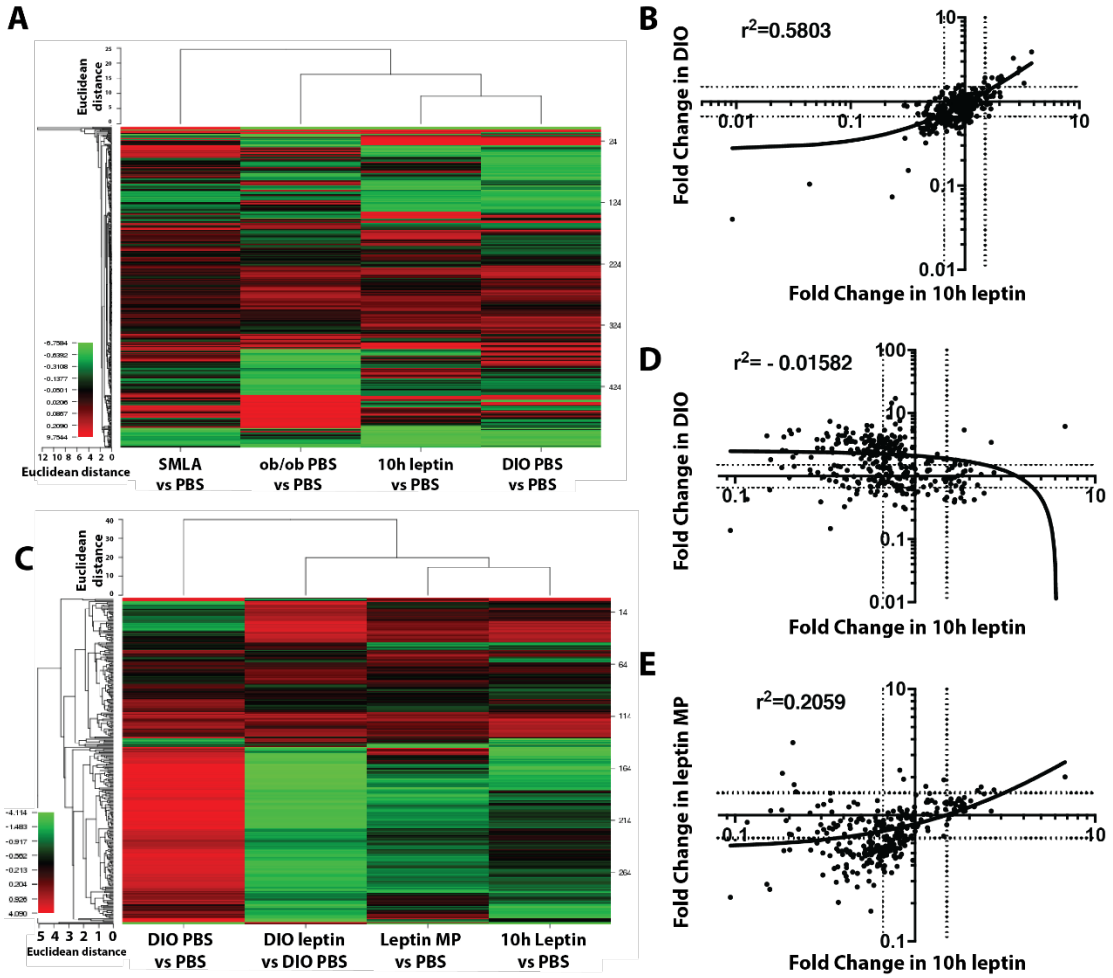

Figure 2.9: Fold change similarities in non-LepRb genes in the hypothalamus and the arcuate nucleus. Translating ribosome affinity purification (TRAP) was performed in LepR^{eGFP} and LepR^{eGFP}*ob/ob* mice fed either normal chow or high-fat diet and treated with either PBS or leptin by injection or 2-week minipump implantation (leptin: 5mg/kg i.p. injection or 2.2mg/kgday minipump). Fold change values for the non-LepRb fraction of each group were calculated and compared to littermate control PBS-treated LepR^{eGFP} mice. Those genes that were significantly changed and that were not enriched in the LepRb fraction were included. **(A)** Heat map detailing the relationship via dendrogram between genes (left axis) and conditions (top axis) in whole hypothalamic dissections. **(B)** Hypothalamic fold change in 10-hour leptin treated mice versus fold change in DIO mice. **(C)** Those genes from the arcuate nuclei dissections and were significantly changed are mapped here with the relationships revealed in the dendrograms on the top and left axis. **(D)** Arcuate specific fold change in 10-hour leptin treated mice vs fold change in DIO mice. **(E)** Arcuate specific fold change in 10-hour leptin treated mice vs fold change in leptin minipump implanted mice. Genes enriched (FPKM in TRAP/FPKM in TRAP-depleted > 1.5) at baseline or in any of the conditions were not included in this analysis. Dashed lines are at FC=1.5 and FC=0.667 for axis in **(B, D-E)**. Each sample comprised of pooled hypothalami for 4-6 adult mice or pooled arcuate for 10-22 adult mice. N=3-4 samples per group.

References:

1. Cutler, D. M., Glaeser, E. L. & Shapiro, J. M. American Economic Association Why Have Americans Become More *Ob*ese? *Source J. Econ. Perspect.* **17,** 93–118 (2003).
2. Elmquist, J. K., Coppari, R., Balthasar, N., Ichinose, M. & Lowell, B. B. Identifying Hypothalamic Pathways Controlling Food Intake , Body Weight , and Glucose Homeostasis. **71,** 63–71 (2005).
3. Bates, S. H. & Myers, M. G. The role of leptin receptor signaling in feeding and neuroendocrine function. *Trends Endocrinol. Metab.* **14,** 447–452 (2003).
4. Ahima, R. S. *et al.* Role of leptin in the neuroendocrine response to fasting. *Nature* **382,** 250–252 (1996).
5. Ring, L. E. & Zeltser, L. M. Disruption of hypothalamic leptin signaling in mice leads to early-onset *ob*esity, but physiological adaptations in mature animals stabilize adiposity levels. *J. Clin. Invest.* **120,** 2931–2941 (2010).
6. Bates, S. H. *et al.* STAT3 signalling is required for leptin regulation of energy balance but not reproduction. *Nature* **421,** 856–859 (2003).
7. Jiang, L. *et al.* Tyrosine-dependent and -independent actions of leptin receptor in control of energy balance and glucose homeostasis. *Proc. Natl. Acad. Sci. U. S. A.* **105,** 18619–18624 (2008).
8. Patterson, C. M., Leshan, R. L., Jones, J. C. & Myers, M. G. Molecular mapping of mouse brain regions innervated by leptin receptor-expressing cells. *Brain Res.* **1378,** 18–28 (2011).
9. Cowley, M. a *et al.* Leptin activates anorexigenic POMC neurons through a neural network in the arcuate nucleus. *Nature* **411,** 480–484 (2001).
10. Elias, C. F. *et al.* Chemical characterization of leptin-activated neurons in the rat brain. *J. Comp. Neurol.* **423,** 261–281 (2000).
11. Ollmann, M. *et al.* Antagonism of Central Melanocortin Receptors in Vitro and in Vivo by Agouti-Related Protein. *Science (80-.).* **278,** 135–138 (1997).
12. Frederich, R. C. *et al.* Leptin Levels Reflect Body Lipid-Content in Mice - Evidence for Diet-Induced Resistance To Leptin Action. *Nat. Med.* **1,** 1311–1314 (1995).
13. T*ob*e, K. *et al.* Relationship between serum leptin and fatty liver in Japanese male adolescent university students. *Am. J. Gastroenterol.* **94,** 3328–3335 (1999).
14. Heymsfield, S. B. *et al.* Recombinant Leptin for Weight Loss in *Ob*ese and Lean Adults. *JAMA* **282,** 1568 (1999).
15. El-Haschimi, K., Pierroz, D. D., Hileman, S. M., Bjørbæk, C. & Flier, J. S. Two defects contribute to hypothalamic leptin resistance in mice with diet-induced *ob*esity. *J. Clin. Invest.* **105,** 1827–1832 (2000).
16. Münzberg, H., Flier, J. S. & Bjørbæk, C. Region-specific leptin resistance within the hypothalamus of diet-induced *ob*ese mice. *Endocrinology* **145,** 4880–4889 (2004).
17. Thaler, J. *et al. Ob*esity is associated with hypothalamic injury in rodents and humans. *J. Clin. Investig.* **122,** 153 (2011).
18. Milanski, M. *et al.* Saturated Fatty Acids Produce an Inflammatory Response Predominantly through the Activation of TLR4 Signaling in Hypothalamus: Implications for the Pathogenesis of *Ob*esity. *J. Neurosci.* **29,** 359–370 (2009).

19. Valdearcos, M., Xu, A. W. & Koliwad, S. K. Hypothalamic Inflammation in the Control of Metabolic Function. *Annu. Rev. Physiol.* **77,** 131–160 (2015).
20. Cani, P. D. *et al.* Metabolic Endotoxemia Initiates *Ob*esity and Insulin Resistance. *Diabetes* **56,** 1761–1772 (2007).
21. Radilla-Vazquez, R. B. *et al.* Gut micr*ob*iota and metabolic endotoxemia in young *ob*ese mexican subjects. *Obes. Facts* **9,** 1–11 (2016).
22. Dorfman, M. D. *et al.* Sex differences in microglial CX3CR1 signalling determine *ob*esity susceptibility in mice. *Nat. Commun.* **8,** 14556 (2017).
23. Allison, M. B. *et al.* TRAP-seq defines markers for novel populations of hypothalamic and brainstem LepRb neurons. *Mol. Metab.* **4,** 299–309 (2015).
24. Guh, D. P. *et al.* The incidence of co-morbidities related to *ob*esity and overweight: a systematic review and meta-analysis. *BMC Public Health* **9,** 88 (2009).
25. Cawley, J., Rizzo, J. A. & Haas, K. Occupation-Specific Absenteeism Costs Associated With *Ob*esity and Morbid *Ob*esity. *J. Occup. Environ. Med.* **49,** 1317–1324 (2007).
26. Cawley, J. & Meyerhoefer, C. The medical care costs of *ob*esity: An instrumental variables approach. *J. Health Econ.* **31,** 219–230 (2012).
27. Ogden, C. L., Carroll, M. D., Fryar, C. D. & Flegal, K. M. Prevalence of *Ob*esity Among Adults and Youth: United States, 2011-2014. *NCHS Data Brief* 1–8 (2015). doi:10.1017/S1368980017000088
28. Ottaway, N. *et al.* Diet-Induced *Ob*ese Mice Retain Endogenous Leptin Short Article Diet-Induced *Ob*ese Mice Retain Endogenous Leptin Action. *Cell Metab.* **21,** 1–6 (2015).
29. Leshan, R. L., Björnholm, M., Münzberg, H. & Myers, M. G. Leptin receptor signaling and action in the central nervous system. *Obesity (Silver Spring).* **14 Suppl 5,** 208S–212S (2006).
30. Krashes, M. J. *et al.* An excitatory paraventricular nucleus to AgRP neuron circuit that drives hunger. *Nature* **507,** 238–42 (2014).
31. Langmead, B., Trapnell, C., Pop, M. & Salzberg, S. Ultrafast and memory-efficient alignment of short DNA sequences to the human genome. *Genome Biol.* **10,** R25 (2009).
32. Trapnell, C. *et al.* Transcript assembly and quantification by RNA-Seq reveals unannotated transcripts and isoform switching during cell differentiation. *Nat. Biotechnol.* **28,** 511–515 (2010).
33. Magrane, M. & Consortium, U. P. UniProt Knowledgebase: A hub of integrated protein data. *Database* **2011,** 1–13 (2011).
34. Weinstein, J. N. *et al.* Predictive statistics and artificial intelligence in the U.S. National Cancer Institute's drug discovery program for cancer and AIDS. *Stem Cells* **12,** 13–22 (1994).
35. Kuleshov, M. V *et al.* Enrichr: a comprehensive gene set enrichment analysis web server 2016 update. *Nucleic Acids Res.* **44,** W90-7 (2016).

CHAPTER 3

LACK OF STAT1 DOES NOT EXACERBATE LACK OF STAT3 IN LEPTIN RECEPTOR NEURONS

Chapter Summary

Leptin is the key hormone responsible for regulating energy balance by signaling through its receptor (LepRb) in the brain an individual's approximate energy stores. The majority of leptin's anorectic action is mediated through the phosphorylation of Tyr_{1138} on the intracellular tail of LepRb. In cell culture, Tyr_{1138} recruits and phosphorylates both STAT1 and STAT3, and while STAT3 is the transcription factor responsible for much of leptin action, leptin action through STAT1 has not been examined closely. Here, we employed LepRb specific TRAP-seq to identify the transcriptome of leptin-deficient *ob/ob* mice and STAT3 null ($STAT3^{LepR}KO$) mice. Surprisingly, the transcriptional difference between the obese *ob/ob* and marginally less obese $STAT3^{LepR}KO$ mice involves genes known to be involved in STAT1 action. Furthermore, in $STAT3^{LepR}KO$ mice, STAT1 mRNA and protein both increase dramatically, suggesting a compensatory

mechanism consistent with the overlapping function of STAT proteins in other systems. To determine the role STAT1 plays on energy balance, we conditionally deleted STAT1 in LepRb neurons and found metabolic parameters to be unchanged. Additionally, the further ablation of STAT1 on top of STAT3 null mice did not exacerbate the obesity. Thus, STAT1 does not appear to contribute to energy balance; however, it's increase in neighboring glia when deleted in neurons highlights the importance of interactions among multiple cell types.

Introduction

Obesity is an ever-increasing problem in the United States. And as the rate of obesity increases, its costs rise proportionally: in addition to driving diabetes, cardiovascular disease and a variety of cancers, obesity is responsible over 20% of current US health care costs.[1]

Leptin is produced in white adipocytes in proportion to the individual's triglyceride content and travels through the circulation to the central nervous system, where it binds to its receptor (LepRb) to regulate energy balance.[2–4] Bound LepRb results in the autophosphorylation and activation of Janus-activated Kinase 2 (JAK2) and consequent phosphorylation of the three tyrosine residues (Tyr_{985}, Tyr_{1077}, Tyr_{1138}) on the intracellular tail of the receptor.[5–8] Tyr_{985} recruits SHP2 and Socs3 to attenuate LepRb signaling, Tyr_{1077} recruits STAT5, and Tyr_{1138} recruits STAT3. Together, these tyrosines and downstream transcriptional signals are largely responsible for leptin action, for mice with these three tyrosine mutated ($LepRb^{123F}$) or the receptor truncated ($LepRb^{\Delta 65}$) are phenotypically similar to LepRb-deficient *db/db* animals.[9,10] Furthermore, genetic mutation analysis revealed no phenotypic difference between mutation of all three tyrosines ($LepRb^{123F}$) and of only Tyr_{1138} ($LepRb^{3F}$), pointing to Tyr_{1138} as the tyrosine responsible for the majority of LepRb action.[9] Importantly, phosphorylation of Tyr_{1138} results in the recruitment and activation of STAT3.[7,11] This JAK2-STAT3 pathway mediates the majority of leptin's control of energy balance.[12]

And while much of the Tyr_{1138}-mediated control of energy balance is mediated by STAT3, recent transcriptome analysis of LepRb neurons revealed novel genes enriched

in LepRb neurons that may be separate from STAT3 action but part of Tyr_{1138} signaling.[13] Additionally, in cultured cells, Tyr_{1138} recruits and activates both STAT1 and STAT3.[14] And, due to the overlapping function of STAT proteins, STAT1 may, like STAT3, mediate part of leptin action through Tyr_{1138}.

Results

STAT3 in leptin receptor neurons is critical for energy balance

$LepR^{eGFP}$ mice (homozygous for $Rosa26^{eGFP\text{-}L10a}$) were crossed to $STAT3^{flox}$ mice to generate $LepR^{cre/cre}STAT3^{flox/flox}$ ($STAT3^{LepR}KO$) and $LepR^{cre/cre}STAT3^{+/+}$ ($LepR^{eGFP}$) mice. In $STAT3^{LepR}KO$ mice, exons 18-20 of STAT3 (which encode the SH2 domain) are conditionally deleted in LepRb-expressing neurons (Figure 3.1A). To confirm the ablation of STAT3 in LepRb neurons, $STAT3^{LepR}KO$ and $LepR^{eGFP}$ mice were treated with PBS vehicle or leptin (5mg/kg; i.p.) for 90 minutes and pSTAT3-IR in eGFP-labeled LepRb neurons was assessed (Figure 3.1B). As expected, in $LepR^{eGFP}$ mice, leptin treatment strongly induces pSTAT3; however, in $STAT3^{LepR}KO$ mice, pSTAT3 is absent with leptin treatment (Figure 3.1B). Given the importance of LepRb→STAT3, $STAT3^{LepR}KO$ mice have expectedly more adiposity and decreased lean mass (Figure 3.1C). In addition, these obese $STAT3^{LepR}KO$ mice have markedly elevated leptin and insulin levels (Figure 3.1D, 3.1E).

Transcriptional profiling of leptin-active and leptin-deficient animals.

Mice on the eGFP-L10a background were in one of seven conditions: 1. $STAT3^{LepR}KO$, 2. $LepR^{eGFP}$ treated with PBS 10 hours prior to sacrifice, 3. $LepR^{eGFP}$ treated with leptin (5mg/kg, i.p.) 3 hours prior to sacrifice, 4. $LepR^{eGFP}$ treated with leptin

(5mg/kg, i.p.) 10 hours prior to sacrifice, 5. LepR^{eGFP} mice fasted for 24 hours, 6. LepR^{eGFP}*ob/ob* (on the *ob/ob* background) treated with PBS 10 hours prior to sacrifice, and 7. LepR^{eGFP}*ob/ob* treated with leptin (5mg/kg, i.p.) 10 hours prior to sacrifice. Hypothalami from all groups were pooled, at least three independently pooled samples from each condition were sequenced and the differentially expressed genes were analyzed. Gene expression comparisons were analyzed between the LepRb neuron fraction (pull-down) and the non-LepRb cell fraction (supernatant) to generate a list of enriched genes. Then, further comparisons were performed between the gene expression values from the various conditions against the control PBS-treated LepR^{eGFP} condition to identify the genes that were differentially regulated (the leptin-treated LepR^{eGFP}*ob/ob* condition was the only one not compared to the PBS-treated LepR^{eGFP} sample; rather, the PBS-treated LepR^{eGFP}*ob/ob* condition was used as the baseline). From these six comparisons, over 150 genes were found to be differentially regulated and enriched in LepRb neurons and are displayed in the heatmap, which demonstrates the clear dichotomy of relationships between the conditions of leptin action (3h leptin, 10h leptin, *ob/ob* leptin) and leptin deficiency (STAT3^{LepR}KO and *ob/ob*) (Figure 3.2A). Due to the similar hyperphagic obesity experienced in STAT3^{LepR}KO and LepR^{eGFP}*ob/ob* mice, it is unsurprising that STAT3^{LepR}KO and LepR^{eGFP}*ob/ob* mice share a close transcriptional relationship, particularly given the importance of STAT3 in leptin action. Comparison of the fold expression changes observed in STAT3^{LepR}KO and LepR^{eGFP}*ob/ob* (versus LepR^{eGFP} PBS) would determine genes that are regulated by LepRb→STAT3, by LepRb action independent of STAT3, and by STAT3 signaling independent of LepRb (Figure 3.2B, Table 3.2). Genes that are coordinately regulated

by both STAT3 and leptin are labeled as I and I' (red background in 2B) and include many of the neuropeptides known to be involved in leptin action, including *Pomc*, *Agrp*, *Npy*, *Nts* and *Cartpt*. However, when all these genes were analyzed, there were no significantly enriched terms that appeared through transcription factors protein-protein interactions (TF-PPIs) (data not shown). The genes with significant fold changes in *ob/ob*, but not in STAT3^{LepR}KO mice, are denoted in green with II and II' (Figure 3.2B, Table 3.2). Through TF-PPI analysis, these group II genes are most enriched for EP300, which has been implicated in leptin action (Figure 3.2C, Table 3.3).[15,16] Last, fold change expression of the genes in group III is significantly altered in STAT3^{LepR}KO mice, but not in LepR^{eGFP}*ob/ob* mice, suggesting that these genes are leptin regulated but independent of STAT3 action (Figure 3.2, Table 3.2). Through TF-PPI, group III genes are highly significant for a number of pathways, including IRF3, STAT1 and STAT2 (Figure 3.2C, Table 3.3). This, together with the significantly increased *Stat1* transcript in STAT3^{LepR}KO mice and participation of STAT1 in LepRb signaling in cultured cells,[14] suggests that STAT1 may drive the expression of these group III genes in the absence of STAT3. It is important to note that STAT1 activity disappears with complete leptin absence (*ob/ob* group), further confirming the existence of a leptin→STAT1 signal.

RT-qPCR confirms TRAP-seq gene expression

Previously, Allison et. al. demonstrated that differential expression of genes determined by TRAP-seq not only follows trends in quantitative RT-qPCR gene expression levels, but is also more specific for LepRb neurons.[13] We similarly confirmed our LepRb transcriptome findings with RT-qPCR, and as expected, the discovered

changes in gene expression of target genes by RT-qPCR in *ob/ob* and STAT3^{LepR}KO mice align with the observed changes by TRAP-seq (Table 3.1). Additionally, we employed RT-qPCR on LepR$^{s/s}$ mice (which contain a mutation in Tyr_{1138} that prevents recruitment of STAT3 to LepRb while leaving global STAT3 signaling intact) and found expression levels to be similar to either that of *ob/ob* mice or that of the STAT3^{LepR}KO mice, depending on the gene (Table 3.1). All together, our analysis confirms the elevation of *Stat1* and STAT1-induced transcripts (*Irf1* and *Psmb8*) in STAT^{3LepR}KO mice, but not in LepR$^{s/s}$ or *ob/ob* mice; thus, STAT1's upregulation in the absence of STAT3 may be downstream of LepRb→Tyr_{1138}.

STAT3 absence results in increased STAT1 protein expression

To explore this coupling of STAT1 and STAT3, the fold expression changes of *Stat1* in LepRb neurons (LepR^{STAT1}) and of *Stat3* in LepRb neurons (LepR^{STAT3}) under a number of conditions are plotted (Figure 3.3A). Excluding the STAT3^{LepR}KO condition, the fold change relationship between LepR^{STAT1} and LepR^{STAT3} is remarkably linear (r^2=0.9172) (Figure 3.3A). The outlier is the STAT3^{LepR}KO condition, which is expected due to the deletion of *Stat3* in LepRb neurons; although, perhaps more interesting is the 3.49-fold change of *Stat1*. This dramatic increase of *Stat1* is confirmed with immunohistochemical studies demonstrating a robust increase in STAT1 protein in LepRb neurons of STAT3^{LepR}KO mice (Figure 3.3B-E).

Conditional ablation of STAT1 in LepR neurons

STAT3^{LepR}KO mice, while obese, are not as obese as *ob/ob* mice, suggesting the presence of other LepRb-specific anorectic signals that contribute to the *ob/ob*

phenotype. Therefore, we conditionally deleted *Stat1* in LepRb neurons to generate $LepR^{cre/cre}STAT1^{flox/flox}$ ($STAT1^{LepR}KO$) and $LepR^{cre/cre}STAT1^{+/+}$ ($LepR^{cre}$) control mice (Figure 3.4A). Through *in situ hybridization*, we confirmed the deletion of *Stat1* from LepRb neurons in $STAT1^{LepR}KO$ (Figure 3.4C). Interestingly, both immunohistochemistry and ISH suggest that STAT1 ablation in LepRb neurons results in the increase of STAT1 in neighboring tanycytes/glia (Figure 3.4B, 3.4C). In addition, we crossed these $STAT1^{LepR}KO$ to $STAT3^{LepR}KO$ to generate $STAT3^{LepR}KO$ single conditional knock-out mice and littermate $STAT1STAT3^{LepR}KO$ double knock-out mice, which lose the robust STAT1 expression seen in $STAT3^{LepR}KO$ (Figure 3.6).

Absence of STAT1 in LepR neurons does not perturb energy balance

Generally, male and female $STAT1^{LepR}KO$ have comparable body weights, food intake, body composition, blood glucose, serum leptin and serum insulin to littermate control $LepR^{eGFP}$ mice (Figure 3.5, Figure 3.8). $STAT1^{LepR}KO$ mice also responded similarly to glucose and insulin tolerance tests when compared to $LepR^{eGFP}$ controls (Figure 3.5, Figure 3.8, Figure 3.10). Moreover, the further deletion of STAT1 in $STAT3^{LepR}KO$ mice did not exacerbate the obesity experienced; indeed, $STAT1STAT3^{LepR}KO$ mice had similar body weights, food intake, body composition, blood glucose, serum leptin, serum insulin levels compared to $STAT3^{LepR}KO$ mice (Figure 3.7, Figure 3.9). Glucose and insulin tolerance were also comparable between $STAT1STAT3^{LepR}KO$ and $STAT3^{LepR}KO$ mice (Figure 3.6, 3.9, 3.10).

Markers of gliosis present in $STAT1^{LepR}KO$ animal

Microglial activation and astrogliosis are markers of injury and have been postulated to play a role in obesity.[17] In male STAT1^{LepR}KO animals (compared to their LepR^{eGFP} littermate controls), the number of microglia are elevated in the ARC using immunohistochemical microglia specific marker Iba1 (Figure 3.11a, 3.11b, 3.11e). Additionally, the number of astrocytes is also higher in the ARC with a concomitant increase in the average area of each astrocyte (Figure 3.11c, 3.11d, 3.11g, 3.11h). These findings, when coupled to the increase of STAT1 in neighboring glia with its ablation in LepRb neurons may point to a new mechanism of DIO-induced gliosis (Figure 3.4B, Figure 3.4C).

Discussion

Tyr_{1138} is responsible for the majority of leptin's actions and STAT3 is the main downstream signal that mediates those effects. Another STAT protein, STAT1, is also recruited by Tyr_{1138} and is tightly coupled to STAT3 activity under various metabolic conditions. Of particular interest is our data demonstrating the upregulation of STAT1 when STAT3 is deleted in LepRb-expressing neurons (STAT3^{LepR}KO), suggesting that at least part of Tyr_{1138} is preserved in STAT3 absence. Furthermore, the gene expression differences between STAT3^{LepR}KO, LepRb$^{s/s}$, and *ob/ob* mice point to the existence of leptin-dependent STAT1 signaling.

Our data, however, show that STAT1, although regulated by leptin→Tyr_{1138} and coupled to STAT3 signaling, does not provide a significant metabolic signal or exacerbate STAT3 deficiency when deleted in LepRb neurons. While its absence does not appear to have a metabolic consequence, it does result in increased gliosis in the

hypothalamus and STAT1 expression in neighboring non-LepRb neurons. STAT1^{LepR}KO animals are then an example of lean mice that experiences gliosis and points to the importance of the LepRb neuronal interaction with neighboring cells. Therefore, the gliosis observed in diet-induced obesity (DIO) may not necessarily drive obesity but it may instead be a consequence of the cross-talk between LepRb neurons and microglia/astrocytes.[17]

Finally, DIO is at times considered a state of STAT3-deficiency; there are clear phenotypic similarities between DIO and STAT3^{LepR}KO mice: both are obese, hyperleptinemic, and do not phenotypically or immunohistochemical (via pSTAT3-IR) respond to exogenous leptin treatment. However, our TRAP-seq analyses demonstrate that *Stat1* and *Stat3* fold change expression in LepRb neurons under DIO are dissimilar to those in STAT3^{LepR}KO. While this body of work examined the metabolic consequence of deleting STAT proteins, future work should examine the interactions between STAT1 and STAT3 during elevated states like DIO.

Materials and Methods

Mice.

Mice were bred in our colony in the Unit for Laboratory Animal Medicine at the University of Michigan; these mice and the procedures performed were approved by the University of Michigan Committee on the Use and Care of Animals and in accordance with AALAC and NIH guidelines. We purchased male and female C57BL/6 mice (Jackson stock #000664) and *ob/ob* mice (Jackson stock #000632) for experiments and breeding studies from Jackson Labs. STAT1^{flox} (Jackson stock #012901) and STAT3^{flox}

(Jackson stock #016923) mice were also from Jackson. Mice were bred at the University of Michigan and provided with food and water *ad libitum* in temperature controlled rooms on a 12-hour light-dark cycle.

We generated $LepR^{eGFP}$ mice by crossing $LepR^{cre}$ mice[18] onto the eGFP-L10a background to generate $LepR^{cre/+}$;$Rosa26^{eGFP\text{-}10a/+}$ mice,[19] which we then intercrossed to generate double homozygous $LepR^{cre/cre}$;$Rosa^{eGFP\text{-}10a/eGFP\text{-}L10a}$ ($LepR^{eGFP}$) study animals. $LepR^{eGFP}$ mice were backcrossed to *ob/ob* mice until $LepR^{cre/cre}$;$Rosa^{eGFP\text{-}L10a/eGFP\text{-}L10a}$;*ob*/+ mice were obtained. These mice were subsequently intercrossed to generate $LepR^{cre/cre}$;$Rosa^{eGFP\text{-}L10a/eGFP\text{-}L10a}$;*ob/ob* ($LepR^{eGFP}$*ob/ob*) and $LepR^{crecre}$;$Rosa^{eGFP\text{-}L10a/eGFP\text{-}L10a}$;+/+ ($LepR^{eGFP}$) control mice for study. $STAT3^{flox}$ mice were backcrossed to $LepR^{eGFP}$ mice to generate $LepR^{eGFP\text{-}L10a}$;$STAT3^{flox/+}$ mice. These mice were then intercrossed to generate $LepR^{cre/cre}$;$Rosa^{eGFP\text{-}L10a/eGFP\text{-}L10a}$;$STAT3^{flox/flox}$ ($STAT3^{LepR}$KO) and $LepR^{cre/cre}$;$Rosa^{eGFP\text{-}L10a/eGFP\text{-}L10a}$;STAT3+/+ ($LepR^{eGFP}$) control mice for study. $STAT1^{flox}$ mice were then crossed to $STAT3^{LepR}$KO mice to generate $LepR^{cre/cre}$;$Rosa^{eGFP\text{-}L10a/eGFP\text{-}L10a}$;$STAT3^{flox/+}$;$STAT1^{flox/+}$, which were intercrossed to generate $LepR^{cre/cre}$;$Rosa^{eGFP\text{-}L10a/eGFP\text{-}L10a}$;$STAT3^{flox/flox}$ ($STAT3^{LepR}$KO), $LepR^{cre/cre}$;$Rosa^{eGFP\text{-}L10a/eGFP\text{-}L10a}$;$STAT1^{flox/flox}$;$STAT3^{flox/flox}$ (STAT1$STAT3^{LepR}$KO) mice for study. $LepR^{s/s}$ mice and controls were generated as previously described.[20]

Leptin treatment, high-fat diet, SMLA treatment, and fasting.

For $LepR^{STAT1}$ and $LepR^{STAT3}$ fold induction TRAP-seq experiments, mice were weaned onto either a standard chow diet (Purina Lab Diet 5001) or a 60% high-fat diet (Research Diets D12492, 60% kcal from fat) for at least 8 weeks and were dissected at

12-14 weeks of age. Food was removed at the onset of the light cycle and mice were treated four hours later with metreleptin (5mg/kg, i.p.), PASylated superactive mouse leptin antagonist (SMLA; Protein Laboratories Rehovot; 100pmol/g; i.p.), vehicle (0.9% sodium chloride; Hospira; i.p.). For the fasting condition, mice were fasted for 24 hours. All conditions were compared to the control $LepR^{eGFP}$ vehicle injected animals raised on standard chow. For immunohistochemistry, mice had food removed at the onset of the light cycle. Animals were treated four hours later with metreleptin (5mg/kg, i.p.) and subjected to perfusion 90 minutes after treatment.

Immunohistochemistry.

Prior to perfusion, mice were anesthetized with a lethal dose of pentobarbital and transcardially perfused with phosphate buffered saline (PBS) followed by 10% buffered formalin. Brains were removed, placed in 10% buffered formalin overnight, and dehydrated in 30% sucrose for one week. Using a freezing microtome (Leica), brains were cut into 30 um sections. Sections were treated sequentially with 1% hydrogen peroxide/0.5% sodium hydroxide, 0.3% glycine, 0.03% sodium dodecyl sulfate, and blocking solution (PBS with 0.1% triton, 3% Normal Donkey Serum). Immunostaining was performed using primary antibodies for pSTAT3 (Cell Signaling #9145, 1:1000), GFP (Aves Labs #GFP1020, 1:1000), STAT1 (Santa Cruz sc-346, 1:250), dsRed (Living Colors #632496, 1:1000), Iba1 (Wako, 1:1000), and GFAP (Millipore, 1:500). All antibodies were reacted with species-specific Alexa Fluor-488 or -568 conjugated secondary antibodies (Invitrogen, 1:200) or processed with the avidin-biotin/diaminobenzidine (DAB) method (ABC kit, Vector Labs, 1:500; DAB reagents, Sigma). Images were collected on an Olympus BX53F microscope. DAB images were

pseudocolored using Photoshop software. Quantification was performed on anatomically matched brain regions with pre-set regions of interest using the Olympus BX53F software. Both sides of the arcuate nucleus were counted and groups means were determined (n=10-14 animals per group).

In situ hybridization.

For *in situ hybridization* (ISH), adult STAT1^{LepR}KO, STAT3^{LepR}KO, STAT1STAT3^{LepR}KO and wildtype control mice were anesthetized with isoflurane and then euthanized by decapitation. Whole brains were dissected, flash frozen in isopentane, chilled on dry ice and stored at -80°C. 16 µm-thick coronal sections were cut on a cryostat (Leica), thaw-mounted to SuperFrost Plus slides, allowed to dry at -20°C for one hour and then stored at -80°C. Slides were then processed for ISH using RNAScope technology per the manufacturer's protocol (Advanced Cell Diagnostics). For all slides, the multiplex fluorescent assay (320850) was used to visualize Stat1 (11ZZ) and Cre (312281-C3) probes using Amp 4 Alt-A. Images were obtained with an Olympus BX53F and QImaging Retiga 6000 monochrome camera under 40X objective. All images were processed identically in CellProfiler (Lamprecht MR 2007 Biotechniques) to reduce nonspecific background. Serial images (16 per arcuate nucleus) were taken and stitched together using Photoshop (Adobe).

Phenotyping of STAT-null mice and control mice.

STAT1^{LepR}KO, STAT3^{LepR}KO, STAT1STAT3^{LepR}KO and littermate control (LepR^{cre}) mice were weaned into individual housing at 21 days and fed normal chow (Purina Lab Diet 5001). Weekly body weight and food intake were monitored. Unfasted

blood glucose sample was take every other week from 4-12 weeks of age. Glucose tolerance test (2g/kg body weight, i.p.) and insulin tolerance test (1 unit/kg body weight, Humulin (Eli Lilly), i.p.) were performed in 13 and 14 week old mice, respectively, after a 5 hour fast three hours after the start of the light-cycle. Analysis of body fat and lean mass was performed at 15 weeks of age using NMR-based analyzer (Minispec LF90II, Bruker Optics). Leptin and insulin were assayed by commercial ELISA (Crystal Chem).

Hypothalamic and arcuate dissections for TRAP-seq and RT-PCR.

At the midpoint of the light cycle, adult homozygous mice were anesthetized with isoflurane, had their brains removed and placed onto a mouse coronal brain matrix (1mm sections). For whole hypothalamic dissections, a 3x3x3mm block was dissected from the ventral diencephalon immediately caudal to the optic chiasm and immediately homogenized for TRAP-seq analysis. For arcuate specific dissections, 3 consecutive 1mm sections were removed immediately caudal to the optic chiasm, and arcuate nuclei were dissected bilaterally by hand from the mediobasal hypothalamus of each section, pooled and snap frozen for later processing.

Translating Ribosome Affinity Purification with deep sequencing (TRAP-seq).

We employed anti-eGFP Translating Ribosome Affinity Purification (TRAP) using hypothalamic material from PBS and leptin treated $LepR^{eGFP}$, $LepR^{LepR}$*ob/ob*, and $STAT3^{LepR}$KO mice (which all express an eGFP-tagged ribosomal subunit in LepR cells). Messenger RNA isolated from eGFP-tagged ribosomes and from the eGFP-depleted fraction was assessed for quality using TapeStation (Agilent, Santa Clara, CA) and samples with RNA Integrity Numbers (RINs) of 8 or greater were prepared using

the Illumina TruSeq mRNA Sample Prep v2 kit (Catalog # RS-122-2001 and #RS-122-2002) (Illumina, San Diego, CA), where 0.1-3ug of RNA was converted to mRNA using a polyA purification. The mRNA was chemically fragmented and copied into first strand cDNA using reverse transcriptase and random primers. The 3' ends of the cDNA were adenylated and the 6-nucleotide-barcoded adapters ligated. These products were then purified and enriched by PCR to create the cDNA library, which were checked for quality and quantity by TapeStation (Agilent) and qPCR using Kapa's library quantification kit for Illumina Sequencing platforms (catalog #KK4835) (Kapa Biosystems, Wilmington MA). They were clustered on cBot (Illumina) and sequenced 4 samples per lane on a 50 cycle single end run on a HiSeq 2000 (Illumina) using version 2 reagents according to manufacturer's protocols.

RNA-seq analysis

50 base pair single end reads underwent QC analysis prior to alignment to mouse genome build mm10 using TopHat and Bowtie alignment software.[21] Differential expression was determined using Cufflinks Cuffdiff analysis, with thresholds for differential expression set to fold change >1.5 or <0.66 and a false discovery rate of </0.05 [22]. Lists of differentially expressed genes were then queried against the Uniprot Database for gene ontology and protein class analysis.[23]

RNA extraction of arcuate nuclei and analysis by RT-qPCR.

RNA was extracted from microdissected hypothalamic using Trizol (Invitrogen) according to manufacturer's protocol and subsequently converted to cDNA using iScript cDNA synthesis kit (Biorad #170-8891) for use in reverse transcription PCR. cDNA was

analyzed in triplicate by quantitative real time PCR on an Applied Biosystems StepOnePlus Real-Time PCR System for TBP (endogenous control) and the following: *Socs3*, *Atf3*, *JunB*, *Arid5a*, *Etv6*, *Fos*, *Slco1a4*, *Ghrh*, *Agrp*, *Pomc*, *Serpina3h*, *Tbx19*, *Pltp*, and *Gdd45g*. All Taqman assays were acquired from Applied Biosystems (Foster City, CA). We calculated relative mRNA expression values using the $2^{-\Delta\Delta Ct}$ method with normalization of each sample ΔCt value to the average ΔCt value from the control mice.

Statistics.

Data are reported as mean +/- SEM. RT-qPCR data are reported as mean fold change compared to normalized vehicle. Statistical analysis of physiological data was performed with Prism software (version 7). Unpaired t-test was used to compare results between two groups. Body weight gain, cumulative food intake, body length, GTT and ITT were analyzed by two-way ANOVA. $P<0.05$ was considered statistically significant.

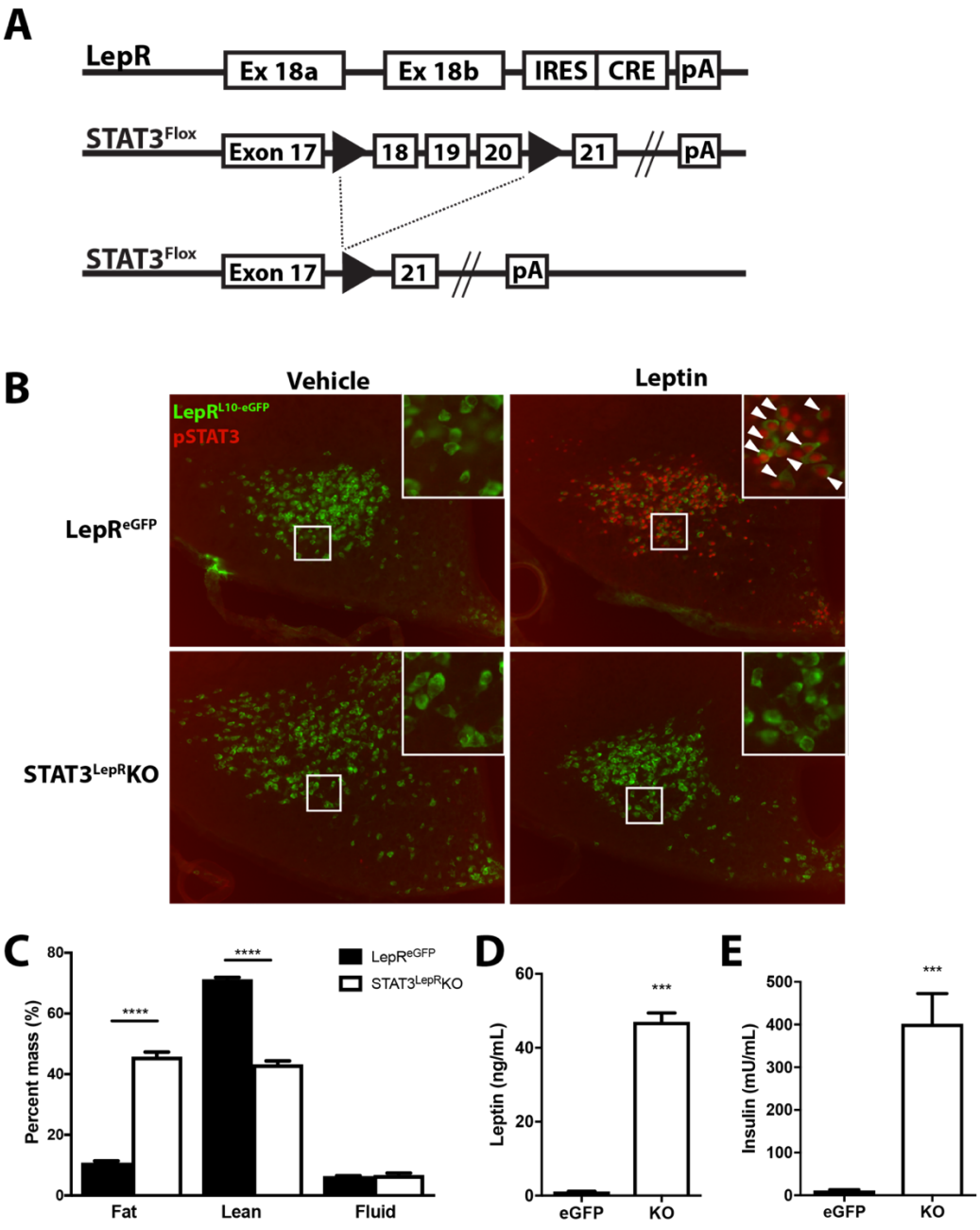

Figure 3.1: Deletion of STAT3 in LepRb neurons. (A) Schematic diagram showing the cross of $LepR^{cre}$ with $STAT3^{flox}$ mice to generate $STAT3^{LepR}KO$ mice through excision of exons 18 to 20 of the STAT3 gene. **(B)** Representative images showing colocalization of pSTAT3-IR (red) with GFP-IR (green) in the PMv of $STAT3^{LepR}KO$ and $LepR^{cre}$ control mice (both of which are on the $Rosa^{26eGFP-L10a}$ background) treated with leptin (5mg/kg; i.p.) or PBS vehicle for 90 minutes. Arrows denote dual labeled neurons. **(C)** $STAT3^{LepR}KO$ and $LepR^{cre}$ control mice underwent body composition analysis by NMR spectroscopy. Blood serum from mice were assayed for leptin **(D)** and insulin **(E)**. n=15 per group. Mean +/- SEM; ***p<0.001 by unpaired t-test; ***p<0.0001 by unpaired t-test for **(C-E)**; PMv: ventral premammillary nucleus.

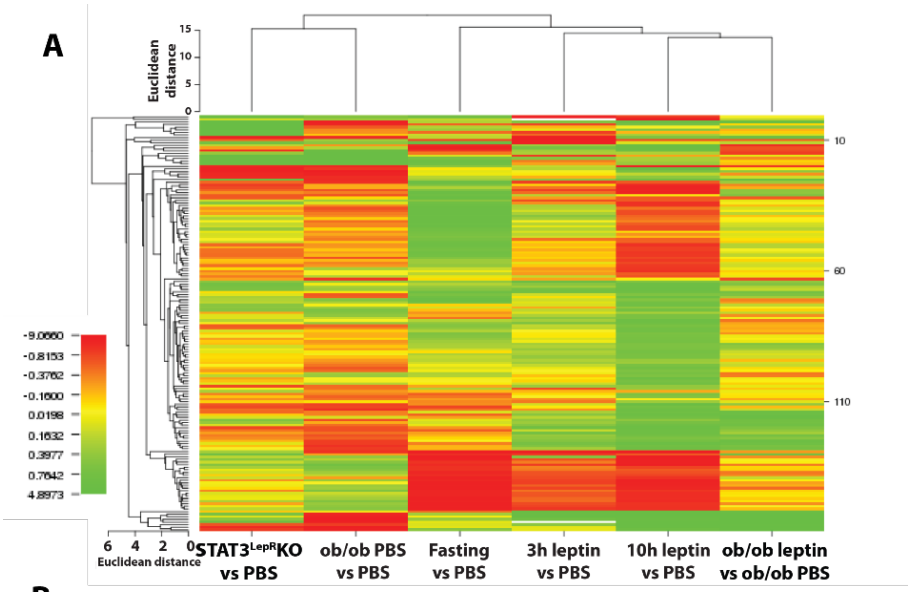
A
Euclidean distance
15
10
5
0
10
60
110
-9.0660
-0.8153
-0.3762
-0.1600
0.0198
0.1632
0.3977
0.7642
4.8973
6 4 2 0
Euclidean distance
STAT3LepRKO vs PBS
ob/ob PBS vs PBS
Fasting vs PBS
3h leptin vs PBS
10h leptin vs PBS
ob/ob leptin vs ob/ob PBS

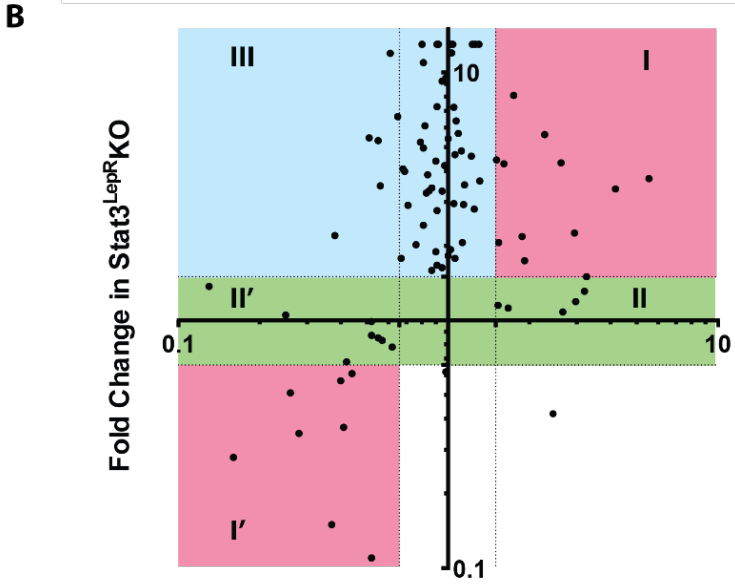
B
III
I
II′
II
I′
10
0.1
10
0.1
Fold Change in Stat3LepRKO
Fold change in ob/ob

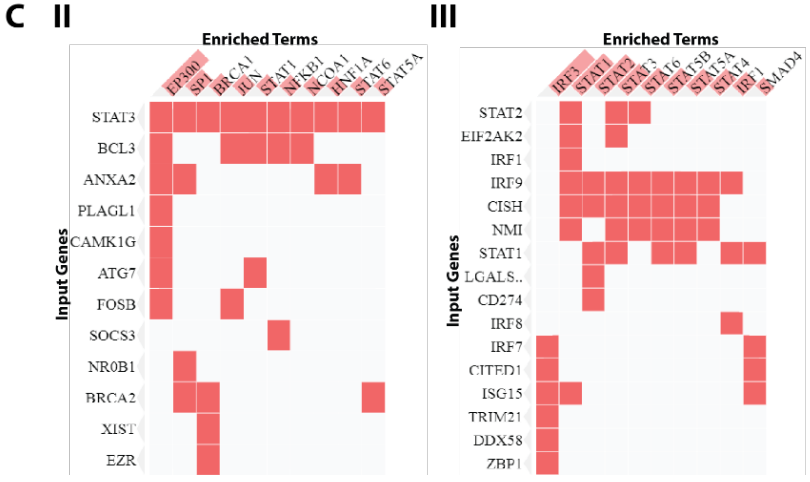
C
II
Enriched Terms
EP300
SP1
BRCA1
JUN
STAT1
NFKB1
NCOA1
HNF1A
STAT6
STAT5A
STAT3
BCL3
ANXA2
PLAGL1
CAMK1G
ATG7
FOSB
SOCS3
NR0B1
BRCA2
XIST
EZR
Input Genes
III
Enriched Terms
IRF3
STAT1
STAT2
STAT3
STAT6
STAT5B
STAT5A
STAT4
IRF1
SMAD4
STAT2
EIF2AK2
IRF1
IRF9
CISH
NMI
STAT1
LGALS..
CD274
IRF8
IRF7
CITED1
ISG15
TRIM21
DDX58
ZBP1
Input Genes

Figure 3.2: LepRb-enriched genes regulated by STAT3 and leptin action. Translating ribosome affinity purification (TRAP) was performed in STAT3^{LepR}KO, LepR^{eGFP}*ob/ob*, and LepR^{eGFP} mice. **(A)** Fold change values for each of the groups were calculated and compared to littermate control PBS-treated LepR^{eGFP} or PBS-treated LepR^{eGFP}*ob/ob* mice. Each sample comprised of pooled hypothalamic for 5-8 adult animals. n=3-4 pooled samples per condition. **(B)** Both fold change values for STAT3^{LepR}KO mice and LepR^{eGFP} *ob/ob* mice were calculated compared to control LepR^{eGFP} mice; fold change values are plotted and dashed lines are at FC=1.5 and FC=0.667 for both axes. **(C)** The genes in groups II and III are detailed with their corresponding list of transcription factors, as determined by the Transcription Factors Protein Protein Interactions database through Enrichr.

	Fold Change in TRAP			Fold Change in Arcuate		
Gene	**Enrichment**	***ob/ob***	**STAT3^{LepR}KO**	***ob/ob***	**STAT3^{LepR}KO**	***Lepr$^{s/s}$***
Agrp	75.34	***5.55***	***3.73***	***1.75***	***3.28***	***3.87***
Stat1	1.43	***0.56***	***3.49***	***0.73***	***1.46***	0.96
Stat3	2.61	***0.52***	0.87	***0.79***	0.94	0.89
Psmb8	2.37	0.8	***13.81***	1.74	***4.65***	1.4
Irf1	1.88	0.71	***2.91***	0.98	1.51*	0.78
Irf9	2.19	***0.38***	***2.2***	***0.66***	1.2	***0.67***
Gch1	8.99	***0.51***	0.81	***0.57***	1.04	1.03
Socs3	2.51	***0.25***	1.05	***0.48***	0.76	1.34

Table 3.1: Fold change in *ob/ob*, STAT3^{LepR}KO, and Lepr$^{s/s}$ mice as determined by TRAP or qPCR. TRAP-Seq was performed on STAT3^{LepR}KO, LepRb^{eGFP} and LepRb^{eGFP}*ob/ob* mice. Genes enriched (FPKM in TRAP/FPKM in TRAP-depleted >1.5) at baseline, or that became enriched in a condition in which they were also significantly changed, were included in this analysis. Enrichment and expression (FPKM) values displayed are from LepRb^{eGFP} mice. Fold change values as determined by RNA-Seq for STAT3^{LepR}KO mice were versus LepRb^{eGFP} controls **(Column 4)**, Fold change values as determined by RNA-Seq for LepRb$^{eGFP\text{-}L10a}$*ob/ob* **(Column 3)** are versus 10-hour vehicle treated LepRb^{eGFP}. N=3-4 samples per treatment group. Each sample was comprised of pooled hypothalami of 4-6 adult animals. Whole RNA was also isolated from the arcuate nuclei of adult *ob/ob* and c57bl6 controls, Lepr$^{s/s}$ and Lepr$^{+/+}$ controls, and STAT3^{LepR}KO and LepRb^{eGFP} mice (n=8-10 mice per group). Changes in transcript expression were assayed by RT-qPCR using ABI Taqman assays for the listed genes, and *Tbp* as an endogenous control. p<.05 for values in bold and italics. *p=0.053.

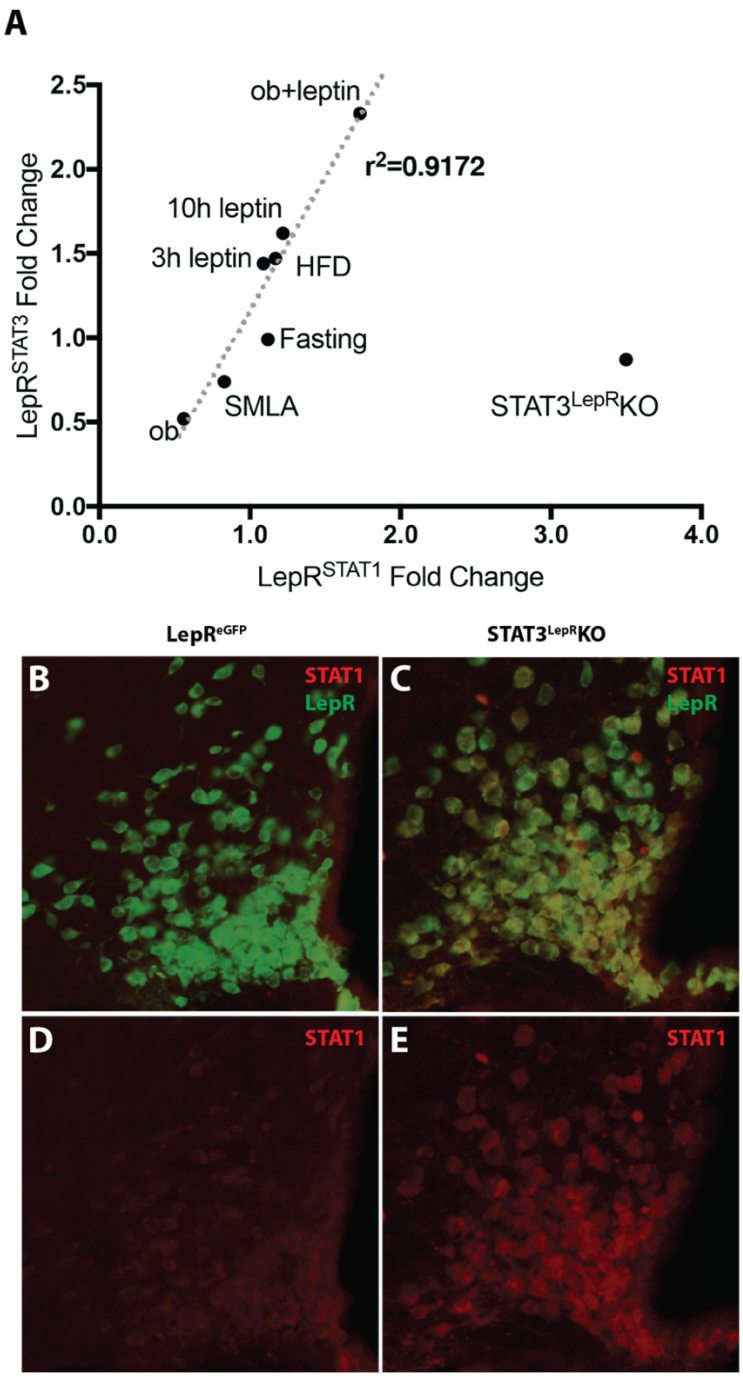

Figure 3.3: STAT1 increases in STAT3 absence. (A) TRAP-seq was performed on STAT3^{LepR}KO mice; LepR^{eGFP}*ob/ob* mice treated with PBS or leptin; and LepR^{eGFP} mice treated with leptin, SMLA antagonist, HFD, or fasting; STAT1 and STAT3 fold changes values (compared against control LepR^{eGFP} STAT1 and STAT3 expression) are plotted and the line of best fit is shown for all conditions except the STAT3^{LepR}KO outlier. **(B-E)** Representative images showing colocalization of STAT1-IR (red) and GFP-IR (green) in LepR^{eGFP} mice, and STAT3^{LepR}KO mice.

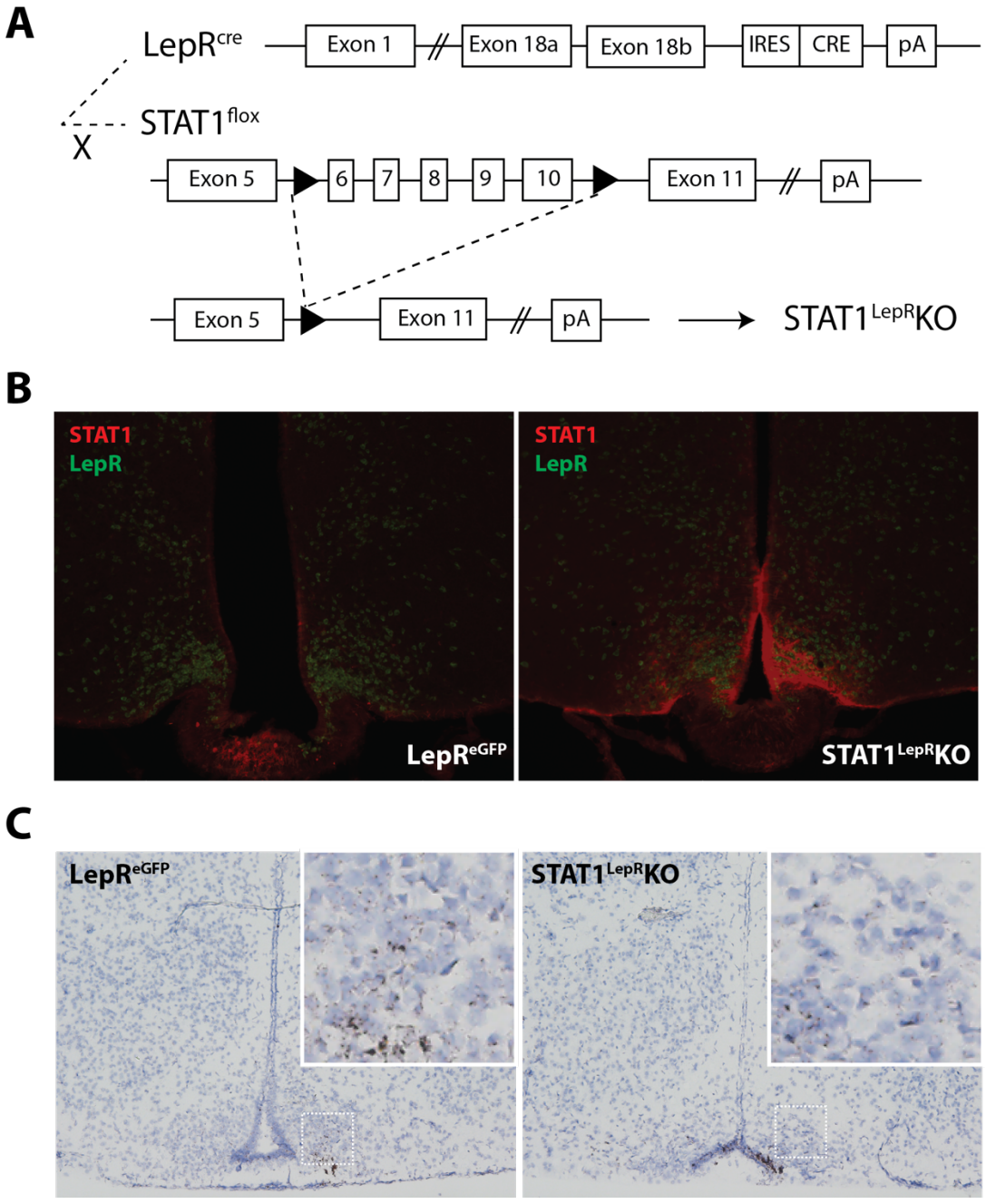

Figure 3.4: Deletion of STAT1 in LepRb neurons. (A) Schematic diagram showing the cross of $LepR^{cre}$ with $STAT1^{flox}$ mice to generate $STAT1^{LepR}KO$ mice through excision of exons 6 to 10 of the STAT1 gene. **(B)** Representative images showing colocalization of STAT1-IR (red) with GFP-IR (green) in the hypothalamus of $STAT1^{LepR}KO$ and $LepR^{cre}$ control mice (both of which are on the $Rosa^{26eGFP-L10a}$ background). **(C)** Representative ISH images showing Stat1 (brown) in the arcuate nucleus of control $LepR^{cre}$ and $STAT1^{LepR}KO$ mice.

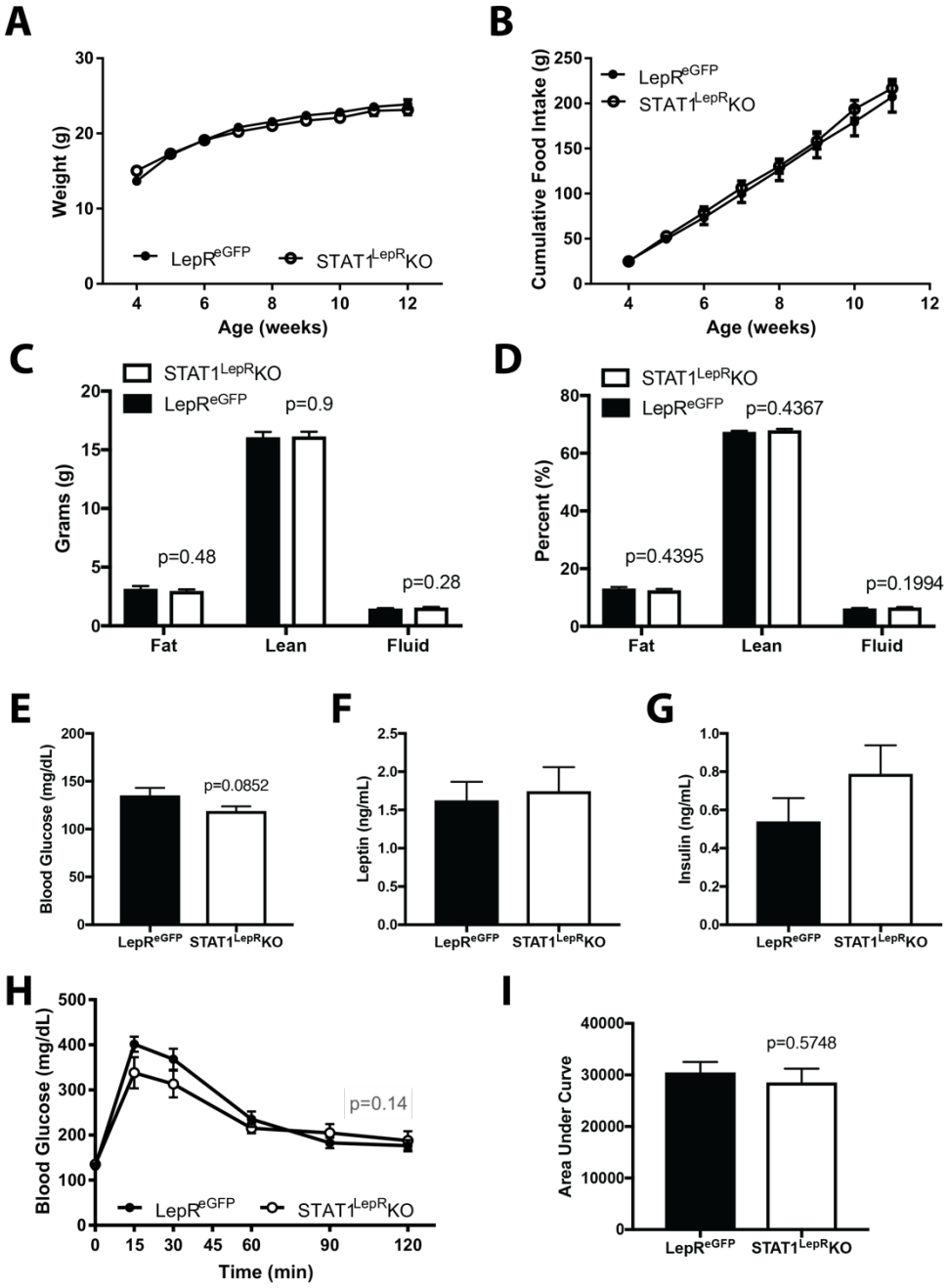

Figure 3.5: LepR^{STAT1} does not regulate energy balance. (A) Male STAT1^{LepR}KO and LepR^{eGFP} (littermate control) mice were placed on chow and body weight **(A)** measured weekly, and cumulative food intake **(B)** measured weekly. **(C-D)** At 14 weeks of age, animals underwent body composition by NMR spectroscopy. **(E)** Glucose concentration for male 12-week-old mice. Serum from 12-week-old mice were assayed for leptin **(F)** and insulin **(G)**. Mice at weeks 12-14 of age were treated with **(H)** glucose (2g/kg; i.p.) and blood glucose concentrations were measured, and area under the curve analysis **(I)** was performed. N=10-15 for all genotypes. ANOVA analysis was performed for **(A, B, H)**; unpaired t-test was performed for **(C-G, I)**.

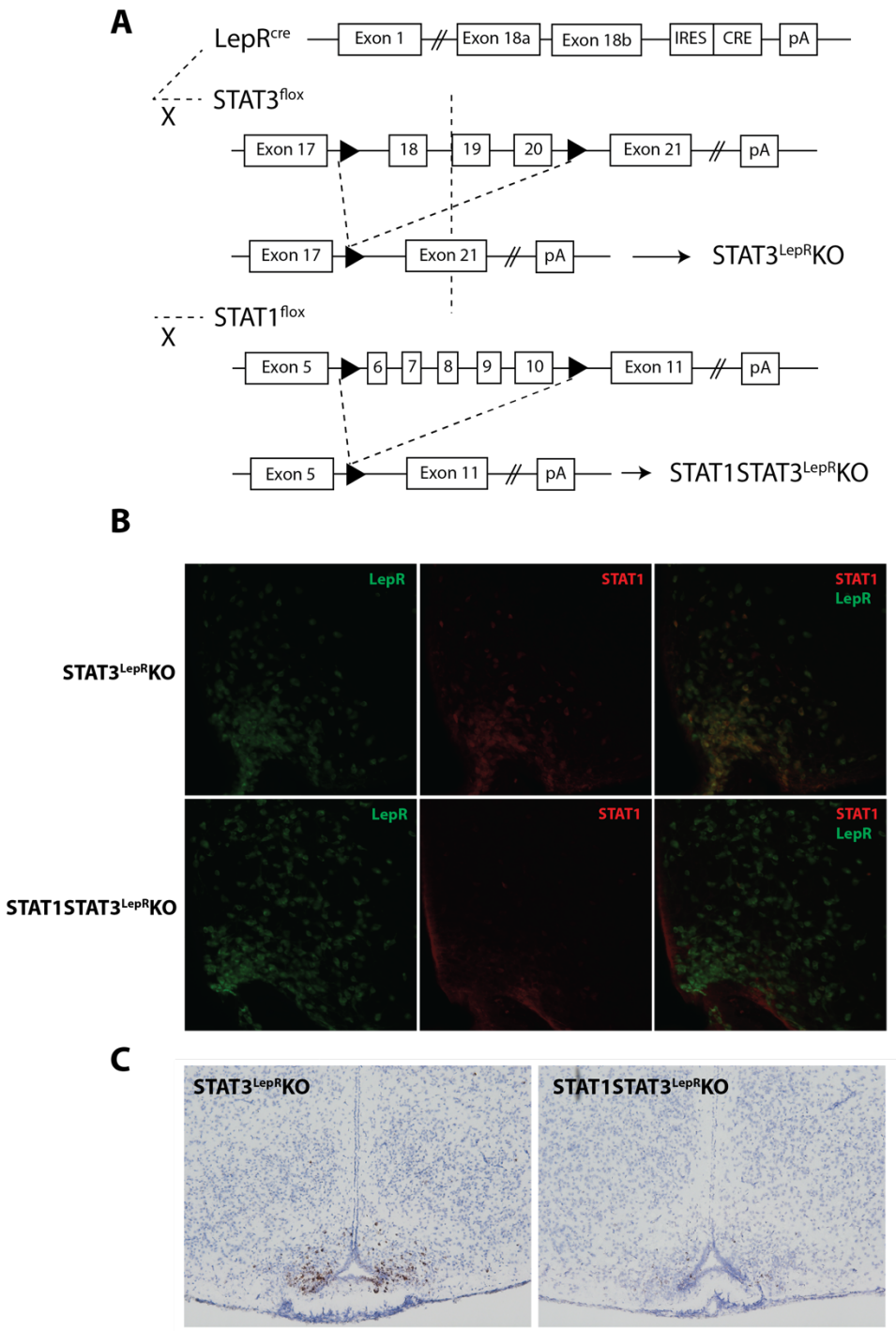

Figure 3.6: Deletion of STAT1 and STAT3 in LepRb expressing neurons. (A) Schematic diagram showing the cross of LepR^{cre} with STAT1^{flox} and STAT3^{flox} mice to generate STAT3^{LepR}KO and STAT1STAT3^{LepR}KO mice. pA: polyadenylation signal. **(B)** Representative images showing colocalization of STAT1-IR (red) with GFP-IR (green) in the arcuate nucleus of STAT3^{LepR}KO and STAT1STAT3^{LepR}KO (both of which are on the Rosa26$^{eGFP-L10a}$ background) mice. **(C)** Representative ISH images showing *Stat1* (brown) in the ARC of STAT3^{LepR}KO and STAT1STAT3^{LepR}KO mice.

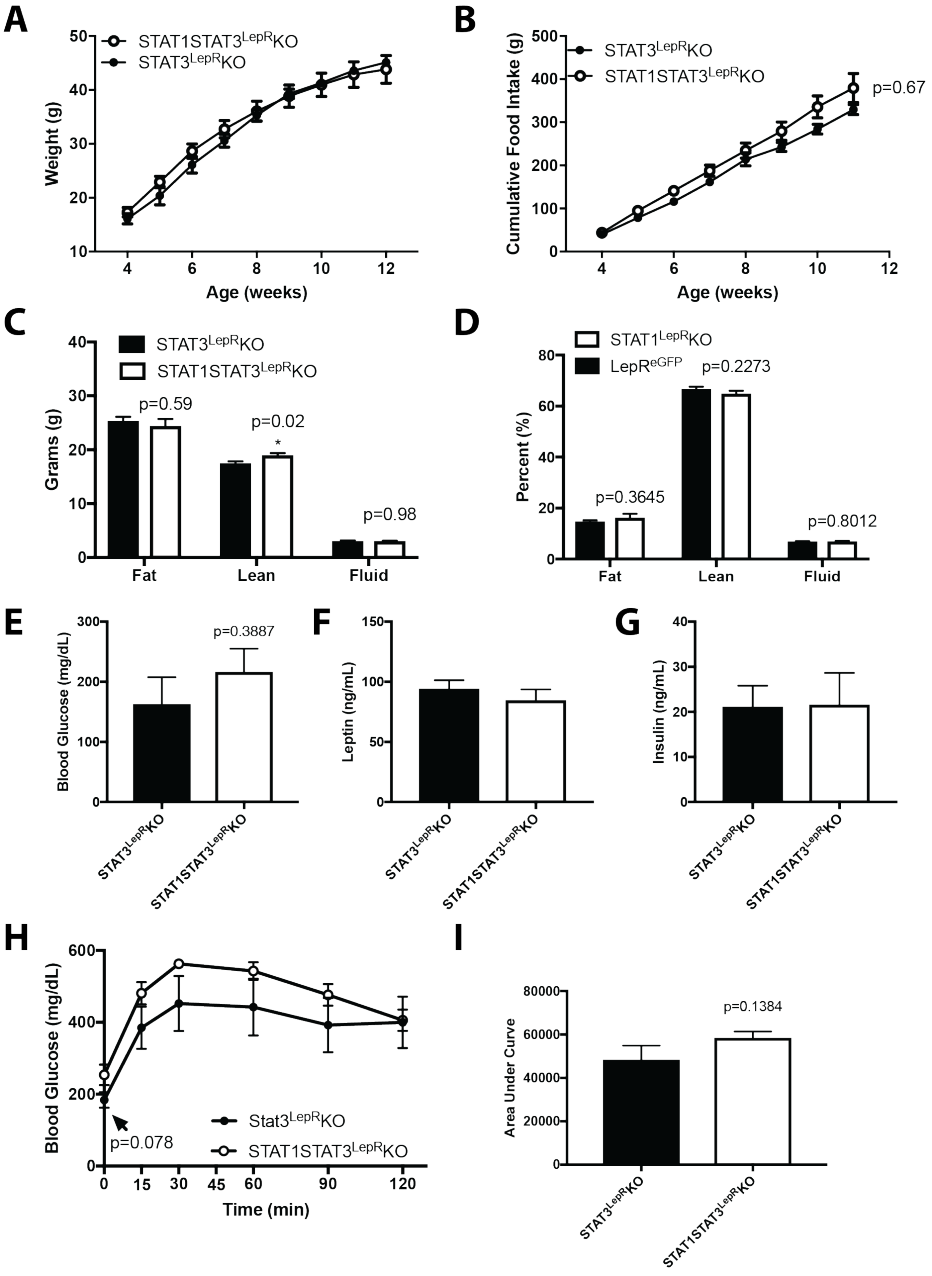

Figure 3.7: Ablation of STAT1 does not exacerbate metabolic parameters in mice that lack STAT3 in LepRb-expressing neurons. Male STAT3^{LepR}KO and STAT1STAT3^{LepR}KO mice were placed on chow and body weight **(A)** and cumulative food intake **(B)** were measured weekly. **(C, D)** At 14-15 weeks of age, animals underwent body composition analysis by NMR spectroscopy. **(E)** Blood glucose concentrations for 12-week-old male STAT3^{LepR}KO and STAT1STAT3^{LepR}KO mice. Serum from 12-week-old mice were assayed for leptin **(F)** and insulin **(G)**. **(H)** Mice at 12-14 weeks of age were treated with glucose (2g/kg; i.p) and blood glucose concentrations were measured. **(I)** Area under the curve analysis for GTT was performed. N=8-14 per genotype. ANOVA analysis was performed for **(A, B, H)**; unpaired t-test was performed for **(C-G, I)**.

Combined total enriched list	Enrichment (WT)	FPKM (WT)	*ob/ob*	Stat3 KO	Stat3/ob	Group
9230105E10Rik	0.40	0.34	1.61	***4.28***	***4.97***	I
Adrb2	0.86	0.34	2.07	***3.08***	1.34	
Agrp	75.34	229.60	***5.55***	***3.73***	0.73	
Apoa1	0.93	0.73	***2.25***	1.99	0.73	
Apol9a	1.87	0.14	1.75	***8.08***	***6.57***	
Ccl17	1.73	1.81	***2.62***	***4.32***	0.85	
Cdhr3	1.60	0.46	***1.84***	1.89	0.73	
Fam159a	4.79	6.09	***2.94***	***2.25***	0.88	
Fosl2	0.95	2.31	***3.26***	1.50	***0.65***	
Gdpd3	1.34	4.79	***1.54***	***2.06***	0.90	
Gm885	1.81	0.30	***7.88***	3.01	1.11	
Il18bp	0.32	0.65	2.28	***5.62***	***4.37***	
Isg20	0.34	0.20	2.64	***7.83***	1.90	
Krtap17-1	2.88	1.35	***2.07***	1.56	0.53	
Maff	1.47	1.37	***1.88***	***2.18***	0.83	
Nmb	0.93	3.45	***4.14***	1.73	0.54	
Npy	24.98	1152.79	***4.17***	***3.39***	0.86	
Rbp4	2.05	10.30	***1.92***	***1.74***	0.93	
Samd9l	0.65	0.34	1.51	***4.44***	***5.80***	
Spink8	0.59	0.56	3.50	***5.07***	1.55	
Cartpt	11.37	661.42	***0.28***	***0.35***	1.07	I'
Gm5779	1.71	2.17	0.52	***0.11***	***0.14***	
Npy2r	3.72	18.83	***0.44***	***0.61***	***1.78***	
Nts	5.39	113.14	***0.41***	***0.37***	0.93	
Pomc	37.76	539.53	***0.16***	***0.28***	1.39	
Serpina3n	13.18	69.85	***0.26***	***0.51***	***1.97***	
Tmem176a	3.92	32.57	***0.40***	***0.57***	1.38	
Tnfrsf11b	3.22	1.31	***0.42***	0.58	1.77	
Tuba1c	1.42	10.46	***0.37***	***0.15***	***0.21***	
Ucn	14.97	16.44	***0.35***	***0.31***	0.54	
Bahcc1	2.58	5.86	***1.86***	1.02	0.73	II
Brca2	1.22	1.26	***1.56***	1.27	0.85	
Btg1	1.39	11.68	***1.55***	1.29	0.88	
Camk1g	2.41	31.35	***1.53***	1.15	***0.64***	
Ctla2a	0.82	2.47	***2.97***	1.19	***0.52***	

Cyp4v3	1.06	0.99	***2.20***	1.32	0.85	
Ezr	1.41	7.02	***1.51***	1.45	1.08	
Fam46a	1.73	5.37	***1.73***	1.11	0.80	
Fosb	1.32	1.05	***3.20***	1.31	***0.38***	
Gem	1.76	1.91	***1.67***	1.12	***0.50***	
Ghrh	11.83	56.26	***2.66***	1.08	***0.36***	
Ghsr	3.73	2.21	***1.74***	1.24	0.75	
Hs3st1	0.82	7.56	***2.06***	1.33	0.82	
N4bp2l1	1.83	49.33	***1.50***	1.37	0.96	
Rpl22l1	2.30	657.56	***1.51***	1.16	1.14	
Rplp2	1.92	941.48	***1.51***	1.24	0.86	
Snhg8	1.45	24.62	***1.65***	1.28	0.78	
Tnrc18	2.32	14.56	***1.59***	0.92	0.80	
Xist	2.91	1.92	***2.47***	1.48	***2.22***	
Anxa2	1.34	11.51	***0.63***	0.89	1.48	**II'**
Asb4	9.86	63.03	***0.61***	0.76	1.39	
Atg7	8.52	61.48	***0.42***	0.68	***1.83***	
Bcl3	1.86	0.71	***0.43***	0.90	1.45	
Chodl	2.01	4.61	***0.62***	0.79	1.49	
Fam179a	1.89	3.45	***0.66***	0.80	1.02	
Gch1	8.99	14.49	***0.51***	0.81	1.31	
Gstm6	3.04	45.54	***0.62***	0.83	1.03	
Gsx1	12.87	9.73	***0.64***	0.98	1.14	
Irs4	5.62	55.04	***0.60***	0.82	1.39	
Nr0b1	7.73	2.57	***0.49***	0.82	1.33	
Plagl1	2.97	33.71	***0.55***	0.85	***1.54***	
Serpina3i	31.59	0.58	***0.13***	1.37	***6.18***	
Socs3	2.51	1.94	***0.25***	1.05	***3.65***	
Stat3	2.61	31.53	***0.52***	0.87	***1.63***	
Tac1	4.55	301.96	***0.57***	0.83	***1.72***	
Tmem176b	2.79	57.43	***0.55***	0.71	1.29	
Tnfaip8l3	1.71	5.26	***0.53***	0.77	1.58	
Vwa5a	2.27	6.88	***0.52***	0.99	***2.04***	
Yeats2	5.46	37.38	***0.62***	0.78	***1.51***	
1500012F01Rik	1.70	137.17	1.34	***1.69***	1.06	**III**
Apol6	0.94	0.37	1.12	***4.82***	***3.92***	
B2m	1.77	60.49	0.82	***6.09***	***10.66***	
Bst2	1.11	1.45	1.30	***49.14***	***47.84***	

Casp1	0.54	0.37	0.90	***4.39***	***4.66***	
Cd274	2.51	2.52	0.84	***3.87***	***5.49***	
Cish	1.25	3.78	0.67	***1.78***	***2.06***	
Cited1	8.86	122.41	1.22	***1.59***	1.09	
Ddx58	1.11	0.89	1.25	***2.81***	***2.76***	
Dhx58	0.68	0.51	0.83	***3.26***	***3.13***	
Dtx3l	1.28	0.96	0.85	***3.33***	***5.22***	
Eif2ak2	1.20	2.51	1.15	***3.52***	***3.06***	
Gbp2	1.24	0.51	1.00	***5.41***	***9.18***	
Gbp3	0.82	0.53	0.54	***27.82***	***90.13***	
Gbp4	1.58	0.21	0.38	***14.57***	***48.45***	
Gbp6	0.95	0.48	0.69	***3.99***	***6.93***	
Gbp9	2.58	0.46	0.51	***5.45***	***17.25***	
Gm12250	1.05	0.07	1.23	***130.58***	***182.66***	
Gm4841	0.54	0.12	1.03	***11.99***	***13.57***	
Gm4951	0.44	0.09	1.26	***39.21***	***37.92***	
Gm6548	1.33	2.75	1.13	***2.06***	***1.91***	
H2-Aa	0.44	0.76	0.95	***3.32***	***5.27***	
H2-Bl	1.48	2.64	1.27	***3.23***	0.65	
H2-D1	2.22	17.38	0.91	***2.77***	***3.19***	
H2-Gs10	1.31	1.53	0.98	***9.50***	***11.07***	
H2-K1	1.15	4.13	0.81	***10.96***	***16.51***	
H2-Q6	17.57	0.48	0.34	***19.77***	***60.79***	
H2-Q7	2.44	0.73	0.41	***16.87***	***23.98***	
H2-Q8	6.44	0.62	0.65	***6.64***	***5.66***	
H2-T23	1.90	6.47	1.31	***3.65***	***2.87***	
I830012O16Rik	0.60	0.95	0.87	***3.42***	***3.76***	
Ifi35	1.84	2.22	0.79	***5.23***	***6.16***	
Ifi44	1.70	0.13	0.91	***15.12***	***28.50***	
Ifi47	2.23	0.42	0.48	***49.06***	***152.81***	
Ifit1	0.72	0.67	0.92	***29.69***	***39.38***	
Ifit2	0.64	3.66	1.14	***2.93***	***2.93***	
Ifit3	0.51	1.43	1.07	***6.37***	***6.49***	
Igtp	1.83	1.76	0.64	***15.40***	***25.13***	
Iigp1	0.81	0.23	0.60	***33.53***	***90.96***	
Irf1	1.88	4.24	0.71	***2.91***	***3.76***	
Irf7	1.66	0.97	1.09	***5.68***	***4.33***	
Irf8	0.40	0.59	0.97	***4.21***	***5.71***	

Irf9	2.19	7.68	***0.38***	***2.20***	***5.69***	
Irgm1	1.10	5.68	1.05	***7.24***	***7.65***	
Irgm2	0.98	0.65	0.59	***22.91***	***51.99***	
Isg15	0.42	1.03	0.53	***31.03***	***51.26***	
Lgals3bp	2.57	8.76	0.90	***1.89***	***2.14***	
Mpa2l	1.63	0.63	0.61	***16.03***	***30.60***	
Nmi	0.96	2.21	0.76	***2.02***	***2.65***	
Oas1b	1.73	0.45	1.06	***4.66***	***5.14***	
Oasl2	1.31	1.40	1.04	***23.57***	***24.70***	
Parp10	0.86	0.53	0.95	***9.23***	***8.64***	
Prlh	29.22	70.94	0.89	***1.80***	1.54	
Psmb10	1.48	45.60	1.02	***1.93***	***1.56***	
Psmb8	2.37	3.10	0.80	***13.81***	***17.82***	
Psmb9	1.11	1.50	0.61	***11.95***	***15.98***	
Psme2	2.11	102.53	0.87	***1.59***	***1.79***	
Rsad2	2.19	0.34	1.22	***4.59***	***3.04***	
Rtp4	0.64	0.68	1.02	***25.99***	***21.21***	
Samhd1	1.36	7.23	1.06	***1.78***	***1.75***	
Serpina3f	2.56	0.20	0.27	***29.80***	***33.49***	
Serpina3h	2.64	0.46	***0.32***	1.54	1.50	
Stat1	1.43	5.84	***0.56***	***3.49***	***6.02***	
Stat2	0.81	3.08	0.91	***1.67***	***1.79***	
Tap1	2.04	0.83	0.91	***7.28***	***9.08***	
Tapbp	1.75	10.48	0.95	***1.63***	***1.82***	
Trim21	1.30	1.35	0.68	***4.08***	***4.67***	
Trim25	1.59	1.68	1.00	***1.82***	***1.78***	
Uba7	1.87	0.28	0.55	***5.31***	***12.35***	
Ube2l6	1.33	6.04	1.05	***2.96***	***2.84***	
Usp18	1.32	0.48	0.57	***13.53***	***20.30***	
Xaf1	0.39	1.44	0.81	***4.96***	***8.68***	
Zbp1	0.43	0.06	0.66	***127.49***	200.15	
Zc3hav1	1.33	0.59	0.81	***2.42***	***3.11***	
Procr	4.30	1.18	***2.45***	0.42	***0.20***	
St8sia4	1.93	8.06	0.78	***0.64***	1.16	
Npy1r	1.66	7.93	0.72	***0.57***	0.96	
Npy5r	1.91	3.76	0.71	***0.54***	0.90	
Pcsk1n	2.40	401.14	0.98	***0.62***	***0.49***	

Table 3.2: Fold change in LepRb enriched genes in STAT3^{LepR}KO and *ob/ob* mice. TRAP-Seq was performed on STAT3^{LepR}KO, LepRb^{eGFP} and LepRb^{eGFP}*ob/ob* mice. Genes enriched (FPKM in TRAP/FPKM in TRAP-depleted >1.5) at baseline, or that became enriched in a condition in which they were also significantly changed, were included in this analysis. Enrichment and expression (FPKM) values displayed are from LepRb^{eGFP} mice. Fold change values for STAT3^{LepR}KO mice were versus LepRb^{eGFP} controls **(Column 5)**, or against LepRb^{eGFP}*ob/ob* **(Column 6)**. Fold change values for LepRb^{eGFP}*ob/ob* **(Column 4)** are versus 10-hour vehicle treated LepRb^{eGFP}. **(Column 7)** designates the corresponding section of Figure 2B. n=3-4 samples per treatment group. Each sample was comprised of pooled hypothalami of 4-6 adult animals. $p<.05$ for values in bold and italics. FPKM: Fragments Per Kilobase of exon per Million reads mapped.

Term	P-value	Genes	Group
EP300	3.16E-05	ANXA2;PLAGL1;STAT3;BCL3;FOSB;ATG7;CAMK1G	II
SP1	1.67E-03	ANXA2;STAT3;NR0B1;BRCA2	
BRCA1	8.68E-03	STAT3;XIST;EZR;BRCA2	
JUN	1.24E-02	STAT3;BCL3;FOSB	
STAT1	6.54E-03	STAT3;BCL3;ATG7	
NFKB1	1.32E-02	SOCS3;STAT3;BCL3	
NCOA1	1.30E-02	STAT3;BCL3	
HNF1A	4.62E-03	ANXA2;STAT3	
STAT6	1.14E-02	ANXA2;STAT3	
STAT5A	1.51E-02	STAT3;BRCA2	
ESR1	2.62E-02	ANXA2;STAT3;BCL3;NR0B1;EZR	
NR4A1	2.11E-02	STAT3;NR0B1	
SMAD3	3.63E-02	SOCS3;PLAGL1;BRCA2	
HDAC2	3.93E-02	STAT3;FOSB;BRCA2	
CTNNB1	4.22E-02	BCL3;RPLP2;EZR	
PML	4.71E-02	PLAGL1;STAT3	
IRF3	3.43E-07	ZBP1;CITED1;DDX58;IRF7;ISG15;TRIM21	III
STAT1	8.06E-06	CISH;IRF1;STAT2;EIF2AK2;ISG15;NMI;IRF9	
STAT2	1.13E-06	LGALS3BP;CD274;CISH;STAT1;IRF9	
STAT3	3.00E-04	CISH;STAT1;STAT2;EIF2AK2;NMI;IRF9	
STAT6	2.54E-04	CISH;STAT2;NMI;IRF9	
STAT5B	2.32E-04	CISH;STAT1;NMI;IRF9	
STAT5A	4.44E-04	CISH;STAT1;NMI;IRF9	
STAT4	1.49E-04	CISH;NMI;IRF9	
IRF1	6.17E-04	STAT1;IRF8;IRF9	
SMAD4	1.30E-02	CITED1;STAT1;IRF7;ISG15	
EP300	3.08E-02	CITED1;STAT1;IRF1;STAT2;IRF7	
IRF8	6.23E-03	IRF1;TRIM21	
FOS	3.76E-02	STAT1;NMI;IRF9	
ILF2	3.08E-02	EIF2AK2;IFIT1;IFIT2	
SPI1	2.49E-02	IRF1;IRF8	
CHD1	2.42E-02	ISG15;GBP2	
SMARCA4	4.76E-02	STAT1;IRF1;STAT2	
NCOA1	4.30E-02	TRIM21;PSMB9	

Table 3.3: Significantly enriched transcription factor pathways. The list of genes in groups II and III in Figure 2B were analyzed for terms that were signficiantly enriched through Transcription Factor Protein Protein Interaction by Enrichr. The enriched terms, their p-values for significance, and the list of genes that fall into the respective terms are detailed.

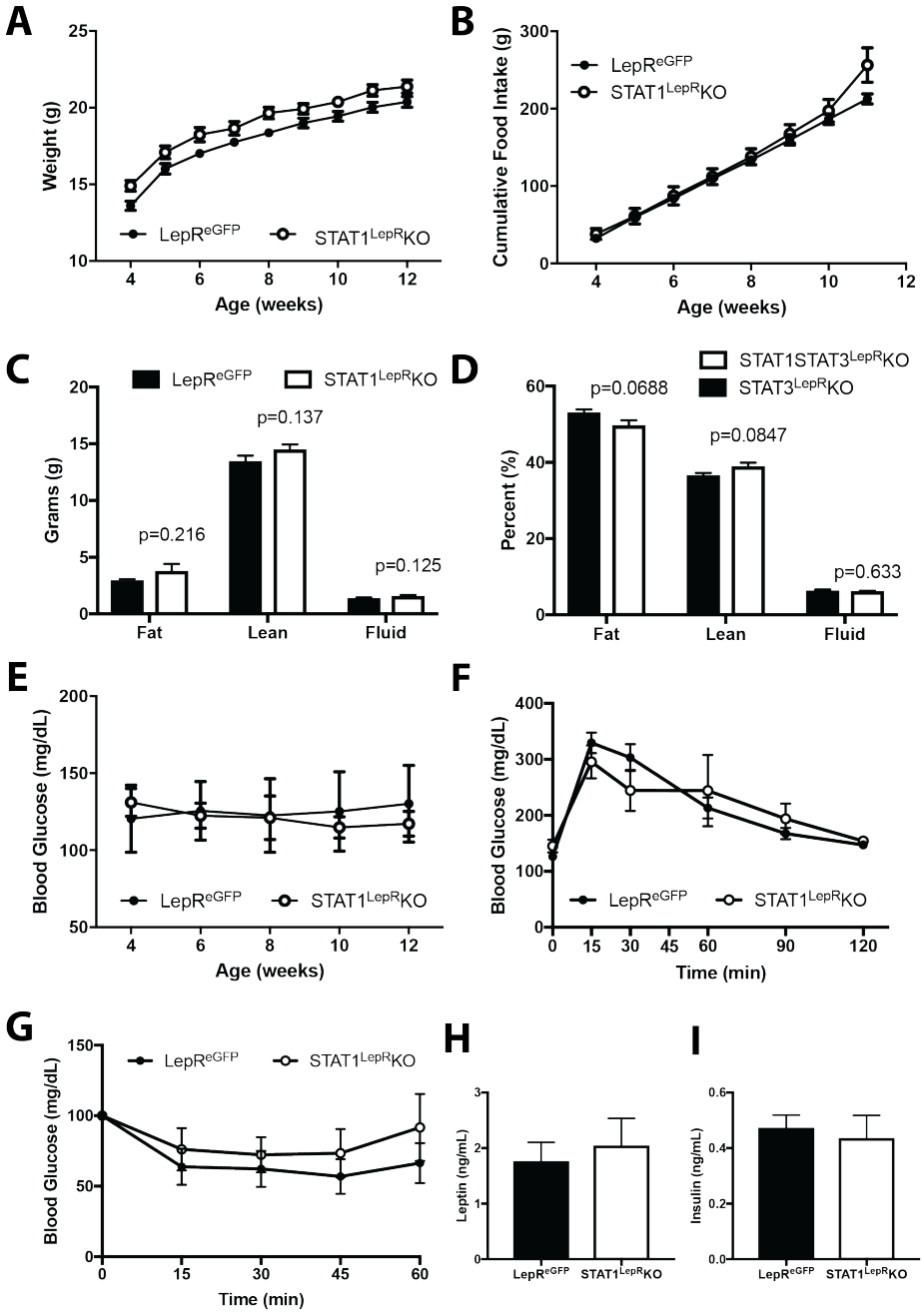

Figure 3.8: LepR^{STAT1} does not regulate energy balance (females). (A) Female STAT1^{LepR}KO and LepR^{eGFP} (littermate control) mice were placed on chow and body weight **(A)** measured weekly, and cumulative food intake **(B)** measured weekly. **(C-D)** At 14 weeks of age, animals underwent body composition by NMR spectroscopy. **(E)** Biweekly blood glucose concentrations for female STAT1^{LepR}KO and LepR^{eGFP} mice at 4-12 weeks of age. Mice at weeks 12-14 of age were treated with **(F)** glucose (2g/kg; i.p.) or **(G)** insulin (1 U/kg; i.p.) and blood glucose concentrations were measured. 10-week old mice had their serum assayed for **(H)** leptin and **(I)** insulin. N=10-18 per condition. ANOVA analysis was performed for **(A-B, E-G)**; unpaired t-test analysis was done in **(C-D, H-I)**.

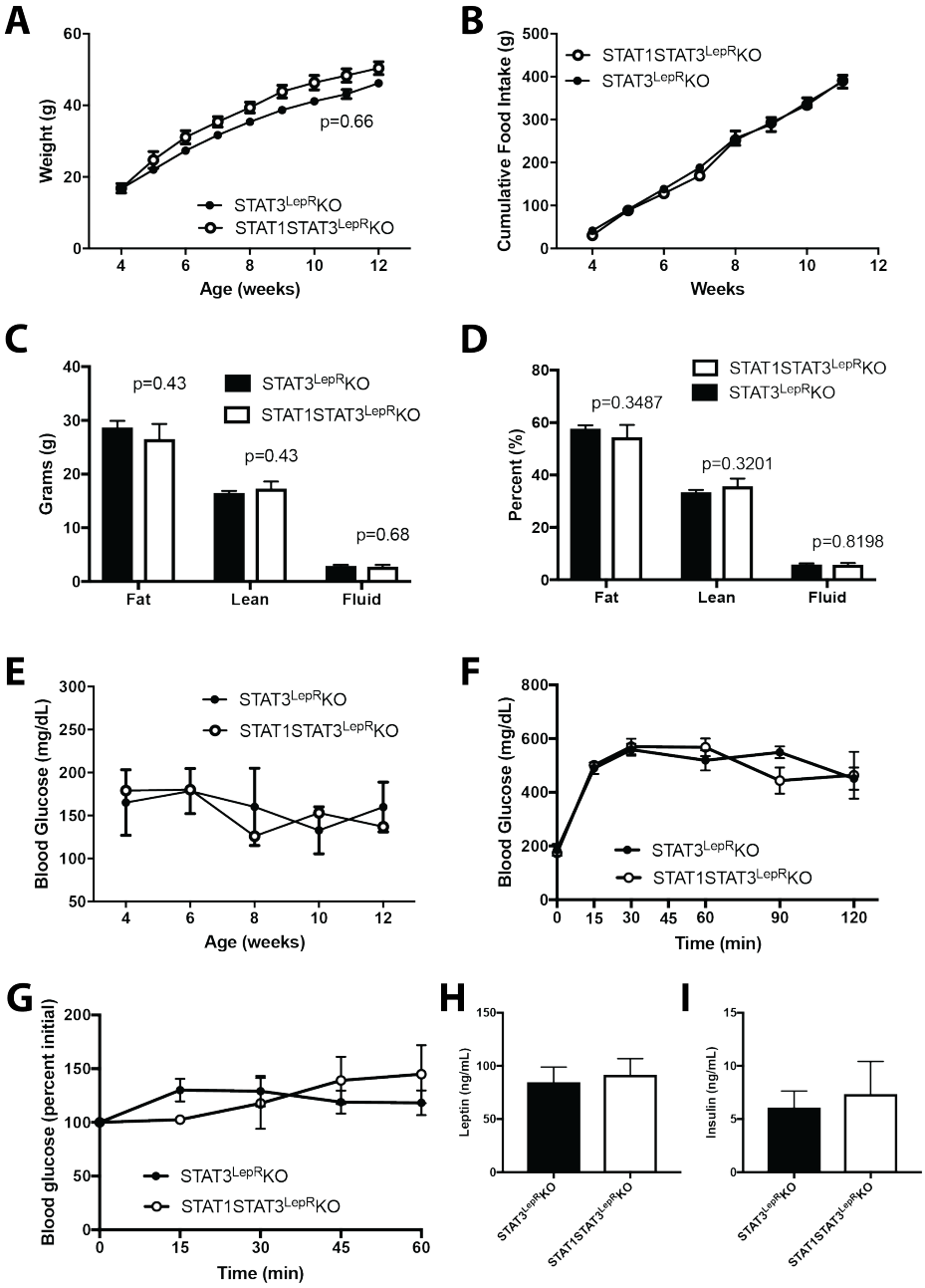

Figure 3.9: Ablation of LepR^{STAT1} in STAT3^{LepR}KO does not exaggerate energy imbalance (females). Female STAT1STAT3^{LepR}KO and STAT3^{LepR}KO mice were placed on chow and body weight **(A)** measured weekly, and cumulative food intake **(B)** measured weekly. **(C-D)** At 14 weeks of age, animals underwent body composition by NMR spectroscopy. **(E)** Biweekly blood glucose concentrations for female STAT1STAT3^{LepR}KO and STAT3^{LepR}KO mice at 4-12 weeks of age. Mice at weeks 12-14 of age were treated with **(F)** glucose (2g/kg; i.p.) or **(G)** insulin (1 U/kg; i.p.) and blood glucose concentrations were measured. 10-week-old mice had their serum assayed for **(H)** leptin and **(I)** insulin. N=7-10 per condition. ANOVA analysis was performed for A-B, E-G; unpaired t-test analysis was done in **(C-D, H-I)**.

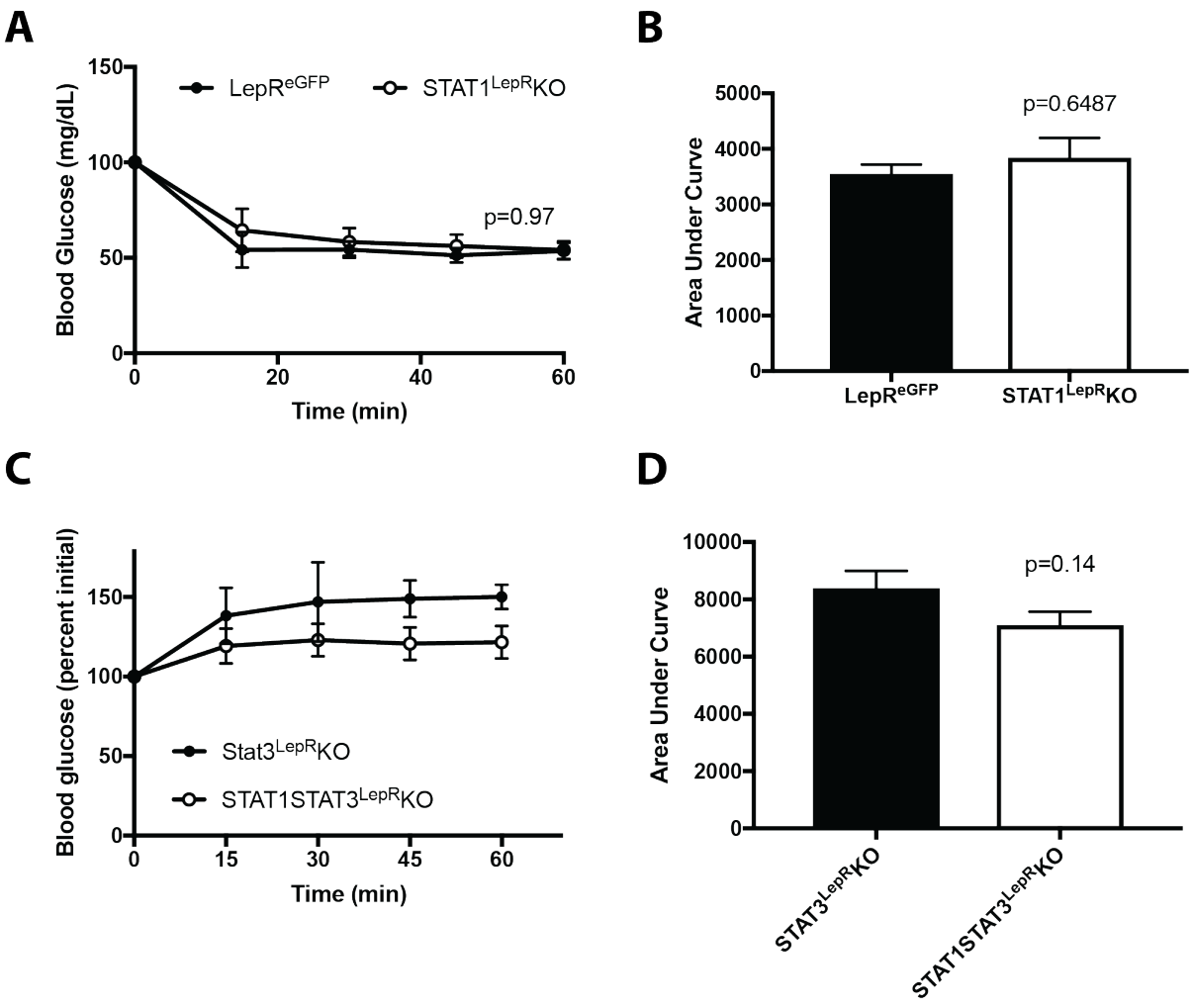

Figure 3.10: LepR^{STAT1} does not cause hypoglycemia. (A-D) At 12-14 weeks of age, male LepR^{eGFP}, STAT1^{LepR}KO, STAT3^{LepR}KO, and STAT1STAT3^{LepR}KO mice were treated with insulin (1U/kg; i.p.) and blood glucose concentrations were measured; area under the curve analysis was performed for insulin tolerance test. ANOVA analysis was performed for **(A, C)**; unpaired t-test was done for **(B, D)**.

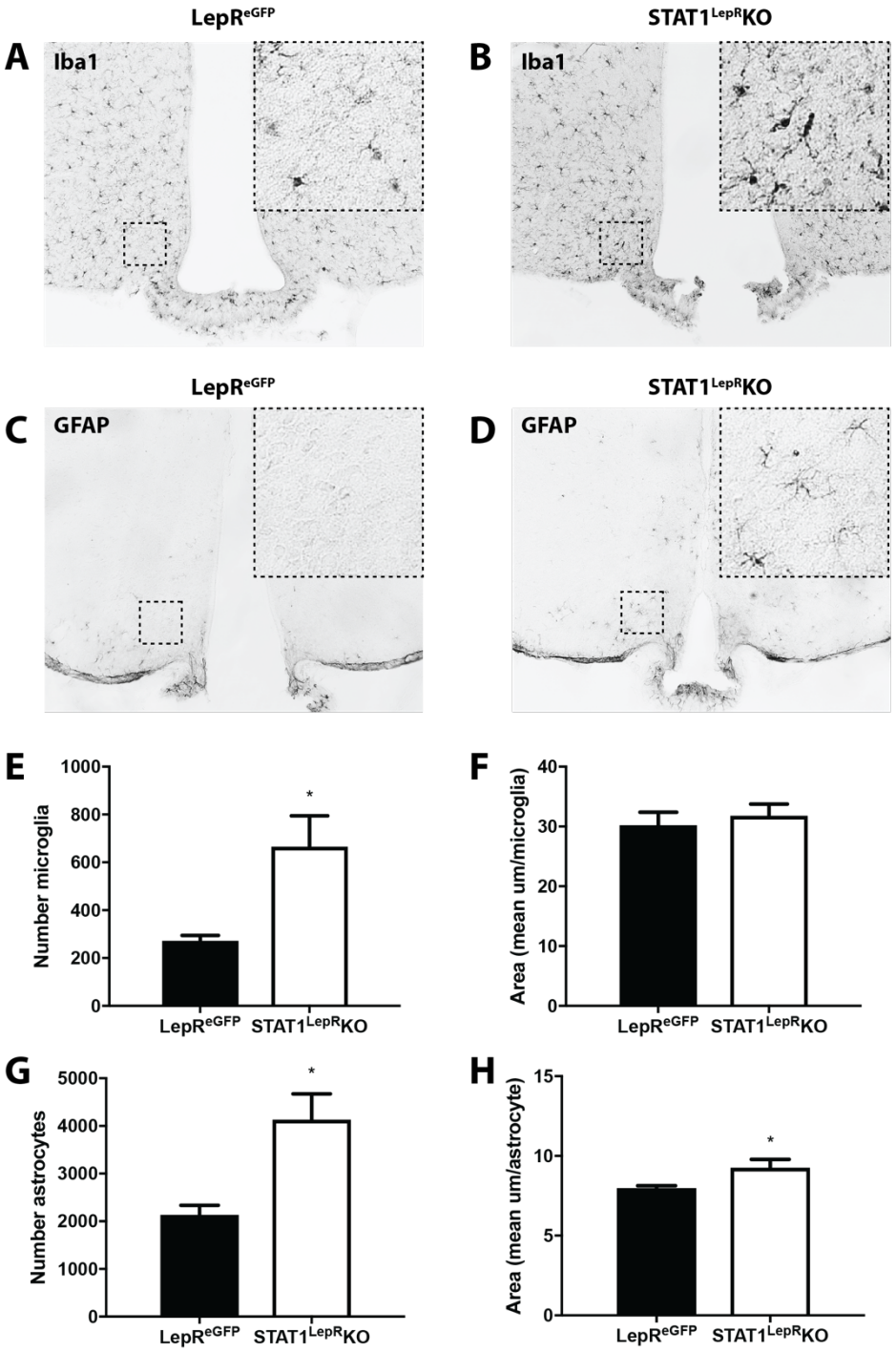

Figure 3.11: Histochemical analysis of hypothalamic microglia and astrocytes in STAT1 deficient animals. Representative images of microglial distribution in the medial basal hypothalamus in **(A)** LepR^{eGFP} and **(B)** STAT1^{LepR}KO mice. Representative sections of astrocytes in **(C)** LepR^{eGFP} and **(D)** STAT1^{LepR}KO mice. Quantification of microglia numbers **(E)** and average area per microglia **(F)** in the ARC; quantification of astrocyte number **(G)** and average area per astrocyte **(H)**. *p<0.05 by unpaired t-test.

References

1. Cawley, J. & Meyerhoefer, C. The medical care costs of obesity: An instrumental variables approach. *J. Health Econ.* **31,** 219–230 (2012).
2. Elmquist, J. K., Coppari, R., Balthasar, N., Ichinose, M. & Lowell, B. B. Identifying Hypothalamic Pathways Controlling Food Intake , Body Weight , and Glucose Homeostasis. **71,** 63–71 (2005).
3. Frederich, R. C. *et al.* Leptin Levels Reflect Body Lipid-Content in Mice - Evidence for Diet-Induced Resistance To Leptin Action. *Nat. Med.* **1,** 1311–1314 (1995).
4. Maffei, M. *et al.* Leptin levels in human and rodent: measurement of plasma leptin and ob RNA in obese and weight-reduced subjects. *Nat. Med.* **1,** 1155–1161 (1995).
5. Tartaglia, L. A. *et al.* Identification and expression cloning of a leptin receptor, OB-R. *Cell* **83,** 1263–1271 (1995).
6. Baumann, H. *et al.* The full-length leptin receptor has signaling capabilities of interleukin 6-type cytokine receptors. *Proc. Natl. Acad. Sci. U. S. A.* **93,** 8374–8 (1996).
7. Banks, A. S., Davis, S. M., Bates, S. H. & Myers, M. G. Activation of downstream signals by the long form of the leptin receptor. *J. Biol. Chem.* **275,** 14563–14572 (2000).
8. Kloek, C. *et al.* Regulation of Jak kinases by intracellular leptin receptor sequences. *J. Biol. Chem.* **277,** 41547–41555 (2002).
9. Jiang, L. *et al.* Tyrosine-dependent and -independent actions of leptin receptor in control of energy balance and glucose homeostasis. *Proc. Natl. Acad. Sci. U. S. A.* **105,** 18619–18624 (2008).
10. Robertson, S. *et al.* Insufficiency of Janus Kinase 2 – Autonomous Leptin Receptor Signals for Most Physiologic Leptin Actions. **59,** (2010).
11. Gong, Y. *et al.* The long form of the leptin receptor regulates STAT5 and ribosomal protein S6 via alternate mechanisms. *J. Biol. Chem.* **282,** 31019–31027 (2007).
12. Bates, S. H. & Myers, M. G. The role of leptin receptor signaling in feeding and neuroendocrine function. *Trends Endocrinol. Metab.* **14,** 447–452 (2003).
13. Allison, M. B. *et al.* TRAP-seq defines markers for novel populations of hypothalamic and brainstem LepRb neurons. *Mol. Metab.* **4,** 299–309 (2015).
14. Takahashi, Y. *et al.* Leptin Induces Tyrosine Phosphorylation of Cellular Proteins Including STAT-1 in Human Renal Adenocarcinoma Cells , ACHN tions including hypertension , hyperlipidemia and NIDDM upon health and longevity . Genetic factors have been supposed to be involved . **864,** 859–864 (1996).
15. Erickson, R. L., Hemati, N., Ross, S. E. & MacDougald, O. A. p300 Coactivates the Adipogenic Transcription Factor CCAAT/ Enhancer-binding Protein ?? *J. Biol. Chem.* **276,** 16348–16355 (2001).
16. Tang, C.-H. *et al.* Leptin-induced IL-6 production is mediated by leptin receptor, insulin receptor substrate-1, phosphatidylinositol 3-kinase, Akt, NF-kappaB, and p300 pathway in microglia. *J. Immunol. (Baltimore, Md 1950)* **179,** 1292–1302 (2007).
17. Thaler, J. *et al.* Obesity is associated with hypothalamic injury in rodents and humans. *J. Clin. Investig.* **122,** 153 (2011).

18. Leshan, R. L., Björnholm, M., Münzberg, H. & Myers, M. G. Leptin receptor signaling and action in the central nervous system. *Obesity (Silver Spring).* **14 Suppl 5,** 208S–212S (2006).
19. Krashes, M. J. *et al.* An excitatory paraventricular nucleus to AgRP neuron circuit that drives hunger. *Nature* **507,** 238–42 (2014).
20. Bates, S. H. *et al.* STAT3 signalling is required for leptin regulation of energy balance but not reproduction. *Nature* **421,** 856–859 (2003).
21. Langmead, B., Trapnell, C., Pop, M. & Salzberg, S. Ultrafast and memory-efficient alignment of short DNA sequences to the human genome. *Genome Biol.* **10,** R25 (2009).
22. Trapnell, C. *et al.* Transcript assembly and quantification by RNA-Seq reveals unannotated transcripts and isoform switching during cell differentiation. *Nat. Biotechnol.* **28,** 511–515 (2010).
23. Magrane, M. & Consortium, U. P. UniProt Knowledgebase: A hub of integrated protein data. *Database* **2011,** 1–13 (2011).

CHAPTER 4

CONSTITUTIVE STAT3 ACTIVITY PROMOTES NEGATIVE ENERGY BALANCE

Chapter Summary

The adipocyte leptin, central to the homeostatic systems that regulate energy balance, activates the transcription factor STAT3 by binding to its receptor (LepRb) in the central nervous system to drive anorexia and weight loss. And, while the necessity of STAT3 in leptin action has been demonstrated, here we examine the sufficiency of STAT3 to normalize energy balance in the absence of other leptin-dependent signals. Using the enhanced STAT3 mutant (CASTAT3), we were able to further drive anorexia in already lean normoleptinemic chow-fed mice and found their sensitivity to exogenous leptin to remain intact. Moreover, our use of LepRb-specific TRAP-seq has identified a number of genes that may be responsible for mediating the observed weight loss and be the sought after signals downstream of STAT3 translocation that mediate its action. However, animals fed a high-fat diet became diet-induced obese (DIO) regardless of whether they had the enhanced STAT3 element or not. Therefore, there must exist a

block to leptin action downstream of STAT3 phosphorylation that prevents the anorexic response observed in lean and leptin-deficient animals.

Introduction

Obesity, defined as a body mass index (BMI) of greater than 30kg/m^2, results from an energy imbalance where energy stores from consumed calories outstrips the metabolic needs of the individual. In the last 50 years, obesity has dramatically increased in prevalence and incidence due to calorically dense diets.[1] Today, over 70% of the US population is overweight (BMI>25kg/m^2) and 37.7% is obese.[2]

Obesity results from a continued imbalance between intake and expenditure where the body's homeostatic systems are unable to completely counter the shift in energy balance. And so, while obese individuals have increased basal metabolic rates compared to lean counterparts, their increased food intake continues, resulting in an ever-increasing positive energy surplus.[3,4] Additionally, when obese individuals lose weight, the endogenous homeostatic systems promote an anabolic response (increase hunger and decrease energy expenditure) reminiscent of lean individuals losing weight.[5] Therefore, even when obese individuals are able to lose weight, homeostatic systems drive them to regain the lost weight.

The metabolic homeostasis our body maintains centers on the hormone leptin, which circulates in proportion to adipose mass and confers a snapshot of the individual's energy stores when it binds to its receptor (LepRb) in the central nervous system.[3,6,7] The type I cytokine receptor LepRb, when bound, activates Janus kinase 2 (JAK2), resulting in a phosphorylation cascade, including Tyr_{1138}, which recruits signal transducer and activator of transcription 3 (STAT3). This leptin activated JAK2→STAT3 pathway mediates the majority of leptin's anorectic action—mice with mutated Tyr_{1138} or

absent STAT3 in LepRb neurons demonstrate hyperphagic obesity similar to that of leptin deficient *ob/ob* animals.[8,9] From these studies, it is clear that STAT3 is necessary in leptin action; however, its sufficiency in LepRb signaling to combat obesity has not been demonstrated.

Unlike leptin deficient or STAT3 ablated mutants, most individuals today are obese from the availability of cheap, calorically rich foods and sedentary lifestyles.[1] These diet-induced obese (DIO) individuals possess high circulating leptin concentrations (hyperleptinemia) expected of their elevated adiposity, instead of the absent leptin (hypoleptinemia) seen in leptin deficient obese indivdiuals.[10] The success of exogenous leptin to treat hypoleptinemic obesity and its failure to treat hyperleptinemic DIO have promulgated the theory of "leptin resistance" in DIO.[11] And, due to the importance of leptin→STAT3, leptin resistance is further supported by the absent pSTAT3 response to exogenous treatment in DIO animals.[12] Therefore, using an enhanced STAT3 mutant, we investigated whether STAT3 signaling in the absence of all other leptin signals is sufficient to mediate leptin action. Furthermore, this constitutively active STAT3 mutant would determine whether the blockade of leptin action is upstream of STAT3 translocation/activity and whether obesity would be cured if exogenous leptin were able to expectedly increase STAT3 translocation.

Results

LepR^{CASTAT3} mice have enhanced STAT3 activity

A constitutively active STAT3 mutant (CASTAT3) on the Rosa 26 locus was crossed with the LepR^{cre} and Rosa26$^{eGFP\text{-}L10a}$ mice to generate

$LepR^{cre/cre}Rosa26^{CASTAT3/eGFP-L10a}$ ($LepR^{CASTAT3}$) and $LepR^{cre/cre}Rosa26^{eGFP-L10a/+}$ ($LepR^{eGFP}$) control mice (Figure 4.1A). To confirm the expression of the Stat3-C transgene in CASTAT3 mice, anti-eGFP translating ribosome affinity purification (TRAP) against hypothalamic material from $LepR^{CASTAT3}$ and $LepR^{eGFP}$ (both of which have one copy of the eGFP-L10a fusion protein) resulted in the sequencing of the actively translating messenger RNA. Sequenced reads that were perfectly matched to unique regions of the Stat3-C transgene or the endogenous Stat3 gene were aligned and quantified (Figure 4.1B-C, Figure 4.6). This confirmed the active translation of the Stat3-C transgene previously shown to result in transcriptional activity and function.[13,14]

Anorexia in $LepR^{CASTAT3}$ mice on chow

Weekly body weight measurements of male $LepR^{CASTAT3}$ and $LepR^{eGFP}$ mice revealed a lower body weight in $LepR^{CASTAT3}$ mice due largely to decreased food intake (Figure 4.2A, 4.2B). The lower body weight was due to a significant decrease in adipose mass, both in grams and proportionally (Figure 4.2C, 4.2D). This decreased body weight did not affect blood glucose, serum leptin, serum insulin, or crown-rump length (Figure 4.2E, 4.2F, 4.2G, Figure 4.7A). Maximal oxygen consumption (VO_2), both adjusted to body weight and to lean body mass, and total locomotor activity are also comparable between $LepR^{CASTAT3}$ and $LepR^{eGFP}$ mice (Figure 4.2H, 4.2I, Figure 4.7B-4.7E). Thus, these results indicate that enhanced STAT3 in LepRb neurons results in decreased body weights due to anorexia. In females, however, body weight and food intake remain largely unchanged between $LepR^{CASTAT3}$ and $LepR^{eGFP}$ mice (Figure 4.9A, 4.9B). And, while female $LepR^{CASTAT3}$ mice did have significantly less fat and fluid mass, when compared by percentage, there was no significant difference in percent adiposity

or fluid (Figure 4.9C, 4.9D). Additionally, glycemic parameters and body length similarly remained comparable (Figure 4.9E-H).

Leptin sensitivity remains intact in LepR^{CASTAT3} mice

To investigate leptin sensitivity in mice with enhanced STAT3 activity, 10-week-old male LepR^{CASTAT3} and control LepR^{eGFP} mice were injected twice daily for 3 days with 0.9% sodium chloride, then twice daily for 3 days with metreleptin (5mg/kg; i.p.), followed by twice daily for 2 days with 0.9% sodium chloride. Leptin treatment significantly decreased body weight and food intake in both LepR^{CASTAT3} and LepR^{eGFP} mice (Figure 4.3). This suggests that despite the augmented STAT3 signaling that drives anorexia, exogenous boli of leptin is effective in further decreasing food intake and body weight to a comparable extent in LepR^{CASTAT3} mice versus littermate controls.

Transcriptional profiling of enhanced STAT3 animals

Mice on the eGFP-L10a background were in one of six conditions: 1. LepR^{CASTAT3} ,2. LepR^{eGFP} treated with PBS 10-hours prior to sacrifice, 3. LepR^{eGFP} treated with leptin (5mg/kg, i.p.) 3-hours prior to sacrifice, 4. LepR^{eGFP} treated with leptin (5mg/kg, i.p.) 10-hours prior to sacrifice, 5. LepR^{eGFP}*ob/ob* (on the *ob/ob* background) treated with PBS 10-hours prior to sacrifice, and 7. LepR^{eGFP}*ob/ob* treated with leptin (5mg/kg, i.p.) 10-hours prior to sacrifice. 5-7 hypothalami from each of the groups were pooled and 3-4 of the independently pooled samples for each of the conditions were sequenced and the differential expressed genes were analyzed. Gene expression comparisons were analyzed between the LepRb neuron fraction (pull-down) and the non-LepRb cell fraction (supernatant) to generate a list of enriched genes. Additional

comparisons were performed between the gene expression values from the various conditions against the control PBS-treated LepR^{eGFP} condition to identify the genes that were differentially regulated (the leptin-treated LepR^{eGFP}*ob/ob* condition was the only one not compared to the PBS-treated LepR^{eGFP} sample; rather, it was compared to the PBS-treated LepR^{eGFP}*ob/ob* condition). The over 150 genes that were differentially regulated and enriched in LepRb neurons are shown in the heatmap, which highlights the clear dichotomy between the transcriptome of leptin deficient *ob/ob* mice and the transcriptome of the other 4 states of leptin action (Figure 4.4). Even though the leptin-treated *ob/ob* (vs PBS-treated *ob/ob*) should be most similar to the 10h leptin v PBS condition, it is instead most closely coupled to the LepR^{CASTAT3} condition. This suggests that the profound metabolic normalization seen with leptin-treated *ob/ob* animals may be driven partly by enhanced STAT3 activity. Under the LepR^{CASTAT3} condition, those genes that were enriched in LepRb neurons and that experienced differential expression changes when compared to LepR^{eGFP} controls are listed in Table 4.1.

LepR^{CASTAT3} is sufficient to partially normalize leptin-deficient hyperphagic obesity

Whereas the hyperphagic obesity in STAT3 null mice in LepRb neurons demonstrates the necessity of STAT3 in leptin action, the sufficiency of STAT3 to mediate leptin action in the absence of other LepRb signals has not previously been demonstrated. To investigate this, LepR^{CASTAT3} mice were bred onto the *ob/ob* background. LepR^{CASTAT3};*ob/ob* mice gained significantly less weight versus their *ob/ob* littermate controls (Figure 4.5A). This weight loss is reflected in less adiposity and

increased lean body mass (Figure 4.5B, 4.5C). Furthermore, unfasted blood glucose values in LepR^{CASTAT3};*ob/ob* mice are lower than in *ob/ob* controls (Figure 4.5D).

Enhanced STAT3 is ineffective in diet-induced obesity

LepR^{CASTAT3} is effective in driving anorexia in both lean chow-fed animals and obese leptin-deficient animals, so we next investigated its effectiveness in diet-induced obesity (DIO). Male and female LepR^{CASTAT3} mice had comparable weights and food intakes to control LepR^{eGFP} mice when weaned onto a high-fat diet (Figure 4.8A, 4.8B; Figure 4.10A, 4.10B). Their body compositions, unfasted glucose, serum leptin and serum insulin values likewise remained comparable (Figure 4.8C-4.8G; Figure 4.10C-4.10G). This suggests that the enhanced STAT3 action that suffices to drive weight loss in lean chow-fed animals and leptin deficient *ob/ob* mice may be insufficient to drive weight loss in DIO animals.

Discussion

The world-wide obesity epidemic is only growing as more and more individuals are exposed to cheap, calorically-rich foods. Today's obesogenic environment is effective in overcoming individuals' endogenous homeostatic systems meant to protect them from transient fluctuations in food intake. The inability of leptin, a major anorectic driver of these systems, to combat diet-induced obesity (DIO) has warranted continued investigation in the notion of leptin resistance. Indeed, DIO animals share many characteristics with STAT3 null mice: both are obese, hyperleptinemic, and do not respond phenotypically to exogenous leptin, presumably due to an absence of pSTAT3

activation. We, therefore, sought to determine whether enhanced STAT3 activity can drive the system towards negative energy balance during obesity.

Previously, a mutant transcriptionally active form of STAT3 (CASTAT3) was found to promote leanness or mild obesity when placed in AgRP or POMC neurons, respectively.[13,14] And while many AgRP and POMC neurons express LepRb, we found $LepR^{CASTAT3}$ mice experienced anorexia and decreased adiposity compared to controls, suggesting that chronically augmented STAT3 activity results in additional negative energy balance in already-lean animals. This finding, coupled with previous work demonstrating effective anorexia from DIO hyperleptinemia, is further evidence that chronically enhanced STAT3 action (i.e. hyperleptinemia) is effective in driving additional weight loss.[15]

Surprisingly, these CASTAT3 animals have intact leptin sensitivity when given exogenous leptin, intimating that increased STAT3 activity alone does not prohibit further exogenous leptin induced anorexia. These findings suggest that the increased STAT3 action during DIO-hyperleptinemia should not alone prohibit effective exogenous leptin treatment. There may therefore be other signals, perhaps leptin dependent, that block the effectiveness of exogenous leptin therapy. Furthermore, our DIO animals with the enhanced STAT3 action exhibited the same levels of adiposity and food intake compared to controls, suggesting that during DIO-induced hyperleptinemia either STAT3 activity is already exhausted or there exists a blockade of STAT3-induced anorexia downstream of its translocation.

Our data show that STAT3 action is sufficient to normalize much of the metabolic dysfunction in leptin deficient *ob/ob* animals. Therefore, leptin therapy in leptin deficient patients must be mediated primarily by leptin→STAT3 action. Obesity, strictly speaking, is then not what limits leptin therapy in DIO patients. Knight et. al. also recently demonstrated that high-fat diet itself does not dampen the effectiveness of leptin therapy in DIO mice.[16] All together, it would seem that obesity, high-fat diet, and enhanced STAT3 activity (like under hyperleptinemia) are not responsible for the failure of exogenous leptin to provoke weight loss in DIO individuals. Perhaps other leptin-dependent signals (e.g. negative regulators) during DIO-hyperleptinemia are responsible. Regardless, it is clear that further examination of hyperleptinemia and its functional and transcriptional consequences is necessary to inform the development of new targets in the battle against obesity.

Materials and Methods

Mice.

Mice were bred in our colony in the Unit for Laboratory Animal Medicine at the University of Michigan; these mice and the procedures performed were approved by the University of Michigan Committee on the Use and Care of Animals and in accordance with AALAC and NIH guidelines. We purchased male and female C57BL/6 mice (Jackson stock #000664) and *ob/ob* mice (Jackson stock #000632) for experiments and breeding studies from Jackson Labs. Rosa26-CASTAT3-eGFP mice were generously provided by Sergei Koralov.[13] Mice were bred at the University of Michigan and

provided with food and water *ad libitum* in temperature controlled rooms on a 12-hour light-dark cycle.

LepR^{cre} mice[17] were crossed with Rosa26-loxSTOPlox-eGFP-L10a and Rosa26-CASTAT3-eGFP to generate LepR$^{cre/cre}$;Rosa$^{eGFP\text{-}L10a/CASTAT3}$ mice,[18] which were then crossed with LepR^{cre} mice to generate LepR$^{cre/cre}$;Rosa$^{eGFP\text{-}L10a/CASTAT3}$ (LepR $^{eGFP\text{-}L10a/CASTAT3}$) and LepR$^{cre/cre}$;Rosa$^{eGFP\text{-}L10a/+}$ (LepR $^{eGFP\text{-}L10a/+}$) study animals. LepR^{cre} and LepR$^{cre/cre}$;Rosa$^{eGFP\text{-}L10a/CASTAT3}$ mice were backcrossed to *ob/ob* mice until LepR$^{cre/cre}$; *ob/*+ mice and LepR$^{cre/cre}$;Rosa$^{eGFP\text{-}L10a/CASTAT3}$;*ob/*+ were obtained, which were crossed to obtain LepR$^{cre/cre}$;Rosa$^{eGFP\text{-}L10a/CASTAT3}$;*ob/ob* and LepR$^{cre/cre}$;Rosa$^{eGFP\text{-}L10a/+}$;*ob/ob* study animals.

Leptin sensitivity.

10-month-old male LepR^{CASTAT3} and LepR^{eGFP} mice were injected twice daily for three days with 0.9% soldium chloride (Hospira; i.p.), followed with metreleptin (5mg/kg, i.p.) (a generous gift from AstraZenica, Inc.), then again with 0.9% sodium chloride (Hospira; i.p.) for 2 days. Body weight and food were measured twice per day during the injection period.

Phenotyping of LepR $^{eGFP\text{-}L10a/CASTAT3}$ and control mice.

LepR $^{eGFP\text{-}L10a/CASTAT3}$ and control LepR $^{eGFP\text{-}L10a/+}$ were weaned into individual housing at 21 days and fed normal chow (Purina Lab Diet 5001) or 60% high-fat diet (Research Diets D12492, 60% kcal from fat). Similarly LepR$^{cre/cre}$;Rosa$^{eGFP\text{-}L10a/CASTAT3}$;*ob/ob* and LepR$^{cre/cre}$;Rosa$^{eGFP\text{-}L10a/+}$;*ob/ob* study animals were weaned into individual housing at 21 days and fed normal chow (Purina Lab Diet 5001). Weekly

body weight and food intake were monitored. Unfasted blood glucose was take every other week from 4-20 weeks of age. Analysis of body fat and lean mass was performed at 21-22 weeks of age using NMR-based analyzer (Minispec LF90II, Bruker Optics). Leptin and insulin were assayed by commercial ELISA with serum collected in 14-week old animals (Crystal Chem). One subset of male mice (10 weeks old) were analyzed for oxygen consumption (VO_2) and locomotor activity using the Comprehensive Laboratory Animal Monitoring System (CLAMS, Columbus Instruments).

Hypothalamic dissections for TRAP-seq.

At the midpoint of the light cycle, 13- to 15-week-old adult homozygous mice were anesthetized with isoflurane, had their brains removed and placed onto a mouse coronal brain matrix (1mm sections). A 3x3x3 mm block was dissected from the ventral diencephalon immediately caudal to the optic chiasm and immediately homogenized for TRAP-seq analysis.

Translating Ribosome Affinity Purification with deep sequencing (TRAP-seq).

We employed anti-eGFP Translating Ribosome Affinity Purification (TRAP) using hypothalamic material from PBS or leptin treated $LepR^{eGFP}$, $LepR^{LepR}$*ob/ob*, $LepR^{CASTAT3}$ mice (which all express an eGFP-tagged ribosomal subunit in LepR cells). Messenger RNA isolated from eGFP-tagged ribosomes and from the eGFP-depleted was assessed for quality using TapeStation (Agilent, Santa Clara, CA) and samples with RNA Integrity Numbers (RINs) of 8 or greater were prepared using the Illumina TruSeq mRNA Sample Prep v2 kit (Catalog # RS-122-2001 and #RS-122-2002) (Illumina, San Diego, CA), where 0.1-3ug of RNA was converted to mRNA using a polyA purification. The

mRNA was chemically fragmented and copied into first strand cDNA using reverse transcriptase and random primers. The 3' ends of the cDNA were adenylated and the 6-nucleotide-barcoded adapters ligated. These products were then purified and enriched by PCR to create the cDNA library, which were checked for quality and quantity by TapeStation (Agilent) and qPCR using Kapa's library quantification kit for Illumina Sequencing platforms (catalog #KK4835) (Kapa Biosystems, Wilmington MA). They were clustered on cBot (Illumina) and sequenced 4 samples per lane on a 50 cycle single end run on a HiSeq 2000 (Illumina) using version 2 reagents according to manufacturer's protocols.

RNA-seq analysis.

50 base pair single end reads underwent QC analysis prior to alignment to mouse genome build mm10 using TopHat and Bowtie alignment software.[19] Differential expression was determined using Cufflinks Cuffdiff analysis, with thresholds for differential expression set to fold change >1.5 or <0.66 and a false discovery rate of <0.05.[20] Lists of differentially expressed genes were then queried against the Uniprot Database for gene ontology and protein class analysis.[21]

Statistics.

Data are reported as mean +/- SEM. RT-qPCR data are reported as mean fold change compared to normalized vehicle. Statistical analysis of physiological data was performed with Prism software (version 7). Unpaired t-test was used to compare results between two groups. Body weight gain, cumulative food intake and body length, were analyzed by two-way ANOVA. $P<0.05$ was considered statistically significant.

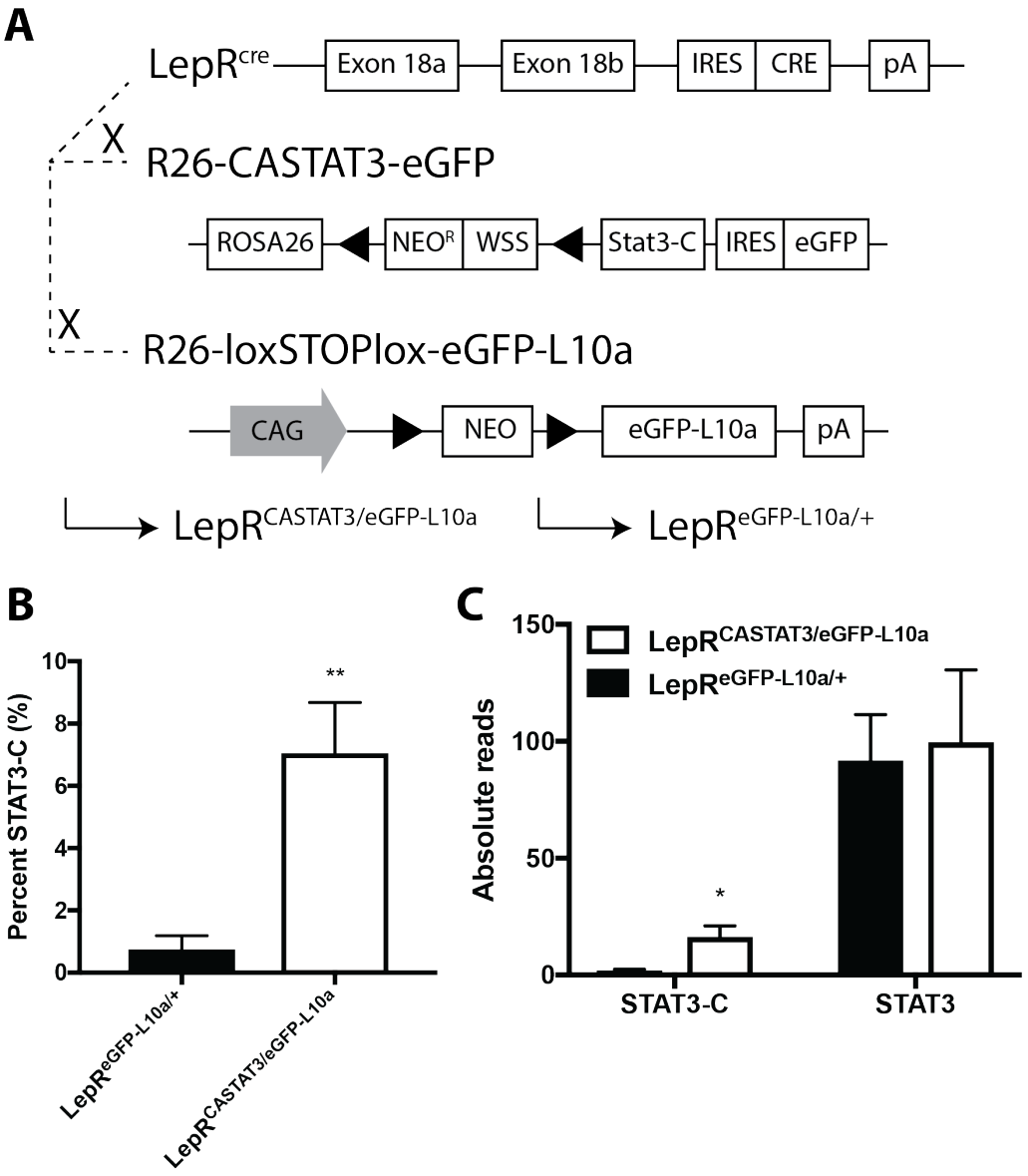

Figure 4.1: Enhanced STAT3 activity in LepRb neurons. (A) Schematic diagram showing the cross of $LepR^{cre}$ with Rosa26-CASTAT3-eGFP and Rosa26-loxSTOPlox-eGFP-L10a to generate $LepR^{CASTAT3/eGFP-L10a}$ ($LepR^{CASTAT3}$) and $LepR^{eGFP-L10a/+}$ ($LepR^{eGFP}$) mice through excision of loxP-flanked Neo^R, Neo, and Stop sequence only in cell types expressing LepRb. IRES: internal ribosome entry site; filled triangles: loxP sites; Neo^R: neomycin resistance gene driven by the TK promoter; WSS: Westphal stop sequence; Stat3-C: constitutively active STAT3. **(B)** RNA sequencing percent reads of the inserted Stat3-C (Stat3-C divided by total Stat3-C and endogenous Stat3) in $LepR^{CASTAT3}$ and control $LepR^{eGFP}$. **(C)** The number of perfectly mapped reads at the unique sites for STAT3-C and endogenous STAT3 in both $LepR^{CASTAT3}$ and $LepR^{eGFP}$ controls. n=3-4 per group. Mean +/- SEM; *p<0.05 by unpaired t-test; **p<0.01 by unpaired t-test for **(B-C)**.

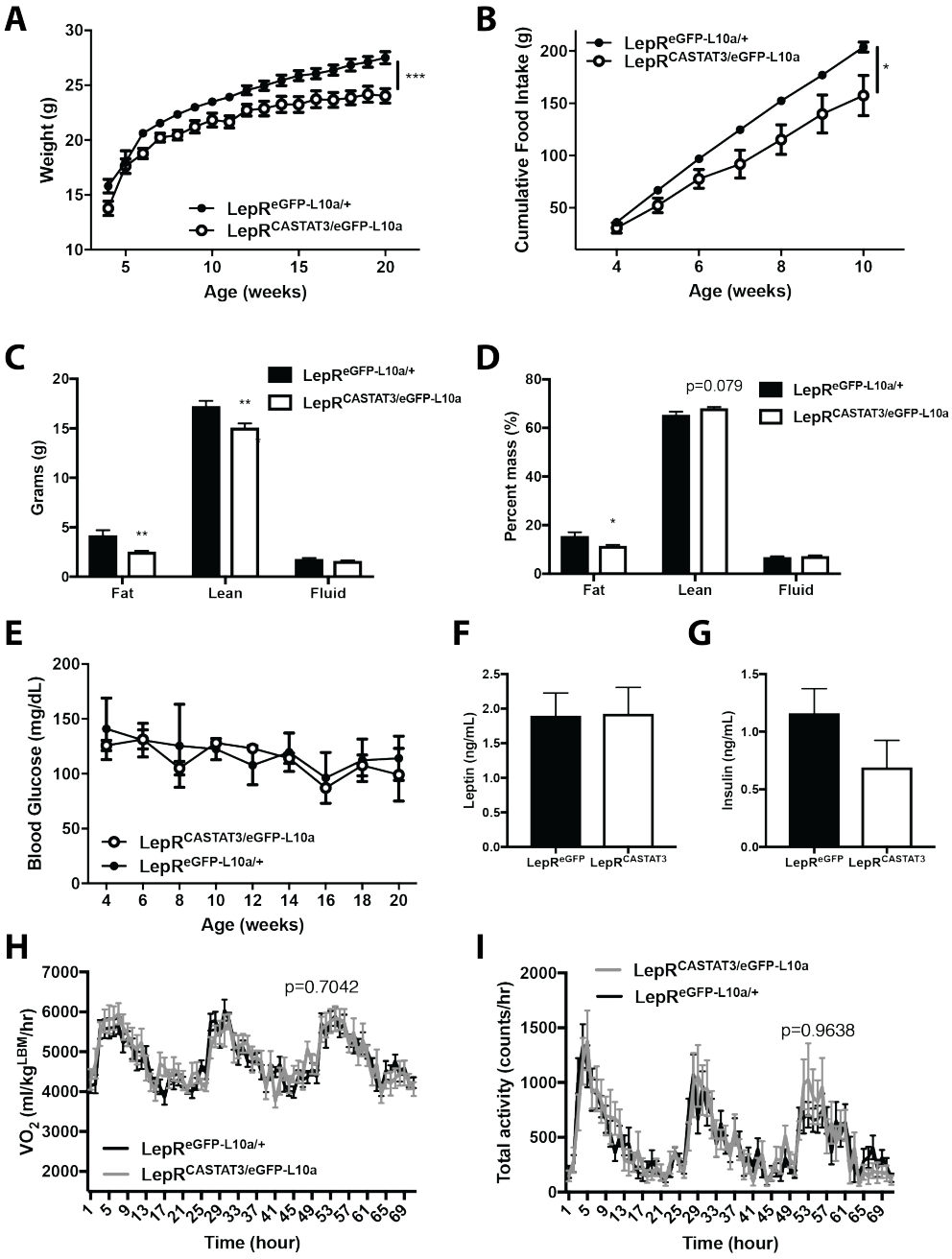

Figure 4.2: Constitutive STAT3 activity in LepRb neurons decreases body weight and adiposity. Male LepR$^{CASTAT3/eGFP-L10a}$ and LepR$^{eGFP-L10a/+}$ mice were placed on chow and body weight **(A)** and food intake **(B)** were measured weekly. At 21-22 weeks of age, animals underwent body composition analysis **(C-D)** by NMR spectroscopy. **(E)** Unfasted blood glucose was measured biweekly. Serum from 16-week-old mice were assayed for leptin **(F)** and insulin **(G)**. 10-12 week-old mice were subjected to CLAMS analysis to determine VO_2 normalized to total body mass **(H)**, and locomotor activity **(I)** over a 72-hour period. n=15-20 for **(A, B)**, n=8-14 for **(C-I)**. Mean +/- SEM is shown;

*p<0.05, **p<0.01, ***p<0.001, ****p<0.0001 by ANOVA **(A, B, H, I)** or unpaired t-test **(C, D)**.

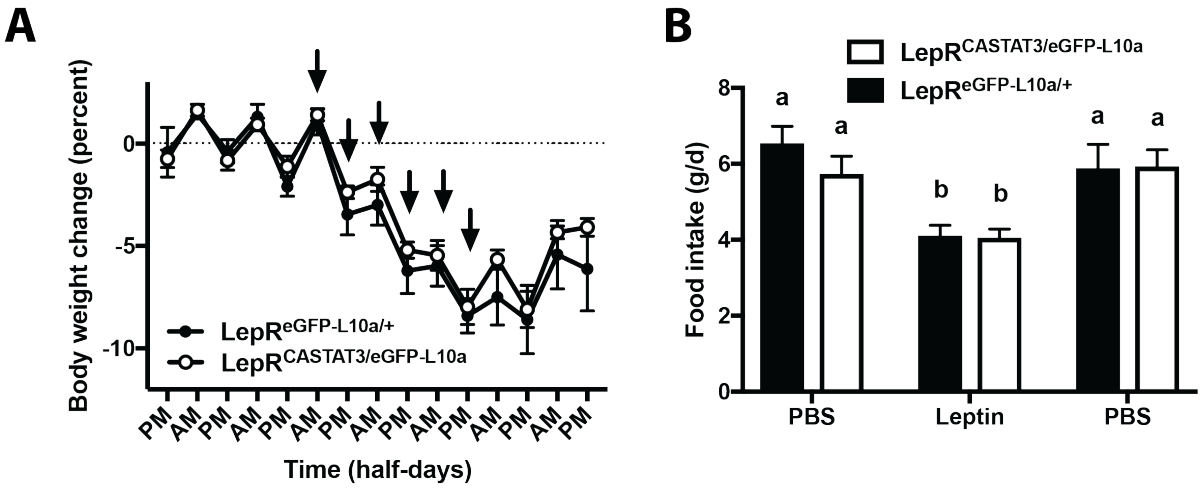

Figure 4.3: Effect of exogenous leptin in already enhanced STAT3-expressing animals. Eight-week-old male $LepR^{CASTAT3/eGFP-L10a}$ and $LepR^{eGFP-L10a/+}$ mice fed normal chow were injected twice daily (at 8:30AM and 4:30PM) with PBS for 3 days, with leptin for 3 days (5mg/kg; i.p.), and then with PBS for 2 days. **(A)** Body weight was measured twice per day during the injection period; arrows indicate times of leptin injections. **(B)** Food intake was measured daily and compiled for the initial PBS period, the leptin period, and the second PBS period. n=9-12 per genotype. **p<0.01 for a to b, no significance between a-a or b-b.

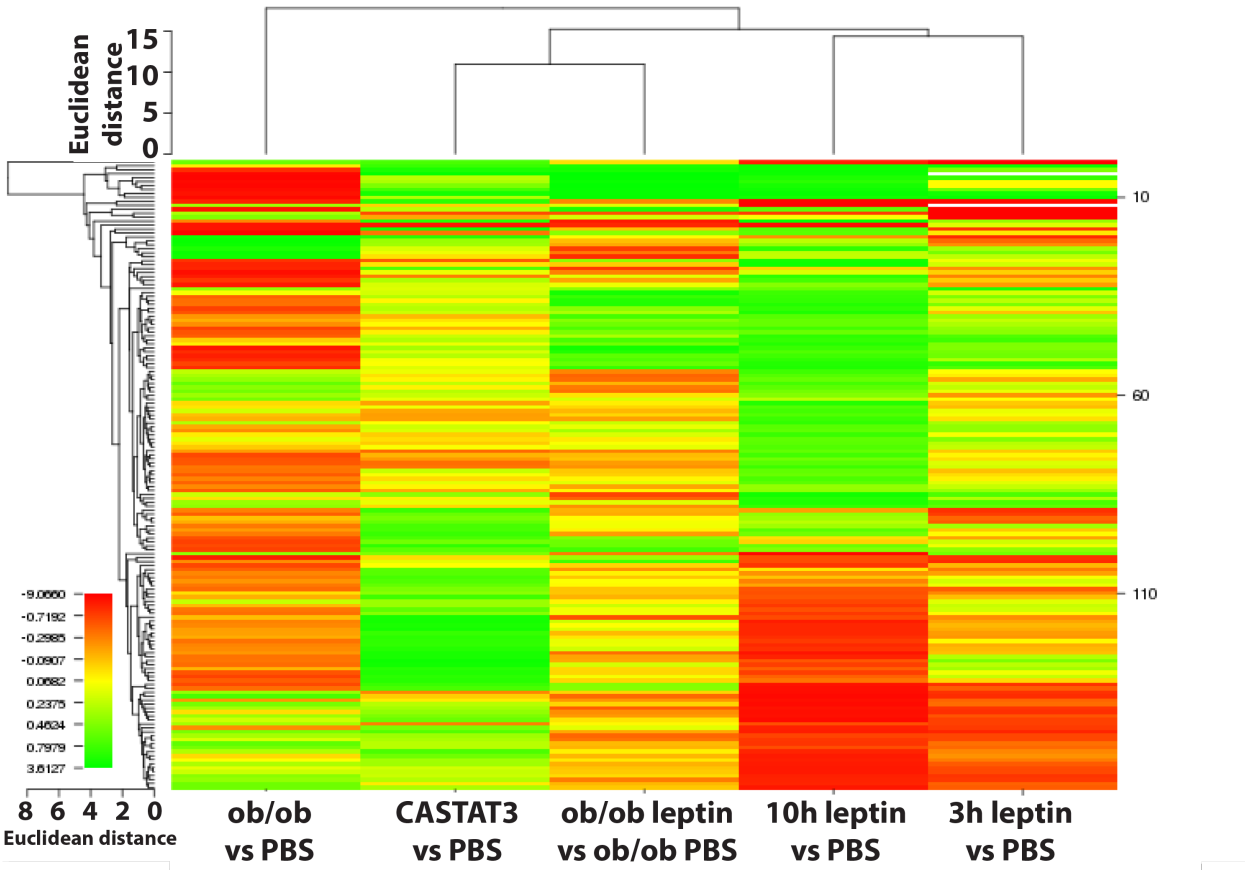

Figure 4.4: TRAP-seq reveals similarities between LepR^{CASTAT3} and leptin treated *ob/ob* animals. Translating ribosome affinity purification (TRAP) was performed in LepR^{eGFP}*ob/ob*, LepR^{CASTAT3} and LepR^{eGFP} mice treated with PBS or leptin and compared to the control PBS treated LepR^{eGFP} group. Fold change values for each of the groups were calculated and compared to littermate control PBS-treated LepR^{eGFP} or PBS-treated LepR^{eGFP}*ob/ob* mice. Each sample comprised of pooled hypothalamic for 6-8 adult animals. n=3-4 pooled samples per condition.

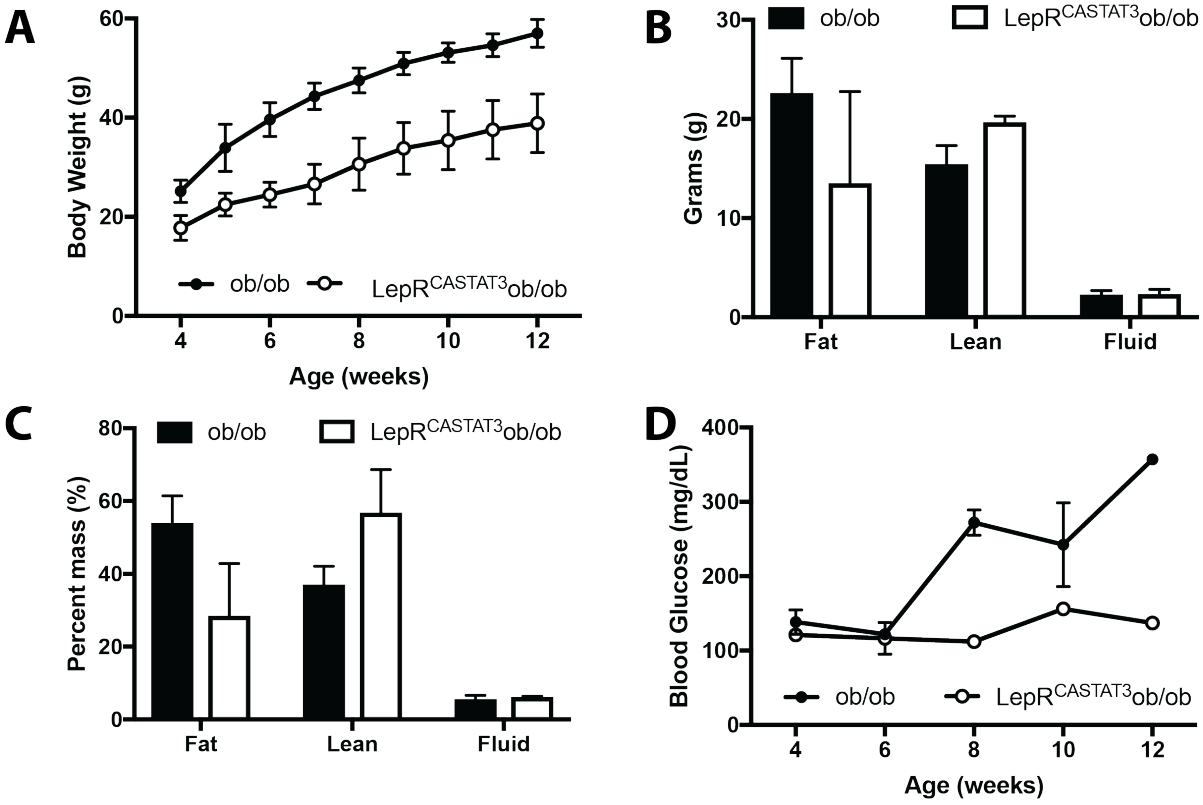

Figure 4.5: LepR^{CASTAT3} partially normalizes *ob/ob* mice. Male LepR^{CASTAT3};*ob/ob* and LepR^{eGFP};*ob/ob* mice were placed on chow and body weight **(A)** was measured weekly. At 14-15 weeks of age, animals underwent body composition analysis **(B-C)** by NMR spectroscopy. **(D)** Unfasted blood glucose was measured biweekly. Mean +/- SEM is shown. N=2-4 per condition.

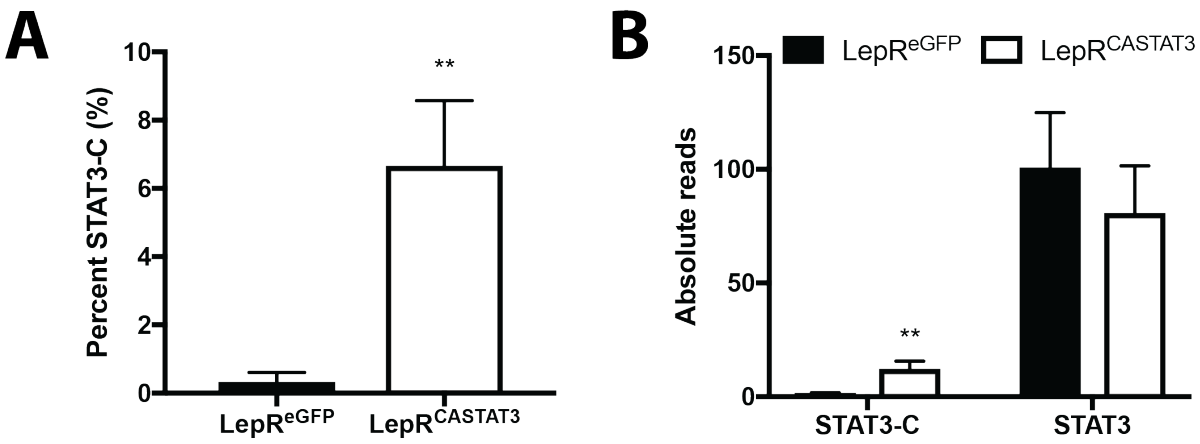

Figure 4.6: Enhanced STAT3 activity in LepRb neurons (females). (A) RNA sequencing percent reads of the inserted Stat3-C (Stat3-C divided by total Stat3-C and Stat3) in female $LepR^{CASTAT3}$ and control $LepR^{eGFP}$. **(B)** The number of perfectly mapped reads at the unique sites for STAT3-C and endogenous STAT3 in female $LepR^{CASTAT3}$ and $LepR^{eGFP}$ controls. n=3-4 per pooled group. Mean +/- SEM; **p<0.01 by unpaired t-test.

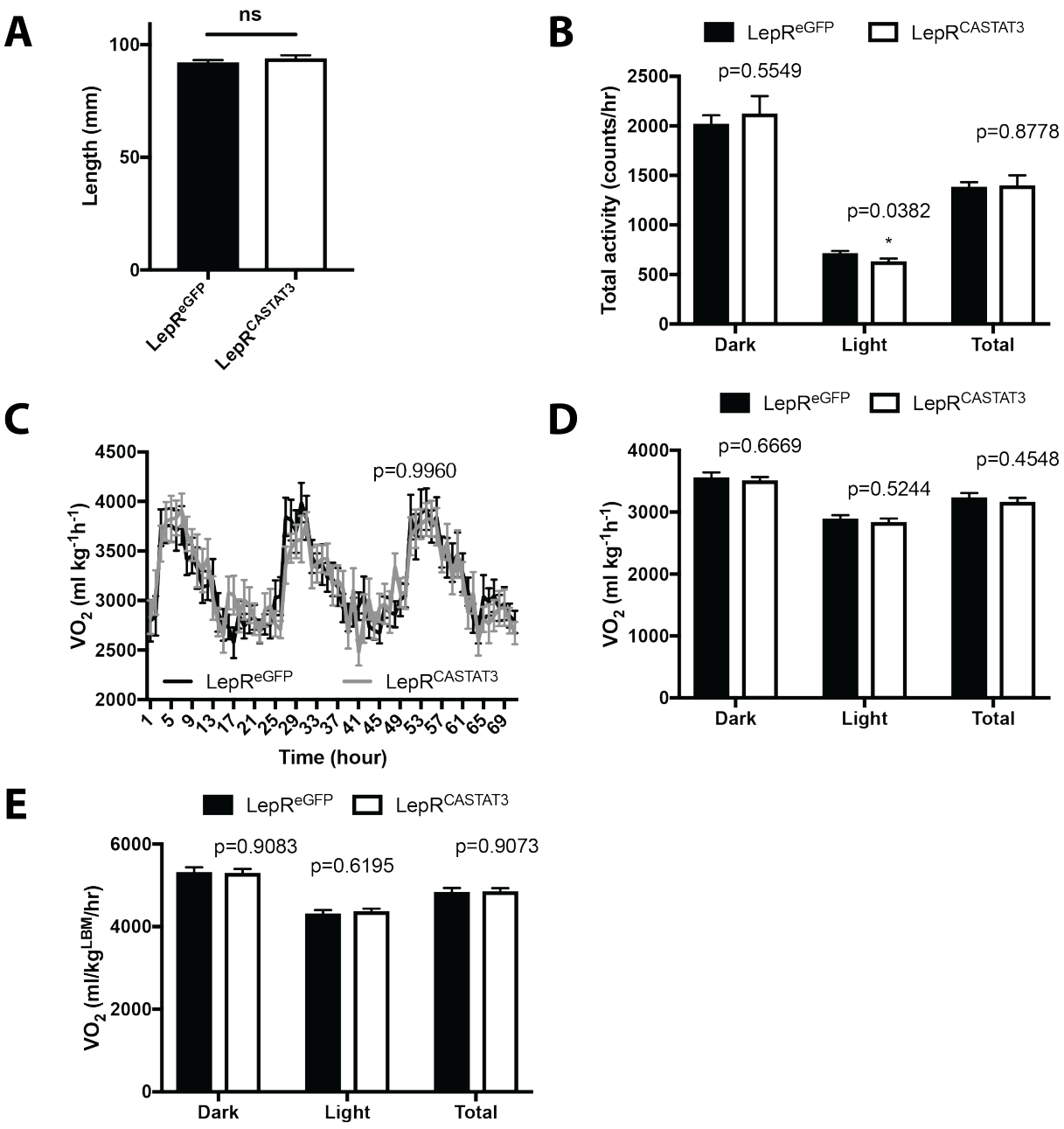

Figure 4.7: Male LepR^{CASTAT3} body length and energy expenditure. (A) Body lengths of male mice were measured at 12 weeks. 10-week old LepR^{eGFP} and LepR^{CASTAT3} mice were placed in CLAMS and locomotor activity **(B)**, VO_2 normalized to total body mass **(C, D)**, and VO_2 adjusted to lean body mass **(E)** were measured. Data are shown for the dark cycle (Dark), light cycle (Light), and 24 hour (Total) period. *p<0.05 by unpaired t-test. n=8-14 per genotype.

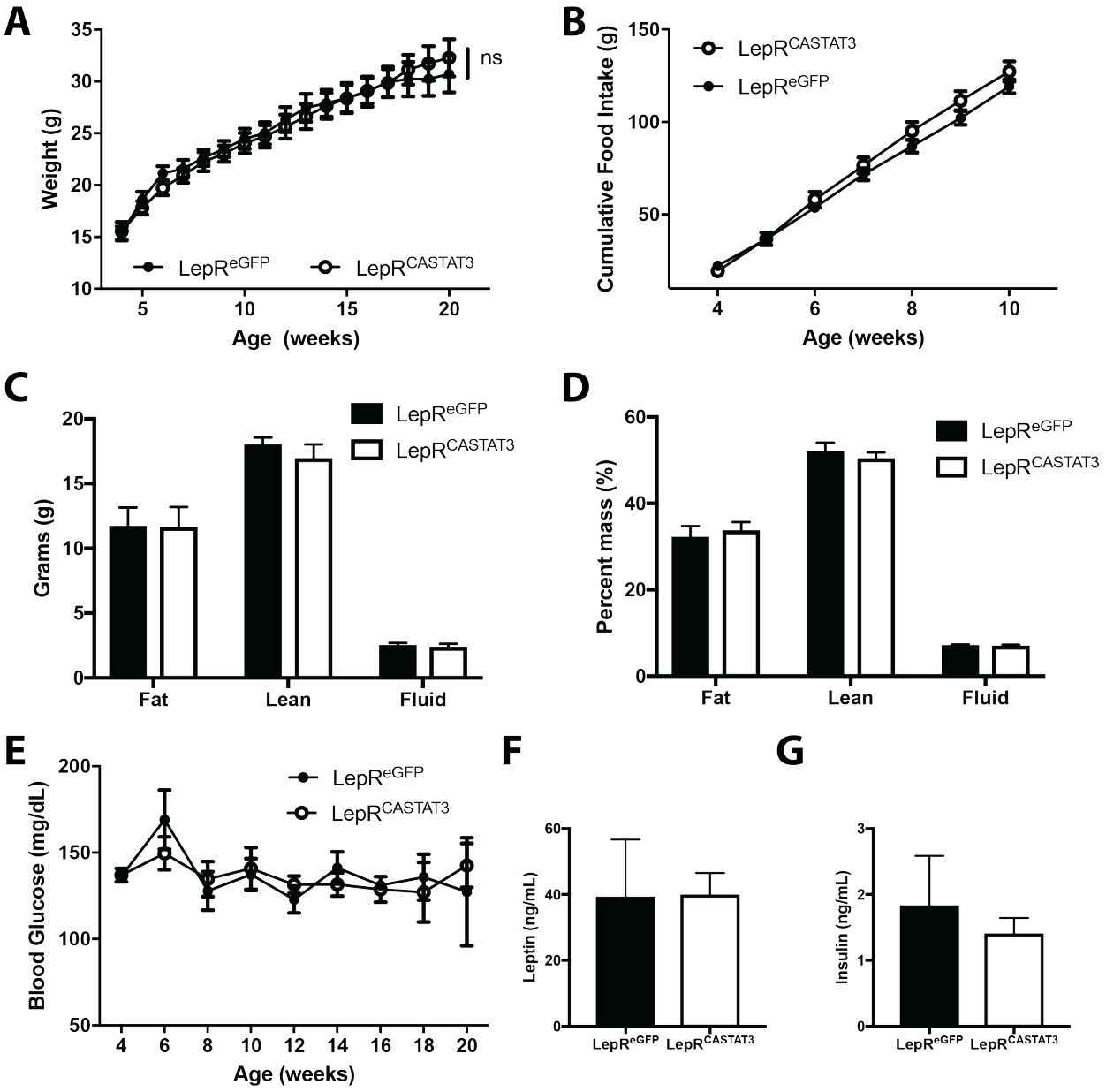

Figure 4.8: Enhanced STAT3 activity does not counter high-fat diet-induced obesity. Male LepR^{CASTAT3} and LepR^{eGFP} mice were placed on 60% high-fat diet and body weight **(A)** and food intake **(B)** were measured weekly. At 21-22 weeks of age, animals underwent body composition analysis **(C-D)** by NMR spectroscopy. **(E)** Unfasted blood glucose was measured biweekly. Serum from 16-week-old mice were assayed for leptin **(F)** and insulin **(G)**. No significance was found by ANOVA or unpaired t-test. N=8-12 per genotype.

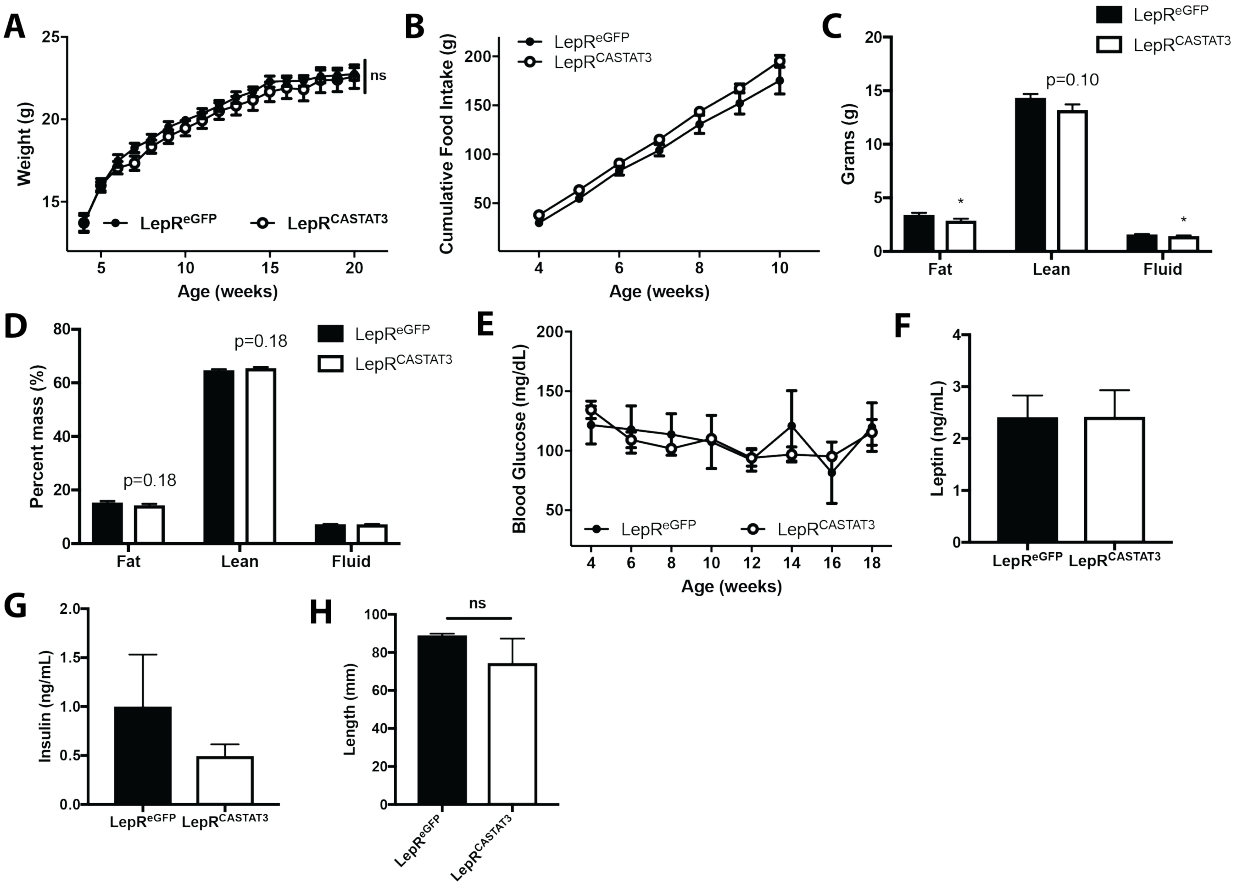

Figure 4.9: Constitutive STAT3 activity in LepRb neurons does not affect energy expenditure (females). Female LepR^{CASTAT3} and LepR^{eGFP} mice were placed on chow and body weight **(A)** and food intake **(B)** were measured weekly. At 21-22 weeks of age, animals underwent body composition analysis **(C-D)** by NMR spectroscopy. **(E)** Unfasted blood glucose was measured biweekly. Serum from 16-week-old mice were assayed for leptin **(F)** and insulin **(G)**. **(H)** Body length was measured in 12-week-old female mice. N=16-20 per group **(A, B)**; n=10-12 per genotype **(C-H)**. Mean +/- SEM is shown; *p<0.05 by unpaired t-test.

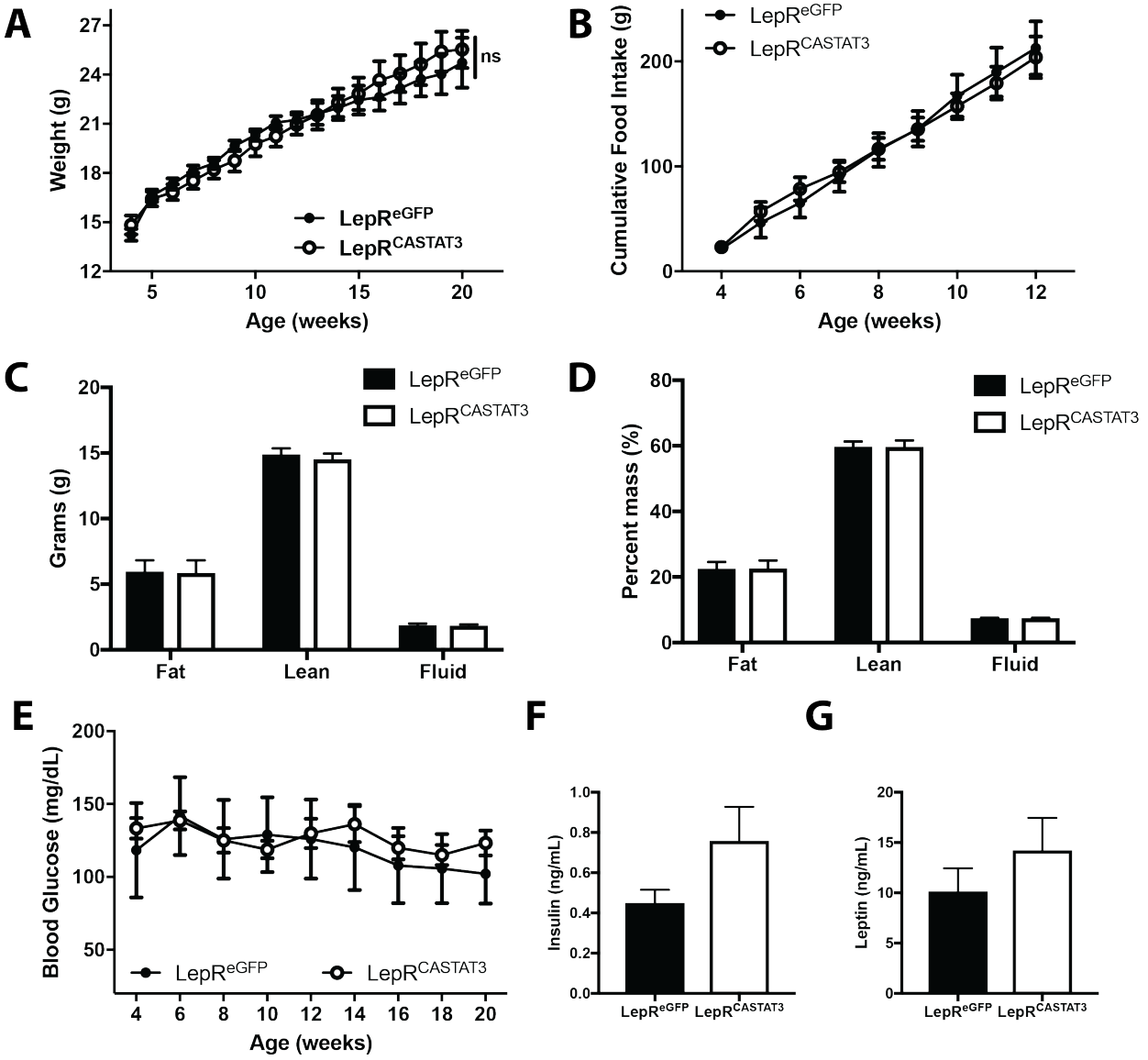

Figure 4.10: Enhanced STAT3 activity does not counter high-fat diet-induced obesity (females). Female LepR^{CASTAT3} and LepR^{eGFP} mice were placed on high-fat diet and body weight **(A)** and food intake **(B)** were measured weekly. At 21-22 weeks of age, animals underwent body composition analysis **(C-D)** by NMR spectroscopy. **(E)** Unfasted blood glucose was measured biweekly. Serum from 16-week-old mice were assayed for leptin **(F)** and insulin **(G)**. No significance was found by ANOVA or unpaired t-test. N=8-12 per genotype.

Gene	FPKM (WT)	Enrichment (WT)	CASTAT3
Aldh1a1	26.00	1.34	2.33
Aldh1a7	0.82	2.81	2.06
Atf3	1.53	3.72	1.84
C130021I20Rik	6.28	2.52	1.63
Ccnb1ip1	0.28	0.97	1.90
Chrna6	2.74	2.39	2.54
Chrnb3	0.85	2.14	2.86
Crhbp	12.94	1.70	1.58
Cubn	0.10	0.89	1.67
Ddc	102.09	2.98	1.53
Egflam	1.13	2.17	1.58
En1	3.13	3.91	3.39
Fgf20	0.21	1.64	2.76
Foxa1	6.88	4.20	1.70
Foxa2	0.79	2.49	2.19
Gbp6	0.68	1.82	1.58
Gm5105	0.13	1.29	1.92
Gucy2c	1.30	6.66	1.96
Gzmk	1.07	1.16	1.62
H2-Q6	0.36	2.56	3.11
Ifi47	0.20	0.77	1.96
Igtp	1.57	1.65	1.65
Irgm2	0.66	0.95	2.05
Irx5	2.82	2.25	1.68
Irx6	2.60	4.08	1.50
Lmx1a	2.85	1.84	1.61
Myh6	0.43	1.35	1.53
Nr4a2	12.80	3.10	1.52
Ntf3	0.65	1.97	1.75
Ntn1	2.27	1.13	1.89
O3far1	0.11	3.03	2.17
Pitx3	0.88	2.24	3.13
Psmb8	3.19	1.60	1.83
Ret	9.81	2.50	1.97
Rnase6	3.03	1.32	0.64
Serpina3h	0.34	3.09	2.74
Serpina3m	0.24	2.42	2.51

Slc10a4	15.05	2.19	2.26
Slc18a2	5.89	1.63	2.06
Slc6a3	14.53	3.65	2.88
Spink8	0.40	0.67	2.24
Sprr1a	0.37	2.60	2.11
Tap1	0.86	1.47	1.52
Th	74.98	2.66	2.01
Ucn	2.00	5.22	0.39
Usp18	0.40	0.87	1.97

Table 4.1: Fold change in LepRb enriched genes in LepR^{CASTAT3} mice. TRAP-Seq was performed on LepR^{CASTAT3} and littermate control LepRb^{eGFP} mice. Genes enriched (FPKM in TRAP/FPKM in TRAP-depleted >1.5) at baseline or that became enriched in the CASTAT3 condition were included in this analyses. Enrichment and expression (FPKM) values displayed are from LepRb^{eGFP} mice. Fold change values for LepR^{CASTAT3} mice were compared to LepR^{eGFP} controls **(Column 4)**. n=3-4 samples per treatment group. Each sample was comprised of pooled hypothalami of 6-8 adult animals.

References

1. Cutler, D. M., Glaeser, E. L. & Shapiro, J. M. American Economic Association Why Have Americans Become More Obese? *Source J. Econ. Perspect.* **17,** 93–118 (2003).
2. Flegal, K. M. *et al.* Trends in Obesity Among Adults in the United States, 2005 to 2014. *Jama* **315,** 2284 (2016).
3. Schwartz, M. W., Woods, S. C., Porte, D., Seeley, R. J. & Baskin, D. G. Central nervous system control of food intake. *Nature* **404,** 661–671 (2000).
4. Hebebrand, J., Muller, T. D., Holtkamp, K. & Herpertz-Dahlmann, B. The role of leptin in anorexia nervosa: clinical implications. *Mol. Psychiatry* **12,** 23–35 (2007).
5. Rosenbaum, M. *et al.* Low-dose leptin reverses skeletal muscle, autonomic, and neuroendocrine adaptations to maintenance of reduced weight. *J. Clin. Invest.* **115,** 3579–3586 (2005).
6. Patterson, C. M., Leshan, R. L., Jones, J. C. & Myers, M. G. Molecular mapping of mouse brain regions innervated by leptin receptor-expressing cells. *Brain Res.* **1378,** 18–28 (2011).
7. Hayes, M. R. *et al.* Endogenous Leptin Signaling in the Caudal Nucleus Tractus Solitarius and Area Postrema Is Required for Energy Balance Regulation. *Cell Metab.* **11,** 77–83 (2010).
8. Piper, M. L., Unger, E. K., Myers, M. G. & Xu, A. W. Specific physiological roles for signal transducer and activator of transcription 3 in leptin receptor-expressing neurons. *Mol. Endocrinol.* **22,** 751–759 (2008).
9. Bates, S. H. *et al.* STAT3 signalling is required for leptin regulation of energy balance but not reproduction. *Nature* **421,** 856–859 (2003).
10. Frederich, R. C. *et al.* Leptin Levels Reflect Body Lipid-Content in Mice - Evidence for Diet-Induced Resistance To Leptin Action. *Nat. Med.* **1,** 1311–1314 (1995).
11. El-Haschimi, K., Pierroz, D. D., Hileman, S. M., Bjørbæk, C. & Flier, J. S. Two defects contribute to hypothalamic leptin resistance in mice with diet-induced obesity. *J. Clin. Invest.* **105,** 1827–1832 (2000).
12. Münzberg, H., Flier, J. S. & Bjørbæk, C. Region-specific leptin resistance within the hypothalamus of diet-induced obese mice. *Endocrinology* **145,** 4880–4889 (2004).
13. Ernst, M. B. *et al.* Enhanced Stat3 activation in POMC neurons provokes negative feedback inhibition of leptin and insulin signaling in obesity. *J. Neurosci.* **29,** 11582–11593 (2009).
14. Mesaros, A. *et al.* Activation of Stat3 Signaling in AgRP Neurons Promotes Locomotor Activity. *Cell Metab.* **7,** 236–248 (2008).
15. Ottaway, N. *et al.* Diet-Induced Obese Mice Retain Endogenous Leptin Short Article Diet-Induced Obese Mice Retain Endogenous Leptin Action. *Cell Metab.* **21,** 1–6 (2015).
16. Knight, Z. A., Hannan, K. S., Greenberg, M. L. & Friedman, J. M. Hyperleptinemia is required for the development of leptin resistance. *PLoS One* **5,** 1–8 (2010).
17. Leshan, R. L., Björnholm, M., Münzberg, H. & Myers, M. G. Leptin receptor signaling and action in the central nervous system. *Obesity (Silver Spring).* **14 Suppl 5,** 208S–212S (2006).

18. Krashes, M. J. *et al.* An excitatory paraventricular nucleus to AgRP neuron circuit that drives hunger. *Nature* **507,** 238–42 (2014).
19. Langmead, B., Trapnell, C., Pop, M. & Salzberg, S. Ultrafast and memory-efficient alignment of short DNA sequences to the human genome. *Genome Biol.* **10,** R25 (2009).
20. Trapnell, C. *et al.* Transcript assembly and quantification by RNA-Seq reveals unannotated transcripts and isoform switching during cell differentiation. *Nat. Biotechnol.* **28,** 511–515 (2010).
21. Magrane, M. & Consortium, U. P. UniProt Knowledgebase: A hub of integrated protein data. *Database* **2011,** 1–13 (2011).

CHAPTER 5

LEPTIN ACTION THROUGH HYPOTHALAMIC CALCITONIN RECEPTOR-EXPRESSING NEURONS CONTROLS ENERGY BALANCE

Chapter Summary

Obesity, and its vast negative implications on health, is an epidemic only growing in incidence. Central to our understanding of obesity is the adipocyte leptin, which binds to its receptor (LepRb) in the hypothalamus to provide a snap shot of fat stores and to drive anorexia. Unfortunately, leptin therapy is ineffective in promoting weight loss in diet-induced obese (DIO) individuals. However, leptin-amylin combination treatment is effective. Here, we explore the hypothalamic neurons that express both LepRb and amylin's cognate receptor, calcitonin receptor (CalcR), by conditionally deleting LepRb in CalcR-expressing neurons. Not only are these mice obese from hyperphagia and decreased energy expenditure, but these LepRb- and CalcR-expressing neurons are a previously unstudied subpopulation of LepRb neurons. Thus, the regulation of energy balance by leptin clearly involves $LepR^{CalcR}$ neurons.

Introduction

Obesity is a growing epidemic in the United States and accounted for over $147 billion of total health care costs in 2008.[1] The adipocyte leptin is produced in proportion to triglyceride content and binds to its receptors (LepRb) to not only provide a summary of the body's energy stores, but to also regulative energy balance.[2–4] These LepRb-expressing neurons are located throughout the brain and are heterogeneous in nature; those in the hypothalamus are perhaps the most involved in energy balance, for their ablation results in profound obesity and metabolic dysfunction.[5]

Of the many subpopulations of LepRb neurons in the hypothalamus, those located in the arcuate nucleus (ARC), which lies adjacent to the median eminence (a circumventricular organ that permits passage of circulating factors like leptin), are best characterized. Many of these ARC LepRb neurons express the melanocortin precursor POMC (termed POMC neurons) or the inhibitory hormone neuropeptide Y (NPY), the melanocortin antagonist agouti-related protein (AgRP), and the inhibitory neurotransmitter GABA. Partially through the melanocortin system, POMC neurons drive a negative energy balance while NAG (NPY, AgRP, GABA) neurons promote a positive energy balance.[6] Leptin thereby promotes negative energy balance by increasing POMC neuronal activity while decreasing NAG action.[6] Despite the central roles POMC and NAG neurons play in leptin action, deletion of LepRb from POMC and/or NAG neurons only modestly affect energy balance.[7] Recent single-cell sequencing of ARC cells reveals the existence of other non-POMC and non-NAG LepRb neurons in the arcuate nucleus, some of which express calcitonin receptor (CalcR).[8]

The hormone calcitonin and its family of structurally and functionally related neuropeptides, including amylin, calcitonin gene-related peptide (CGRP), and adrenomedullin, all bind to CalcR in the brain to promote satiety, glycemic control and slowing of gastric empyting.[9–12] In the context of the obesity epidemic, the interaction between leptin and CalcR agonists has been a promising area of research: combination leptin-amylin therapy is effective in producing synergistic and consistent weight loss in diet-induced obese (DIO) humans and rodents.[13–15] Recently, Li et. al. demonstrated that the precursor to amylin is secreted in hypothalamic neurons and may synergize with LepRb-expressing neighboring neurons.[16] This, coupled with the high expression and fold enrichment of CalcR in hypothalamic LepRb neurons, underscores not only the importance of these dual-expressing neurons on energy balance, but also highlights a new population of LepRb neurons that may mediate a portion of leptin signaling in the hypothalamus.[17] Therefore, we conditionally ablated LepRb in CalcR-expressing neurons to determine whether those $LepRb^{CalcR}$ neurons are important in energy balance. Additionally, we aimed to identify this subpopulation of LepRb neurons that also express CalcR and genes that may be involved in their activity.

Results:

Calcitonin activates LepRb neurons in the ARC

Salmon calcitonin (sCT), a powerful calcitonin receptor (CalcR) agonist, has particularly effective anorexigenic properties in the state of diet-induced obesity (DIO) and leptin resistance.[18] Intraperitoneal injection of sCT resulted in the activation of CalcR neurons using immunohistochemically detectable cfos induction as marker in

CalcR;Rosa26$^{L10a\text{-}eGFP}$ (CalcR^{eGFP}) mice that express an L10a-GFP fusion protein in CalcR neurons (Figure 5.8). As suggested by previous *in-situ hybridization* experiments,[19] many of these cfos-induced regions are in leptin receptor- (LepRb) rich regions of the hypothalamus. Indeed, cfos induction with sCT injection was found in neurons that not only express CalcR, but also express LepRb—specifically NPY expressing LepRb neurons (Figure 5.1). Quantification reveals that approximately 60% of cfos-positive neurons also express NPY, 2% express POMC, and the remaining 37% are arcuate neurons that express neither NPY or POMC (Figure 5.1e). In addition, there was no colocalization between CalcR and POMC when CalcR^{eGFP} mice were crossed to POMC^{sdred} mice (Figure 5.12). Thus, the existence of these hypothalamic neurons expressing both LepRb and CalcR may impart clues on the synergistic weight loss demonstrated with amylin-leptin combination therapy in diet-induced obesity [20].

Generation and characterization of CalcR-cre mice

To study LepRb and CalcR dual expressing neurons, we inserted a 2a element plus the coding sequences for Cre recombinase into the 3'untranslated region of CalcR in mice to promote CalcR-restricted Cre expression (CalcRcre mice) (Figure 5.2a). We verified that this cre expression overlaps with CalcR mRNA by ISH (Figure 5.7). These CalcRcre mice were then bred to R26-loxSTOPlox-eGFP-L10a and LepR$^{flox/flox}$ mice to generate CalcR$^{cre/cre}$;LepR$^{flox/flox}$;Rosa26$^{eGFP\text{-}10a/eGFP\text{-}10a}$ (LepR^{CalcR}KO) mice and littermate control CalcR$^{cre/cre}$;Rosa$^{eGFP\text{-}10a/eGFP\text{-}L10a}$ (CalcR^{eGFP}) mice (Figure 5.2a). Analysis of CalcR^{eGFP} and LepR^{CalcR}KO mice show an absence of pSTAT3 in the CalcR neurons of LepR^{CalcR}KO with leptin treatment compared to littermate controls (Figure 5.2b, 5.2c, and Figure 5.9). We quantified the conditional ablation of LepRb in CalcR

neurons with pSTAT3 immunoreactivity (compared to control mice) in regions where there was potential overlap between pSTAT3 and CalcR expression: the arcuate nucleus (ARC), dorsomedial hypothalamus (DMH), lateral hypothalamic area (LHA) and nucleus of the solitary tract (NTS) (Figure 5.2d, 5.2e, and Figure 5.9).

Leptin receptors in calcitonin receptor expressing neurons regulate energy balance

Both male and female $LepR^{CalcR}KO$ mice have higher body weights and food intakes compared to control $CalcR^{eGFP}$ mice (Figure 5.3a, 5.3f, and Figure 5.10a, 10f). The excess weight in $LepR^{CalcR}KO$ mice was largely due to elevated adipose mass (Figure 5.3c, 5.3d, and Figure 5.10c, 5.10d), and is reflected in elevated serum leptin levels (Figure 5.3e, and Figure 5.10e). $LepR^{CalcR}KO$ mice have unchanged crown to rump lengths when compared to $CalcR^{eGFP}$ mice (Figure 5.3b, and Figure 5.10b). Interestingly, while $LepR^{CalcR}KO$ mice have more absolute adipose tissue, lean mass, and fluid; in percentage terms, $LepR^{CalcR}KO$ mice are less lean, more obese, and have comparable fluid levels (Figure 5.3c, 5.3d, Figure 5.10c, 5.10d). The maximal oxygen consumption (VO_2) in male $LepR^{CalcR}KO$ mice was lower than in $CalcR^{eGFP}$ mice (Figure 5.4a, 5.4b), but when VO_2 was adjusted to lean body mass, VO_2 was comparable between $LepR^{CalcR}KO$ and $CalcR^{eGFP}$ mice (Figure 5.4c, 5.4d). A decrease in dark and total locomotor activity was also observed in $LepR^{CalcR}KO$ mice when compared to $CalcR^{eGFP}$ control mice (Figure 5.4e, 5.4f). Thus, leptin action in $LepR^{CalcR}$ neurons is crucial for regulation of feeding and the control of body weight and adiposity.

Glucose homeostasis is not disrupted in $LepR^{CalcR}KO$ animals

To determine the potential role for leptin action through $LepR^{CalcR}$ neurons on glucose homeostasis, unfasted serum glucose levels were measured biweekly from 4-12 weeks of age in $LepR^{CalcR}KO$ and $CalcR^{eGFP}$ control mice and were comparable (Figure 5.5a, and Figure 5.11a). 10-week-old $LepR^{CalcR}KO$ mice were found to have higher serum insulin levels when compared to 10-week-old littermate controls (Figure 5.5b, and Figure 5.11b). Glucose tolerance and insulin tolerance test were performed but neither were altered in $LepR^{CalcR}KO$ mice (Figure 5.5c, 5.5d; Figure 5.11c, 5.11d).

Gene expression, enrichment and regulation of CalcR neurons.

We employed translating ribosome affinity purification (TRAP) using hypothalamic material from both $CalcR^{eGFP}$ and $LepR^{CalcR}KO$ mice (which both express an eGFP-tagged ribosomal subunit fusion protein in CalcR neurons) to separate hypothalamic CalcR cell transcripts from non-CalcR expressing cell mRNA. The expression levels of key genes involved in regulation of food intake were measured and fold changes are detailed for enrichment (between CalcR and non-CalcR cells) and expression (between CalcR cells in control $CalcR^{eGFP}$ and CalcR cells in $LepR^{CalcR}KO$ mice) (Figure 5.6a, 5.6b). Corroborating our finding of cfos expression with sCT injection seen in many NPY neurons (Figure 5.1c-e), *AgRP* and *Npy* are highly enriched in both $CalcR^{eGFP}$ and $LepR^{CalcR}KO$ mice, while *Pomc* is de-enriched (Figure 5.6a). As expected, *CalcR* is highly enriched in CalcR neurons, although *Sst* was also found to be highly enriched in both $CalcR^{eGFP}$ and $LepR^{CalcR}KO$ mice (Figure 5.6a). *Socs3*, *Cartpt*, and *Serpina3N* were all enriched in $CalcR^{eGFP}$ but not in $LepR^{CalcR}KO$ mice (Figure 5.6a). Examination of relative expression differences between control $CalcR^{eGFP}$ to $LepR^{CalcR}KO$ mice reveal a significant decrease in expression of *Socs3* (a surrogate for

LepRb action) and *Serpina3N* (Figure 5.6b). Deletion of LepRb from $LepR^{CalcR}$ neurons also resulted in increased expression of *Pomc* (although *Pomc* still remains de-enriched in CalcR neurons), *AgRP* and *Npy* (Figure 5.6a, 5.6b). Together, these data reveal a population of LepRb neurons that express CalcR/AgRP/Npy/Sst critical for leptin action and energy balance. Furthermore, given the severe metabolic phenotype of $LepR^{CalcR}$KO mice, the differential expression of certain genes like SERPINA3N may underlie mechanisms responsible for the obesity.

Discussion

Previous studies have examined the phenotypic significance of amylin-leptin combination treatment in obese individuals, and the synergistic weight loss seen suggests the existence of interactions between the two hormones.[13,15] Consistent with previous TRAP-seq and single-cell sequencing analyses, we found that LepRb is expressed in a number of CalcR neurons throughout the hypothalamus including the ARC, DMH and LHA.[8,17] Unexpectedly, even though LepRb neurons and CalcR neurons are both expressed in the hindbrain and both mediate satiety, there is no overlap between the two. We found that most of the dual LepRb- and CalcR-expressing neurons are located in the ARC, which was confirmed with salmon calcitonin (sCT) treatment. Interestingly, many of these LepRb- and CalcR-expressing neurons in the ARC are NAG neurons and genetic ablation of LepRb from CalcR neurons resulted in a obesity from increased food intake and decreased energy expenditure. This would point to the importance of these CalcR-expressing LepRb neurons in the arcuate and identifies a population of non-Npy non-Pomc LepRb neurons that mediates a significant degree of leptin action, given the modest effects seen with LepRb ablation in AgRP/Npy

expressing neurons.[7] Worthy of further investigation is the role sCT-activated NAG neurons play in satiety. Because NAG neurons promote a positive energy balance and sCT is a potent satiety compound, it should be explored whether directed delivery of sCT to non-NAG areas can amplify the satiety experienced.

Clearly, leptin action through $LepR^{CalcR}$ neurons is important for energy balance. Gene expression analysis of these CalcR neurons demonstrate the enrichment of a number of genes that may mediate part of the demonstrated metabolic effects of LepRb ablation. Specifically, the enrichment of *Sst* is an interesting candidate for mediating leptin action; even more exciting is the significant decrease in expression of *Serpina3N* with LepRb deletion. Previous studies have identified SERPINA3N as a gene downstream of leptin action that may be an important enzyme in the regulation of leptin action and body weight homeostasis.[8,17] Together, this work demonstrates the heterogeneous nature of LepRb neurons and the role leptin action plays in multiple homeostatic systems involved in energy balance. Given the promise of dual therapy in the treatment of obesity, the continued investigation of complementary hormones may reveal novel therapeutic targets to cure obesity. And while these studies demonstrate the importance of $LepRb^{CalcR}$ neurons, additional research on the deletion of CalcR from LepRb-expressing neurons need to be performed to strengthen the idea that the amylin-leptin synergistic weight loss occurs in these CalcR- and LepRb-expressing neurons. Specifically, the question of whether DIO $CalcR^{LepR}$KO mice responds to amylin-leptin therapy like their littermate DIO controls needs to be answered. Furthermore, while we point to SERPINA3N and SST as genes of interest in these neurons, TRAP-seq on $LepR^{flp}CalcR^{cre}$ mice with a flp and cre dependent eGFP-L10a fusion protein (especially

when comparing PBS treated DIO to amylin-leptin treated DIO animals) would really identify the genes and molecular mechanisms that may be responsible for the synergistic weight loss observed.

Materials and Methods

Mice.

Mice were bred in our colony at the Unit for Laboratory Animal Medicine at the University of Michigan; these mice and the procedures performed were approved by the University of Michigan Committee on the Use and Care of Animals and in accordance with AALAC and NIH guidelines. We purchased male and female C57BL/6 mice for experiments and breeding studies from Jackson Labs. Mice were bred at the University of Michigan and provided with food and water *ad libitum* in temperature controlled rooms on a 12-hour light-dark cycle.

We generated $LepR^{eGFP}$ mice by crossing $LepR^{cre}$ mice[21] onto the eGFP-L10a background to produce $LepR^{cre/+}$;$Rosa26^{eGFP\text{-}10a/+}$ mice,[22] which we then intercrossed to generate double homozygous $LepR^{cre/cre}$;$Rosa^{eGFP\text{-}10a/eGFP\text{-}L10a}$ ($LepR^{eGFP}$) study animals. Pomc-dsRed transgenic mice (gift from Malcolm Low) and Npy-GFP transgenic mice (Jackson stock #006417) were crossed to generate $Pomc^{dsRed}Npy^{GFP}$ mice.

To generate CalcR-2aCre mice, a selection cassette containing the porcine teschoviral 2A cleavage sequence linked to Cre recombinase and a Frt-flanked kanamycin resistance gene was targeted to replace the stop codon of the CalcR gene in a bacterial artificial chromosome (RP24-193M22; Children's Hospital Oakland Research Institute). A targeting plasmid containing the Cre-containing selection cassette and ~4

kb genomic sequence upstream and downstream of the CalcR stop codon was isolated and used for embryonic stem cell targeting by the University of Michigan Transgenic Core. Correctly targeted clones were identified by loss of native allele quantitative PCR in blastocysts. Chimeric animals generated from blastocyst implantation were then bred for germline transmission of the CalcR-2aCre allele. Flp-deleter mice were then used to remove the neomycin selection cassette. Mice were subsequently intercrossed to generate homozygous Cre reporter strains and bred to Cre-dependent reporter lines. $CalcR^{eGFP}$ mice were produced by crossing CalcRcre mice onto the eGFP-L10a background to produce $CalcR^{cre/+}$;$Rosa26^{eGFP\text{-}10a/+}$ mice, which were then intercrossed to generated double homozygous $CalcR^{cre/cre}$;$Rosa^{eGFP\text{-}10a/eGFP\text{-}L10a}$ ($CalcR^{eGFP}$) study animals. $LepR^{flox/flox}$ mice[23] were bred to $CalcR^{eGFP}$ mice to generate $CalcR^{cre/+}$;$LepR^{flox/+}$;$Rosa26^{eGFP\text{-}10a/+}$ mice, which were bred to $CalcR^{eGFP}$ mice to produce $CalcR^{cre/cre}$;$LepR^{flox/+}$;$Rosa26^{eGFP\text{-}10a/eGFP\text{-}10a}$ mice. The intercross of $CalcR^{cre/cre}$;$LepR^{flox/+}$;$Rosa26^{eGFP\text{-}10a/eGFP\text{-}10a}$ mice resulted in $CalcR^{cre/cre}$;$LepR^{flox/flox}$;$Rosa26^{eGFP\text{-}10a/eGFP\text{-}10a}$ ($LepR^{CalcR}$KO) mice and littermate control ($CalcR^{cre/cre}$;$LepR^{+/+}$;$Rosa26^{eGFP\text{-}10a/eGFP\text{-}10a}$ ($CalcRe^{GFP}$)) mice for study. $Pomc^{dsRed}CalcR^{eGFP}$ were generated by crossing CalcRcre onto the eGFP-L10a background then crossing with the Pomc-dsRed transgenic mice. We genotyped offspring using PCR.

Leptin treatment, salmon calcitonin treatment and immunohistochemistry.

Mice had food removed at the onset of the light cycle and were treated four hours later with metreleptin (5mg/kg; i.p.), salmon calcitonin (150ug/kg; i.p.), or vehicle and subsequently perfused 90 minutes later. Prior to perfusion, mice were anesthetized with

a lethal dose of pentobarbital and transcardially perfusion with phosphate buffered saline (PBS) followed by 10% buffered formalin. Brains were removed, placed in 10% buffered formalin overnight, and dehydrated in 30% sucrose for one week. Using a freezing microtome (Leica), brains were cut into 30 um sections. Sections were treated sequentially with 1% hydrogen peroxide/ 0.5% sodium hydroxide, 0.3% glycine, 0.03% sodium dodecyl sulfate, and blocking solution (PBS with 0.1% triton, 3% Normal Donkey Serum). Immunostaining was performed using primary antibodies for pSTAT3 (Cell Signaling #9145, rabbit, 1:1000), GFP (Aves Labs #GFP1020, chicken, 1:1000), c-fos (Santa Crus sc-52, rabbit, 1:1000), dsRed (Living Colors #632496, 1:1000). All antibodies were reacted with species-specific Alexa Fluor-488 or -568 conjugated secondary antibodies (Invitrogen, 1:200) or processed with the avidin-biotin/diaminobenzidine (DAB) method (ABC kit, Vector Labs, 1:500; DAB reagents, Sigma). Images were collected on an Olympus BX53F microscope. DAB images were pseudocolored using Photoshop software. The number of c-Fos and pSTAT3 positive nuclei and those colocalizing with GFP and dsRed expressing cells were counted.

In situ hybridization.

For *in situ hybridization* (ISH), adult *CalcR*-Cre and wildtype control mice were anesthetized with isoflurane and then euthanized by decapitation. Whole brains were dissected, flash frozen in isopentane, chilled on dry ice and stored at -80°C. 16 µm-thick coronal sections were cut on a cryostat (Leica), thaw-mounted to SuperFrost Plus slides, allowed to dry at -20°C for one hour and then stored at -80°C. Slides were then processed for ISH using RNAScope technology per the manufacturer's protocol (Advanced Cell Diagnostics). For all slides, the multiplex fluorescent assay (320850)

was used to visualize CalcR (477791) and Cre (312281-C3) probes using Amp 4 Alt-A. Images were obtained with an Olympus BX53F and QImaging Retiga 6000 monochrome camera under 40X objective. All images were processed identically in CellProfiler (Lamprecht MR 2007 Biotechniques) to reduce nonspecific background. Serial images (16 per arcuate nucleus) were taken and stitched together using Photoshop (Adobe).

Phenotyping of LepR^{CalcR}KO and control mice.

LepR^{CalcR}KO and littermate control (LepR^{cre}) mice were weaned into individual housed cages at 21 days and fed normal chow (Purina Lab Diet 5001). Weekly body weight and food intake were monitored. Unfasted blood glucose sample was take every other week from 4-12 weeks of age. Glucose tolerance test (2g/kg body weight, i.p.) and insulin tolerance test (1 unit/kg body weight, Humulin (Eli Lilly), i.p.) were performed in 13 and 14 week old mice, respectively, after a 5-hour fast three hours after the start of the light-cycle. Analysis of body fat and lean mass was performed at 15 weeks of age using NMR-based analyzer (Minispec LF90II, Bruker Optics). One subset of mice (9-11 weeks old) were analyzed for oxygen consumption (VO_2), food intake, and locomotor activity using the Comprehensive Laboratory Animal Monitoring System (CLAMS, Columbus Instruments). Leptin and insulin were assayed by commercial ELISA (Crystal Chem).

TRAP RT-qPCR.

At the midpoint of the light cycle, adult homozygous mice were anesthetized with isoflurane, had their brains removed and placed onto a mouse coronal brain matrix

(1mm sections). A 3x3x3mm block was dissected from the ventral diencephalon immediately caudal to the optic chiasm; this hypothalamic dissection was homogenized for TRAP-seq analysis. We employed anti-eGFP Translating Ribosome Affinity Purification (TRAP) using hypothalamic material from $CalcR^{eGFP}$ and $LepR^{CalcR}KO$ mice (which both express an eGFP-tagged ribosomal subunit in CalcR cells). The messenger RNA isolated from eGFP-tagged ribosomes and from the eGFP-depleted was assessed for quality using the TapeStation (Agilent, Santa Clara, CA) and samples with RINs (RNA Integrity Numbers) of 8 or greater were converted to cDNA using iScript cDNA synthesis kit (Biorad #170-8891) for use in reverse transcription PCR. cDNA was analyzed in triplicate by quantitative real time PCR on an Applied Biosystems StepOnePlus Real-Time PCR System for GAPDH (endogenous control) and the following: *AgRP*, *Pomc*, *Serpina3n*, *Socs3*, *Npy*, *Cartpt*, *Sst*, and *CalcR*. All Taqman assays were acquired from Applied Biosystems (Foster City, CA). We calculated relative mRNA expression values using the $2^{-\Delta\Delta Ct}$ method with normalization of each sample ΔCt value to the average ΔCt value from the control mice.

Statistics.

Data are reported as mean +/- SEM. Statistical analysis of physiological data was performed with Prism software (version 7). Unpaired t-test was used to compare results between two groups. Body weight gain, cumulative food intake, body length, GTT and ITT were analyzed by two-way ANOVA. $P<0.05$ was considered statistically significant.

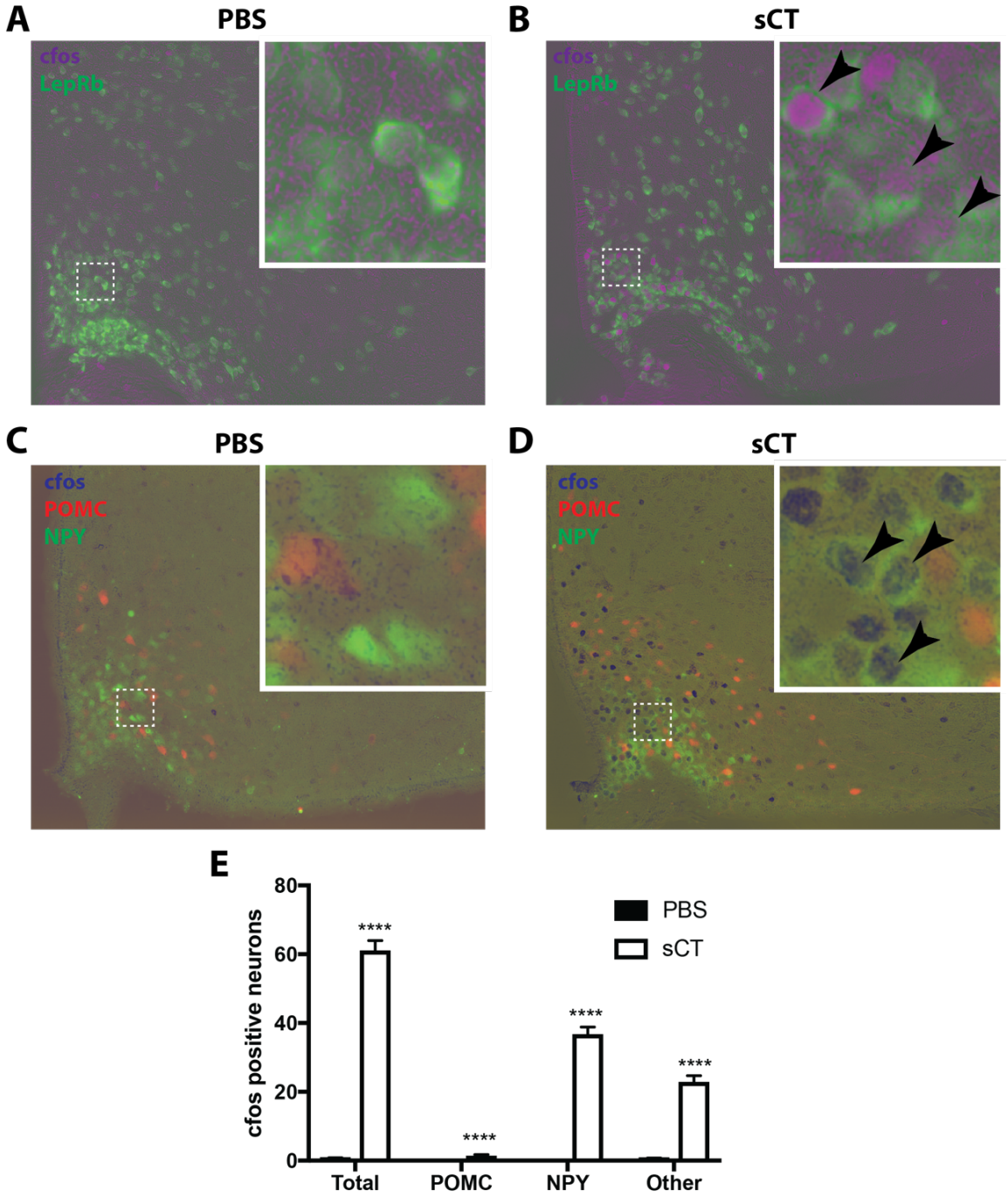

Figure 5.1: Salmon calcitonin-stimulated cfos-IR in LepRb, POMC and NPY neurons. (**A-B**) Representative images showing colocalization of cfos-IR (purple) with GFP-IR (green) in $LepR^{eGFP}$ mice treated with salmon calcitonin (sCT; 150ug/kg, i.p.) or PBS vehicle. (**C-D**) Representative images showing colocalization of cfos-IR (blue) with dsRed-IR (red) and GFP-IR (green) in $POMC^{dsred}NPY^{GFP}$ mice. (**E**) Counts of cfos-IR in the arcuate nucleus (Total), those dual-labeled with dsred-IR (POMC), those dual-labeled with GFP-IR (NPY), and those not colocalized with either (Other). Arrows indicate colocalized neurons.

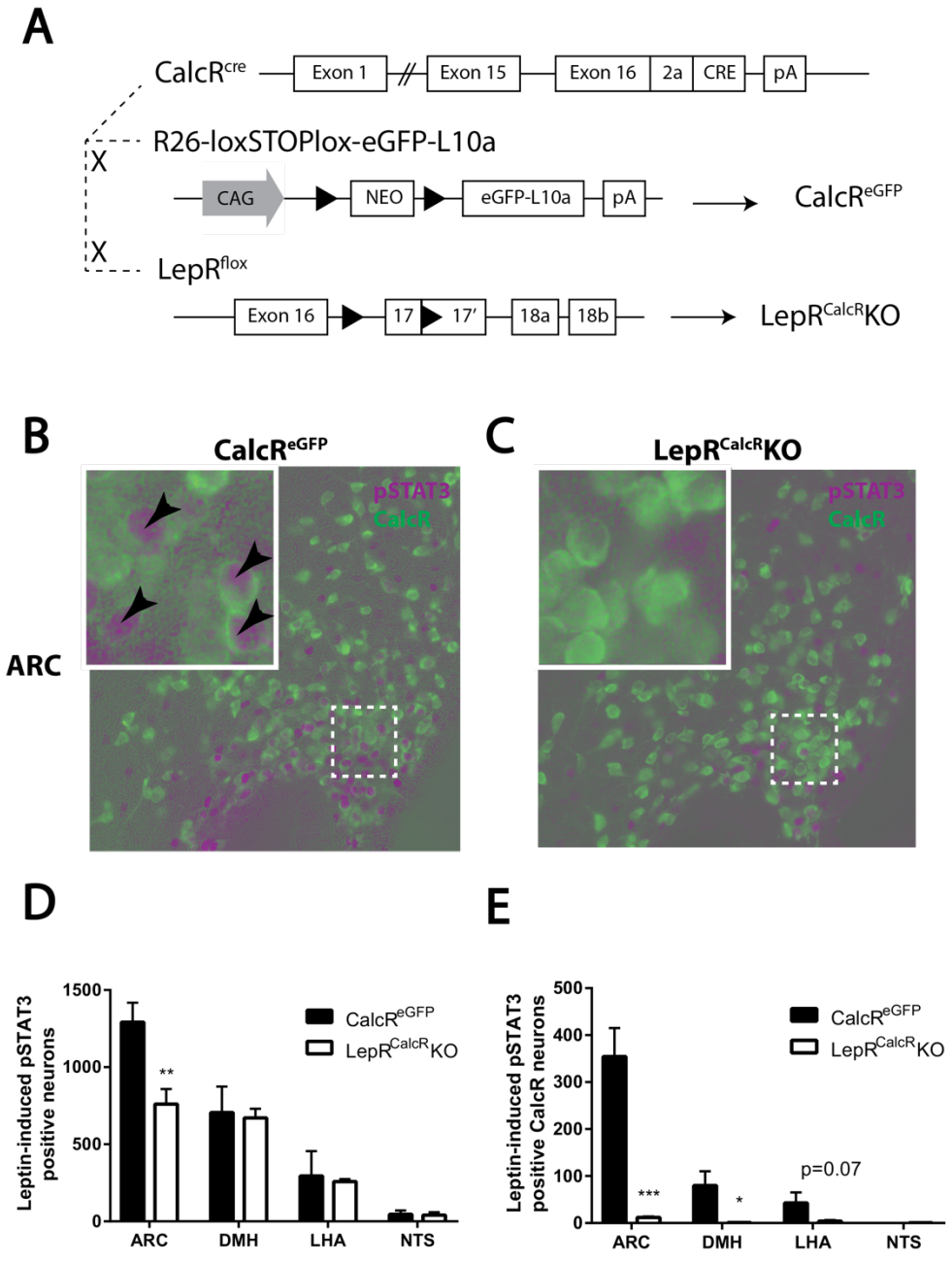

Figure 5.2: Generation of CalcR^{cre} and the lack of LepRb in CalcR expressing neurons. (**A**) Schematic diagram showing the cross of CalcR^{cre} with R26-loxSTOPlox-eGFP-L10a (Rosa26$^{eGFP\text{-}L10a}$) mice to generate CalcR^{eGFP} mice and the cross of CalcR^{cre} with LepR$^{flox/flox}$ mice to generate LepR^{CalcR}KO mice. pA: polyadenylation signal. (**B-C**) Representative images showing colocalization of pSTAT3-IR (purple) with GFP-IR (green) in the arcuate nucleus of four-week-old CalcR^{eGFP} and LepR^{CalcR}KO (both of which are on the Rosa26$^{eGFP\text{-}L10a}$ background) mice treated with leptin (5mg/kg, i.p.) for 90 minutes. Arrows indicate colocalized neurons. (**D-E**) The number of cells positive for pSTAT3 and doubled-labeled pSTAT3+GFP cells are plotted by region.

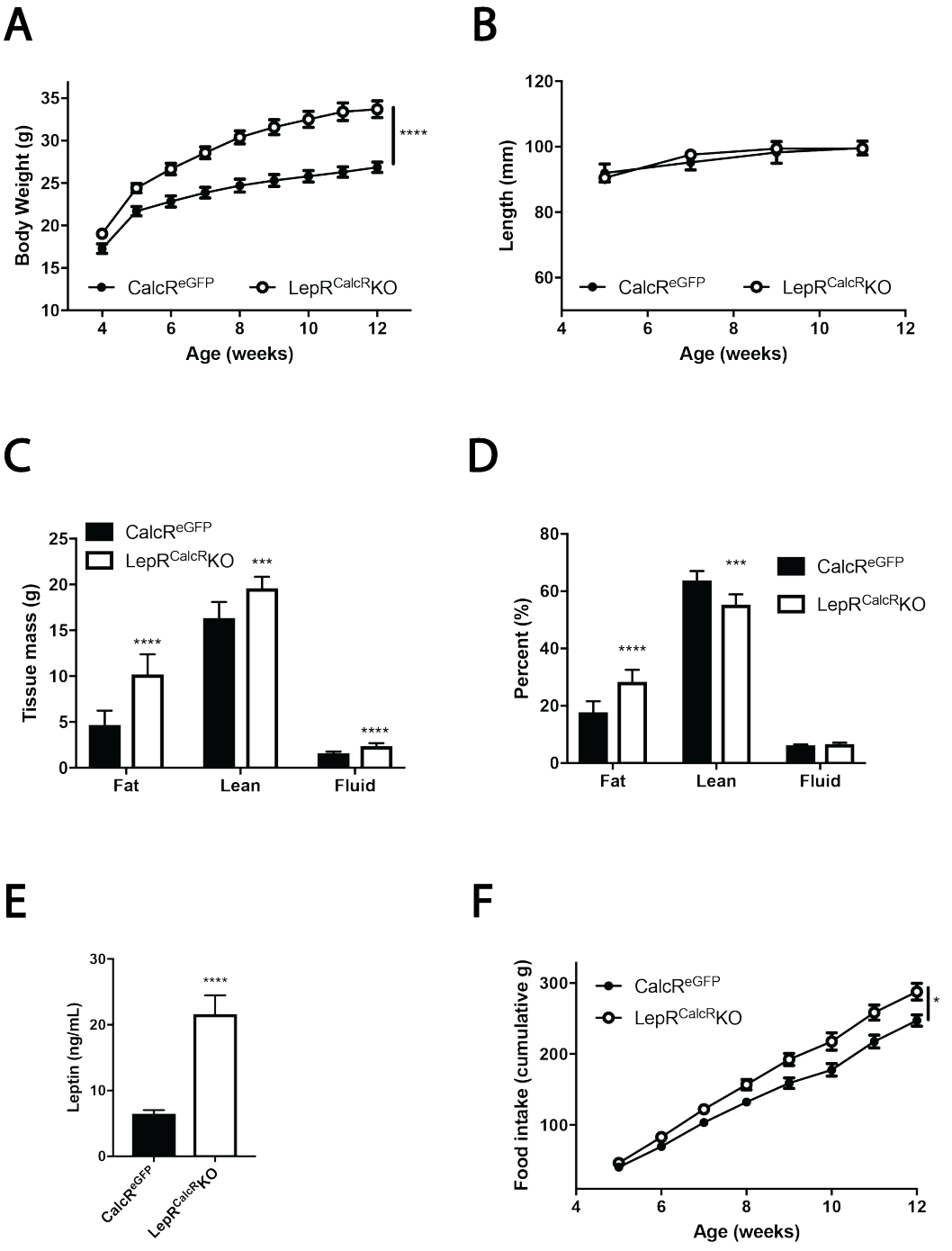

Figure 5.3: LepR^{CalcR} neurons regulate energy balance. (**A**) Male LepR^{CalcR}KO and CalcRe^{GFP} (littermate control) mice were placed on chow and body weight (**A**) measured weekly (****p<0.0001 by ANOVA), and crown-rump length (**B**) measured biweekly. At 14-15 weeks of age, animals underwent body composition analysis (**C-D**) by NMR spectroscopy (***p<0.001; ****p<0.0001 by unpaired t-test). Serum from 10-week-old mice were assayed for leptin (**E**) (****p<0.0001 by unpaired t-test). Cumulative food intake (**F**) was measured weekly for mice at 4-12 weeks of age (*p<0.05 by ANOVA).

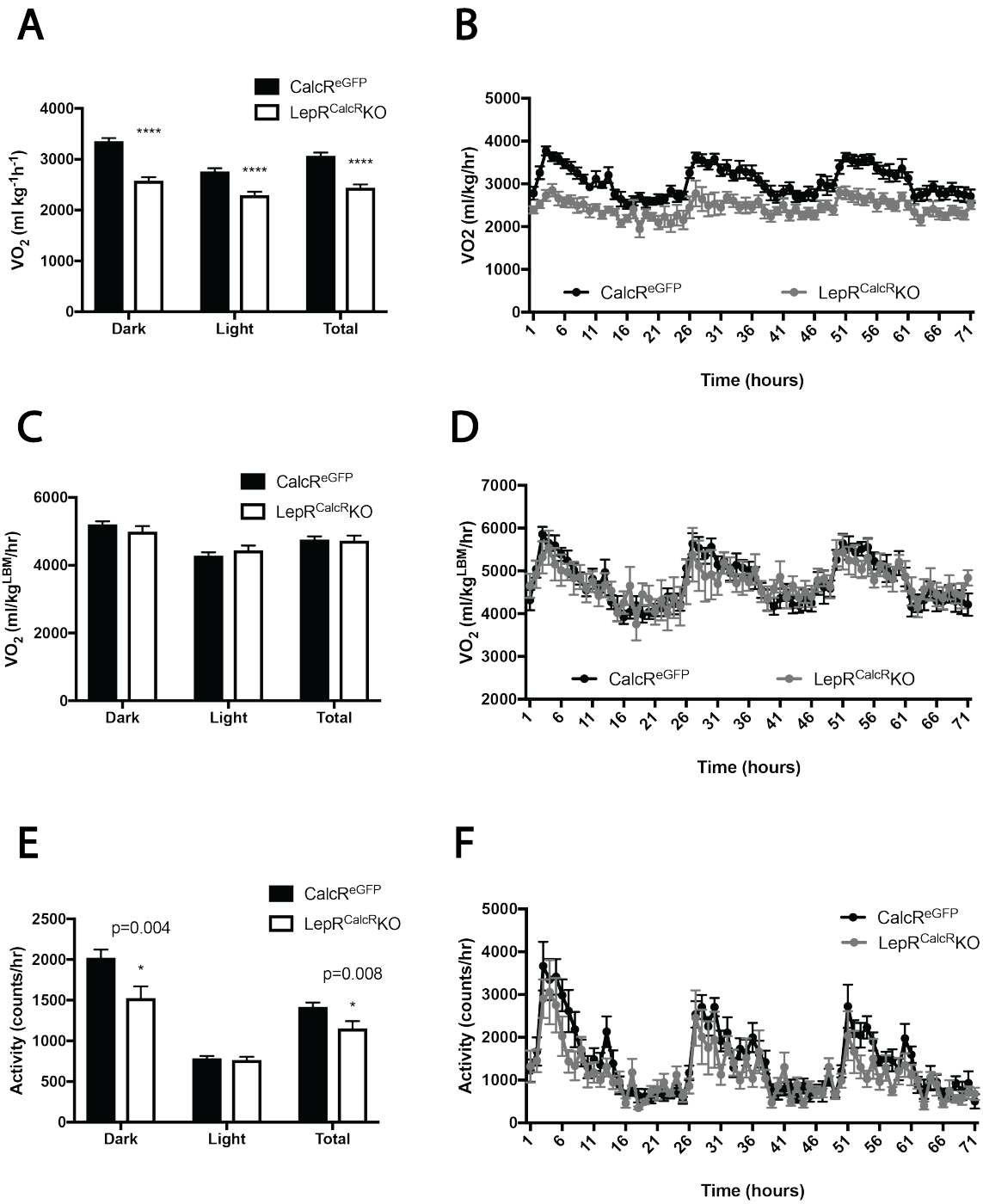

Figure 5.4: Leptin acts on LepR^{CalcR} neurons to regulate VO_2 and locomotor activity. 9-11 week-old male CalcR^{eGFP} (n=12) and LepR^{CalcR}KO (n=8) mice were subjected to CLAMS analysis to determine (**A-B**) VO_2 normalized to total body mass, (**C-D**) VO_2 adjusted to lean body mass, and (**E-F**) locomotor activity. Data are shown for dark cycle (Dark), light cycle (Light), 24 hours (Total), and the entire hour-by-hour 72-hour period. Mean +/- SEM is shown; ANOVA, *p<0.05, ****p<0.0001.

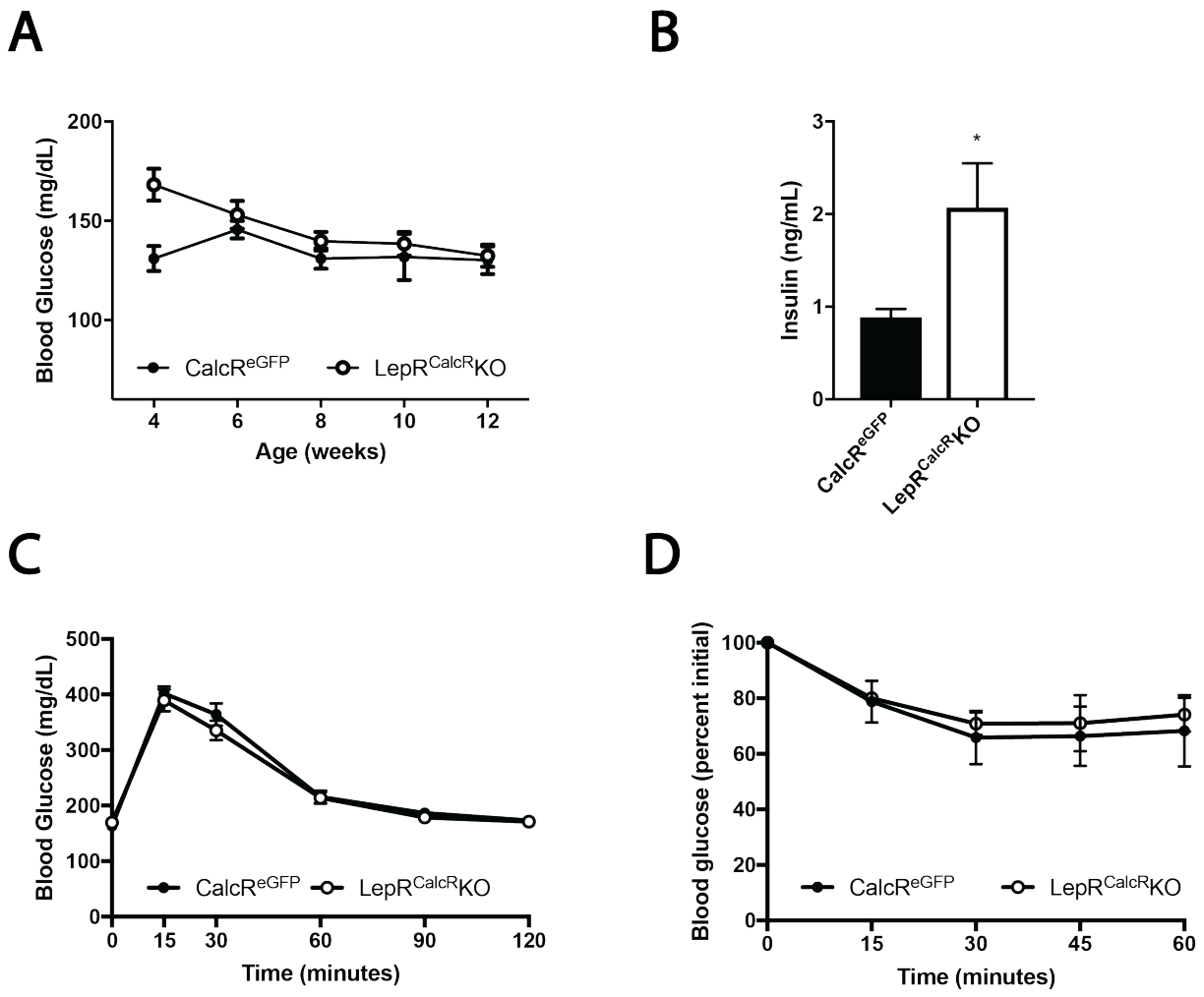

Figure 5.5: Glycemic indices are unaffected by LepR^{CalcR} neurons. (**A**) Biweekly blood glucose concentrations for male CalcR^{eGFP} (control) and LepR^{CalcR}KO mice at 4-12 weeks of age. (**B**) Serum insulin concentrations for 10-week-old mice (*$p<0.05$ by unpaired t-test). Mice at 12-14 weeks of age were treated with (**C**) glucose (2g/kg; i.p.) or (**D**) insulin (1 U/kg; i.p.) and blood glucose concentrations were measured.

A

	CalcR^{eGFP}		LepR^{CalcR}KO	
Gene	Enrichment	SEM	Enrichment	SEM
Pomc	0.63	0.04	0.73	0.07
AgRP	14.15	0.49	26.32	2.33
Npy	12.76	0.97	17.25	0.68
Socs3	1.55	0.23	0.62	0.21
Cartpt	1.75	0.10	1.20	0.07
Serpina3n	1.83	0.08	1.42	0.04
Sst	7.59	1.17	7.40	1.37
CalcR	30.48	12.27	23.33	4.31

B

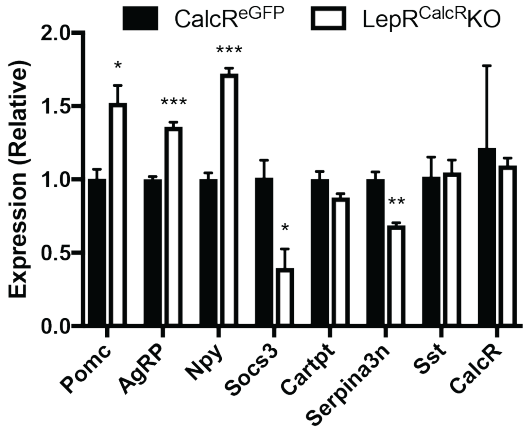

Figure 5.6: Gene expression and fold change in the hypothalamus of CalcR^{eGFP} and LepR^{CalcR}KO mice. Translating ribosome affinity purification (TRAP) was performed on CalcR^{eGFP} (n=11) and LepR^{CalcR}KO mice (n=16). Changes in transcript expression were assayed by RT-qPCR using ABI Taqman assays for the listed genes and for GAPDH as the control. Transcript expression in CalcR-expressing neurons and nonCalcR neurons in the hypothalamus was measured and **(A)** mean enrichment (Enrichment) with standard error (SEM) are detailed with enrichment values >1.5 bolded. **(B)** Relative expression of genes are plotted for both genotypes (*p<0.05; **p<0.01; ***p<0.001 by unpaired t-test).

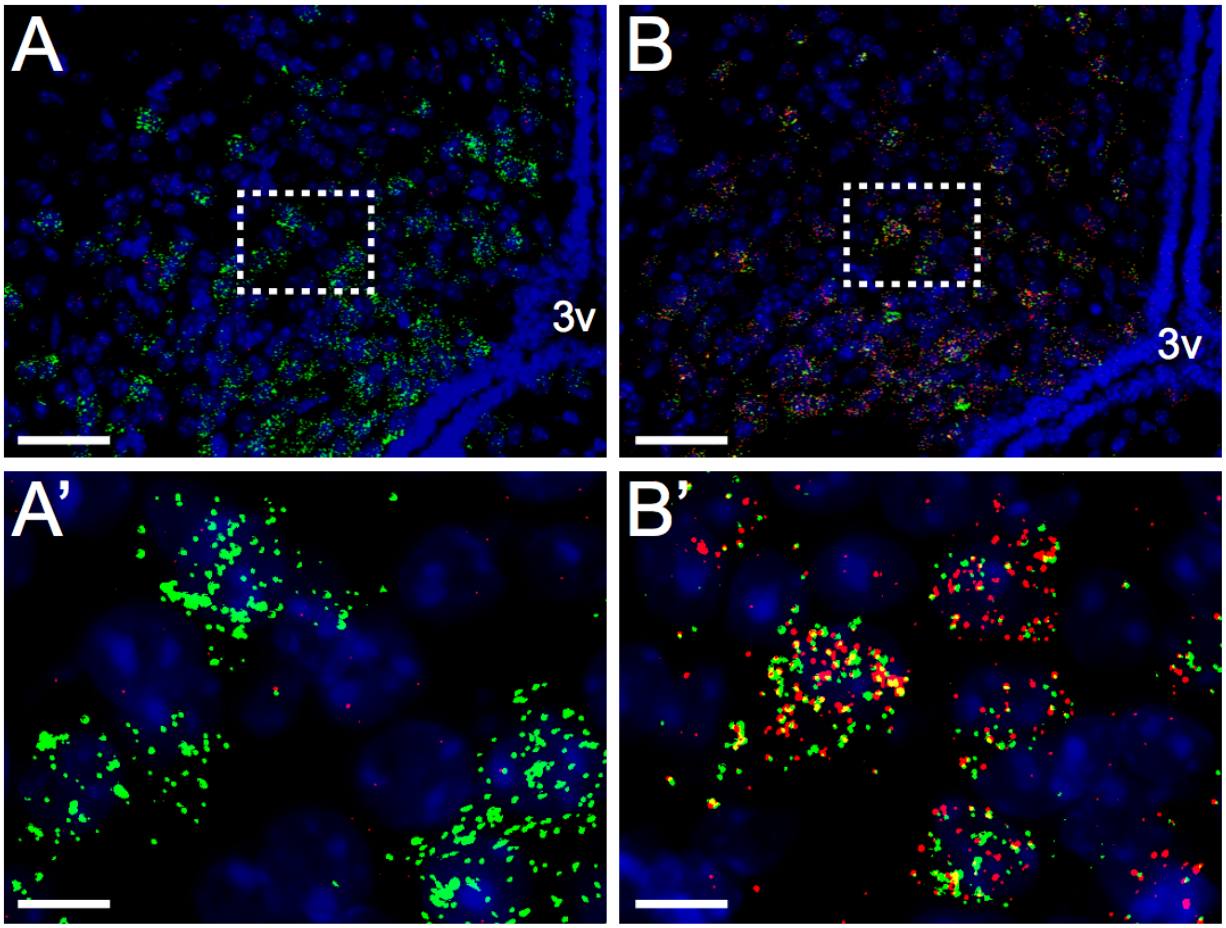

Figure 5.7: Verification of CalcR-Cre mouse strain. Representative ISH images showing *Calcr mRNA* (green) and *Cre mRNA* (red) signal in the arcuate nucleus of wildtype (**A**) and CalcR-Cre (**B**) mice. **A**' and **B**' are more magnified images of the area indicated by the dotted rectangles in **A** and **B**. Blue is DAPI. Scale bar = 50 μm (**A,B**) and 10 μm (**A',B'**). 3v = 3rd ventricle.

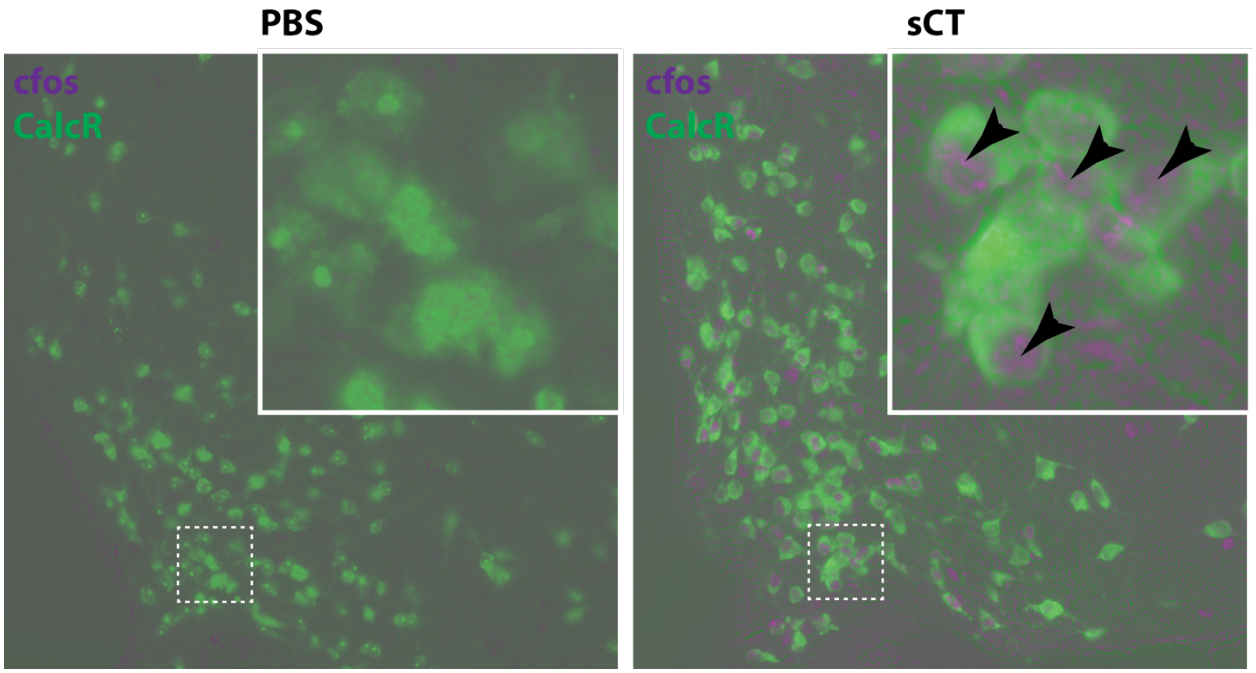

Figure 5.8: Salmon calcitonin-stimulated cfos-IR in CalcR^{eGFP} mice. Representative images show colocalization of cfos-IR (purple) with GFP-IR (green) in CalcR^{eGFP} mice treated with salmon calcitonin (sCT; 150ug/kg, i.p.) or PBS vehicle.

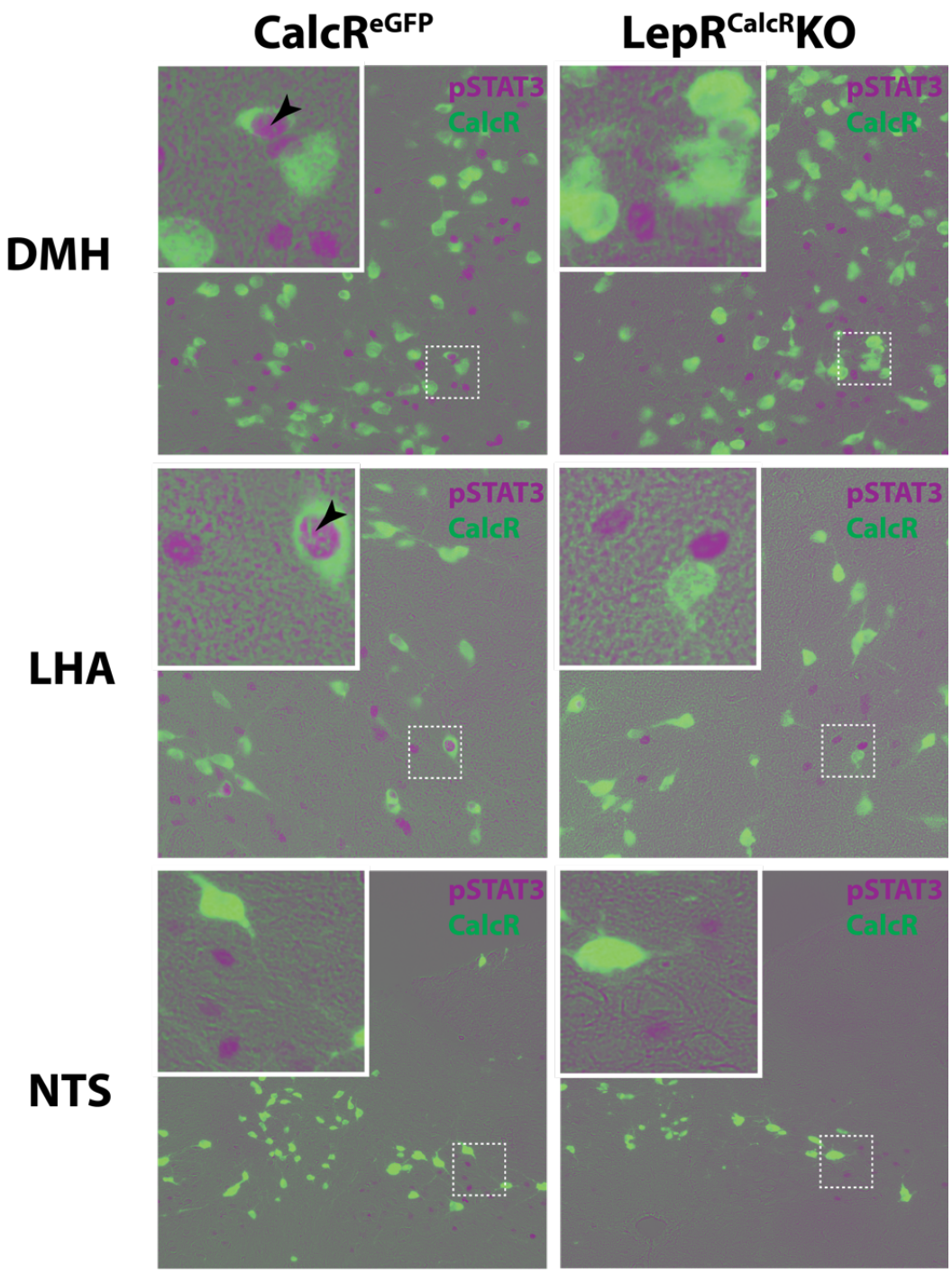

Figure 5.9: Conditional ablation of LepRb in CalcR neurons. Representative images showing colocalization of pSTAT3-IR (purple) with GFP-IR (green) in the dorsomedial hypothalamus (DMH), lateral hypothalamic area (LHA) and nucleus of the solitary tract (NTS) of four-week-old CalcR^{eGFP} and LepR^{CalcR}KO (both of which are on the Rosa$^{26eGFP\text{-}L10a}$ background) mice treated with leptin (5mg/kg, i.p.) for 90 minutes. Arrows indicate colocalized neurons.

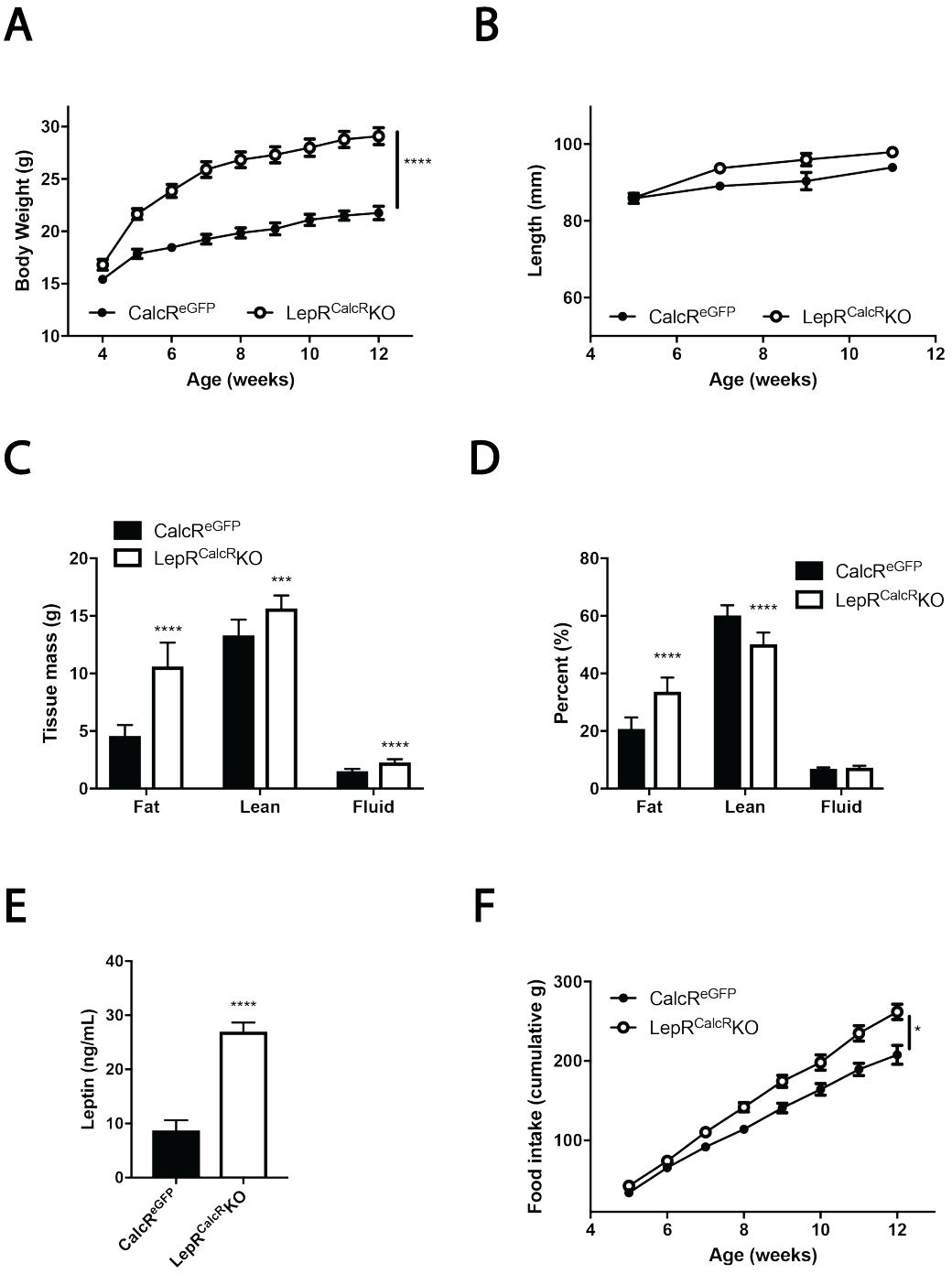

Figure 5.10: LepR^{CalcR} neurons regulate energy balance (females). (**A**) Female LepR^{CalcR}KO and CalcRe^{GFP} (littermate control) mice were placed on chow and body weight (**A**) was measured weekly (****p<0.0001 by ANOVA), and crown-rump length (**B**) was measured biweekly. At 14-15 weeks of age, animals underwent body composition analysis (**C-D**) by NMR spectroscopy (***p<0.001; ****p<0.0001 by unpaired t-test). Serum from 10-week-old mice were assayed for leptin (**E**) (****p<0.00001 by unpaired t-test). Cumulative food intake (**F**) was measured weekly for mice at 4-12 weeks of age (*p<0.05 by ANOVA).

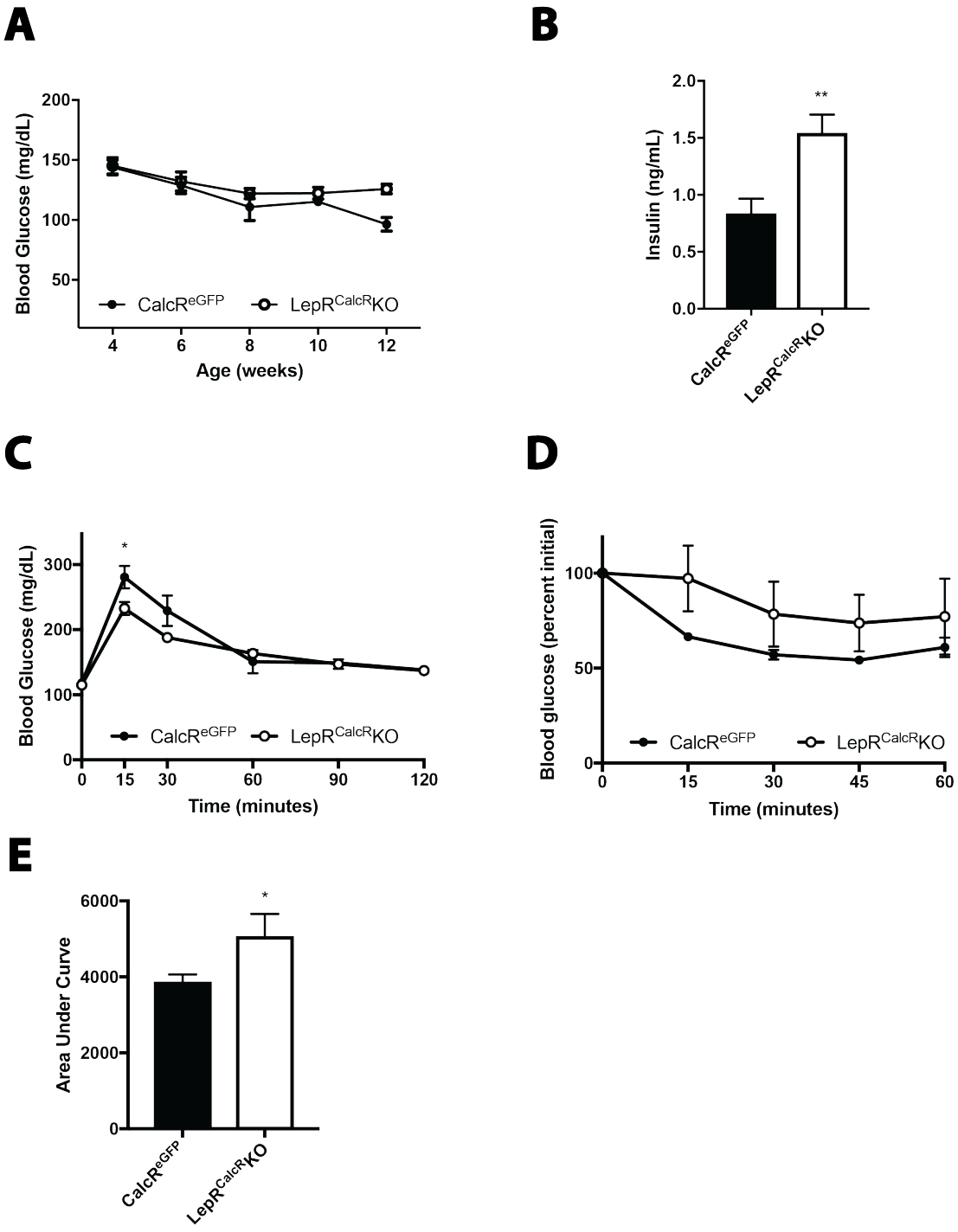

Figure 5.11: Glycemic indices are controlled by LepR^{CalcR} neurons (females). (**A**) Biweekly blood glucose concentrations for female CalcR^{eGFP} (control) and LepR^{CalcR}KO mice at 4-12 weeks of age. (**B**) Serum insulin concentrations for 10-week-old mice (**p<0.01 by unpaired t-test). Mice at 12-14 weeks of age were treated with (**C**) glucose (2g/kg; i.p.) or (**D**) insulin (1 U/kg; i.p.) and blood glucose concentrations were measured (*p<0.05 by ANOVA). (**E**) Area under the curve analysis was performed for insulin tolerance test (*p<0.05 by unpaired t-test).

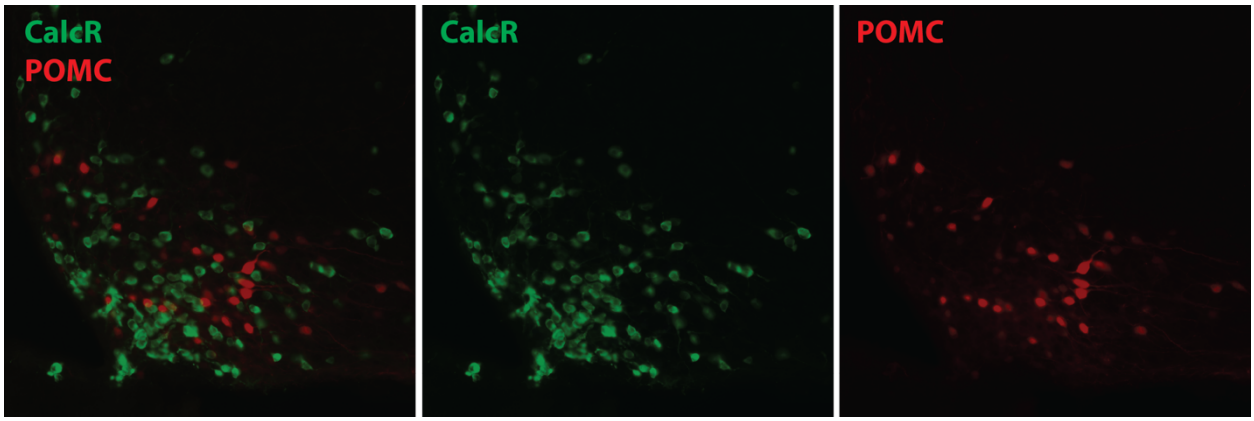

Figure 5.12: Lack of colocalization between ARC CalcR and POMC neurons. Representative images from the ARC of CalcR^{eGFP} mice crossed with POMC^{dsred} to generate CalcR^{eGFP}POMC^{dsred} mice. No colocalization was observed between GFP-IR and dsRed-IR.

References

1. Finkelstein, E. A., Trogdon, J. G., Cohen, J. W. & Dietz, W. Annual medical spending attributable to obesity: Payer-and service-specific estimates. *Health Aff.* **28,** (2009).
2. Patterson, C. M., Leshan, R. L., Jones, J. C. & Myers, M. G. Molecular mapping of mouse brain regions innervated by leptin receptor-expressing cells. *Brain Res.* **1378,** 18–28 (2011).
3. Hayes, M. R. *et al.* Endogenous Leptin Signaling in the Caudal Nucleus Tractus Solitarius and Area Postrema Is Required for Energy Balance Regulation. *Cell Metab.* **11,** 77–83 (2010).
4. Schwartz, M. W., Woods, S. C., Porte, D., Seeley, R. J. & Baskin, D. G. Central nervous system control of food intake. *Nature* **404,** 661–671 (2000).
5. Ring, L. E. & Zeltser, L. M. Disruption of hypothalamic leptin signaling in mice leads to early-onset obesity, but physiological adaptations in mature animals stabilize adiposity levels. *J. Clin. Invest.* **120,** 2931–2941 (2010).
6. Flak, J. N. & Myers, M. G. Minireview : CNS Mechanisms of Leptin Action. **30,** 3–12 (2016).
7. Van De Wall, E. *et al.* Collective and individual functions of leptin receptor modulated neurons controlling metabolism and ingestion. *Endocrinology* **149,** 1773–1785 (2008).
8. Campbell, J. N. *et al.* A molecular census of arcuate hypothalamus and median eminence cell types. *Nat. Neurosci.* (2017). doi:10.1038/nn.4495
9. Hay, D. L., Christopoulos, G., Christopoulos, A., Poyner, D. R. & Sexton, P. M. Pharmacological discrimination of calcitonin receptor: receptor activity-modifying protein complexes. *Mol Pharmacol* **67,** 1655–1665 (2005).
10. Beaumont, K., Kenney, M. A., Young, A. A. & Rink, T. J. High affinity amylin binding sites in rat brain. *Mol Pharmacol* **44,** 493–497 (1993).
11. Pittner, R. A. *et al.* Molecular physiology of amylin. *J. Cell. Biochem.* **55,** 19–28 (1994).
12. Lutz, T. a. The role of amylin in the control of energy homeostasis. *Am. J. Physiol. Regul. Integr. Comp. Physiol.* **298,** R1475-84 (2010).
13. Trevaskis, J. L. *et al.* Amylin-mediated restoration of leptin responsiveness in diet-induced obesity: Magnitude and mechanisms. *Endocrinology* **149,** 5679–5687 (2008).
14. Turek, V. F. *et al.* Mechanisms of amylin/leptin synergy in rodent models. *Endocrinology* **151,** 143–152 (2010).
15. Roth, J. D. *et al.* Leptin responsiveness restored by amylin agonism in diet-induced obesity: Evidence from nonclinical and clinical studies. *Proc. Natl. Acad. Sci.* **105,** 7257–7262 (2008).
16. Li, Z., Kelly, L., Heiman, M., Greengard, P. & Friedman, J. M. Hypothalamic Amylin Acts in Concert with Leptin to Regulate Food Intake. *Cell Metab.* **22,** 1059–1067 (2015).
17. Allison, M. B. *et al.* TRAP-seq defines markers for novel populations of hypothalamic and brainstem LepRb neurons. *Mol. Metab.* **4,** 299–309 (2015).
18. Eiden, S., Daniel, C., Steinbrueck, A., Schmidt, I. & Simon, E. Salmon calcitonin -

a potent inhibitor of food intake in states of impaired leptin signalling in laboratory rodents. *J. Physiol.* **541,** 1041–8 (2002).
19. Sheward, W. J., Lutz, E. M. & Harmar, A. J. The expression of the calcitonin receptor gene in the brain and pituitary gland of the rat. *Neurosci. Lett.* **181,** 31–34 (1994).
20. Ravussin, E. *et al.* Enhanced weight loss with pramlintide/metreleptin: an integrated neurohormonal approach to obesity pharmacotherapy. *Obesity (Silver Spring).* **17,** 1736–43 (2009).
21. Leshan, R. L., Björnholm, M., Münzberg, H. & Myers, M. G. Leptin receptor signaling and action in the central nervous system. *Obesity (Silver Spring).* **14 Suppl 5,** 208S–212S (2006).
22. Krashes, M. J. *et al.* An excitatory paraventricular nucleus to AgRP neuron circuit that drives hunger. *Nature* **507,** 238–42 (2014).
23. McMinn, J. E. *et al.* An allelic series for the leptin receptor gene generated by CRE and FLP recombinase. *Mamm. Genome* **15,** 677–685 (2004).

CHAPTER 6

CONCLUSIONS AND FUTURE DIRECTIONS

Leptin and diet-induced obesity

Chapter 2 of this dissertation explores the transcriptional state of high-fat diet-induced obesity (DIO) in leptin receptor (LepRb) neurons and compares it to conditions of leptin deficiency and leptin activity. Through the TRAP-seq approach, we are able to evaluate the relationships between seemingly similar (or dissimilar) conditions by examining the translatome of LepRb neurons in the hypothalamus of mice. This approach has revealed the similarity in the expected conditions of leptin deficient *ob/ob* mice and mice treated with leptin antagonist SMLA; however, a more surprising relationship was discovered between the seemingly disparate conditions of high-fat DIO and leptin-injected lean mice. Far from the postulated “leptin resistance” that occurs in diet-induced obesity, these data suggest that DIO is a leptin active state more similar to a 10-hour intraperitoneal injection of exogenous leptin than any other condition.

Because “leptin resistance” is thought to mostly occur in the arcuate nucleus (ARC) of the hypothalamus,[1] further clarification of the relationship between leptin treatment and DIO in the ARC was necessary. One advantage of the TRAP-seq technique is the ability to micro-dissect any area of interest and examine the transcriptional profile compared across various conditions. Thus, ARC-specific TRAP-seq analysis reveals that DIO is indeed similar to 10-hour leptin treatment. This finding further confirms the finding that the hyperleptinemia in DIO does not denote “resistance” and inactivity of leptin; instead, it effectively decreases energy balance (to an extent).[2]

But, this does not mean that leptin “resistance” is entirely incorrect in DIO. The ARC TRAP-seq analysis further reveals that DIO is more similar to leptin treated DIO mice than any other condition. Given the previous findings that exogenous leptin therapy is an ineffective weight-loss treatment in DIO, it is unsurprising that transcriptionally, the ARC remains unchanged with leptin injection on the background of DIO. What this may suggest, however, is that while the hyperleptinemia in DIO is euleptinemic (in proportion to the individual’s fat stores) and effective, further exposure to exogenous leptin treatment results in an ineffective level of additional leptin past that euleptinemic level. One potentially important avenue for further exploration is whether an individual’s euleptinemic level can be artificially manipulated. Indeed, if in the DIO setting, the euleptinemic level were reset to normoleptinemic levels (leptin levels expected of lean individuals), the excess endogenous leptin may be even more potent in exerting negative energy balance.[3] Another possibility is that there is an innate ceiling of leptin action where additional leptin is ineffective. This warrants careful investigation, however, for obese individuals do not exponential gain weight—if there indeed is a firm

threshold of leptin action, then the endogenous leptin action of an obese individual (BMI=30kg/m^2) should be similar to that of super obese individual (BMI=50kg/m^2). While super obesity is not uncommon, the vast majority of overweight individuals do not proceed to super obesity despite their continued positive energy balance.[4] A third possibility is that high-fat diet itself may have effects on energy homeostasis and short circuit LepRb neurons from responding appropriately to the hyperleptinemia and exogenous leptin. While a previous publication would argue against this,[3] our understanding of this possibility is still lacking. Last, excess leptin action may overwhelm LepRb neurons such that they are constantly activated to the point of exhaustion. I will expound upon this last possibility later in this chapter. Regardless of what may truly be occurring, if leptin is the means by which our adipocytes communicate the status of our energy stores, understanding LepRb neurons and their response in various conditions is critical.

A current area of investigation that ties in these possibilities is the finding of gliosis in the ARC of DIO animals.[5] Our findings of gliosis under chronic leptin infusion (and lack there of in leptin deficient animals) suggest that the gliosis seen in DIO is a consequence of hyperleptinemia, rather than a marker (or driver) of obesity. This suggests that gliosis may serve as a useful surrogate of LepRb neuronal (over)activity. However, gliosis is also involved in inflammation and many reports have categorized DIO as a state of low-grade hypothalamic inflammation, perhaps as a consequence of the saturated fatty acids in the high-fat diets (HFD) consumed to cause DIO.[6,7] The most provocative interpretation of gliosis (whose presence in the ARC precedes obesity in the body) causing obesity warrants further attention due to the paradigm-shifting nature of

this idea, if true.[5] Experiments eliciting gliosis (through viral or optogenetic means) independent of body weight, inflammation state or fatty acid intake would help disentangle this hypothesis. Thus, the role of gliosis in the genesis of obesity is a complicated one and requires further investigation.

We have used TRAP-seq to untangle some of these different metabolic phenomena by identifying and comparing the relative expression of genes responsive to leptin action, obesity, and inflammation. Furthermore, we have used sex-specific TRAP-seq to understand the sex differences in DIO gliosis (i.e. the absence of gliosis in female DIO mice). Fractalkine has recently been implicated; however, while our sex-specific TRAP-seq analysis does show a demonstrable difference in expression levels between male and female DIO animals, the absolute expression levels (FPKM) are extremely low and fractalkine was not significantly enriched in LepRb neurons for any of the conditions.[8] Instead, our sex-specific experiments suggest that the gliosis difference may not contribute much to the activity of LepRb neurons. It is worth noting that much of our efforts here have focused exclusively on LepRb neurons and the transcriptional changes unique to that population. While we have analyzed transcriptional changes in non-LepRb cells, those analyses have not been cell-type specific. Therefore, to further elucidate the phenomena occurring, future investigators should identify the transcriptional changes of other cells involved in metabolism in the hypothalamus (e.g. microglia, astrocytes, tanycytes, etc). Moreover, given the cross-talk and interactive nature of glia, it is critical to investigate the relationships among cells.

Leptin is, without a doubt, important in obesity. However, the heterogeneity of LepRb neurons and their interactions with neighboring cells complicate our

understanding of DIO. And, while our efforts to profile the transcriptional changes exclusively in LepRb neurons through TRAP-seq has reveals new insights in DIO, more needs to be done. LepRb neurons do not exist in a vacuum. They are constantly interacting, modifying and being modulated by neighboring (and not so neighboring) neurons, glia, and cells. Our analyses of the transcriptional changes in non-LepRb cells provide a gestalt that requires more detailed investigation. It is my hope that when the data here in this dissertation is combined with other sequencing data (microglial TRAP-seq, single-cell sequencing, etc.), new hypotheses and interpretations will be generated and tested. Indeed, while our sex-specific LepRb and non-LepRb TRAP-seq data may be insufficient to understand the sex differences in DIO gliosis, a more complete depiction of how various cells respond to different conditions may inform our thinking of whether gliosis is a potential therapeutic target for obesity, or whether it is an artifact.

STAT proteins in leptin action

The work in Chapter 2 identified expected and novel gene patterns in LepRb neurons in a variety of metabolic insults; one of these unexpected findings is the transcriptional differences of leptin deficient *ob/ob* mice and STAT3 ablated mice. STAT3 is the major anorectic signal of leptin, and both *ob/ob* and $STAT3^{LepR}KO$ mice manifest hyperphagic obesity. Yet, their transcriptional profiles are quite dissimilar. Much of this dissimilarity is due to STAT1 compensation/upregulation (and the genes downstream of it) in STAT3-deficient mice. The TRAP-seq data, coupled with previous studies showing leptin activating STAT1 cell lines, implicates STAT1 as an important signal of leptin action.

However, our finding that ablation of STAT1 in LepRb neurons does not result in obesity or phenotypically exacerbate the obesity in $STAT3^{LepR}KO$ mice partially rebukes the importance of the transcriptional analyses. This illustrates a limitation of TRAP-seq: the transcriptional patterns of neurons may change under various conditions, but it may not be functionally/phenotypically relevant. It is, therefore, unclear how to prioritize the changing gene patterns under the various conditions: whether by directionality, amplitude or number of genes. Despite this drawback, the extensive transcriptional data do provide novel targets to explore (even if many are red herrings) and perhaps with collaboration and new perspectives, new insights can be gleaned.

Additionally, if diet-induced obesity is a state of “leptin resistance”, the $STAT3^{LepR}KO$ model would most mimic it: it is hyperleptinemic, obese, and unresponsive to exogenous leptin injections. Despite the transcriptional dissimilarity between DIO and $STAT3^{LepR}KO$ mice under TRAP-seq, the TRAP-seq data does identify a number of STAT3 independent leptin signals elevated in DIO that may be responsible for the failure of exogenous leptin to promote weight loss in DIO.

The upregulation of STAT1 in tanycytes with its deletion from LepRb neurons and the ARC gliosis seen in $STAT1^{LepR}KO$ mice demonstrate the importance of understanding the interaction between neurons and glia. Metabolically, these mice are comparable to littermate controls; however, the brain does much more than regulate metabolism. The brain is the most complex organ and compared to other organs, we know relatively little. Given its complexity and the multitude of diseases that affect it, these negative metabolic findings and the available transcriptional data may be informative to other neuroscientists examining STAT proteins in different cell types. The

differential expression of STAT1 from different cells when it is deleted from one cell type underscores the importance of investigation into how various cells communicate and interact. Therefore, in addition to the cell-autonomous transcriptional regulation revealed through sequencing techniques, additional methods delineating how the differential expression of genes like STAT1 modulate and influence other cells in the CNS milieu should be pursued.

Enhanced STAT3 and leptin action

Chapter 3 highlighted the necessity of STAT3 in metabolism; chapter 4 examines the sufficiency of STAT3 in leptin action. STAT3 mediates the majority of leptin's anorexic action and immunohistochemical staining for pSTAT3 is regularly used as a proxy for leptin action. Using a constitutively active STAT3 (CASTAT3) mutant, we enhanced STAT3 action in LepRb neurons, causing decreased food intake and body weight. On the leptin deficient *ob/ob* background, $LepR^{CASTAT3}$ normalized metabolic parameters; however, on high-fat diet (HFD), $LepR^{CASTAT3}$ were similarly obese compared to littermate controls. Therefore, STAT3 signaling in LepRb neurons suffices to mediate part of physiologic leptin action in the absence of other leptin signals; however, enhanced STAT3 signaling is unable to suppress body weight in DIO. This is reminiscent of our findings where chronic leptin (leptin minipump) significantly decreased adiposity and body weight in lean animals and previous studies demonstrating exogenous leptin treatment's ineffectiveness in diet-induced obese animals and patients. Again, the concept of "leptin resistance" arises where while lean normoleptinemic animals lose adiposity when their effective leptin action is increased (through minipumps or $LepR^{CASTAT3}$), DIO animals, which are hyperleptinemic (though in

proportion to their elevated adiposity), do not lose weight when leptin action is increased (hence they are leptin “resistant”). Because $LepR^{CASTAT3}$ and leptin are effective weight loss therapies for leptin deficient animals, it is not obesity that prohibits leptin sensitivity; rather, it must be, leptin, fatty acids or something else that is responsible for the difference in leptin therapy between DIO and *ob/ob* animals. Knight et. al. demonstrated that *ob/ob* mice clamped to different leptin levels and fed HFD are still responsive to leptin when going from a normoleptinemic (hypoleptinemic relative to fat stores) to a hyperleptinemic (euleptinemic relative to fat stores) state, suggesting that leptin action (at least from normoleptinemia to hyperleptinemia levels) is not curbed by HFD. Thus, endogenous leptin levels may determine the effectiveness of leptin therapy.

The immunohistochemical evidence for “leptin resistance” is the absence of an exogenous leptin-induced pSTAT3 response; however, it is worth noting that the baseline (not treated with exogenous leptin) levels of pSTAT3 are elevated in DIO animals compared to chow-fed controls. If DIO results from the absence of an appropriate elevation of pSTAT3 activity from the hyperleptinemia, an attractive therapy is to enhance STAT3 activity; however, our findings would argue that even with constitutive STAT3 activity, DIO persists to the same degree as DIO controls. The blockade to an acute anorectic response to exogenous leptin may, therefore, be downstream of STAT3 translocation. Further exploration into transcriptional outcomes of STAT3 in DIO may yield new insights into a feasible leptin therapy for DIO.

A separate, but related, aspect of leptin resistance is the elevated endogenous pSTAT3-IR observed in DIO.[1,2] While there is a preoccupation with DIO pSTAT3-IR not exactly mirroring the extent of expression in 1-hour leptin treated chow-fed animals, a

more apt comparison would be to compare DIO pSTAT3 expression at baseline with chronic (or 10-hour) leptin treatment. This comparison not only aligns immunohistochemically, but is also more similar transcriptome-wise when compared to a short-term leptin treatment (i.e. the 3-hour leptin treated condition). This shift of examining DIO as a condition of leptin resistance to one of constant leptin bombardment raises a few questions. The most prominent of which is whether leptin (over)activity is detrimental or beneficial. Clearly, endogenous leptin action in DIO has negative energy balance effects; however, the level of anorectic control falls short of our (perhaps unrealistic) expectations. To illustrate this, I cannot help but draw a comparison to neuronal membrane potentials. Leptin treatment in chow-fed animals elicits an impressive anorexia, much like how a depolarization event results in an exaggerated action potential. The excess of leptin action in DIO may then be analogous to a membrane potential that is unable to repolarize, where the leptin bombardment may still elicit smaller “graded potentials” but it is unable to continually induce large action potentials. This analogy may help explain the perplexing phenomenon of weight rebound after weight loss. The textbook 72kg man who has been the same weight for decades can eat significantly more than a similar 72kg man who just lost 80kg of weight, all else being equal. The normoleptinemic states of both these 72kg men cannot explain this disparity; additional studies examining whether the latter’s bombardment of leptin from his recent hyperleptinemia may be preventing his ability to mount exaggerated “action potential” level responses to leptin are necessary. This phenomenon of homeostatic systems responding to weight loss by mounting an anabolic response (increased food intake and decreased energy expenditure) often

results in rebound weight-gain. Interestingly, this phenomenon coincides with the continued existence of gliosis months after DIO mice have normalized their weights switching from a high-fat diet to a normal chow diet.[9] So, if gliosis is a marker of LepRb neuronal activity, the gliosis, weight rebound and inability to mount “action potential” level responses to leptin could be manifestations of the same condition. Because LepRb neurons do recover/repolarize (at least in some individuals) and individuals who lose weight eventually do mostly normalize energy balance, weight gain in DIO appears reversible; additional research in this area would further our understanding of sustainable weight loss.

The over-activity of LepRb neurons can itself drive gliosis in the area, which would explain why the ARC is the only area to experience the gliosis (it is adjacent to the median eminence and so constantly exposed to the elevated circulating leptin levels in hyperleptinemia). Interestingly, the absence of gliosis in other LepRb hypothalamic populations like the DMH or LHA correlates with the pSTAT3 responsiveness of those regions as well.[1,5] The lack of a phenotypic response from exogenous leptin, instead of demonstrating leptin resistance, illustrates the importance of ARC LepRb neurons in mediating leptin’s anorectic effects. There has been some evidence suggesting that leptin exposure in the hypothalamus begins in the ARC and then spreads laterally into the rest of the hypothalamus. Indeed, an experiment that needs to be performed is one that clamps leptin levels to ever-increasing levels of hyperleptinemia and examines the gliosis and pSTAT3-IR response to exogenous leptin. This study would help determine if the ARC is unique or if other regions can also be made unresponsive and experience

gliosis. My expectation is that the level of hyperleptinemia in DIO is just enough to induce leptin over-activity in the ARC (and not in other regions).

Furthermore, the absence of gliosis in females may be due to the exclusively female experience of pregnancy. During pregnancy, adiposity and leptin levels increase significantly and from a teleological perspective, it would follow that females have an imbedded capacity and expectation to experience fluctuations in adiposity and leptin levels. An interesting study that should be performed is the examination of whether female DIO animals experience rebound weight-gain to the same extent as their male counterparts. The sex differences observed may be the perfect lens by which to link endogenous leptin inactivity, gliosis, and rebound weight-gain together.

If this recovery period (i.e. repolarization of LepRb neurons) were shortened and rebound weight gain were eliminated, the tide of the battle against obesity may finally turn. Then, the cure to obesity would not lie in identifying new weight loss drugs, for we have very effective therapies already in diet and exercise; rather, it may be in the pharmacologic targeting of LepRb neurons to allow individuals to sustain their weight loss. Thus, the exploration and use of leptin and LepRb antagonists like SMLA may reveal the development of an approachable regimen to effectively combating obesity.

LepRb- and CalcR-expressing neurons

Whereas the previous Chapters 2-4 focus exclusively on leptin signaling, Chapter 5 examines the existence of hypothalamic neurons that express both LepRb and calcitonin receptor (CalcR). Not only is CalcR the cognate receptor for salmon calcitonin (sCT), a potent anorectic agent, but it is also the receptor for amylin, a hormone that

promotes satiety. Additionally, many previous studies have demonstrated effective synergistic weight loss in DIO humans and rodents with dual therapy of leptin and amylin; therefore, the identification of the locations and molecular interactions between leptin and amylin may uncover the mechanisms responsible for a proven treatment to DIO.[10–12] Our data reveal the significance of LepRb neurons on energy balance that also express CalcR, which supports the possibility of these LepRb- and CalcR-expressing neurons as the site of synergistic weight loss. The complimentary set of experiments that need to be performed is the deletion of CalcR in LepRb neurons; if leptin-amylin dual therapy on $CalcR^{LepR}$KO DIO mice is ineffective compared to DIO controls, then these hypothalamic LepRb- and CalcR-expressing neurons may indeed be the location of the synergy.

Understanding the molecular underpinnings of leptin-amylin synergistic weight loss would identify pharmacological targets that could treat DIO. To accomplish this feat, multiple recombinase systems (i.e. LepRb- FLP/FRT and CalcR- cre/lox) should be combined with a FLP- and cre-dependent eGFP-L10a element that would enable TRAP-seq of neurons that only express both LepRb and CalcR. Characterizing the transcriptome of these neurons under the conditions of DIO and DIO treated with leptin and/or amylin would produce a target list of genes and molecular mechanisms that may be responsible for the synergistic weight loss demonstrated.

The other avenue worth investigating is the finding that sCT activates CalcR neurons that also express NPY, AgRP and GABA (NAG neurons), which are known to drive positive energy balance. This is surprising because sCT is a potent satiety drug. Therefore, a deeper understanding and investigation of sCT-driven NAG neuronal

activation would have implication on energy homeostasis, regardless of the outcome. These possible outcomes are: 1. hunger, 2. satiety, or 3. no observable metabolic effect. If sCT-dependent NAG activity results in hunger, then the overall satiety experienced with sCT therapy could be amplified by silencing NAG neurons or directing the sCT activity only to non-NAG neuronal sites (presumably in the hindbrain). If, however, NAG neurons cause satiety, the current understanding of NAG neurons exclusively driving hunger would need re-evaluation. Finally, if there is no observed metabolic impact, this may provide a system to study the negative valence of NAG neurons uncoupled from hunger.[13] Clearly, these questions need to be answered with viral, DREADD, optogenetic and localized injection approaches.

The continued characterization of the many homeostatic systems responsible for energy balance and leptin's roles in them is the next step in understanding the neurobiology of obesity. For me, this has demonstrated the hidden synergy in multiple complementary systems, whose investigation may reveal an approachable pharmaceutical cure to obesity.

Conclusions

Twenty years ago, leptin fell short of expectations as the cure to all obesity. Since then, a deeper and more nuanced understanding of the neuroendocrine regulation of obesity and leptin has developed. Innovations in deep sequencing technologies have begun to reveal the transcriptome of cells responsive to leptin, and ongoing efforts to identify how cells communicate with one another in response to leptin and other metabolic insults are developing. Many exciting findings (like the synergistic

weight loss with amylin-leptin therapy) provide new evidence that leptin signaling may hold the key after all to curing obesity even if the mechanisms remain opaque. Moreover, the advent and utilization of new technologies have afforded researchers the opportunity to test hypotheses and to further the understanding of the field. There has, therefore, never been a more exciting time to investigate the nuances of leptin action.

The data and chapters presented in this dissertation represent only a portion of the many and varied approaches investigators can take in solving the mystery of obesity. The 21st century in research has been marked with the importance of genes; consequently, genetic techniques have been instrumental tools in the investigation of obesity. In line with this, much of the data detailed in this dissertation revolves around transcriptional analyses and the role LepRb-expressing neurons play in these various metabolic conditions. Our use of these genetic techniques have allowed us to better characterize diet-induced obesity as a state of leptin over-activity (instead of one of leptin deficiency/resistance). Additionally, the identification and investigation of novel genes like calcitonin receptor (CalcR) in leptin action have begun to complete our understanding of previously discovered interactions between leptin and amylin that may hold the key to treating diet-induced obesity. Furthermore, the finding that STAT3 is sufficient to mediate leptin action is thanks to the genetic manipulations that allow many of these hypotheses to be tested.

Despite these findings, it is clear that these genetic data need to be anchored to physiological studies and examined carefully. The importance of the transcriptional data generated in Chapter 2 cannot be understated; however, it also highlights the importance of examining other cell types like glia. The interactions among cells in the

CNS milieu are necessary to contextualize the transcriptional findings from sequencing techniques. The interaction between neurons and glia is exemplified in Chapter 3, which additionally provides a cautionary tale of relying too heavily on transcriptional analyses. Therefore, while genetic techniques are extraordinary powerful, they are insufficient to fully inform our understanding of physiology.

Research has become increasingly collaborative. This has been necessary with the explosion of technologies and our ever-increasing complex understanding of the natural world. Additionally, the sharing of data and expertise has allowed for the rapid progress in all fields. One of the many valuable lesson I will take with me is the importance of the re-examination and re-interpretation of previous data contextualized to the ever-evolving understanding of the field. I hope that the data generated in this dissertation will help inform and guide investigators in their research to improve the human condition today and in the future.

References

1. Münzberg, H., Flier, J. S. & Bjørbæk, C. Region-specific leptin resistance within the hypothalamus of diet-induced obese mice. *Endocrinology* **145,** 4880–4889 (2004).
2. Ottaway, N. *et al.* Diet-Induced Obese Mice Retain Endogenous Leptin Short Article Diet-Induced Obese Mice Retain Endogenous Leptin Action. *Cell Metab.* **21,** 1–6 (2015).
3. Knight, Z. A., Hannan, K. S., Greenberg, M. L. & Friedman, J. M. Hyperleptinemia is required for the development of leptin resistance. *PLoS One* **5,** 1–8 (2010).
4. Sturm, R. & Hattori, A. Morbid obesity rates continue to rise rapidly in the United States. *Int. J. Obes.* **37,** 889–891 (2013).
5. Thaler, J. *et al.* Obesity is associated with hypothalamic injury in rodents and humans. *J. Clin. Investig.* **122,** 153 (2011).
6. Cani, P. D. *et al.* Metabolic Endotoxemia Initiates Obesity and Insulin Resistance. *Diabetes* **56,** 1761–1772 (2007).
7. Milanski, M. *et al.* Saturated Fatty Acids Produce an Inflammatory Response Predominantly through the Activation of TLR4 Signaling in Hypothalamus: Implications for the Pathogenesis of Obesity. *J. Neurosci.* **29,** 359–370 (2009).
8. Dorfman, M. D. *et al.* Sex differences in microglial CX3CR1 signalling determine obesity susceptibility in mice. *Nat. Commun.* **8,** 14556 (2017).
9. Berkseth, K. E. *et al.* Hypothalamic gliosis associated with high-fat diet feeding is reversible in mice: A combined immunohistochemical and magnetic resonance imaging study. *Endocrinology* **155,** 2858–2867 (2014).
10. Roth, J. D. *et al.* Leptin responsiveness restored by amylin agonism in diet-induced obesity: Evidence from nonclinical and clinical studies. *Proc. Natl. Acad. Sci.* **105,** 7257–7262 (2008).
11. Turek, V. F. *et al.* Mechanisms of amylin/leptin synergy in rodent models. *Endocrinology* **151,** 143–152 (2010).
12. Trevaskis, J. L. *et al.* Amylin-mediated restoration of leptin responsiveness in diet-induced obesity: Magnitude and mechanisms. *Endocrinology* **149,** 5679–5687 (2008).
13. Betley, J. N. *et al.* Neurons for hunger and thirst transmit a negative-valence teaching signal. *Nature* **521,** 180–185 (2015).